



## City Research Online

### City, University of London Institutional Repository

---

**Citation:** Wang, X. (1998). Separate adjustment of close range photogrammetric measurements. (Unpublished Doctoral thesis, City, University of London)

This is the accepted version of the paper.

This version of the publication may differ from the final published version.

---

**Permanent repository link:** <https://openaccess.city.ac.uk/id/eprint/30999/>

**Link to published version:**

**Copyright:** City Research Online aims to make research outputs of City, University of London available to a wider audience. Copyright and Moral Rights remain with the author(s) and/or copyright holders. URLs from City Research Online may be freely distributed and linked to.

**Reuse:** Copies of full items can be used for personal research or study, educational, or not-for-profit purposes without prior permission or charge. Provided that the authors, title and full bibliographic details are credited, a hyperlink and/or URL is given for the original metadata page and the content is not changed in any way.

**A thesis submitted for the award of the degree of Doctor of Philosophy**

**Separate Adjustment of  
Close Range Photogrammetric Measurements**

**By Xinchu Wang**

**Optical Metrology Centre  
Department of Electrical, Electronic and Information Engineering  
City University  
London**

**July, 1998**

## Acknowledgement

I would like to thank Dr. T.A. Clarke, my supervisor, for his suggestion of the research area and invaluable guidance during the course of the research work. His initial introduction guided me into the area of photogrammetry and his suggestion of the starting point enabled me to get into the area quickly. His continuous encouragement and advice were the driving resources of my progress, especially in the early stage when I was embarrassed by language barriers. His careful reading and correcting of my  
” throughout the thesis led to its current form. I would also want to express my special appreciation for his arrangement of financial support during the last three and half years which allowed me to concentrate on the research work. Without his help, this thesis would not have been finished smoothly.

I wish to thank Professor M.A.R. Cooper for his excellent guidance on the theory of photogrammetry. It was my pleasure to have many opportunities to discuss my ideas with him. His comments on least squares and statistical analysis were very helpful in extending my knowledge. His rigorous research attitude and logical thought influenced me very much. His critical remarks on the method of separate adjustment compelled me to do more fundamental research on least squares and make the method more credible. I also wish to thank him for spending his precious time reading through the whole thesis, making many corrections and providing some constructive suggestions.

I would like to give my thanks to Dr. S. Robson. He was always ready to respond to my questions and comment on them quickly. Discussions with him over technical problems in photogrammetry were always fruitful. He also let me use the bundle adjustment programs, GAP and CUBA, and provided many real data sets which allowed me to test the separate adjustment method and compare its results with the traditional bundle adjustment method.

Finally, I would like to extend my thanks to my colleagues Dr. X. Pan, Dr. J. Chen, Mr. D.D.A.P. Ariyawansa, Mr. S. Cowhig and Dr. R. Gooch for their help and collaboration over the past three years at the Centre of Digital Image Measurement and Analysis.

## **Declaration**

“I grant powers of discretion to the University Librarian to allow this thesis to be copied in whole or in part without further reference to me. This permission covers only single copies made for study process, subject to normal conditions of acknowledgement”.

## Abstract

Photogrammetry is a non-contact measurement technique of obtaining 3D information in the object space by processing 2D information on the image planes. This thesis mainly concerns the data reduction methods used in close range multiple camera photogrammetry. The objective was to develop a fast method which could be used in real-time measurement systems. Traditional methods such as the bundle adjustment are investigated and the advantages and disadvantages are discussed. It was found that the bottle-neck which restricts the speed was the computation of matrices, especially the inverse of the coefficient matrix, in the simultaneous least squares estimation process.

In this thesis, an alternative method named the separate adjustment is developed and successfully used in close range photogrammetry. This method can give the same results as the traditional bundle adjustment, but with a significant saving of computation time and memory requirements. It was found that the computation time required by the separate adjustment is directly proportional to the numbers of the object points and cameras, and the memory required is independent of how many object points or cameras are involved. A thorough comparison between the two methods is given and some results from simulation and practical tests are presented.

The separate adjustment is a separate least squares estimation process which estimates the unknown parameters separately in groups rather than simultaneously. In this way the sizes of the matrices in the least squares process are reduced. Therefore time and memory are reduced accordingly. Due to the special structures of the design matrix and the coefficient matrix in close range photogrammetry the separate adjustment method is very efficient and very easy to apply, especially when it is used in real-time applications.

# Contents

<b>Acknowledgements</b> .....	i
<b>Declaration</b> .....	ii
<b>Abstract</b> .....	iii
<b>Contents</b> .....	iv
<b>Chapter 1 Introduction</b> .....	1
1.1 A brief review of photogrammetry .....	2
1.2 A brief review of least squares .....	7
1.3 Applications of least squares in close range photogrammetry ....	10
1.3.1 Least squares in intersection .....	11
1.3.2 Least squares in resection .....	12
1.3.3 Least squares in bundle adjustment .....	12
1.4 Separate adjustment of photogrammetric measurements .....	13
1.5 Thesis structure .....	15
<b>Chapter 2 Observations and Least Squares Estimation</b> .....	17
2.1 Functional model and linearization .....	18
2.2 Stochastic model and error propagation .....	20
2.2.1 Concepts of weight, variance-covariance and cofactor matrices ....	20
2.2.2 Error propagation through the functional model .....	22
2.3 The least squares method .....	25
2.4 Sequential LSE .....	30
2.5 Iterative LSE .....	34
2.6 Step-by-step LSE .....	38
2.7 Datum and constraints .....	39
2.7.1 Datum .....	39
2.7.2 Constraints .....	40
2.8 LSE with constraints .....	43
2.8.1 LSE with inner constraints .....	43
2.8.2 LSE with previously estimated coordinates .....	46
2.9 The unified LSE .....	49
2.10 Summary of the chapter .....	55
<b>Chapter 3 Least Squares Estimation of Photogrammetric Measurements</b> <b>---- The Traditional Methods</b> .....	57
3.1 Functional models .....	58
3.1.1 Collinearity equations .....	60
3.1.2 DLT model .....	61
3.1.3 Camera interior parameters .....	62

3.1.3.1	Principal distance and principal point .....	62
3.1.3.2	Radial distortion and decentring distortion .....	63
3.1.4	Modification of the collinearity equations .....	66
3.2	Intersection .....	66
3.2.1	Direct solution .....	68
3.2.2	Iterative solution .....	69
3.2.3	Discussion .....	71
3.3	Resection .....	72
3.3.1	Iterative solution .....	73
3.3.2	Closed solution (Direct solution) .....	75
3.3.3	Discussion .....	78
3.4	The bundle adjustment .....	78
3.5	Bundle adjustment with constraints .....	84
3.5.1	Inner constraints on the object points .....	85
3.5.2	Inner constraints on the camera parameters .....	86
3.5.3	Discussion .....	88
3.6	The unified bundle adjustment .....	89
3.7	Summary of the chapter .....	93

#### **Chapter 4    Separate Least Squares Estimation**

	.....	95
4.1	Introduction .....	95
4.2	Separate LSE .....	100
4.2.1	Linear case .....	101
4.2.2	Non-linear case .....	105
4.3	Discussion .....	108
4.4	A numerical example .....	110
4.4.1	Simultaneous solution .....	112
4.4.2	Separate solution .....	113
4.5	Datum problem of the separate LSE .....	116
4.6	Separate LSE with constraints .....	117
4.6.1	With fixed control points .....	118
4.6.2	With weighted control points .....	118
4.7	An application of surveying .....	119
4.8	Summary of the chapter .....	125

#### **Chapter 5    Separate Adjustment of Photogrammetric Measurements**

	.....	127
5.1	Free network adjustment .....	127
5.1.1	Adjusting the object points .....	128
5.1.2	Adjusting the cameras .....	130
5.1.3	Iteration between the two steps .....	132
5.1.4	Datum definition .....	133
5.1.5	Precision estimation .....	133
5.1.6	Number of iterations .....	135

5.1.7	Consistency with the bundle solution .....	136
5.1.8	Computational complexity .....	137
5.1.9	Feasible area of the separate adjustment .....	138
5.2	Continuous adjustment .....	138
5.3	Separate adjustment with controls .....	142
5.3.1	With fixed control points .....	143
5.3.2	With weighted control points .....	143
5.3.3	With scale .....	144
5.3.4	Number of iterations .....	145
5.4	Separate adjustment with DLT model .....	145
5.5	Self-calibration separate adjustment .....	149
5.5.1	Three step separate adjustment .....	151
5.5.2	Two step separate adjustment .....	152
5.5.3	A simulation test .....	153
5.6	Summary of the chapter .....	155
 <b>Chapter 6    Coordinate Transformation</b> .....		 157
6.1	Two dimensional transformation .....	157
6.1.1	Estimation of the transformation parameters .....	158
6.1.2	Estimation of transformed coordinates .....	166
6.2	Three dimensional transformation .....	170
6.2.1	Conventional method .....	170
6.2.2	Linear coordinate transformation .....	173
6.2.2.1	Estimation of the transformation parameters .....	173
6.2.2.2	Estimation of the transformed coordinates .....	178
6.2.2.3	Estimation of seven parameters from twelve parameters .....	181
6.3	Applications .....	183
6.3.1	Datum transformation .....	183
6.3.2	Relative positioning of a moving object .....	184
6.3.2	Relative positioning of two rigid objects .....	184
6.4	Summary of the chapter .....	186
 <b>Chapter 7    Simulation Tests</b> .....		 187
7.1	Test of resection with the 2D DLT model .....	187
7.1.1	Test for camera positions .....	188
7.1.2	Error propagation from 3D to cameras .....	191
7.1.3	Error propagation from 2D to cameras .....	192
7.2	Test of resection followed by intersection with the DLT model ....	194
7.3	Test of the bundle adjustment .....	197
7.4	Tests of the separate adjustment .....	198
7.4.1	Free network adjustment .....	198
7.4.2	With control points .....	201
7.5	Speed of the separate adjustment .....	201
7.6	More comparisons between BA and SA .....	202
7.7	More tests with separate adjustment .....	203
7.8	Tests of separate adjustment with DLT models .....	205

7.9	Tests of self calibration adjustment .....	206
7.10	Tests of continuous measurement of a moving object .....	214
<b>Chapter 8</b>	<b>A practical test .....</b>	<b>222</b>
<b>Chapter 9</b>	<b>Conclusions .....</b>	<b>237</b>
<b>Appendix I</b>	<b>Derivations of some partial derivatives .....</b>	<b>240</b>
<b>Appendix II</b>	<b>Some results from the simulation tests .....</b>	<b>248</b>
<b>References and Bibliography</b>	<b>.....</b>	<b>261</b>

## **Chapter 1**

### **Introduction**

Photogrammetry is defined as (Karara, 1989)

“The art, science, and technology of obtaining reliable quantitative information about physical objects and the environment through the process of recording, measuring, and interpreting photographic images and patterns of radiant imagery derived from sensor systems”.

Since it was developed more than a hundred years ago, photogrammetry has been widely used in geology, forestry, agriculture, architecture, industry and medicine (Slama 1980; Karara 1989; Atkinson 1996) where spatial 3-dimensional (3D) coordinates are required. These 3D coordinates can be used to derive other useful information, such as position, size and shape of an object or relative positions between objects. Since it is a non-contact measurement technique by taking photographs/images with cameras, photogrammetry can be used to measure objects which are inaccessible or inconvenient to access when they are measured. Each image records a 2D perspective projection of the object to be measured in the 3D space. With two or more images taken from different positions, the 3D object can be reconstructed indirectly.

High accuracy is an important property of photogrammetric measurement. Like many other measurement techniques, redundant measurements are always needed in photogrammetry for high accuracy. This means that the number of measured elements (observations) is more than the minimum required to determine the unknown parameters. In close range photogrammetry, a measurement process with thousands of degrees of freedom is not unusual. In this case, least squares is useful to determine these parameters uniquely. By adjusting the observations so that the sum of the weighted squares of all the residuals fitting to the functional model is minimised, least squares estimation can give the maximum likelihood results (if the errors are normally

distributed and independent). In close range photogrammetry, least squares estimation is used in data deduction such as intersection, resection, camera calibration and simultaneous bundle adjustment. It is almost inevitable in close range photogrammetry.

In this chapter photogrammetry and least squares methods are briefly reviewed. In particular the applications of least squares to photogrammetry is discussed. An alternative method of least squares, named *separate least squares estimation*, is introduced.

### **1.1 A brief review of photogrammetry**

Photogrammetry has been increasingly used in areas where 3D information is required. One of the early application of photogrammetry is the compilation of topographic maps and surveys (Karara 1989). In 1851 the Frenchman Laussedat began to develop photogrammetric methods for mapping using terrestrial photographs. He constructed a city map based on geometric information deducted from the photographs taken from the roofs of Paris. This is believed to be the first application of topographic photogrammetry. Laussedat also published books on his methods and instrumentation for the compilation of topographic maps. The first application of non-topographic photogrammetry was due to a Prussian architect, Meydenbauer. In 1858 he used Laussedat's technique to survey churches and historical monuments for reconstruction after damage and determination of deformation. In 1885 Meydenbauer established a state institute in Berlin to carry out architectural recording.

Since the invention of aeroplane early this century, aerial photogrammetry has played, and will continue to play, an important role in geological survey, topographic mapping, military operations and agriculture. Close range photogrammetry, which is widely used in architecture, industrial engineering, biomedical and bioengineering applications, has developed into a highly reliable and precise measurement technique and is rapidly expanding in many other areas. The digital era of photogrammetry has arrived in the 1990s with the technology of video cameras, frame grabbers and computers. Real-time photogrammetry is becoming possible with powerful hardware and advanced software.

The term 'close range photogrammetry' refers to the situation where object-to-camera distances are not more than 300 metres. Unlike aerial photogrammetry where camera axes are normally parallel, in close range photogrammetry images are taken from camera positions all around the object pointing towards the middle of the object. So the measurement networks are highly convergent and the cameras are often stationary. Close range photogrammetric applications are becoming the dominant activity for the successful implementation of modern digital photogrammetry. High accuracy can be achieved in close range photogrammetry, and a relative accuracy of one part in a million has been reported (Fraser 1992).

In a close range photogrammetric measurement process, there are normally three major steps:

- (i) 2D image data acquisition;
- (ii) Image processing, target location and matching between different images; and
- (iii) Least squares estimation to reconstruct the 3D coordinates of the interested points in the object space.

Image acquisition is a procedure which converts 3D information in the object space into 2D information on the camera image planes. In close range photogrammetry targets are normally put on the object to be measured for high precision. Locations of the target image on the camera image plane are measured. These targets are then labelled and matched between different cameras. Based on the geometric perspective principle, a set of so called collinearity equations can be derived to establish the relationships between 2D observations on the camera image planes and the 3D coordinates of object points. By solving the collinearity equations with least squares estimation the 3D coordinates of these points can be reconstructed in the object space.

In practice, some objects are difficult to measure by other means for reasons such as irregular shape, inaccessible, etc. However, if the objects can be imaged, they can be measured by close range photogrammetry. Figure 1-1 to 1-3 illustrate the close range photogrammetric measurement procedure.

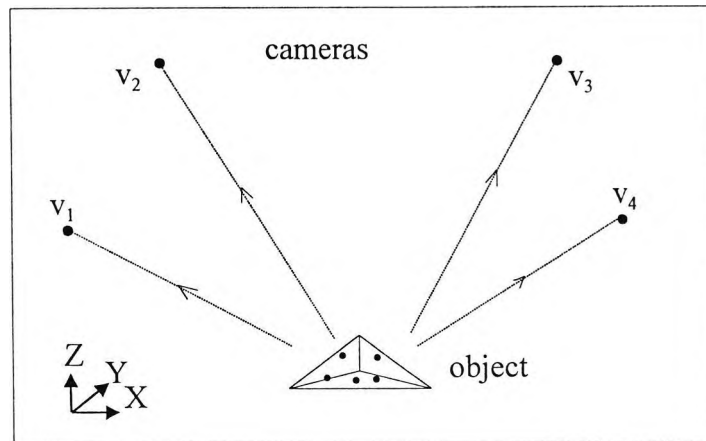


Figure 1-1 Image acquisition (From 3D to 2D)

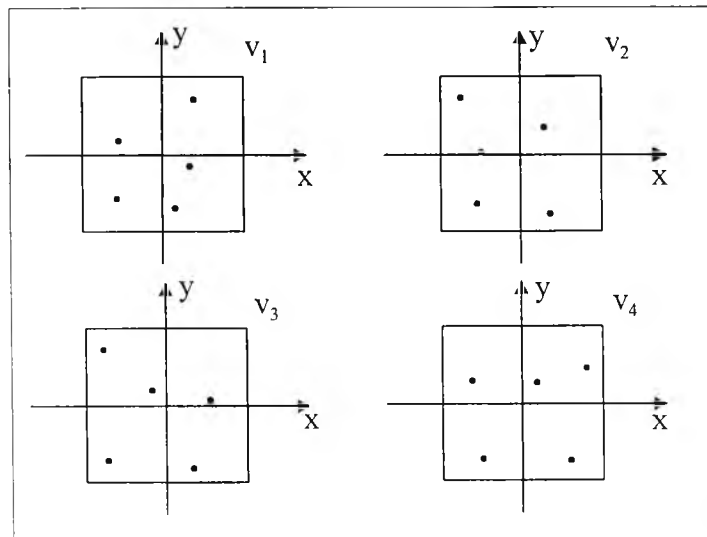


Figure 1-2 Image processing, target location and matching

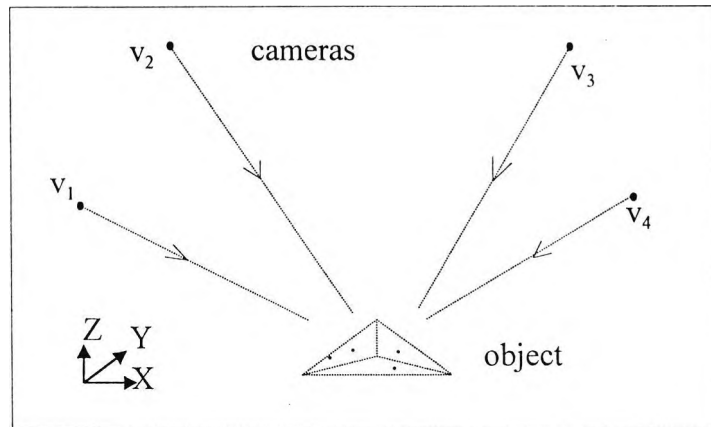


Figure 1-3 Object reconstruction (From 2D to 3D)

Figure 1-4 shows a marine propeller. The geometric shape makes it a difficult object to measure. With close range photogrammetry, the targeted marine propeller is imaged by multi-cameras from different view points all around it (Figure 1-5). The locations (2D coordinates) of the targets on the camera image planes are then calculated and matched between different images. By a least squares estimation process the 3D coordinates of the targets can be estimated and the marine propeller can be reconstructed in the object space (Figure 1-6).

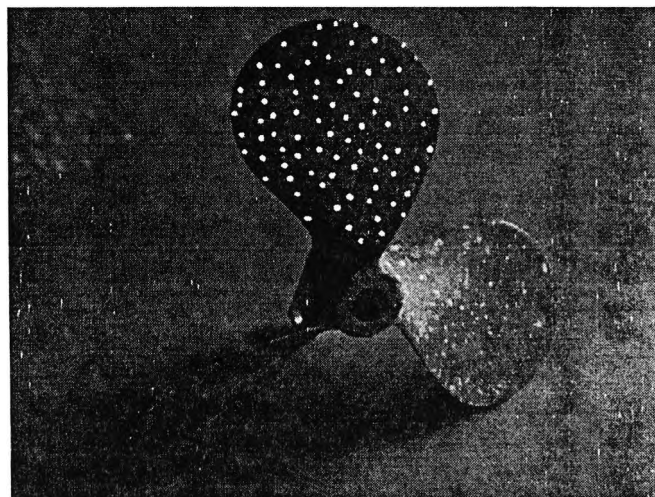


Figure 1-4 A marine propeller

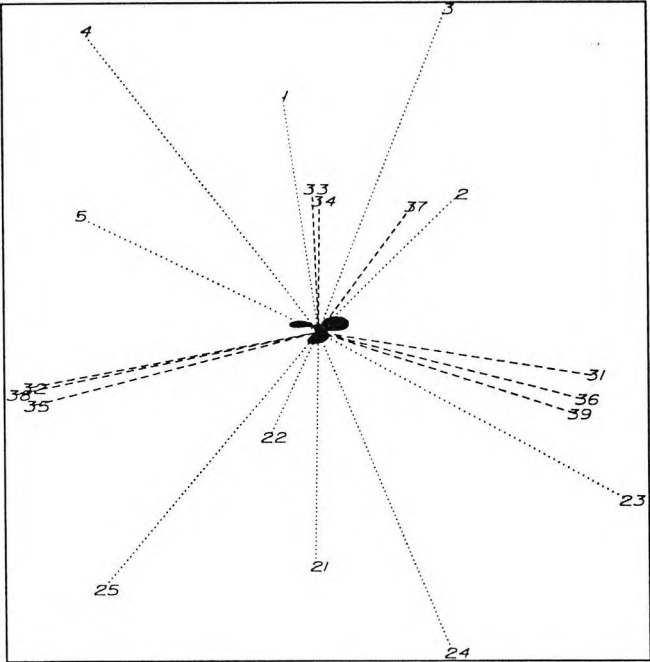


Figure 1-5 Image acquisition

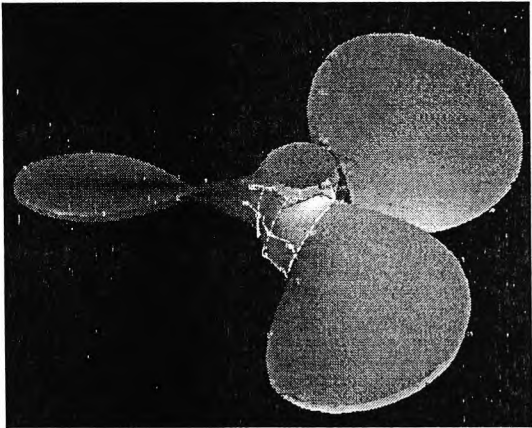


Figure 1-6 3D reconstruction of the marine propeller

## 1.2 A brief review of least squares

Least squares estimation is a method of adjusting observations so that the sum of the weight squares of the residuals from the functional model is minimised. The method was developed independently by Gauss and Legendre about two hundred years ago. It has been widely used in surveying and photogrammetry to deal with redundant measurements (Kissam 1956; Mikhail 1976, 1981; Cross 1983; Anderson & Mikhail 1985; Methley 1986; Cooper 1987).

It has been proven that no matter whether or not the observations are normally distributed, whether or not they are independent, the least squares estimate is a Best Linear Unbiased Estimate, which is often referred to as *BLUE*. If the observations are normally distributed and independent, the least squares estimate will give the maximum likelihood solution.

In surveying and photogrammetry, the observations are obtained to derive other unknown parameters. A general functional model, which establishes the relationship between the observations and the unknown parameters, can be described as

$$f(\mathbf{x}, \mathbf{l}) = \mathbf{0} \quad (1.1)$$

where  $\mathbf{x} = (x_1, x_2, \dots, x_u)$  is a vector of  $u$  unknown parameters,  $\mathbf{l} = (l_1, l_2, \dots, l_m)$  is a vector of  $m$  observations and  $f$  is a vector of the  $c$  functions  $(f_1, f_2, \dots, f_c)$ .

For a given functional model, there is always a minimum number of independent observations ( $m_0$ ) to determine those unknown parameters uniquely. If the number of observations is not sufficient, say  $m < m_0$ , the situation will obviously be deficient. However in practice  $m$  is usually much larger than  $m_0$ . So *redundancy* is said to exist and *adjustment* of the observations is required to determine the unknown parameters uniquely. The number of redundancies or the *degrees of freedom*  $r$  is given by

$$r = m - m_0 \quad (1.2)$$

In close range photogrammetry,  $r$  could be several hundreds or even more. Any sufficient subset of observations can be used to estimate the unknown parameters. However, due to the random errors of the observations, each minimum subset would give a different result. It is impossible to obtain a unique result from these redundant observations unless an additional criterion is introduced. Many criteria can be used for this purpose. However *least squares estimation* is the most popular method used in science and engineering. It is by far the predominant technique of data deduction method in photogrammetry and surveying.

In a data deduction process, the original set of observations  $l$ , which is inconsistent with the functional model, is replaced by an adjusted set  $\hat{l}$  which satisfies the model. The differences between the two set of observations, which are termed *residuals*, is given by

$$\mathbf{v} = \hat{\mathbf{l}} - \mathbf{l} \quad (1.3)$$

The least squares estimation is usually described as a process to minimise a specified target function  $\phi$ , i.e.,

$$\phi = \mathbf{v}' \mathbf{W}_l \mathbf{v} \quad (1.4)$$

where  $\mathbf{v} = (v_1, v_2, \dots, v_m)$  is a vector of residuals from Eq (1.3) and  $\mathbf{W}_l$  is the weight matrix of the observations. A simple case is when all the observations are independent and equally weighted so that the weight matrix is a scalar matrix. The target function to be minimised becomes

$$\phi = \mathbf{v}' \mathbf{v} = \sum_{i=1}^m v_i^2 \quad (1.5)$$

This is the oldest and most classical case from which the name *Least Squares* came.

In practice, the functional models are usually non-linear. Linearization is needed before least squares estimation can be applied. This procedure is often accomplished by

Taylor's expansion to the first order accuracy. The linearized functional model is then expressed as

$$A\Delta x + Bv = b \quad (1.6)$$

where  $A = (\partial f/\partial x)^0$ ,  $B = (\partial f/\partial l)^0$ ,  $b = -f(x^0, l)$ , and  $\Delta x$  is a vector of corrections to the unknown parameters.

There are two special cases of the general linearized functional model which often occur in practice (Mikhail 1976, 1981). The most common case in photogrammetry is the *observation equations*. In this case each equation in the functional model (1.1) contains only one observation which is explicit and the number of the equations is equal to that of the observations ( $c = m$ ). Suppose that  $l_i$  appears in  $f_i$  as  $-l_i$ , so matrix  $B = -I$ . The linearized functional model becomes

$$A\Delta x = b + v \quad (1.7)$$

In this case the unknown parameters can be determined by a least squares estimation, which gives (if  $A$  is of full rank)

$$\Delta x = (A'W_l A)^{-1} A'W_l b \quad (1.8)$$

It is followed by

$$x = x^0 + \Delta x \quad (1.9)$$

where  $x^0$  is a vector of the starting values of the unknown parameters. Least squares estimation is an iterative process when the functional model is non-linear. After each iteration,  $x$  is updated. The iterative process terminates when a stop criterion is met, corresponding to the first order approximation in Taylor expansion.

The second special case of the linearized model occurs when the observations must satisfy the functional model while the unknown parameters do not appear in it. So matrix  $A$  is a null matrix. Therefore the general linearized functional model becomes

$$Bv = b \quad (1.10)$$

These equations are called *condition equations*.

Most simple problems can be modelled by either observation equations or condition equations. But for more complicated problems, such as 3D coordinate transformation between two coordinate systems when the coordinates from both systems are considered as observations, the general case (1.6) is used.

An important property of the least squares estimation process in (1.8) is that at the same time as the unknown parameters are estimated, their covariance matrix is obtained. The covariance matrix can be used to analyse error propagation from the observations into the derived results through the measurement system. The reverse procedure (network design) can also be carried out, i.e., with a given covariance matrix it is possible to deduce how many observations should be measured and with what variances.

### 1.3 Applications of least squares estimation in close range photogrammetry

In close range photogrammetry, 2D coordinates of target images are measured on camera image planes as observations. These observations can be used to derive the unknown parameters, such as the 3D coordinates of the object points and the camera parameters. The relationships between the observations and the unknown parameters are established by the collinearity equations (Wolf 1983), which can generally be expressed as

$$f(x_1, x_2) = l \quad (1.11)$$

where the unknown parameters  $\mathbf{x}_1$  denotes the 3D coordinates of the object points,  $\mathbf{x}_2$  denotes the camera parameters and  $l$  is the 2D coordinates (observations) on camera image planes. This is the typical case of observation equations. In each equation, there is only one observation (image coordinate of one object point,  $x$  or  $y$ ) and it appears explicitly on one side of the equation. If  $m$  images are taken to measure  $n$  object points, the total number of the equations is  $2mn$  and the total number of the unknown parameters is  $3n+6m$ , assuming all the points are imaged on each image.

### 1.3.1 Least squares in intersection

If the camera parameters are known beforehand, the 3D coordinates of the object points can be determined by intersecting lines projected from their corresponding points on the camera image planes. This procedure is called *intersection*. It is the standard situation using metric cameras with fixed bases or when using photo-theodolites (Karara 1989). Intersection is also used to locate object points from two overlapping horizontal terrestrial photos or highly oblique photos (Wolf 1983). In close range photogrammetry intersection is often used to estimate the starting values of the object points using approximately estimated camera parameters. These starting values can be used in the subsequent bundle adjustment for better estimates.

Ideally, for each object point the  $m$  lines projected from the cameras should intersect at one point in the object space. However, due to the errors in the measurement process these lines will not intersect at the same point. Since  $\mathbf{x}_2$  are considered as constants, the linearized observation equations can be expressed as

$$A_1 \Delta \mathbf{x}_1 = \mathbf{b} \quad (1.12)$$

For each object point, there are  $2m$  equations and 3 unknown parameters. In this case least squares estimation can be used for the unique solution.

### 1.3.2 Least squares in resection

*Resection* is a procedure of determining camera exterior parameters with known spatial control points (Thompson 1975; Slama 1980; Atkinson 1996). Theoretically, three control points, which will give six equations, can be used to determine the six camera exterior parameters uniquely. In practice, more control points are used for a more reliable solution. Since  $x_1$  are considered as constants, the linearized observation equations can be expressed as

$$A_2 \Delta x_2 = b \quad (1.13)$$

For each camera, there are  $2n$  equations and 6 unknown parameters. When  $2n > 6$ , least squares estimation can be used for the best solution.

### 1.3.3 Least squares in bundle adjustment

*Bundle adjustment* is a procedure in which both  $x_1$  and  $x_2$  are treated as unknown parameters and adjusted simultaneously (Brown 1976; Granshaw 1980; Karara 1989; Fraser 1992; Atkinson 1996). This is the general case in close range photogrammetry where neither the 3D coordinates of the object points nor the camera parameters are known, except for their approximately estimated starting values. The linearized observation equations can be expressed by Eq (1.7), in which

$$A = [A_1 \ A_2] \quad (1.14)$$

and

$$\Delta x = \begin{bmatrix} \Delta x_1 \\ \Delta x_2 \end{bmatrix} \quad (1.15)$$

If all the object points appear on all of the cameras, there will be totally  $2mn$  equations, and  $(3n+6m)$  unknown parameters to be solved. The number of equations  $2mn$  is usually

much larger than the number of unknown parameters  $(3n+6m)$ . So these unknown parameters can be solved by a simultaneous least squares estimation. The size of the matrix  $A'W_rA$  in Eq (1.8) is  $(3n+6m) \times (3n+6m)$ . If 20 images are taken to measure 200 object points, the size of  $A'W_rA$  will be  $720 \times 720$ . Calculating the inverse of such a big matrix is very expensive in terms of both computation time and memory requirements.

The principles of simultaneous least squares estimation are well known (Mikhail 1976, 1981; Cooper 1987). It is clear that this method provides the *de facto* standard for the *output* from an adjustment. However, the requirement for large matrix inversions places large demands on storage and computing power. To avoid this a *sequential adjustment* may be used as a means of providing fast updates for the parameters while not requiring a full matrix inversion (Shortis 1980; Cross 1983; Gruen 1985; Cooper 1987). For most true real-time applications the direct linear transform (DLT) (Abdel-Aziz & Karara 1971) has been used but it does not provide the highest accuracy due to its modelling deficiencies and the reliance on accurately measured control points for camera parameter estimation (Marzan 1975; Karara 1980). For situations where interior and exterior camera parameters are known a direct spatial intersection may be used (Granshaw 1980; Shmutter 1974). Because each of these methods have deficiencies research is necessary to find an alternative fast, robust and flexible solution.

#### 1.4 Separate adjustment of photogrammetric measurements

In this thesis, an alternative method, named the *separate adjustment*, is introduced. It can be shown that this method gives the same results as the simultaneous bundle adjustment but with a significant decrease in storage requirements and computational time.

The separate adjustment is a technique of division. The theoretical background is that in a least squares estimation process the unknown parameters can be estimated separately, one by one or group by group, and same results can be expected as that obtained by a simultaneous estimation. In close range photogrammetry, the unknown parameters are naturally divided into two parts, the 3D coordinates of the object points and the camera

parameters. Instead of estimating the unknown parameters simultaneously, the unknown parameters can be estimated separately in two steps. In the first step, the 3D coordinates of the object points are estimated while the camera parameters are considered as constants. The computational complexity in terms of time is linear with respect to the number of the object points and the maximum size of the matrices to be inverted is  $3 \times 3$ . In the second step, the camera parameters are estimated while the 3D coordinates of the object points are considered as constants. The computational complexity in terms of time is linear with respect to the number of the images and the maximum size of the matrices to be inverted is  $6 \times 6$ .

After each circulation, the unknown parameters in the two parts are updated and another iteration is followed. The iterative process terminates when the maximum correction of the unknown parameters is less than a given significant value. Since same functional model and same target function of the least squares estimation are used in the separate adjustment and the bundle adjustment, the same results can be obtained from the two methods. But the speed of the separate adjustment is much faster than the bundle adjustment. Table 1-1 illustrates a comparison of speed between the two methods for a four camera close range photogrammetric measurement network (the test was conducted on a SUN Sparc Classic).

Table 1-1 A comparison of speed between the bundle adjustment and the separate adjustment

No. of points	Bundle Adjustment (seconds)	Separate Adjustment (seconds)
100	45	0.86
200	389	1.72
300	1269	2.58
400	2967	3.44

In the early stage of photogrammetry, image acquisition and processing were time consuming works which could have taken a few days before the 2D coordinates on the photographs (observations) were ready for the 3D reconstruction. Therefore a few hours calculation by computer for the 3D coordinates was quite endurable. However as

photogrammetry enters the digital era, the scope of its applications has been extended. With digital cameras, powerful PC's and DSP's, the 2D coordinates on the image planes can be obtained in real-time. Hence real-time 3D measurement by photogrammetry becomes possible. The demand for real-time algorithm of 3D reconstruction becomes urgent. From this point of view, the separate adjustment method is developed and introduced in this thesis.

The words "adjustment" and "estimation" are commonly used terms in least square processes. When redundant measurements (observations) are used to estimate the unknown parameters, adjustments are required to the observations according to the least squares criterion, no matter whether the functional models are linear or non-linear. The result of these adjustments is a unique solution of the unknown parameters -- a least squares estimate. The word "estimation" is more suitable for the least squares process and it has a proper statistical meaning whereas "adjustment" has not (Cooper 1987). Therefore the phrase "least squares estimation" (LSE) will be used in the thesis. However, considering the extensive use of the word "adjustment" in photogrammetry, such as "bundle adjustment" and "sequential adjustment", the phrase "separate adjustment" is chosen for the method developed in the thesis. The background of the "separate adjustment" is a "separate least squares estimation" (SLSE).

## **1.5 Thesis Structure**

The thesis is composed of nine chapters, two appendices and a bibliography.

Chapter 2 describes the basic concepts of observations and least squares estimation. Some conventional methods of least squares estimation, such as sequential adjustment, iterative adjustment and step-by-step method, are discussed.

Chapter 3 describes the basic theories of the photogrammetric measurement. The conventional bundle adjustment is discussed. Datum problems are addressed. A unified bundle adjustment is introduced.

In Chapter 4, an alternative method of least squares estimation, the separate least squares estimation, is developed. Some numerical examples are given to verify the results of the method.

In Chapter 5, the separate adjustment method, which is based on the theory of the separate least squares estimation, is developed and used in close range photogrammetry. Issues such as datum definition, precision estimation, consistency with the bundle solution are discussed.

In Chapter 6, a linear coordinate transformation method is introduced. It can be used to transform the results of the separate least squares estimation from one coordinate system to another.

In Chapter 7, some results of simulation tests are presented to test the theories discussed in the previous chapters.

In Chapter 8, some results from a practical test are given.

Chapter 9 summarizes the thesis and gives the conclusions.

Appendix I includes some partial derivatives required in the thesis and Appendix II gives some output data from the simulation tests.

## Chapter 2

### Observations and Least Squares Estimation

In surveying and close range photogrammetry, measured elements are used to estimate other quantities (the unknown parameters). For instance, distances and zenith angles may be measured to estimate the positions of the ground stations in a geodetic positioning system. In close range photogrammetry images are taken to measure the spatial object points. The measured elements are the 2D coordinates on the image planes projected from the spatial object points. The unknown parameters to be estimated are the 3D coordinates of the object points. These measured elements are known as *observations*.

The relationship between the observations and the unknown parameters is established by the functional models and stochastic models. In close range photogrammetry the commonly used functional model is based on the well-known collinearity equations. The stochastic models are associated with the weights of the measured 2D coordinates on image planes. By solving for the unknown parameters in the functional model the 3D coordinates of the object points can be estimated.

In practice, the observations can never be measured perfectly due to limitations in the measuring instruments, hence observational errors will be introduced during the measurement process. In order to reduce the effect of the observational errors it has become a routine procedure to make redundant measurements (Mikhail 1976, 1981; Cooper 1987; Kuang 1996). So the unknown parameters become over-determined. Different results will be obtained from each subset of the observations because of their inconsistencies unless an additional criterion is introduced. Many criteria can be used in practice. The principle of least squares is one of the most popular criterion used in surveying (Kissam 1956; Cross 1983; Anderson & Mikhail 1985; Cooper 1987) and close range photogrammetry (Slama 1980; Methley 1986; Karara 1989; Atkinson 1996) and has been proved to be an efficient method of dealing with redundant measurements.

In this chapter the concepts of functional model and stochastic model are introduced. The least squares methods are reviewed. The methods of sequential adjustment, iterative adjustment and step-by-step adjustment are also discussed.

## 2.1 Functional model and linearization

The functional model establishes the mathematical relationship between the observations and the unknown parameters. If  $m$  observations are measured to estimate  $u$  unknown parameters, the functional model can generally be written as

$$F(x, l) = 0 \quad (2.1)$$

in which  $x = (x_1, x_2, \dots, x_u)$ , is a vector of the unknown parameters to be estimated,

$l = (l_1, l_2, \dots, l_m)$ , is a vector of the observations, and

$F$  denotes the  $c$  functions  $F_i$  ( $i = 1, 2, \dots, c$ ).

It is often the case that each equation in the functional model (2.1) contains only one observation which is explicit and the number of the equations is then equal to that of the observations ( $c = m$ ). So the functional model (2.1) can be expressed as

$$F(x, l) = f(x) - l = 0 \quad (2.2)$$

i.e.

$$f(x) = l \quad (2.3)$$

Eq (2.3) are generally known as *observation equations*, which are mostly used in surveying and close range photogrammetry.

If the observation equations are linear, the least squares process can be applied directly. This is called a *linear least squares estimation*. However in most cases the observation equations are non-linear. So linearization is often the first step needed for the subsequent least squares estimation. Taylor

purpose. Expanding Eq (2.3) by Taylor's series to the first order accuracy, the linearized observation equations become

$$f(x^0) + \left(\frac{\partial f}{\partial x}\right)^0(x - x^0) = l \quad (2.4)$$

in which vector  $x^0$  is the first-order approximation to  $x$ , and the partial differential coefficient is calculated at the approximate value  $x = x^0$ . If symbol  $\Delta x$  is used for  $(x - x^0)$ ,  $b$  for  $l - f(x^0)$  and matrix  $A$  for  $\left(\frac{\partial f}{\partial x}\right)^0$ , Eq (2.4) can be written as

$$A\Delta x = b \quad (2.5)$$

in which

$\Delta x = (\Delta x_1, \Delta x_2, \dots, \Delta x_u)^t$ , is a vector of corrections of the unknown parameters;

$b = (l_1 - f_1(x^0), l_2 - f_2(x^0), \dots, l_m - f_m(x^0))^t$ ;

$x^0 = (x_1^0, x_2^0, \dots, x_u^0)^t$  is a vector of the starting values; and

$A$  is the Jacobian matrix, i.e.,

$$A = \begin{bmatrix} \frac{\partial f_1}{\partial x_1} & \frac{\partial f_1}{\partial x_2} & \dots & \frac{\partial f_1}{\partial x_u} \\ \frac{\partial f_2}{\partial x_1} & \frac{\partial f_2}{\partial x_2} & \dots & \frac{\partial f_2}{\partial x_u} \\ \dots & \dots & \dots & \dots \\ \frac{\partial f_m}{\partial x_1} & \frac{\partial f_m}{\partial x_2} & \dots & \frac{\partial f_m}{\partial x_u} \end{bmatrix} \quad (2.6)$$

All the partial derivatives in the Jacobian matrix  $A$  are calculated with the given value  $x^0 = (x_1^0, x_2^0, \dots, x_u^0)$ . Eq (2.5) are generally called *linearized observation equations*.

## 2.2 Stochastic model and error propagation

In a measurement process, the unknown parameters are estimated from the measured elements. It is important to know the quality of the estimated results, mainly the precision of the estimated unknown parameters. It is also important to know the influence of the quality of the measured elements on the estimated results.

Generally there are three types of errors which will influence the estimated results: *systematic errors*, *gross errors* and *random errors*. Systematic errors are related to the functional model. They can be reduced by systematic calibration and numerical correction to the measured elements before using the functional model or by including additional parameters. Gross errors are normally caused by the mistakes during the measurement process. These can be detected and eliminated by independent checks on the measured data or least squares. Random errors arise when repeated measurements of the same element are inconsistent. These errors are more complicated and can be described by a stochastic model.

### 2.2.1 Concept of weight, variance-covariance and cofactor matrices

Observations can be regarded as random variables subject to the laws of statistics. It is possible to analyse the precision of the estimated results by the stochastic model of the measured elements and its propagation through the functional model. In the functional model (2.3), each observation has a variance  $\sigma_i^2$  which is related to the precision of the observation. The higher the precision, the lower the variance. Another evaluation of the precision of an observation is the weight  $w_i$  which is inversely proportional to the variance  $\sigma_i^2$ , i.e.,

$$w_i = \sigma_0^2 / \sigma_i^2 \quad (2.7)$$

$\sigma_0^2$  is referred as the *reference variance* or *variance factor*. The term *reference variance* is used in this thesis. The square root of the variance  $\sigma_i$  is known as the standard

deviation which is used directly for the precision of the observations and the estimated results.

With multiple observations, their variances are expressed by an  $m \times m$  matrix. It is a diagonal matrix for the uncorrelated measurements and is called the variance matrix. The variance matrix is expressed as

$$C = \begin{bmatrix} \sigma_1^2 & 0 & \cdots & 0 \\ 0 & \sigma_2^2 & \cdots & 0 \\ \cdots & \cdots & \cdots & \cdots \\ 0 & 0 & \cdots & \sigma_m^2 \end{bmatrix} \quad (2.8)$$

Its corresponding weight matrix is expressed as

$$W = \begin{bmatrix} w_1 & 0 & \cdots & 0 \\ 0 & w_2 & \cdots & 0 \\ \cdots & \cdots & \cdots & \cdots \\ 0 & 0 & \cdots & w_m \end{bmatrix} \quad (2.9)$$

where  $w_i = \sigma_0^2 / \sigma_i^2$  ( $i = 1, 2, \dots, m$ ). Therefore

$$W = \sigma_0^2 C^{-1} \quad (2.10)$$

In case of the correlated measurements,  $C$  is expressed as

$$C = \begin{bmatrix} \sigma_1^2 & \sigma_{12} & \cdots & \sigma_{1m} \\ \sigma_{21} & \sigma_2^2 & \cdots & \sigma_{2m} \\ \cdots & \cdots & \cdots & \cdots \\ \sigma_{m1} & \sigma_{m2} & \cdots & \sigma_m^2 \end{bmatrix} \quad (2.11)$$

The off-diagonal elements reflect the correlations between the measured elements. This is called the *covariance matrix*.

The *cofactor matrix*  $\mathbf{Q}$ , which is defined as  $\mathbf{Q} = \sigma_0^{-2} \mathbf{C} = \mathbf{W}^{-1}$ , represents the relative covariances of the observations. When the reference variance  $\sigma_0^2$  is unity, the cofactor matrix  $\mathbf{Q}$  is identical to the variance matrix  $\mathbf{C}$ . In this case,  $\mathbf{W}$  is often called the *inverse of the cofactor matrix* instead of the *weight matrix* since it is no longer a diagonal matrix. To simplify the terminology, the name *weight matrix* is extended to the general case in this thesis.

### 2.2.2 Error propagation through the functional model

If an element  $x$  is measured to estimate an unknown parameter  $y$ , and the relationship between them is defined by an explicit function

$$y = f(x) \quad (2.12)$$

then

$$\Delta y \approx \frac{dy}{dx} \Delta x$$

So the standard deviation of  $y$  is given by

$$\sigma_y = \frac{dy}{dx} \sigma_x \quad (2.13)$$

in which  $\sigma_x$  is the standard deviation of  $x$ . The variance of  $y$  is then obtained from

$$\sigma_y^2 = \left(\frac{dy}{dx}\right)^2 \sigma_x^2 \quad (2.14)$$



Therefore  $C_y$  is a  $u \times u$  matrix and can be expressed as

$$C_y = \begin{bmatrix} \sigma_{y_1}^2 & \sigma_{y_1 y_2} & \cdots & \sigma_{y_1 y_u} \\ \sigma_{y_2 y_1} & \sigma_{y_2}^2 & \cdots & \sigma_{y_2 y_u} \\ \cdots & \cdots & \cdots & \cdots \\ \sigma_{y_u y_1} & \sigma_{y_u y_2} & \cdots & \sigma_{y_u}^2 \end{bmatrix} \quad (2.20)$$

The variances of the estimated parameters are obtained directly from the corresponding diagonal elements of  $C_y$  and a global precision estimation of the measured elements is generally given by the *trace* of  $C_y$  which is equal to the sum of these diagonal elements. The off-diagonal element  $\sigma_{y_i y_j}$  is connected with the correlation between the parameters  $y_i$  and  $y_j$ . The *correlation coefficient* designated by  $\rho$  is normally used to state the relationship and

$$\rho_{y_i y_j} = \frac{\sigma_{y_i y_j}}{\sigma_{y_i} \sigma_{y_j}} \quad (2.21)$$

Another commonly used error propagation formula is

$$Q_y = J_{yx} Q_x J_{yx}^t \quad (2.22)$$

in which  $Q_x$  and  $Q_y$  are the cofactor matrices of the observations and the unknown parameters respectively. Eq (2.18) and (2.22) are known as *the general laws of propagation of variances and covariances* (Mikhail, 1981).  $C_y$  and  $Q_y$  are two important matrices which are closely related to the quality of the estimated unknown parameters and the measurement system.

In the special case when the functional model is linear, i.e.,

$$y = Ax + B \quad (2.23)$$

in which  $A$  is a  $u \times m$  coefficient matrix and  $B$  is constant vector, the covariance and the cofactor matrices of the unknown parameters will be given by

$$C_y = AC_x A^t \quad (2.24)$$

and

$$Q_y = A Q_x A^t \quad (2.25)$$

### 2.3 The least squares method

In surveying and close range photogrammetry, redundant measurements are always necessary. This means that the number of observation is more than the minimum for a unique solution of the unknown parameters. The reasons for making redundant measurements are: first, the redundant measurements can provide a check on gross errors; second, they can give a more precise evaluation of the unknown parameters than would the minimum number of measurements (Cooper, 1987); and third, statistics are available with the redundant measurements.

Since errors are inevitable in the measurement process, residuals  $v$  are introduced in the observation equations to make up the differences. So Eq (2.5) becomes

$$A\Delta x = b + v \quad (2.26)$$

where  $v = (v_1, v_2, \dots, v_m)^t$  is a vector of residuals for the observations. There are obviously many possible values for  $v_i$ . Many methods exist to give a minimum value using different combinations of residuals. Among them, the least squares method is the most popular one used in surveying and close range photogrammetry.

The general criterion of the least squares method states:

*the sum of the weighted squares of the residuals must be a minimum, i.e.,*

$$\phi = w_1 v_1^2 + w_2 v_2^2 + \dots + w_m v_m^2 = \sum_{i=1}^m w_i v_i^2 = \mathbf{v}' \mathbf{W} \mathbf{v} \rightarrow \min \quad (2.27)$$

in which  $w_1, w_2, \dots, w_m$  are the weights of the corresponding observations. For the uncorrelated observations with equal precision, the criterion of the least squares method becomes

$$\phi = v_1^2 + v_2^2 + \dots + v_m^2 = \sum_{i=1}^m v_i^2 = \mathbf{v}' \mathbf{v} \rightarrow \min \quad (2.28)$$

From Eq (2.26), the residual vector can be derived as

$$\mathbf{v} = \mathbf{A} \Delta \mathbf{x} - \mathbf{b} \quad (2.29)$$

So the sum of the weighted squares of residuals is

$$\begin{aligned} \phi &= (\mathbf{A} \Delta \mathbf{x} - \mathbf{b})' \mathbf{W} (\mathbf{A} \Delta \mathbf{x} - \mathbf{b}) \\ &= \Delta \mathbf{x}' \mathbf{A}' \mathbf{W} \mathbf{A} \Delta \mathbf{x} - \Delta \mathbf{x}' \mathbf{A}' \mathbf{W} \mathbf{b} - \mathbf{b}' \mathbf{W} \mathbf{A} \Delta \mathbf{x} + \mathbf{b}' \mathbf{W} \mathbf{b} \end{aligned} \quad (2.30)$$

To minimise  $\phi$ , its partial derivatives with respect to  $\Delta \mathbf{x}$  are derived and equated to zero, i.e.,

$$\frac{\partial \phi}{\partial \Delta \mathbf{x}} = 2 \Delta \mathbf{x}' \mathbf{A}' \mathbf{W} \mathbf{A} - 2 \mathbf{b}' \mathbf{W} \mathbf{A} = 0 \quad (2.31)$$

So

$$\Delta \mathbf{x}' \mathbf{A}' \mathbf{W} \mathbf{A} = \mathbf{b}' \mathbf{W} \mathbf{A} \quad (2.32)$$

Transposing both sides of the equation gives

$$\mathbf{A}' \mathbf{W} \mathbf{A} \Delta \mathbf{x} = \mathbf{A}' \mathbf{W} \mathbf{b} \quad (2.33)$$

or

$$N\Delta\mathbf{x} = \mathbf{A}'\mathbf{W}\mathbf{b} \quad (2.34)$$

where  $N = \mathbf{A}'\mathbf{W}\mathbf{A}$  is a  $u \times u$  coefficient matrix and  $\mathbf{A}$  is the often called *design matrix* of the measurement network. If  $N$  is of full rank,  $\Delta\mathbf{x}$  can be solved as

$$\begin{aligned} \Delta\mathbf{x} &= N^{-1}\mathbf{A}'\mathbf{W}\mathbf{b} \\ &= N^{-1}\mathbf{t} \end{aligned} \quad (2.35)$$

where  $\mathbf{t} = \mathbf{A}'\mathbf{W}\mathbf{b}$ . By computing the inverse of the coefficient matrix  $N$  and some products of matrices, all the corrections can be determined and the updated unknown parameters is obtained by

$$\mathbf{x} = \mathbf{x}^0 + \Delta\mathbf{x} \quad (2.36)$$

Because the higher order terms are omitted in the linearization, the least squares solution requires an iterative procedure for the non-linear functional model. From the updated unknown parameters the design matrix  $\mathbf{A}$  is reconstructed and new corrections are calculated again for the next adjustment. This procedure is repeated until a stop criterion is met. The starting values of the unknown parameters must be realistic and reasonably close (i.e. close enough for the assumption of linearity to be valid) to the final solution. Otherwise the iterative process may diverge.

For a linear functional model, the least squares estimates can be obtained directly, i.e.,

$$\mathbf{x} = N^{-1}\mathbf{A}'\mathbf{W}\mathbf{b} \quad (2.37)$$

As mentioned in section 2.2, the precision of the estimated unknown parameters is evaluated from their covariance matrix. By the general law of propagation of the covariance, from Eq (2.35) and Eq (2.36), the cofactor matrix of the unknown parameters is given by

$$\mathbf{Q}_x = \mathbf{Q}_{\Delta x} = \mathbf{N}^{-1} \mathbf{A}' \mathbf{W} \mathbf{Q}_b (\mathbf{N}^{-1} \mathbf{A}' \mathbf{W})' \quad (2.38)$$

Since  $\mathbf{b} = \mathbf{I} - \mathbf{f}(\mathbf{x}^0)$  and  $\mathbf{x}^0$  are non-stochastic,

$$\mathbf{Q}_b = \mathbf{Q}_I = \mathbf{W}_I^{-1} \quad (2.39)$$

Therefore

$$\mathbf{Q}_x = \mathbf{N}^{-1} \mathbf{A}' \mathbf{W}_I \mathbf{W}_I^{-1} \mathbf{W}_I \mathbf{A} \mathbf{N}^{-1} \quad (2.40)$$

So

$$\mathbf{Q}_x = \mathbf{N}^{-1} = (\mathbf{A}' \mathbf{W}_I \mathbf{A})^{-1} \quad (2.41)$$

and

$$\mathbf{C}_x = \sigma_0^2 \mathbf{Q}_x = \sigma_0^2 (\mathbf{A}' \mathbf{W}_I \mathbf{A})^{-1} \quad (2.42a)$$

If  $\sigma_0$  is not known beforehand, the *a posteriori* reference variance can be calculated by

$\hat{\sigma}_0^2 = \frac{\mathbf{v}' \mathbf{W} \mathbf{v}}{r}$  (Mikhail 1976), in which  $r$  is the number of degrees of freedom. Therefore

$$\mathbf{C}_x = \hat{\sigma}_0^2 \mathbf{Q}_x = \hat{\sigma}_0^2 (\mathbf{A}' \mathbf{W}_I \mathbf{A})^{-1} \quad (2.42b)$$

It is generally accepted that Gauss was the first to use least squares at the end of eighteenth century. A historical background and justification can be found in Cross (1983). Two properties of the least squares adjustment are

- (i) it is unbiased; and
- (ii) it has a minimum trace of the covariance matrix of the parameters and a minimum variance of derived parameters.

So the least squares estimate is known as the BLUE (Best Linear Unbiased Estimate). There are a number of reasons why least squares adjustment is widely used (Cross, 1983):

- (i) the method is extremely easy to apply because it yields a linear set of normal equations;
- (ii) the solution is unique, i.e., there is only one solution to a given problem;
- (iii) it is, generally speaking, “unobjectionable”: it is very difficult to form an argument against least squares in favour of some other procedure;
- (iv) the method leads to an easy quantitative assessment of quality, e.g., via the covariance matrix; and
- (v) it is a general method that can be applied to any problem.

As a result of these, the least squares estimation (LSE) has been applied increasingly in survey and close range photogrammetry. The method will continue to be used until an alternative procedure, more economical and more practical, is devised (Cooper 1987). Obviously, this alternative has not been found yet.

Traditionally in surveying and close range photogrammetry all the observations are used at the same time to estimate all the unknown parameters simultaneously. This simultaneous LSE has been proved to be effective and rigorous. Problems may arise when large number of unknown parameters need to be estimated by the simultaneous LSE if speed and memory are considered, since inverting large matrix is very expensive in terms of speed and memory. For instance, in close range photogrammetry, if 20 images are used to measure 200 object points by the bundle adjustment, which is basically a simultaneous LSE process, there will be 600 unknown parameters for the object points and 120 unknown parameters for the cameras, so a total of 720 unknown parameters need to be estimated. The size of the coefficient matrix  $N$  is  $720 \times 720$ . Inverting such a large matrix requires significant resources by computers. The computational complexities to computing the inverse of a matrix are:  $O(u^3)$  and  $O(u^2)$  for time and memory respectively (Bunch & Parley, 1971), where  $u \times u$  is the size of  $N$ .

In some applications where time and memory are critical, the conventional methods of least squares estimation need to be improved.

It may be helpful to divide the simultaneous least squares estimation into parts to reduce both time and memory. One strategy is to divide the observations and the other is to divided the unknown parameters. The former leads to *sequential* LSE and the latter leads to *iterative* LSE. A combination of both leads to *step-by-step* LSE or the *Helmert-Wolf* method.

## 2.4 Sequential LSE

Sequential LSE has been used in photogrammetry since the 1960's (Brown 1960 & 1964; Gruen 1978 & 1985; Shortis 1980; Gruen & Kersten 1992, Edmundson & Fraser 1995). It is a technique of division which puts the observations in groups and uses them sequentially to estimate the unknown parameters. Sequential LSE is useful in the situations where more observations are added or removed to estimate the parameters which have been estimated from an initial set of observations. It is also named *phased* LSE. From each phase of the estimation the unknown parameters and their covariance matrix are kept for the next phase, while the observations can be discarded. This is particularly useful for the computers with limited memory storage. The results from the sequential LSE are identical to those that obtained from the simultaneous LSE where all the observations are involved at the same time.

If two sets of observations  $p$  and  $q$  with the weight matrices  $W_p$  and  $W_q$  have been taken to estimate a same set of unknown parameters, the normal observation equations can be expressed as

$$\begin{bmatrix} A_p \\ A_q \end{bmatrix} \Delta x = \begin{bmatrix} b_p \\ b_q \end{bmatrix} \quad (2.66)$$

From the first set of observations  $p$ , the unknown parameters are estimated as (if  $A_p$  is of full rank)

$$\begin{aligned}\Delta \mathbf{x}_p &= (\mathbf{A}_p' \mathbf{W}_p \mathbf{A}_p)^{-1} \mathbf{A}_p' \mathbf{W}_p \mathbf{b}_p \\ &= \mathbf{N}_p^{-1} \mathbf{t}_p\end{aligned}\quad (2.67)$$

and

$$\mathbf{Q}_x = (\mathbf{A}_p' \mathbf{W}_p \mathbf{A}_p)^{-1} \quad (2.68)$$

When a second set of observations  $q$  is obtained, it can be added to the resultant equation (2.67) to update the estimates of the parameters. The extended observation equations become

$$\begin{bmatrix} \mathbf{I} \\ \mathbf{A}_q \end{bmatrix} \Delta \mathbf{x}_{p+q} = \begin{bmatrix} \mathbf{N}_p^{-1} \mathbf{t}_p \\ \mathbf{b}_q \end{bmatrix} \quad (2.69)$$

or

$$\mathbf{A}' \Delta \mathbf{x}_{p+q} = \mathbf{b}' \quad (2.70)$$

The extended weight matrix for  $\mathbf{b}'$  is given by

$$\mathbf{W}_{b'} = \begin{bmatrix} \mathbf{N}_p & \\ & \mathbf{W}_q \end{bmatrix} \quad (2.71)$$

Therefore

$$\begin{aligned}\Delta \mathbf{x}_{p+q} &= (\mathbf{A}' \mathbf{W}_{b'} \mathbf{A}')^{-1} \mathbf{A}' \mathbf{W}_{b'} \mathbf{b}' \\ &= (\mathbf{N}_p + \mathbf{N}_q)^{-1} [\mathbf{t}_p + \mathbf{t}_q]\end{aligned}\quad (2.72)$$

and

$$\mathbf{Q}_x = (\mathbf{N}_p + \mathbf{N}_q)^{-1} \quad (2.73)$$

These results are identical with that obtained by the simultaneous solution from Eq (2.66). The major advantage of sequential LSE is that after each stage of the estimation the observations can be discarded, and the results (the parameters and their cofactor matrix) retained for the next stage. The number of the unknown parameters need not be constant during the sequential LSE process. Additional parameters can be included by a small extension (Shortis 1980, Cooper 1987).

It is noticed that Eq (2.72) and (2.73) have no advantages in computing time since the size of  $N_q$  is still  $u \times u$  even if only a few observations are added. Therefore the size of the matrix to be inverted remains unchanged for each sequence. However this can be improved by using a special technique of matrix algebra (Cross 1983, Cooper 1987), i.e., if

$$P = U \pm RST$$

then

$$P^{-1} = U^{-1} \mp U^{-1}R(S^{-1} \pm TU^{-1}R)^{-1}TU^{-1} \quad (2.74)$$

provided that  $P$ ,  $U$  and  $S$  are non-singular. Now rearrange Eq (2.72) as

$$\Delta x_{p+q} = (N_p + A_q^t W_q A_q)^{-1} (t_p + t_q) \quad (2.75)$$

applying Eq (2.74) gives

$$\Delta x_{p+q} = (N_p^{-1} - N_p^{-1} A_q^t (W_q^{-1} + A_q N_p^{-1} A_q^t)^{-1} A_q N_p^{-1}) (t_p + t_q) \quad (2.76)$$

Let 
$$K_{pq} = N_p^{-1} A_q^t (W_q^{-1} + A_q N_p^{-1} A_q^t)^{-1} A_q N_p^{-1}$$

So

$$\Delta x_{p+q} = (N_p^{-1} - K_{pq}) (t_p + t_q) \quad (2.77)$$

Since  $N_p^{-1}$  has been obtained from the previous sequence, for the additional observations only the inverse of the matrix  $(W_q^{-1} + A_q N_p^{-1} A_q^t)$  needs to be calculated and the size of it is  $q \times q$ , where  $q$  is the number of new observations. So the sequential method is very efficient when only a few observations are added during each sequence. However if the number of new observations approaches the number of parameters it is more efficient to carry out a new simultaneous LSE in the usual way (Cross, 1983).

The sequential LSE can also be used in the situations where observations are removed rather than added. This can be done by changing the corresponding signs in Eqs (2.74) to (2.77).

There is a restriction for the sequential LSE on the number of observations, i.e., the first sequence must have enough observations to determine the unknown parameters. Furthermore, the process of the first sequence is still a full simultaneous LSE. Therefore the calculation of the inverse of a large matrix (size of  $u \times u$ ) is still inevitable.

Another problem with the sequential method is that the starting values of the unknown parameters must be very close to the final results. If iterations are required many of the advantages will be lost (Cross, 1983).

Sequential LSE may be useful in close range photogrammetry for camera calibration. The camera interior parameters can be updated after each measurement and the knowledge accumulated for the next measurement. Theoretically, the more a camera is used, the better the estimation of its interior parameters provided the blunders are avoided and the camera is not changed physically.

## 2.5 Iterative LSE

As it is used for solving linear algebraic equations, the iterative method can also be applied to LSE. Before iterative LSE is discussed, iterative solution for linear equations is briefly reviewed. References can be found in many *numerical analysis* text books (Traub 1964; Jacoby 1972; Hageman & Young 1981; Phillips & Cornelius 1986)

The basic principle of the iterative methods is described as follows. Suppose a set of linear equations

$$Ax = b \quad (2.78)$$

is to be solved.  $A$  is a  $u \times u$  non-singular matrix with no zero diagonal elements. The matrix  $A$  can be written as

$$A = D + L + U \quad (2.79)$$

where  $D$ ,  $L$  and  $U$  are diagonal, lower triangular and upper triangular parts of  $A$  respectively. If  $A$  is expressed as

$$A = \begin{bmatrix} a_{11} & a_{12} & \cdots & a_{1u} \\ a_{21} & a_{22} & \cdots & a_{2u} \\ \cdots & \cdots & \cdots & \cdots \\ a_{u1} & a_{u2} & \cdots & a_{uu} \end{bmatrix} \quad (2.80)$$

Then

$$D = \begin{bmatrix} a_{11} & 0 & \cdots & 0 \\ 0 & a_{22} & \cdots & 0 \\ \cdots & \cdots & \cdots & \cdots \\ 0 & 0 & \cdots & a_{uu} \end{bmatrix}$$

$$U = \begin{bmatrix} 0 & a_{12} & \cdots & a_{1u} \\ 0 & 0 & \cdots & a_{2u} \\ \cdots & \cdots & \cdots & \cdots \\ 0 & 0 & \cdots & 0 \end{bmatrix}$$

$$L = \begin{bmatrix} 0 & 0 & \cdots & 0 \\ a_{21} & 0 & \cdots & 0 \\ \cdots & \cdots & \cdots & \cdots \\ a_{u1} & a_{u2} & \cdots & 0 \end{bmatrix}$$

Rearranging Eq (2.78) gives

$$Dx = b - (L + U)x \tag{2.81}$$

So

$$x^{[k+1]} = D^{-1}(b - (L + U)x^{[k]}) \tag{2.82}$$

or

$$x_i^{[k+1]} = \frac{1}{a_{ii}} \left( b_i - \sum_{\substack{j=1 \\ j \neq i}}^n a_{ij} x_j^{[k]} \right) \tag{2.83}$$

( $i = 1, 2, \dots, u$ )

where the superscripts  $[k]$  and  $[k+1]$  denote the  $k$ th and  $(k+1)$ st iterations. This is called the *Jacobi method*. As usual with iterative methods, starting values of the unknown parameters are required. If no prior knowledge is available, it is conventional to start with  $x_i^{[0]} = 0$  on the right hand side of Eq (2.83) to obtain  $x_i^{[1]}$ . The iterative process can then be repeated until all the corrections are less than a given tolerance.

In the Jacobi method, the corrected values of the unknown parameters are not used until all of the parameters are solved. It is better to use the corrected values for computing other parameters in the same iteration since the new values are better than the old in

most cases. When this is done, the procedure is called the *Gauss-Seidel method*. It is accomplished by rearranging Eq (2.78) as

$$(D + L)x = b - Ux \quad (2.84)$$

So the iteration becomes

$$x^{[k+1]} = (D + L)^{-1} (b - Ux^{[k]}) \quad (2.85)$$

or

$$x_i^{[k+1]} = \frac{1}{a_{ii}} \left( b_i - \sum_{j=1}^{i-1} a_{ij} x_j^{[k+1]} - \sum_{j=i+1}^n a_{ij} x_j^{[k]} \right) \quad (2.86)$$

$$(i = 1, 2, \dots, u)$$

Normally, the rate of convergence of the Gauss-Seidel method is faster than that of the Jacobi method. It can be proved that the iterations (both Jacobi method and Gauss-Seidel method) will converge for any starting values when the system is *diagonally dominant*, i.e., each diagonal element is larger in magnitude than the sum of the magnitudes of the off-diagonal elements in the row. Mathematically, it is expressed as

$$|a_{ii}| > \sum_{\substack{j=1 \\ j \neq i}}^n |a_{ij}| \quad (2.87)$$

$$(i = 1, 2, \dots, u)$$

This convergence condition is a sufficient condition, which means, if the condition holds, the iteration always converges. However the iteration may converge even if the condition is violated. The greater the left hand side is compared with the right in Eq (2.87), the faster is the convergence.

The third iterative method is an extension of the Gauss-Seidel method. It is achieved by rearranging Eq (2.86), i.e.,

$$x_i^{l_{k+1}} = x_i^{l_{k1}} + \frac{1}{a_{ii}} \left( b_i - \sum_{j=1}^{i-1} a_{ij} x_j^{l_{k+1}} - \sum_{j=i}^n a_{ij} x_j^{l_{k1}} \right) \quad (2.88)$$

$$(i = 1, 2, \dots, u)$$

The second term on the right hand side represents the correction made to  $x_i^{l_{k1}}$  in order to calculate  $x_i^{l_{k+1}}$ . If the correction is multiplied by a factor  $\omega$ , the iteration becomes

$$x_i^{l_{k+1}} = x_i^{l_{k1}} + \frac{\omega}{a_{ii}} \left( b_i - \sum_{j=1}^{i-1} a_{ij} x_j^{l_{k+1}} - \sum_{j=i}^n a_{ij} x_j^{l_{k1}} \right) \quad (2.89)$$

$$(i = 1, 2, \dots, u)$$

With the factor  $\omega$ , the iterative process is relaxed, and when a proper  $\omega$  is selected, the convergent rate of the iteration will be accelerated. The factor  $\omega$  is called relaxation factor. If  $\omega > 1$  (over relaxation), then a larger than normal correction is taken. This is useful when the Gauss-Seidel method converges monotonically, i.e., the unknown parameters move in one direction towards the final solution. If  $\omega < 1$  (under relaxation), then a smaller than normal correction is taken. This is useful when the Gauss-Seidel iterates oscillate, i.e., the unknown parameters fluctuate around the final results. In practice,  $\omega > 1$  is mostly used. So the method is known as *successive over-relaxation* method or *SOR* method

It has been proved that a necessary condition for convergence is that the relaxation factor  $\omega$  should lie between 0 and 2, i.e.,

$$0 < \omega < 2 \quad (2.90)$$

If the coefficient matrix  $A$  is symmetric and positive definite, this condition becomes both necessary and sufficient.

Iterative methods have also been used in LSE process (Brown 1976; Kok 1984; Marel 1988). This iteration is known as *inner iteration*. For the non-linear problem, *outer iteration* is required for LSE. The iterative LSE method was used by Brown (Brown 1976) as the indirect method of Block Successive Over Relaxation (BSOR).

Since the coefficient matrix  $N$  of the least squares estimation is or can be made to be symmetric and positive definite, the three iterative methods discussed will converge with any starting values for inner iteration. The corrections of the unknown parameters are normally around zero provided that the starting values of the outer iteration are reasonably close to the final results, so the inner iteration can start with  $\Delta x^{(0)} = 0$ .

Iterative LSE has the advantage over the simultaneous solution that it avoids direct calculation of the inverse of the coefficient matrix  $N^{-1}$  which is the major cost of the least squares estimation in terms of time and storage, especially when the number of the unknown parameters is very large and  $N$  is sparse. With the iterative method there is no fill-in problem (Kok 1984). The coefficient matrix  $N$  remains unchanged in the inner iterations when it is used repeatedly to compute improved solutions and residuals. For a non-linear problem, the outer iteration will change  $N$ , but not its structure which could be very sparse. By using inner iteration, the storage required is reduced significantly, whilst the speed may not always be fast. Actually, in many cases, the speed of the iterative LSE is slower than that of the simultaneous solution because too many iterations are needed for the inner iteration (Marel 1989). Another disadvantage of the iterative LSE is that full covariance matrix is not available (Brown 1976).

## 2.6 Step-by-step LSE

Step-by-step LSE is a technique of partitioning in which both unknown parameters and observations are divided into parts (Cross 1983, Cooper 1987). It is useful in the situations where parts of the parameters are not required for the purpose in hand but

have to be included in the observation equations. For instance, in close range photogrammetry, the 3D coordinates of the spatial object points are required, whilst the values of the camera parameters may not be needed in some cases, but have to be treated as unknowns in the bundle adjustment. In this case, the observations can be divided into parts and the parameters can be adjusted in steps. The results obtained by the step-by-step method are the same as those obtained by the simultaneous solution. The advantage of the step-by-step method over the simultaneous method is that those parameters not required are not estimated. The size of the matrices to be inverted is reduced.

As with the sequential method, the step-by-step method also requires that the starting values of the unknown parameters are very close to their final results. Otherwise, the advantages of the method will be lost if iterations are needed (Cross, 1983).

## 2.7 Datum and constraints

In the foregoing discussion of the LSE it is assumed that the coefficient matrix  $N$  ( $=A'WA$ ) is of full rank or non-singular, so the Cayley inverse of it exists. Therefore the unknown parameters can be estimated by the normal least squares process. However it is often the case in surveying and close range photogrammetry that the unknown parameters are not estimable by the measured elements because the design matrix  $A$  suffers from column rank defects, therefore the coefficient matrix  $N$  is singular, its Cayley inverse does not exist, and the normal LSE cannot be used. The reason for the column rank defects is that the measured elements do not include enough or any information to define a datum. This assumes that the row rank defects have been eliminated by proper design of the measurements.

### 2.7.1 Datum

A datum is a reference coordinate system, which is usually defined by a number of spatial control points. In surveying and close range photogrammetry, the Cartesian

coordinate system which is a right-hand set of axes ( $X, Y, Z$ ), is commonly used to describe the coordinate system for the measurement network. The datum problem arises when measured elements do not include enough datum information. For instance, in close range photogrammetry the only observations are often the 2D coordinates on the image planes, no observed spatial 3D information is involved in the functional model. Hence, the datum is undefined. The consequence is that the design matrix has column defects and the coefficient matrix  $N$  is singular, so the 3D coordinates of the object points are not obtainable.

The rank defect of the coefficient matrix  $N$  is equal to the number of datum elements undefined. Generally, four datum elements need to be defined for 2D positioning (one scale element, two position elements and one rotation element) and seven datum elements need to be defined for 3D spatial positioning (one scale element, three position elements and three rotation elements).

### 2.7.2 Constraints

The datum problem can be solved by including the spatial control points or applying constraints. In aerial photogrammetry the datum problem is always solved since the ground control points are in place (Karara, 1989). In surveying and close range photogrammetry constraints are sometimes applied in the least squares estimation to remove the datum defects. These constraints are described by a set of constraint equations. Together with the observation equations the unknown parameters can then be estimated. The constraint equations can generally be expressed as

$$g(x) = c \quad (2.91)$$

with associated weight matrix  $W_g$ . The constraint equations are normally non-linear. After linearization they become

$$G\Delta x = b_g \quad (2.92)$$

in which

$$G = \left(\frac{\partial g}{\partial x}\right)^0 \quad \text{and} \quad b_g = c - g(x^0)$$

Therefore the augmented linearised observation equations are expressed as

$$\begin{bmatrix} A \\ G \end{bmatrix} \Delta x = \begin{bmatrix} b \\ b_g \end{bmatrix} + \begin{bmatrix} v \\ v_g \end{bmatrix} \quad (2.93)$$

with associated weight matrix

$$W = \begin{bmatrix} W_l & \\ & W_g \end{bmatrix} \quad (2.94)$$

supposing that the observations and the constraints are independent of each other. Eq (2.93) can be solved by introducing a vector of Lagrangian multipliers (Cooper 1987), so the full set of normal equations for estimated parameters  $\Delta x$  and Lagrangian multipliers  $k$  become

$$\begin{bmatrix} A'W_lA & G \\ G' & 0 \end{bmatrix} \begin{bmatrix} \Delta x \\ k \end{bmatrix} = \begin{bmatrix} A'W_l b \\ b_g \end{bmatrix} \quad (2.95)$$

The augmented coefficient matrix becomes non-singular with  $G'$  and  $G$  involved. So unknown parameters  $\Delta x$  and Lagrangian multipliers  $k$  can be estimated by

$$\begin{bmatrix} \Delta x \\ k \end{bmatrix} = \begin{bmatrix} A'W_lA & G \\ G' & 0 \end{bmatrix}^{-1} \begin{bmatrix} A'W_l b \\ b_g \end{bmatrix} \quad (2.96)$$

There are two disadvantages of this process. First the dimension of the matrix to be inverted is increased, and second the presence of zeros on the leading diagonal makes

the use of algorithms for computing the inverse of a symmetric positive definite matrix invalid. To avoid these, an alternative process is considered.

If the constraint equations in Eq (2.94) are considered as the additional observation equations,  $\Delta\mathbf{x}$  can be estimated by the LSE of the augmented observation equations, i.e.,

$$\Delta\mathbf{x} = \left( \begin{bmatrix} \mathbf{A} \\ \mathbf{G} \end{bmatrix}^t \mathbf{W} \begin{bmatrix} \mathbf{A} \\ \mathbf{G} \end{bmatrix} \right)^{-1} \begin{bmatrix} \mathbf{A} \\ \mathbf{G} \end{bmatrix}^t \mathbf{W} \begin{bmatrix} \mathbf{b} \\ \mathbf{b}_g \end{bmatrix} \quad (2.97)$$

which gives

$$\Delta\mathbf{x} = (\mathbf{A}'\mathbf{W}_l\mathbf{A} + \mathbf{G}'\mathbf{W}_g\mathbf{G})^{-1} (\mathbf{A}'\mathbf{W}_l\mathbf{b} + \mathbf{G}'\mathbf{W}_g\mathbf{b}_g) \quad (2.98)$$

Let  $\mathbf{N}_g = (\mathbf{A}'\mathbf{W}_l\mathbf{A} + \mathbf{G}'\mathbf{W}_g\mathbf{G})$  and  $\mathbf{B}_g = (\mathbf{A}'\mathbf{W}_l\mathbf{b} + \mathbf{G}'\mathbf{W}_g\mathbf{b}_g)$ , therefore

$$\Delta\mathbf{x} = \mathbf{N}_g^{-1} \mathbf{B}_g \quad (2.99)$$

The addition of  $\mathbf{G}'\mathbf{W}_g\mathbf{G}$  to  $\mathbf{A}'\mathbf{W}_l\mathbf{A}$  will remove its rank defects so that the unknown parameters can be estimated by the normal least squares adjustment. Since the size of the matrix  $\mathbf{N}_g$  remains unchanged and it is still a symmetric positive-definite matrix, fast algorithms for computing the inverse of this kind of matrix can still be used.

There are various ways to apply constraints in order to solve the datum problem. For instance, constraints can be applied by fixing values of some coordinates of the object points. This is often the case in aerial photogrammetry where ground control points are involved in the LSE process. These control points can also be considered as the previously estimated results with their cofactor matrix. However, from the point of view of an optimal reference system for an optimum form of the cofactor matrix  $\mathbf{Q}_x$  (Fraser 1984), these two constraints may not be ideal. LSE with inner constraints, which is a free-network adjustment, will yield an optimum mean object point precision and is widely used in surveying and close range photogrammetry. More descriptions on datum

and inner constraints have been given by (Granshaw 1980; Fraser 1984; Caspary 1987; Cooper 1987; Dermanis 1994).

## 2.8 LSE with constraints

### 2.8.1 LSE with inner constraints

Inner constraints can be applied to position, rotation and scale by reference to the centroid of all the object points or a subset of them defined by their starting values (Cooper, 1987). For a 2D network, the constraint equations have the form

$$\begin{bmatrix} 1 & 0 & 1 & 0 & \cdots & 1 & 0 \\ 0 & 1 & 0 & 1 & \cdots & 0 & 1 \\ y_1 & -x_1 & y_2 & -x_2 & \cdots & y_n & -x_n \\ x_1 & y_1 & x_2 & y_2 & \cdots & x_n & y_n \end{bmatrix} \begin{bmatrix} \Delta x_1 \\ \Delta y_1 \\ \Delta x_2 \\ \Delta y_2 \\ \vdots \\ \Delta x_n \\ \Delta y_n \end{bmatrix} = G\Delta x = b_g = \begin{bmatrix} 0 \\ 0 \\ 0 \\ 0 \\ \vdots \\ 0 \\ 0 \end{bmatrix} \quad (2.100)$$

The first two equations provide positional constraints, the third equation provides rotational constraint and the fourth equation provides scale constraint. For a 3D network, the constraint equations have the form

$$\begin{bmatrix} 1 & 0 & 0 & 1 & 0 & 0 & \cdots & 1 & 0 & 0 \\ 0 & 1 & 0 & 0 & 1 & 0 & \cdots & 0 & 1 & 0 \\ 0 & 0 & 1 & 0 & 0 & 1 & \cdots & 0 & 0 & 1 \\ 0 & z_1 & -y_1 & 0 & z_2 & -y_2 & \cdots & 0 & z_n & -y_n \\ -z_1 & 0 & x_1 & -z_2 & 0 & x_2 & \cdots & -z_n & 0 & x_n \\ y_1 & -x_1 & 0 & y_2 & -x_2 & 0 & \cdots & y_n & -x_n & 0 \\ x_1 & y_1 & z_1 & x_2 & y_2 & z_2 & \cdots & x_n & y_n & z_n \end{bmatrix} \begin{bmatrix} \Delta x_1 \\ \Delta y_1 \\ \Delta z_1 \\ \Delta x_2 \\ \Delta y_2 \\ \Delta z_2 \\ \vdots \\ \Delta x_n \\ \Delta y_n \\ \Delta z_n \end{bmatrix} = G\Delta x = b_g = \begin{bmatrix} 0 \\ 0 \\ 0 \\ 0 \\ 0 \\ 0 \\ \vdots \\ 0 \\ 0 \\ 0 \end{bmatrix} \quad (2.101)$$

The first three equations provide positional constraints, the next three equations provide rotational constraint and the last equation provides scale constraint.

Since  $b_g = 0$ , from Eq (2.99) the corrections of the unknown parameters can be estimated by

$$\Delta x = N_g^{-1} A' W_l b \quad (2.102)$$

By the general law of propagation of the cofactor matrices, the cofactor matrix of the estimated parameters is given by

$$\begin{aligned} Q_x &= N_g^{-1} A' W_l Q_b (N_g^{-1} A' W_l)' \\ &= N_g^{-1} A' W_l A N_g^{-1} \end{aligned} \quad (2.103)$$

in which

$$N_g = (A' W_l A + G' W_g G) \quad (2.104)$$

In the above equation,  $W_g$  is the weight matrix which reflects the strength of the constraints. It is interesting to know that changing of  $W_g$  will not influence the estimated results due to the fact that  $b_g = 0$ . To simplify the computation,  $W_g$  is usually set to a unit matrix, i.e.  $W_g = I$ . Therefore the unknown parameters and the cofactor matrix are estimated by

$$N_g = (A' W_l A + G' G) \quad (2.105)$$

$$\Delta x = (A' W_l A + G' G)^{-1} A' W_l b \quad (2.106)$$

$$Q_x = (A' W_l A + G' G)^{-1} A' W_l A (A' W_l A + G' G)^{-1} \quad (2.107)$$

It is important to point out that the structure of the coefficient matrix will change with the addition of  $G'G$ . This may spoil the special structure of the coefficient matrix (e.g.

the block diagonal matrix in close range photogrammetry), which could be made use of for optimisation in the LSE process.

The coordinates in the matrix  $\mathbf{G}$  are initially starting values. These starting values are estimated approximately by other means. After each iteration  $\mathbf{G}$  should be updated by the corrected coordinates. The results of the unknown parameters (the coordinates of the object points) are closely related to these starting values. Different starting values lead to different results but the geometric shape of the network will remain unchanged. So the datum of the results is actually arbitrary depending on choice of the starting values. However, the estimated coordinates and their cofactor matrix can always be transformed to a given reference datum whenever required.

The cofactor matrix gives a precision evaluation of the estimated parameters. However, in some cases the cofactor matrix may not be necessary for the intermediate parameters. When these intermediate parameters are used to estimate other parameters the inverse of the cofactor matrix (the weight matrix) is more useful. For instance, if these parameters (object point coordinates) are used as previously estimated coordinates to solve the datum problem, the weight matrix will be used. Fortunately the weight matrix of the estimated parameters can be obtained from the design matrix directly, i.e.,

$$\mathbf{W}_x = \mathbf{Q}_x^{-1} = \mathbf{A}'\mathbf{W}_l\mathbf{A} \quad (2.108)$$

Matrix  $\mathbf{A}$  is datum related, so the cofactor matrix  $\mathbf{Q}_x$  and the weight matrix  $\mathbf{W}_x$  are datum dependent. Change of datum will cause  $\mathbf{Q}_x$  and  $\mathbf{W}_x$  to change. This will be discussed in Chapter 6. For the final results Eq (2.107) should be used to calculate the cofactor matrix  $\mathbf{Q}_x$  for the evaluation of the precision of the estimated coordinates.

### 2.8.2 LSE with previously estimated coordinates

Constraints can also be applied by adding extra observation equations which describe the results of previously estimated coordinates (control points) with their cofactor matrix. The minimum number of the constraint equations required depends on the deficiency of the design matrix  $A$ . If no datum information is obtained from the observations, the number of rank defects of  $A$  is seven in the 3D case, therefore at least seven constraint equations need to be added. Suppose the first  $p$  coordinates ( $x_1, x_2, \dots, x_p$ ) have been estimated previously with the weight matrix  $W_g$ , the constraint equations have the form

$$\begin{bmatrix} 1 & 0 & \dots & 0 \\ 0 & 1 & \dots & 0 \\ \dots & \dots & \dots & \dots \\ 0 & 0 & \dots & 1 \end{bmatrix} \begin{bmatrix} x_1 \\ x_2 \\ \vdots \\ x_p \end{bmatrix} = \begin{bmatrix} x_1^0 \\ x_2^0 \\ \vdots \\ x_p^0 \end{bmatrix} \tag{2.109}$$

in which  $(x_1^0, x_2^0, \dots, x_p^0)$  are previously estimated coordinates with associated weight matrix  $W_g$ . After Linearization Eq (2.109) become

$$\begin{bmatrix} 1 & 0 & \dots & 0 \\ 0 & 1 & \dots & 0 \\ \dots & \dots & \dots & \dots \\ 0 & 0 & \dots & 1 \end{bmatrix} \begin{bmatrix} \Delta x_1 \\ \Delta x_2 \\ \vdots \\ \Delta x_p \end{bmatrix} = \begin{bmatrix} x_1^0 - x_1 \\ x_2^0 - x_2 \\ \vdots \\ x_p^0 - x_p \end{bmatrix} \tag{2.110}$$

or

$$\begin{bmatrix} & & & & \Delta x_1 \\ & & & & \Delta x_2 \\ & & & & \vdots \\ 1 & 0 & \dots & 0 & 0 & 0 & \dots & 0 \\ 0 & 1 & \dots & 0 & 0 & 0 & \dots & 0 \\ \dots & \dots \\ 0 & 0 & \dots & 1 & 0 & 0 & \dots & 0 \\ & & & & \Delta x_{p+1} \\ & & & & \Delta x_{p+2} \\ & & & & \vdots \\ & & & & \Delta x_n \end{bmatrix} = \begin{bmatrix} x_1^0 - x_1 \\ x_2^0 - x_2 \\ \vdots \\ x_p^0 - x_p \end{bmatrix} \tag{2.111}$$

So

$$\mathbf{G} = \begin{bmatrix} \mathbf{I}_{p \times p} & \mathbf{0}_{p \times (n-p)} \end{bmatrix}_{p \times n} \quad (2.112)$$

and

$$\mathbf{b}_g = \begin{bmatrix} x_1^0 - x_1 \\ x_2^0 - x_2 \\ \vdots \\ x_p^0 - x_p \end{bmatrix} \quad (2.113)$$

From Eq (2.99), the corrections of the unknown parameters are estimated, in which

$$\begin{aligned} \mathbf{N}_g &= \mathbf{A}'\mathbf{W}_l\mathbf{A} + \mathbf{G}'\mathbf{W}_g\mathbf{G} \\ &= \mathbf{A}'\mathbf{W}_l\mathbf{A} + \mathbf{W}_g' \end{aligned} \quad (2.114)$$

and

$$\begin{aligned} \mathbf{B}_g &= \mathbf{A}'\mathbf{W}_l\mathbf{b} + \mathbf{G}'\mathbf{W}_g\mathbf{b}_g \\ &= \mathbf{A}'\mathbf{W}_l\mathbf{b} + \mathbf{W}_g''\mathbf{b}_g \end{aligned} \quad (2.115)$$

where

$$\mathbf{W}_g' = \begin{bmatrix} \mathbf{W}_g & \mathbf{0} \\ \mathbf{0} & \mathbf{0} \end{bmatrix}_{n \times n} \quad \text{and} \quad \mathbf{W}_g'' = \begin{bmatrix} \mathbf{W}_g \\ \mathbf{0} \end{bmatrix}_{n \times p}$$

The addition of  $\mathbf{W}_g$  to the top-left corner of the original coefficient matrix  $\mathbf{A}'\mathbf{W}_l\mathbf{A}$  will remove its rank defects and make the matrix  $\mathbf{N}_g$  non-singular so that the estimates of the parameters are obtainable. The cofactor matrix can be obtained from

$$\begin{aligned} \mathbf{Q}_x &= \mathbf{N}_g^{-1}\mathbf{Q}_{B_g}\mathbf{N}_g^{-1} \\ &= \mathbf{N}_g^{-1}\mathbf{A}'\mathbf{W}_l\mathbf{Q}_b\mathbf{W}_l\mathbf{A}\mathbf{N}_g^{-1} + \mathbf{N}_g^{-1}\mathbf{W}_g''\mathbf{Q}_g\mathbf{W}_g''\mathbf{N}_g^{-1} \end{aligned} \quad (2.116)$$

in which  $\mathbf{Q}_b = \mathbf{W}_l^{-1}$  and  $\mathbf{Q}_g = \mathbf{W}_g^{-1}$ , so

$$\begin{aligned}
Q_x &= N_g^{-1} A' W_l A N_g^{-1} + N_g^{-1} W_g' N_g^{-1} \\
&= N_g^{-1} (A' W_l A + W_g') N_g^{-1} \\
&= N_g^{-1} = (A' W_l A + W_g')^{-1}
\end{aligned}
\tag{2.117}$$

The inverse of the cofactor matrix (the weight matrix) from this adjustment process is

$$W_x = Q_x^{-1} = A' W_l A + W_g' \tag{2.118}$$

It is noticed that  $b_g$  should be updated after each iteration. It is null for the first iteration, but may not be null in the subsequent iterations. If  $b_g$  is set to null for all iterations and the weights of the previously estimated coordinates are let to be infinity (a very big value is given in practice), the least squares estimation will then be constrained by the fixed coordinates. This is a special case when the  $p$  coordinates are selected from fixed control points. These control points will not be adjusted during the least squares process and will be fixed to their starting values. The coordinates of other object points will then be related to the coordinate system defined by the control points.

A distortion (compared with the results from the free network adjustment) will usually be introduced by the constraints of previously estimated coordinates or fixed coordinates if the number of coordinates is more than the minimum required to define the datum. The shape of the object will be different from that obtained by use of inner constraints. Furthermore the global precision is normally worse than that obtained by the inner constraints (assuming that the precision of controls are not as good as current observations), i.e., the trace of the cofactor matrix is larger than that obtained by the inner constraints. The reason is that this constraint is based on only a few which may be biased due to the small number, while inner constraints treat all the coordinates of the object points equally.

The differences in the results between the two kinds of the constraints depend on the significance of the weight matrix  $W_g$ . It can be imagined that if the elements of  $W_g$  are very small, the adjustment of the parameters will be less constrained by the controls and

more dependent on the current observations, and less distortion could be expected but the global accuracy gets worse. If the elements of  $W_g$  are very big (high precision controls) more distortion will be introduced but the global accuracy will be better. The best situation for this type of constraint might be to fix the minimum number of coordinates (which will introduce no distortion) and get the best global precision. However, even under this situation the global precision is still worse than that of inner constraints.

If all the coordinates to be estimated are treated as observations (pseudo observations) and a unique weight (normally very small) is given to them, what will happen? This is actually equivalent to the situation where all the coordinates are free of constraints and these coordinates will be adjusted by the real observations only. Without any bias the same results as obtained by the LSE with inner constraints can be expected. This technique has been called *The unified least square estimation* (Mikhail, 1976). It could be very useful in close range photogrammetry.

## 2.9 The unified LSE

The basic assumption of the unified LSE is that all the unknown parameters in the functional model are treated as observations. A unique weight  $w$  is selected for these observations and two extreme cases are described as follows (Mikhail, 1976):

1. *If an observation (in this case any variable in the model) is given an infinitely large variance, that is, its weight is  $w = 0$ , then it is allowed to vary freely in the adjustment and will therefore assume the role of an unknown parameter in the classical sense.*
2. *If on the other hand the observation is given a zero variance, or a weight that approaches infinity,  $w \rightarrow \infty$  it is simply not allowed to change in the adjustment, with the consequence that its residual will be zero and it would assume the classical meaning of a constant.*

Between the above two extremes lies a large set of possibilities within which actual observations (in the classical sense) fit. Since practically the unknown parameters are not, or not always, observed beforehand, so these parameters can be treated as pseudo observations. The constraint equations can be expressed as

$$\mathbf{x} = \mathbf{x}^0 \quad (2.119)$$

where  $\mathbf{x}^0$  is a vector of the starting values of the unknown parameters. A unique weight is usually given to these pseudo observations, so the weight matrix is

$$\mathbf{W}_g = g\mathbf{I}_{n \times n} \quad (2.120)$$

where  $g$  is the weight factor which defines the strength of the constraints. After linearization the constraint equations become

$$\Delta\mathbf{x} = \mathbf{b}_g \quad (2.121)$$

Together with the real observations equations, the augmented observation equations are expressed as

$$\begin{bmatrix} \mathbf{A} \\ \mathbf{I} \end{bmatrix} \Delta\mathbf{x} = \begin{bmatrix} \mathbf{b} \\ \mathbf{b}_g \end{bmatrix} + \begin{bmatrix} \mathbf{v} \\ \mathbf{v}_g \end{bmatrix} \quad (2.122)$$

with associated weight matrix

$$\mathbf{W} = \begin{bmatrix} \mathbf{W}_l & \\ & g\mathbf{I} \end{bmatrix} \quad (2.123)$$

The sum of the squares of the weight residuals of the observations is given by

$$\begin{bmatrix} \mathbf{v} \\ \mathbf{v}_g \end{bmatrix}' W \begin{bmatrix} \mathbf{v} \\ \mathbf{v}_g \end{bmatrix} = \mathbf{v}' W_l \mathbf{v} + \mathbf{v}_g' g \mathbf{v}_g \quad (2.124)$$

The first term on the right hand side in above equation is the target function which needs to be minimised by the LSE. When  $g$  is very small, the second term can be ignored. So the LSE can be applied to the augmented observation equations and the unknown parameters are estimated by

$$\begin{aligned} \Delta \mathbf{x} &= (A' W_l A + gI)^{-1} \begin{bmatrix} A' & I \end{bmatrix} \begin{bmatrix} W_l & \\ & gI \end{bmatrix} \begin{bmatrix} \mathbf{b} \\ \mathbf{b}_g \end{bmatrix} \\ &= (A' W_l A + gI)^{-1} (A' W_l \mathbf{b} + g \mathbf{b}_g) \end{aligned} \quad (2.125)$$

When  $g$  is very small,  $g \mathbf{b}_g$  can be ignored, so

$$\Delta \mathbf{x} = (A' W_l A + gI)^{-1} A' W_l \mathbf{b} \quad (2.126)$$

Let  $N_l = A' W_l A + gI$ , therefore

$$\Delta \mathbf{x} = N_l^{-1} A' W_l \mathbf{b} \quad (2.127)$$

With the addition of  $gI$  to  $A' W_l A$  the coefficient matrix  $N_l$  becomes non-singular. So the estimates of the unknown parameters are obtainable. Since  $gI$  is a diagonal matrix, the structure of  $A' W_l A$  is not influenced. The cofactor matrix of the parameters is given by

$$Q_x = N_l^{-1} A' W_l A N_l^{-1} \quad (2.128)$$

The magnitude of the weight factor  $g$  plays an important role in the unified LSE. If  $g$  is big, the unknown parameters will be bound more to the starting values which will slow down the adjustment process (more iterations are required). If  $g$  is too small the matrix  $N_l$  will be very ill conditioned ( $g = 0$  makes  $N_l$  singular). Theoretically the smaller the

weight factor  $g$  is, the smaller is the influence of the pseudo observations and the better results can be expected. But numerically  $g$  cannot be too small, otherwise the inverse of  $N_f$  is unobtainable because of the limitation of the computers. When  $g$  approaches zero while the inverse of  $N_f$  is still obtainable, the results of the unified LSE will approach that of the normal LSE with inner constraints. The following simple example verifies the fact.

If a distance is measured 100 units between two points  $x_1$  and  $x_2$  along  $x$  axis. The observation equation for this measurement may be expressed as

$$f(\mathbf{x}) = x_2 - x_1 = 100$$

or

$$\begin{bmatrix} -1 & 1 \end{bmatrix} \begin{bmatrix} \Delta x_1 \\ \Delta x_2 \end{bmatrix} \equiv A \Delta \mathbf{x} = b \equiv 100 - f(\mathbf{x}^0)$$

Due to datum deficiency,  $x_1$  and  $x_2$  are not estimable. Now suppose  $x_1 = 0$  and  $x_2 = 102$  are chosen as the starting values and the normal LSE with inner constraints is applied. The corrections are obtained by

$$\begin{aligned} \Delta \mathbf{x} &= (A' A + G' G)^{-1} A' b \\ &= \begin{bmatrix} 2 & 0 \\ 0 & 2 \end{bmatrix}^{-1} \begin{bmatrix} -1 \\ 1 \end{bmatrix} (-2) \\ &= \begin{bmatrix} 1 \\ -1 \end{bmatrix} \end{aligned}$$

So the updated parameters are given by

$$\hat{\mathbf{x}} = \begin{bmatrix} \hat{x}_1 \\ \hat{x}_2 \end{bmatrix} = \mathbf{x}^0 + \Delta \mathbf{x} = \begin{bmatrix} 1 \\ 101 \end{bmatrix}$$

The cofactor matrix is obtained by

$$\begin{aligned}
 Q_{\hat{x}} &= (A'A + G'G)^{-1} A'A (A'A + G'G)^{-1} \\
 &= \begin{bmatrix} 0.5 & 0 \\ 0 & 0.5 \end{bmatrix} \begin{bmatrix} 1 & -1 \\ -1 & 1 \end{bmatrix} \begin{bmatrix} 0.5 & 0 \\ 0 & 0.5 \end{bmatrix} \\
 &= \begin{bmatrix} 0.25 & -0.25 \\ -0.25 & 0.25 \end{bmatrix}
 \end{aligned}$$

With the unified LSE, the corrections are obtained by

$$\Delta x = (A'A + gI)^{-1} A'b$$

in which

$$\begin{aligned}
 (A'A + gI)^{-1} &= \begin{bmatrix} 1+g & -1 \\ -1 & 1+g \end{bmatrix}^{-1} \\
 &= \frac{1}{2g+g^2} \begin{bmatrix} 1+g & 1 \\ 1 & 1+g \end{bmatrix}
 \end{aligned}$$

and

$$A'b = \begin{bmatrix} -1 \\ 1 \end{bmatrix} \begin{bmatrix} -2 \end{bmatrix} = \begin{bmatrix} 2 \\ -2 \end{bmatrix}$$

Therefore

$$\Delta x = \begin{bmatrix} \frac{2}{2+g} \\ \frac{-2}{2+g} \end{bmatrix}$$

The cofactor matrix is obtained by

$$\begin{aligned}
Q_{\hat{x}} &= (A'A + gI)^{-1} A'A(A'A + gI)^{-1} \\
&= \frac{1}{(2g + g^2)^2} \begin{bmatrix} 1+g & 1 \\ 1 & 1+g \end{bmatrix} \begin{bmatrix} 1 & -1 \\ -1 & 1 \end{bmatrix} \begin{bmatrix} 1+g & 1 \\ 1 & 1+g \end{bmatrix} \\
&= \frac{1}{g^2(2+g)^2} \begin{bmatrix} g^2 & -g^2 \\ -g^2 & g^2 \end{bmatrix} \\
&= \frac{1}{(2+g)^2} \begin{bmatrix} 1 & -1 \\ -1 & 1 \end{bmatrix}
\end{aligned}$$

When  $g$  approaches zero,

$$\Delta x = \begin{bmatrix} I \\ -I \end{bmatrix} \quad \text{and} \quad Q_{\hat{x}} = \frac{1}{4} \begin{bmatrix} I & -I \\ -I & I \end{bmatrix}$$

which are identical with that obtained from the normal LSE with inner constraints.

Simulation tests show that the value of  $g$  can be assigned in a very wide range. Hence instead of adding a rather complicated matrix  $G'G$  (from the inner constraints) to the original matrix  $A'WA$  a small increment to its diagonal elements will remove its defects. When  $g$  is small enough the same results as obtained by the LSE with inner constraints can be expected.

It is very important to notice that the structure of the coefficient matrix will remain unchanged with the unified LSE. Advantages may be taken from this fact when calculating the inverse of the coefficient matrix if the structure of it is special (e.g. a diagonal matrix).

## 2.10 Summary of the chapter

The least squares method is no doubt one of the most important mathematical means to deal with redundant measurement and has been well justified (Cross 1983; Cooper 1987, 1988). Other methods such as the  $L_1$ -norm method and the Danish method have also been used as robust estimation techniques (Kubik 1987; Schuh 1989). However none of them has such a reputation like the least squares method ( $L_2$ -norm method). It is extremely easy to use and gives a unique unbiased solution. Another advantage of the least squares method is that the quality of the estimated results is assessable via the covariance matrix which is provided without any extra computations. The method can almost be used in any measurement problem where redundancy exists.

For the linear problems, solutions of the unknown parameters can be obtained directly by linear least squares estimation. For the non-linear problems, iterations are required to adjust the unknown parameters around their starting values. The starting values of the unknown parameters are important in the non-linear least squares estimation process. They must be realistic and reasonably close to the final solution. Otherwise the iterative process may diverge.

Least squares estimation process involves processing of matrices, in which calculating the inverse of the coefficient matrix is very expensive in term of speed and memory,  $O(u^3)$  and  $O(u^2)$  for time and memory respectively ( $u \times u$  is the size of the coefficient matrix). The conventional least squares estimation deals with the unknown parameters simultaneously. Therefore the size of the coefficient matrix may be very large. In some applications where time and memory are critical the conventional least squares method can be optimised significantly. However for some reason not enough efforts have been made in the algorithmic aspects to improve the conventional least squares method. It is still a bottle-neck in the real-time applications.

The sequential least squares method is a technique which divides the observations into parts. It is useful in situations where additional observations are available to readjust the parameters which have been estimated from an initial set of observations. In this case

the unknown parameters and their covariance matrix are kept for the next estimation, while the observation can be discarded. Therefore the computer resources can be saved. But the first sequence is still a full simultaneous least squares estimation process in which enough observations are required. Another problem with the sequential method is that the starting values of the unknown parameters must be very close to the final result to avoid further iterations. Otherwise many of the advantages will be lost.

The iterative method for solving linear algebraic equations can be used in the least squares estimation. The iteration is applied to the linearized observation equations, therefore is called inner iteration. The unknown parameters are estimated one by one rather than simultaneously. It is obvious that the memory requirement is reduced significantly. But the convergent speed may not be fast since too many iterations are needed for the inner iteration. Furthermore, the full covariance matrix is not provided.

There are two reasons to apply constraints in the LSE process. One reason is to remove the column rank defects from the design matrix so that the unknown parameters can be estimated. Although the Moore-Penrose inverse can be used without constraints, it is very difficult to compute the rank and pseudo-inverse of  $A'WA$  practically (Cooper 1980). The other reason is to define a datum. With inner constraints, the first problem is solved, but not the second. The same thing happens to the unified and the separate LSE. Only when controls are involved can the datum problem be solved properly. However, distortion may be introduced by these controls. The advantages of the unified LSE over the inner constrained LSE are: (i) the unified LSE is easy to apply; and (ii) the structure of the coefficient matrix does not change in the unified LSE process, but does change in the inner constrained LSE. If controls are not included in the least squares process (arbitrary datum), a coordinate transformation may be required to relate the results to a given coordinate system.

## Chapter 3

### Least Squares Estimation of Photogrammetric Measurements

#### ---- The Traditional Methods

Photogrammetry is a technique of obtaining 3D information in the object space by processing 2D information on the camera image planes. In digital close range photogrammetry multiple CCD cameras are used to capture images of the targeted object points from different viewpoints. Based on the geometric perspective principle, a set of so called collinearity equations can be derived to establish the relationships between 2D observations on the camera image planes and 3D coordinates of object points. By solving the collinearity equations the 3D coordinates of these object points can be estimated.

Three major steps are normally needed in the photogrammetric measurement procedure: (i) 2D image data acquisition and target location; (ii) solving target correspondences between different images; and (iii) least squares estimation of the unknown parameters in the functional models. Using powerful processors or hardware, real-time target location can be realised. Various approaches to solve target correspondences are possible such as using epipolar lines and epipolar planes (2D and 3D matching). However, solving collinearity equations by least squares estimation is still a considerable time consuming procedure.

In this chapter the functional relationships between 2D observations on the camera image planes and 3D coordinates of the object points are discussed. Various methods of least squares estimation are investigated to solve the unknown parameters from the functional models.

### 3.1 Functional models

In a photogrammetric 3D measurement system, the 2D coordinates on the image planes are measured and used to estimate the 3D coordinates of the object points. The 2D coordinates on the image planes are known as observations and 3D coordinates of the object points (together with the camera parameters) are the unknown parameters. To solve for these unknown parameters the functional relationships between the observations and the unknown parameters have to be established. The first step in establishing the functional models is to define the coordinate system<sup>3</sup>. The three-dimensional right-handed Cartesian coordinate system is normally used as the object space coordinate system. The image coordinate system is also a three-dimensional right handed Cartesian coordinate system, with the  $x$  and  $y$  axes being in the image plane and  $z$  axis being toward the perspective centre of the camera. Figure 3-1 illustrates the object coordinate system  $XYZ$  and image coordinate system  $xyz$ .

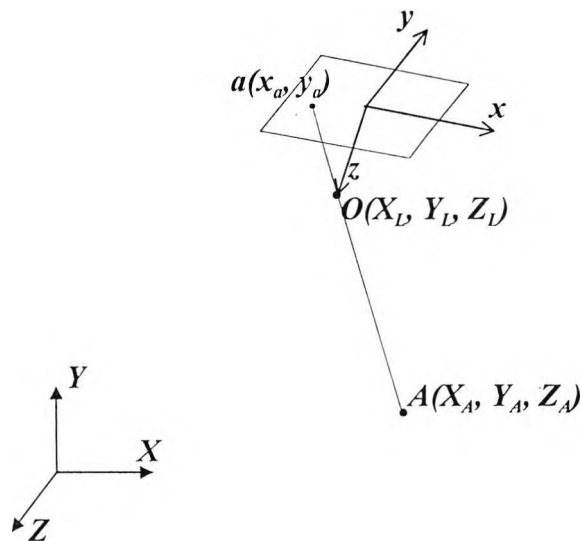


Figure 3-1 The object coordinate system and the image coordinate system

The coordinates of the perspective centre  $O(X_L, Y_L, Z_L)$  of the camera are related to object space coordinate system  $XYZ$  and the angular relationship between the image and the object coordinate systems can be described by a  $3 \times 3$  orthogonal rotation matrix  $M$ . Nine elements are involved in the rotation matrix, but only three independent parameters are involved in the matrix  $M$ . They are  $\omega$ ,  $\phi$  and  $\kappa$ , the three sequential rotation angles around  $X$ ,  $Y$  and  $Z$  axes respectively. The three rotation matrices are obtained as follows (Wolf, 1983)

$$M_\omega = \begin{bmatrix} 1 & 0 & 0 \\ 0 & \cos \omega & \sin \omega \\ 0 & -\sin \omega & \cos \omega \end{bmatrix} \quad (3.1)$$

$$M_\phi = \begin{bmatrix} \cos \phi & 0 & \sin \phi \\ 0 & 1 & 0 \\ -\sin \phi & 0 & \cos \phi \end{bmatrix} \quad (3.2)$$

$$M_\kappa = \begin{bmatrix} \cos \kappa & \sin \kappa & 0 \\ -\sin \kappa & \cos \kappa & 0 \\ 0 & 0 & 1 \end{bmatrix} \quad (3.3)$$

These matrices are multiplied together to give

$$M = M_\omega M_\phi M_\kappa = \begin{bmatrix} m_{11} & m_{12} & m_{13} \\ m_{21} & m_{22} & m_{23} \\ m_{31} & m_{32} & m_{33} \end{bmatrix} \quad (3.4)$$

in which

$$\begin{cases} m_{11} = \cos \phi \cos \kappa \\ m_{12} = \sin \omega \sin \phi \cos \kappa + \cos \omega \sin \kappa \\ m_{13} = -\cos \omega \sin \phi \cos \kappa + \sin \omega \sin \kappa \\ m_{21} = -\cos \phi \sin \kappa \\ m_{22} = -\sin \omega \sin \phi \sin \kappa + \cos \omega \cos \kappa \\ m_{23} = \cos \omega \sin \phi \sin \kappa + \sin \omega \cos \kappa \\ m_{31} = \sin \phi \\ m_{32} = -\sin \omega \cos \phi \\ m_{33} = \cos \omega \cos \phi \end{cases} \quad (3.5)$$

### 3.1.1 Collinearity equations

If an object point  $A(X_A, Y_A, Z_A)$  is imaged by a camera and located at point  $a(x_a, y_a)$  on the image plane, a straight line can be projected from the point  $A$  through the perspective centre  $O(X_L, Y_L, Z_L)$  of the camera onto the point  $a$  on the image plane. Ideally the line segments  $AO$  and  $aO$  should be on the same line, i.e., they are collinear. Based on this condition the well known collinearity equations are established as follows (Wolf, 1983)

$$\begin{aligned} x_a &= -c \frac{m_{11}(X_A - X_L) + m_{12}(Y_A - Y_L) + m_{13}(Z_A - Z_L)}{m_{31}(X_A - X_L) + m_{32}(Y_A - Y_L) + m_{33}(Z_A - Z_L)} \\ y_a &= -c \frac{m_{21}(X_A - X_L) + m_{22}(Y_A - Y_L) + m_{23}(Z_A - Z_L)}{m_{31}(X_A - X_L) + m_{32}(Y_A - Y_L) + m_{33}(Z_A - Z_L)} \end{aligned} \quad (3.6)$$

More generally, if the  $i$ th object point is imaged on the  $j$ th camera, the collinearity equations can be expressed as

$$\begin{cases} f_{jix} = x_{ji} + c_j \frac{M_{ji1}}{M_{ji3}} \\ f_{jiy} = y_{ji} + c_j \frac{M_{ji2}}{M_{ji3}} \end{cases} \quad (3.7)$$

in which

$$\begin{aligned} M_{ji1} &= m_{j11}(X_i - X_{jL}) + m_{j12}(Y_i - Y_{jL}) + m_{j13}(Z_i - Z_{jL}) \\ M_{ji2} &= m_{j21}(X_i - X_{jL}) + m_{j22}(Y_i - Y_{jL}) + m_{j23}(Z_i - Z_{jL}) \\ M_{ji3} &= m_{j31}(X_i - X_{jL}) + m_{j32}(Y_i - Y_{jL}) + m_{j33}(Z_i - Z_{jL}) \end{aligned} \quad (3.8)$$

The collinearity equations establish the relationship between the 2D image coordinates observed on the image planes and the 3D object point coordinates (together with the camera parameters) to be estimated. These collinearity equations are the most commonly used functional models in close range photogrammetry. They can be used in

intersection (estimating the 3D coordinates of the object points with known camera parameters), resection (estimating the camera parameters with known 3D control points) and bundle adjustment (simultaneously estimating the 3D coordinates of the object points and the camera parameters with all of them treated as unknown parameters). Another useful functional model is the DLT model.

### 3.1.2 DLT model

The DLT (Direct Linear Transformation) model proposed by Abdel-Aziz and Karara (1971) is an alternate formulation of the normal functional model. The main advantages of using the DLT model compared with the collinearity equations (3.6) are, (i) it encompasses some camera interior parameters such as the coordinates of the principal point  $(x_p, y_p)$  and the principal distances  $c_x$  and  $c_y$ ; (ii) it simplifies the computation of the photogrammetric adjustment process.

With the principal point  $(x_p, y_p)$  and the principal distances  $c_x$  and  $c_y$  involved, the normal collinearity equations become

$$\begin{aligned} x - x_p &= -c_x \frac{m_{11}(X - X_L) + m_{12}(Y - Y_L) + m_{13}(Z - Z_L)}{m_{31}(X - X_L) + m_{32}(Y - Y_L) + m_{33}(Z - Z_L)} \\ y - y_p &= -c_y \frac{m_{21}(X - X_L) + m_{22}(Y - Y_L) + m_{23}(Z - Z_L)}{m_{31}(X - X_L) + m_{32}(Y - Y_L) + m_{33}(Z - Z_L)} \end{aligned} \quad (3.9)$$

In general, the DLT model for the  $i$ th object point imaged on the  $j$ th camera can be expressed as

$$\begin{cases} f_{jix} = x_{ji} + \frac{D_{ji1}}{D_{ji3}} \\ f_{jiv} = y_{ji} + \frac{D_{ji2}}{D_{ji3}} \end{cases} \quad (3.10)$$

in which

$$\begin{cases} D_{ji1} = L_{j1}X_i + L_{j2}Y_i + L_{j3}Z_i + L_{j4} \\ D_{ji2} = L_{j5}X_i + L_{j6}Y_i + L_{j7}Z_i + L_{j8} \\ D_{ji3} = L_{j9}X_i + L_{j10}Y_i + L_{j11}Z_i + 1 \end{cases} \quad (3.11)$$

where

$$\begin{cases} L_0 = -(m_{31}X_L + m_{32}Y_L + m_{33}Z_L) \\ L_1 = (x_p m_{31} - c_x m_{11}) / L_0 \\ L_2 = (x_p m_{32} - c_x m_{12}) / L_0 \\ L_3 = (x_p m_{33} - c_x m_{13}) / L_0 \\ L_4 = x_p + c_x (m_{11}X_L + m_{12}Y_L + m_{13}Z_L) / L_0 \\ L_5 = (y_p m_{31} - c_y m_{21}) / L_0 \\ L_6 = (y_p m_{32} - c_y m_{22}) / L_0 \\ L_7 = (y_p m_{33} - c_y m_{23}) / L_0 \\ L_8 = y_p + c_y (m_{21}X_L + m_{22}Y_L + m_{23}Z_L) / L_0 \\ L_9 = m_{31} / L_0 \\ L_{10} = m_{32} / L_0 \\ L_{11} = m_{33} / L_0 \end{cases} \quad (3.12)$$

The 11 DLT parameters  $L_1$  to  $L_{11}$  contain 10 camera physical parameters, of which six are exterior parameters ( $X_L, Y_L, Z_L, \omega, \phi, \kappa$ ) and four are interior parameters ( $x_p, y_p, c_x, c_y$ ).

### 3.1.3 Camera interior parameters

#### 3.1.3.1 Principal distance and principal point

The principal distance is the perpendicular distance from the perspective centre of the lens system to the image plane. At infinity focus, it is equal to the focal length. However in close range photogrammetry it is unusual to use a camera focused at infinity. So the principal distance is normally not the same as the focal length. The following equation expresses the relationship between them.

$$c = c_0 + \Delta c \quad (3.13)$$

where  $c$  denotes the principal distance,  $c_0$  denotes the focal length and  $\Delta c$  denotes the difference (offset). With a different focal setting, the value of  $\Delta c$  may change. When  $\Delta c$  is treated as a variable, the principal distance will be adjusted in the least square process and its value can be determined thereafter.

The principal point is defined as that point on the image plane which is at the base of the perpendicular from the 'centre of the lens', or more correctly, from the rear nodal point. Ideally the principal point would coincide with the *fiducial origin*, the origin of the plane coordinate system. The fiducial origin or centre is the intersection of imaginary lines drawn from opposite pairs of fiducial marks in the sides or corners of the image plane. With the digital camera, these fiducial marks may be considered to be on the half sensor size points. So the fiducial centre will be the centre of the sensor or the centre of the image plane. The relationship between the principal point and the fiducial origin can be expressed by

$$\begin{cases} x_p = x_0 + \Delta x_p \\ y_p = y_0 + \Delta y_p \end{cases} \quad (3.14)$$

where  $(x_p, y_p)$  refers to the principal point,  $(x_0, y_0)$  refers to the fiducial origin and  $(\Delta x_p, \Delta y_p)$  is called the *principal point offset*. The principal point  $(x_p, y_p)$  can be determined when it is treated as variable and made adjustable in the least squares process.

### 3.1.3.2 Radial distortion and decentring distortion

Ideally a lens would have the property of collinear imaging geometry over its entire field of view and range of focus. However no real lens has this perfect behaviour and will always suffer from several types of aberration, one of which is described as lens distortion. Lens distortion is usually divided into two types, radial distortion and decentring distortion.

If the image of an off-axis target is displaced radially from the principal point then it is radially distorted. Figure 3-2 shows an error map represents radial lens distortion.

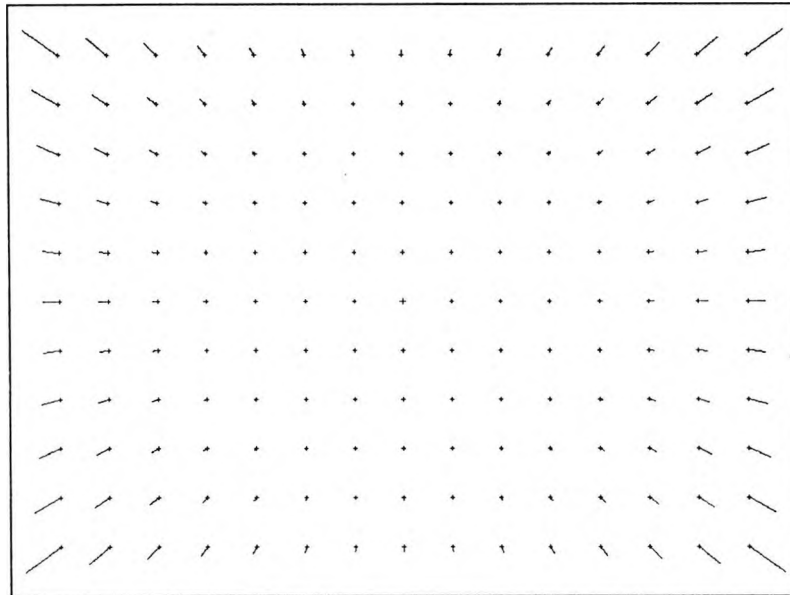


Figure 3-2 An error map caused by radial lens distortion

Radial distortion is a symmetric effect and can normally be modelled by a polynomial series of odd powered terms, i.e.,

$$\Delta r = k_1 r^3 + k_2 r^5 + k_3 r^7 + \dots \quad (3.15)$$

in which

$$r = ((x - x_p)^2 + (y - y_p)^2)^{1/2} \quad (3.16)$$

where  $\Delta r$  is the radial displacement of an image point,  $k_1$ ,  $k_2$ , and  $k_3$  are the coefficients of the radial distortion corresponding to infinity focus,  $x$  and  $y$  are the coordinates of a image point. The displacement of the image point caused by the radial distortion is expressed as

$$\begin{cases} \Delta x_r = (x - x_p) \frac{\Delta r}{r} \\ \Delta y_r = (y - y_p) \frac{\Delta r}{r} \end{cases} \quad (3.17)$$

$\Delta x_r$  and  $\Delta y_r$  are the corrections on  $x$  and  $y$  due to the radial distortion.

Decentering distortion is caused by any vertical displacement or rotation of the lens elements from a perfect alignment. Figure 3-3 shows an error map represents decentering lens distortion.

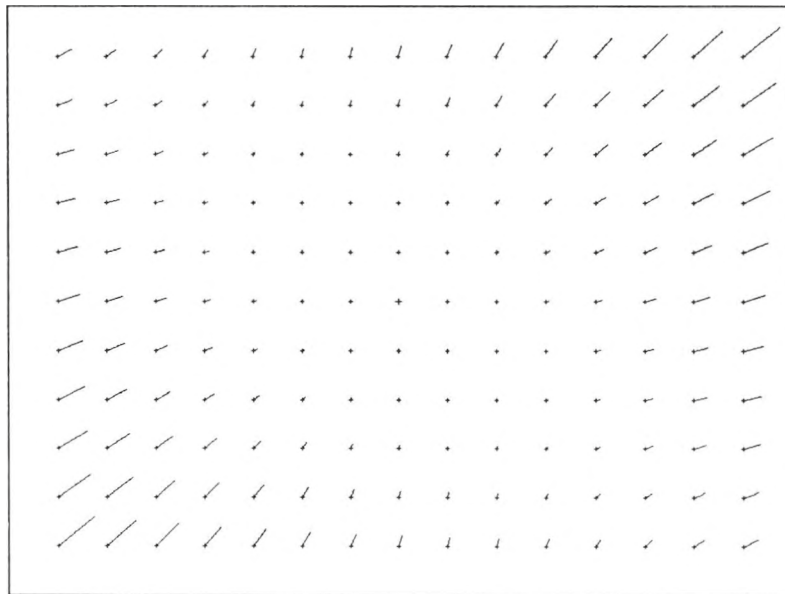


Figure 3-3 An error map caused by decentering lens distortion

The displacement is described by two polynomials, one for the displacement in  $x$  direction and the other for the displacement in  $y$  direction, i.e.,

$$\begin{cases} \Delta x_d = p_1(r^2 + 2(x - x_p)^2) + 2p_2(x - x_p)(y - y_p) \\ \Delta y_d = p_2(r^2 + 2(y - y_p)^2) + 2p_1(x - x_p)(y - y_p) \end{cases} \quad (3.18)$$

where  $p_1$  and  $p_2$  are two coefficients depending on the lens setting, the other notations are the same as used in the radial distortion.

### 3.1.4 Modification of the collinearity equations

With above lens distortions considered, the modified collinearity equations become

$$\begin{cases} f_x = (x - \Delta x_p) + \Delta x_r + \Delta x_d + (c_0 + \Delta c) \frac{M_1}{M_3} \\ f_y = (y - \Delta y_p) + \Delta y_r + \Delta y_d + (c_0 + \Delta c) \frac{M_2}{M_3} \end{cases} \quad (3.19)$$

neglecting subscripts for simplicity. In general, the functional model in close range photogrammetry can be expressed as

$$f(x_1, x_2, x'_2) = l \quad (3.20)$$

where  $x_1 = (X, Y, Z)$  denotes a vector of the 3D coordinates of the object points,  $x_2 = (X_L, Y_L, X_L, \omega, \phi, \kappa)$  denotes a vector of the camera exterior parameters,  $x'_2 = (x_p, y_p, \Delta c, k_1, k_2, k_3, p_1, p_2)$  denotes a vector of the camera interior parameters and  $l$  represents the observed image coordinates.

## 3.2 Intersection

Intersection is the procedure of determining the 3D coordinates of the object points by intersecting lines projected from their corresponding points on the camera image planes. In this process the camera parameters are required to be known. This is the standard situation using metric cameras with fixed bases or when using photo-theodolites (Karara, 1989). Intersection is also used to locate ground points from two overlapping horizontal terrestrial photos or highly oblique photos (Wolf, 1983). In close range photogrammetry intersection is often used to estimate the starting values of the object points with approximately estimated camera parameters. These starting values can be

used in the subsequent bundle adjustment for better estimates. Figure 3-4 illustrates the geometry of the intersection.

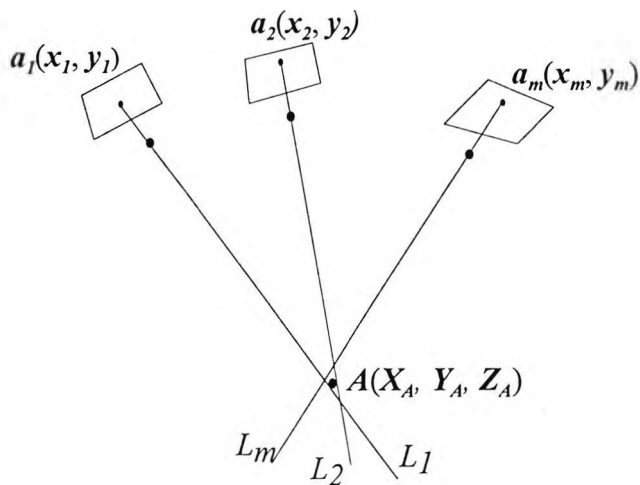


Figure 3-4 The geometry of intersection

If an object point  $A(X_A, Y_A, Z_A)$  is imaged by  $m$  cameras and located at the image points  $a_1(x_1, y_1)$ ,  $a_2(x_2, y_2)$ , ...,  $a_m(x_m, y_m)$  respectively, a straight line can be projected from each image point. Ideally these  $m$  lines should intersect at one point in the object space and that point should be  $A(X_A, Y_A, Z_A)$ . However, errors are inevitable during the measurement procedures. These lines will not intersect at the same point and the coordinates of the point are overdetermined. Using the least squares method (based on the collinearity equations) the 3D coordinates of the object point can be estimated. During the intersection process since the camera parameters are known,  $(X_{iL}, Y_{iL}, Z_{iL})$  and  $(m_{i11} \dots m_{i33})$  are constants, where  $i = 1, 2, \dots, m$ . The only unknown parameters in the collinearity equations are  $(X_A, Y_A, Z_A)$ , the 3D coordinates of each object point. To solve for the three unknown parameters, this object point must appear on at least two images, which will give four equations and the least squares method can be applied for the best solution.

There are two possible ways to solve for the three unknowns ( $X_A, Y_A, Z_A$ ) in the collinearity equations. One is a direct solution which rearranges the collinearity equations into a linear form, the other is an iterative solution which keeps the collinearity equations in the original non-linear form. The latter solution is more rigorous because it minimises the sum of the squares of the residuals on the image planes. However starting values are required for the 3D coordinates. The former solution has no physical meaning, but the unknown parameters can be solved directly without any prior knowledge. The choice of method to use depends on the purpose of the application.

### 3.2.1 Direct solution

The 3D coordinates ( $X_A, Y_A, Z_A$ ) of the object point can be solved directly by rearranging the collinearity equations (3.6) as follows

$$\left\{ \begin{array}{l} (x_j m_{j31} + c_j m_{j11}) X_A + (x_j m_{j32} + c_j m_{j12}) Y_A + (x_j m_{j33} + c_j m_{j13}) Z_A \\ = x_j (m_{j31} X_{jL} + m_{j32} Y_{jL} + m_{j33} Z_{jL}) + c_j (m_{j11} X_{jL} + m_{j12} Y_{jL} + m_{j13} Z_{jL}) \\ \\ (y_j m_{j31} + c_j m_{j21}) X_A + (y_j m_{j32} + c_j m_{j22}) Y_A + (y_j m_{j33} + c_j m_{j23}) Z_A \\ = y_j (m_{j31} X_{jL} + m_{j32} Y_{jL} + m_{j33} Z_{jL}) + c_j (m_{j21} X_{jL} + m_{j22} Y_{jL} + m_{j23} Z_{jL}) \end{array} \right. \quad (3.21)$$

$$(j = 1, 2, \dots, m)$$

or rearranging the DLT model (3.9) as follows

$$\left\{ \begin{array}{l} (L_{j1} - x_j L_{j9}) X_A + (L_{j2} - x_j L_{j10}) Y_A + (L_{j3} - x_j L_{j11}) Z_A = x_j - L_{j4} \\ (L_{j5} - y_j L_{j9}) X_A + (L_{j6} - y_j L_{j10}) Y_A + (L_{j7} - y_j L_{j11}) Z_A = y_j - L_{j8} \end{array} \right. \quad (3.22)$$

In matrix form, these equations can be expressed as

$$\begin{bmatrix} a_{11} & a_{12} & a_{13} \\ a_{21} & a_{22} & a_{23} \\ \vdots & \vdots & \vdots \\ a_{2m1} & a_{2m2} & a_{2m3} \end{bmatrix} \begin{bmatrix} X_A \\ Y_A \\ Z_A \end{bmatrix} = \begin{bmatrix} b_1 \\ b_2 \\ \vdots \\ b_{2m} \end{bmatrix} \quad (3.23)$$

or simply

$$A \begin{bmatrix} X_A \\ Y_A \\ Z_A \end{bmatrix} = B \quad (3.24)$$

The unknown parameters ( $X_A, Y_A, Z_A$ ) can be solved directly by a linear least squares estimation, i.e.,

$$\begin{bmatrix} X_A \\ Y_A \\ Z_A \end{bmatrix} = (A^t A)^{-1} A^t B \quad (3.25)$$

### 3.2.2 Iterative solution

The 3D object point coordinates ( $X_A, Y_A, Z_A$ ) can also be solved with iterative least squares estimation by keeping the collinearity equations in the original non-linear form. In this case, the collinearity equations or the DLT model are Taylor's expansion and the starting values of the 3D coordinates ( $X^0, Y^0, Z^0$ ) are required. Linearizing the collinearity equations (3.7) by Taylor's expansion to the first order accuracy with the coordinates of the object points ( $X, Y, Z$ ) as the variables gives

$$\begin{cases} (f_{ix})^0 + \left(\frac{\partial f_{ix}}{\partial x_i}\right)^0 \Delta x_i = 0 \\ (f_{iy})^0 + \left(\frac{\partial f_{iy}}{\partial x_i}\right)^0 \Delta x_i = 0 \end{cases} \quad (3.26)$$

$$(j = 1, 2, \dots, m)$$

or simply

$$A_1 \Delta x_1 = b \quad (3.27)$$

where

$$\Delta x_1 = \begin{bmatrix} X - X^0 \\ Y - Y^0 \\ Z - Z^0 \end{bmatrix} \quad (3.28)$$

$$\frac{\partial f_{jx}}{\partial x_1} = \begin{bmatrix} \frac{\partial f_{jx}}{\partial X} & \frac{\partial f_{jx}}{\partial Y} & \frac{\partial f_{jx}}{\partial Z} \end{bmatrix} \quad (3.29)$$

$$\frac{\partial f_{jy}}{\partial x_1} = \begin{bmatrix} \frac{\partial f_{jy}}{\partial X} & \frac{\partial f_{jy}}{\partial Y} & \frac{\partial f_{jy}}{\partial Z} \end{bmatrix} \quad (3.30)$$

$$A_1 = \begin{bmatrix} \left( \frac{\partial f_{jx}}{\partial x_1} \right)^0 \\ \left( \frac{\partial f_{jy}}{\partial x_1} \right)^0 \end{bmatrix}_{2m \times 3} \quad \text{and} \quad b = \begin{bmatrix} -(f_{jx})^0 \\ -(f_{jy})^0 \end{bmatrix}_{2m \times 1}$$

The partial derivatives with respect to the object point coordinates ( $X$ ,  $Y$ ,  $Z$ ) are derived and given in Appendix I. So the corrections of the unknown parameters (the 3D coordinates of the object points) can then be estimated by least squares, i.e.,

$$\Delta x_1 = (A_1^t W_1 A_1)^{-1} A_1^t W_1 b \quad (3.31)$$

where  $W_1$  is the weight matrix of the observations. The 3D coordinates of the object points are adjusted by

$$\mathbf{x}_l = \begin{bmatrix} X \\ Y \\ Z \end{bmatrix} = \begin{bmatrix} X^0 \\ Y^0 \\ Z^0 \end{bmatrix} + \Delta \mathbf{x}_l \quad (3.32)$$

The cofactor matrix of the estimated 3D coordinates is given by

$$\mathbf{Q}_{x_l} = (\mathbf{A}_l' \mathbf{W}_l \mathbf{A}_l)^{-1} \quad (3.33)$$

and the covariance matrix is

$$\mathbf{C}_{x_l} = \hat{\sigma}_0^2 (\mathbf{A}_l' \mathbf{W}_l \mathbf{A}_l)^{-1} \quad (3.34)$$

where  $\hat{\sigma}_0^2$  is the *a posteriori* reference variance of the observations.

### 3.2.3 Discussion

Which intersection method to use will depend upon whether speed or statistical rigour is more important (Atkinson, 1996). It is noticed that, due to the rearrangement of the collinearity equations, the minimisation of the least squares for the direct solution is no longer the sum of squares of residuals of the observations. The right hand side terms in equation (3.21) and (3.22) do not have a physical meaning. The iterative solution minimises the sum of squares of residuals of the observations on the image plane. So the iterative solution is statistically rigorous, but starting values are required. The starting values can be obtained by some other non-photogrammetric methods (e.g. surveying) or by the direct solution mentioned above.

If  $m$  images are used for the intersection purpose, the number of observations is  $2m$  and the degrees of freedom are  $(2m-3)$ . These numbers are much smaller than those in the bundle adjustment where a few thousand observations and several hundred unknown parameters are usual. So the results from the intersection are of low reliability compared

with the simultaneous bundle adjustment. Since the camera parameters are known and fixed, the spatial object points can be solved individually. Each time only three unknown parameters need to be solved. This is very efficient in terms of speed and memory.

### 3.3 Resection

Resection is a procedure of determining camera exterior parameters  $(X_L, Y_L, Z_L, \omega, \phi, \kappa)$  with known spatial control points (Thompson 1975; Slama 1980; Atkinson 1996). Figure 3-5 illustrates the geometry of resection.

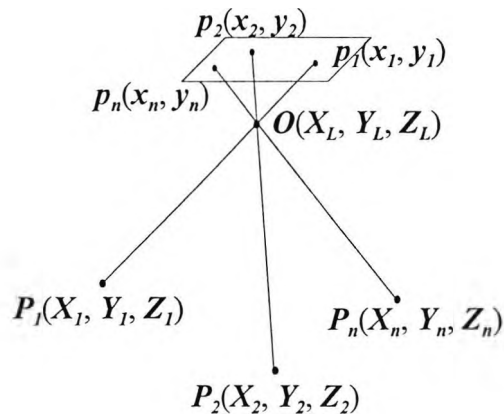


Figure 3-5 The geometry of the resection

Again the collinearity equations can be used for the camera resection purpose. A spatial point  $P_i(X_i, Y_i, Z_i)$  with its image coordinates  $p_i(x_i, y_i)$  measured on a camera will give rise to two collinearity equations. If three non-collinear object points are recorded on a camera and the 3D coordinates of these object points are known, the camera parameters can be determined uniquely by the corresponding collinearity equations. With more than three object points least squares methods are used for the best solution. These spatial object points are referred as spatial control points and their coordinates can be measured by some other non-photogrammetric methods. If enough spatial control points

are available and well distributed in the object space, the camera interior parameters (together with the camera exterior parameters) can also be estimated. As with intersection, two basic procedures can be used in camera resection, i.e., iterative solution and direct solution.

### 3.3.1 Iterative solution

The collinearity equations provide the basic functional model for space resection. Linearizing equations (3.7) by Taylor's expansion to the first order accuracy with the camera exterior parameters ( $X_L, Y_L, Z_L, \omega, \phi, \kappa$ ) as the variables gives

$$\begin{cases} (f_{ix})^0 + \left(\frac{\mathcal{F}_{ix}}{\partial x_2}\right)^0 \Delta x_2 = 0 \\ (f_{iy})^0 + \left(\frac{\mathcal{F}_{iy}}{\partial x_2}\right)^0 \Delta x_2 = 0 \end{cases} \quad (3.35)$$

$$(i = 1, 2, \dots, n)$$

or

$$A_2 \Delta x_2 = b \quad (3.36)$$

where

$$\Delta x_2 = \begin{bmatrix} X_L - X_L^0 \\ Y_L - Y_L^0 \\ Z_L - Z_L^0 \\ \omega - \omega^0 \\ \phi - \phi^0 \\ \kappa - \kappa^0 \end{bmatrix} \quad (3.37)$$

$$\frac{\mathcal{F}_{ix}}{\partial x_2} = \left[ \frac{\mathcal{F}_{ix}}{\partial X_L} \quad \frac{\mathcal{F}_{ix}}{\partial Y_L} \quad \frac{\mathcal{F}_{ix}}{\partial Z_L} \quad \frac{\mathcal{F}_{ix}}{\partial \omega} \quad \frac{\mathcal{F}_{ix}}{\partial \phi} \quad \frac{\mathcal{F}_{ix}}{\partial \kappa} \right] \quad (3.38)$$

$$\frac{\partial f_{iy}}{\partial \alpha_2} = \begin{bmatrix} \frac{\partial f_{iy}}{\partial X_L} & \frac{\partial f_{iy}}{\partial Y_L} & \frac{\partial f_{iy}}{\partial Z_L} & \frac{\partial f_{iy}}{\partial \omega} & \frac{\partial f_{iy}}{\partial \phi} & \frac{\partial f_{iy}}{\partial \kappa} \end{bmatrix} \quad (3.39)$$

$$A_2 = \begin{bmatrix} (\frac{\partial f_{ix}}{\partial \alpha_2})^0 \\ (\frac{\partial f_{iy}}{\partial \alpha_2})^0 \end{bmatrix}_{2n \times 6} \quad \text{and} \quad b = \begin{bmatrix} -(f_{ix})^0 \\ -(f_{iy})^0 \end{bmatrix}_{2n \times 1}$$

The partial derivatives with respect to the camera exterior parameters ( $X_L$ ,  $Y_L$ ,  $Z_L$ ,  $\omega$ ,  $\phi$ ,  $\kappa$ ) are derived and given in Appendix I. The corrections of the camera parameters can then be estimated by least squares, i.e.,

$$\Delta x_2 = (A_2^T W_1 A_2)^{-1} A_2^T W_1 b \quad (3.40)$$

where  $W_1$  is the weight matrix of the 2D observations. The adjusted camera exterior parameters are then obtained by

$$x_2 = \begin{bmatrix} X_L \\ Y_L \\ Z_L \\ \omega \\ \phi \\ \kappa \end{bmatrix} = \begin{bmatrix} X_L^0 \\ Y_L^0 \\ Z_L^0 \\ \omega^0 \\ \phi^0 \\ \kappa^0 \end{bmatrix} + \Delta x_2 \quad (3.41)$$

The full cofactor matrix of the estimated camera exterior parameters is given by

$$Q_{x_2} = (A_2^T W_1 A_2)^{-1} \quad (3.42)$$

The iterative process requires starting values of the camera exterior parameters. Approximate values for the coordinates ( $X_L$ ,  $Y_L$ ,  $Z_L$ ) are relatively easy to obtain but not for the rotation angles ( $\omega$ ,  $\phi$ ,  $\kappa$ ). That makes the space resection method by the iterative process from the standard collinearity equations difficult to use without knowing the

starting values of the camera exterior parameters. Many efforts have been made to obtain the camera exterior parameters by the control points directly without any prior knowledge of the camera. Such approaches are termed *closed solutions*.

### 3.3.2 Closed solution (Direct solution)

Space resection by DLT is one of the well known direct methods which transforms the collinearity equations into the linear form to avoid the requirement for the starting values. The standard DLT equations include 11 parameters which are related to the six camera exterior parameters ( $X_L, Y_L, Z_L, \omega, \phi, \kappa$ ). The interior parameters can normally be ignored in the resection process. The standard DLT equations are:

$$\begin{cases} x = \frac{L_1X + L_2Y + L_3Z + L_4}{L_9X + L_{10}Y + L_{11}Z + 1} \\ y = \frac{L_5X + L_6Y + L_7Z + L_8}{L_9X + L_{10}Y + L_{11}Z + 1} \end{cases} \quad (3.43)$$

Since there are 11 DLT parameters for each camera, a minimum of six control points are needed on the image to give 12 equations for the solution. Eq (3.43) can be transformed into linear form, i.e.,

$$\begin{cases} XL_1 + YL_2 + ZL_3 + L_4 - xXL_9 - xYL_{10} - xZL_{11} = x \\ XL_5 + YL_6 + ZL_7 + L_8 - yXL_9 - yYL_{10} - yZL_{11} = y \end{cases} \quad (3.44)$$

These equations can be solved directly by linear least squares estimation. One of the problems with the standard DLT method is that certain conditions are required for the spatial control points (Karara 1989). If they are in plane, the traditional DLT method will fail. Another disadvantage is that at least six spatial control points are required. This may not be convenient in some situations. To avoid these deficiencies, a two dimensional DLT method can be used (Shih 1988). Only four control targets are required this time and they are required to be in the same plane. This is a good complement to the traditional DLT method. If more than six spatial control points are

available and they have sufficient depth difference, the traditional DLT method can be used. Otherwise, the 2D DLT method will still give a satisfactory solution. This method is discussed here.

In the space resection process, if the control points are supposed to be in the same plane, their  $Z$  coordinates can be considered as zero. The terms including  $Z$  in Eq (3.11) will disappear. Only  $X$  and  $Y$  coordinates are required for these control points. The 11 DLT parameters will be reduced to 8, from which camera exterior parameters can still be derived. The improved 2D DLT equations are expressed as

$$\begin{cases} x = c \frac{L_1 X + L_2 Y + L_3}{L_7 X + L_8 Y + 1} \\ y = c \frac{L_4 X + L_5 Y + L_6}{L_7 X + L_8 Y + 1} \end{cases} \quad (3.45)$$

in which  $L_1 = m_{11}/L$        $L_2 = m_{12}/L$       (3.46a,b)

$$L_3 = -(m_{11}X_L + m_{12}Y_L + m_{13}Z_L)/L \quad (3.46c)$$

$$L_4 = m_{21}/L$$

$$L_5 = m_{22}/L \quad (3.46d,e)$$

$$L_6 = -(m_{21}X_L + m_{22}Y_L + m_{23}Z_L)/L \quad (3.46f)$$

$$L_7 = m_{31}/L$$

$$L_8 = m_{32}/L \quad (3.46g,h)$$

$$L = -(m_{31}X_L + m_{32}Y_L + m_{33}Z_L) \quad (3.46i)$$

The 8 DLT parameters can be solved directly by transforming Eq (3.45) into the linear form as

$$\begin{cases} XL_1 + YL_2 + L_3 - xXL_7 - xYL_8 = x \\ XL_4 + YL_5 + L_6 - yXL_7 - yYL_8 = y \end{cases} \quad (3.47)$$

To solve for the 8 DLT parameters in above equations, a minimum of four control points are needed to give at least eight linear equations. If more than four control points are available, the linear least square estimation is used for the best solution.

Since the 9 rotation parameters  $m_{11}$  to  $m_{33}$  compose a orthogonal matrix, the following conditions hold,

$$\begin{aligned} m_{11}^2 + m_{21}^2 + m_{31}^2 &= 1 \\ m_{12}^2 + m_{22}^2 + m_{32}^2 &= 1 \\ m_{13}^2 + m_{23}^2 + m_{33}^2 &= 1 \end{aligned} \quad (3.48)$$

So  $L$  can be solved as

$$L = \pm \frac{1}{\sqrt{L_1^2 + L_4^2 + L_7^2}} \quad (3.49)$$

or

$$L = \pm \frac{1}{\sqrt{L_2^2 + L_5^2 + L_8^2}} \quad (3.50)$$

Camera rotation parameters ( $\omega$ ,  $\phi$ ,  $\kappa$ ) can then be determined by

$$\begin{cases} \phi = \arcsin(LL_7) \\ \omega = -\arcsin(LL_8 / \cos \phi) \\ \kappa = -\arcsin(LL_4 / \cos \phi) \end{cases} \quad (3.51)$$

and camera positions ( $X_L$ ,  $Y_L$ ,  $Z_L$ ) can be determined by

$$\begin{bmatrix} X_L \\ Y_L \\ Z_L \end{bmatrix} = - \begin{bmatrix} m_{11} & m_{12} & m_{13} \\ m_{21} & m_{22} & m_{23} \\ m_{31} & m_{32} & m_{33} \end{bmatrix}^{-1} \begin{bmatrix} LL_3 \\ LL_6 \\ L \end{bmatrix} \quad (3.52)$$

In the procedure of space resection by direct solution accuracy is not the main consideration and camera interior parameters can be ignored (such as the principal point offset  $\Delta x_p, \Delta y_p$ ) or fixed (such as principal distance  $c$ ) at this stage.

### 3.3.3 Discussion

The two different methods used in the resection will give different results. The difference may not be significant. But theoretically the iterative method is a rigorous least squares process since the sum of squares of residuals is minimised on the camera image plane (observations), while the direct solution does not achieve this. However the direct solution does not need starting values which the iterative solution requires. A good combination could be using direct solution first to obtain the starting values the camera exterior parameters and then further adjusted with the iterative process.

If both the camera parameters and the 3D coordinates of the object points are unknown, they can be treated as variables at the same time in the collinearity equations and solved simultaneously provided that enough observations are available. That leads to the well known *bundle adjustment*.

## 3.4 The bundle adjustment

The bundle adjustment, developed by D.C. Brown in the 1960's has been widely used in the aerotriangulation and self-calibration of the systematic errors which led to substantial improvements in accuracies of aerotriangulation and mapping (Brown 1976). It has also been widely used in the close range industrial photogrammetry (Granshaw 1980; Karara 1989; Fraser 1992; Atkinson 1996) and has been found to be a powerful tool in the high accuracy 3D measurement. Figure 3-6 illustrates the geometric network of the bundle adjustment.

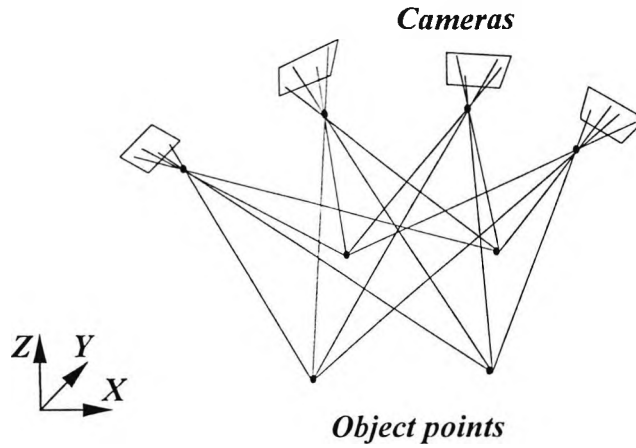


Figure 3-6 The geometric network of the bundle adjustment

Supposing  $m$  cameras are used to measure  $n$  object points. If all of these object points appear on all of the cameras, there will be totally  $2mn$  equations and  $(3n+6m)$  unknown parameters to be solved (provided that the camera interior parameters are fixed). The number of equations  $2mn$  is usually much larger than the number of unknown parameters  $(3n+6m)$ . So these unknown parameters can be solved simultaneously. The collinearity equations (3.7) can generally be expressed as

$$f(x_1, x_2, l) = 0 \tag{3.53}$$

in which

$$x_1 = (X_1, Y_1, Z_1, X_2, Y_2, Z_2, \dots, X_n, Y_n, Z_n)$$

is a vector of the 3D coordinates of the object points,

$$x_2 = (X_{L1}, Y_{L1}, Z_{L1}, \omega_1, \phi_1, \kappa_1, X_{L2}, Y_{L2}, Z_{L2}, \omega_2, \phi_2, \kappa_2, \dots, X_{Lm}, Y_{Lm}, Z_{Lm}, \omega_m, \phi_m, \kappa_m)$$

is a vector of the camera exterior parameters, and

$$l = (x_{11}, y_{11}, \dots, x_{1n}, y_{1n}, \dots, x_{m1}, y_{m1}, \dots, x_{mn}, y_{mn})$$

is a vector of the measured image coordinates (2D observations).

The linearized functional model may be written as

$$\begin{bmatrix} A_1 & A_2 \end{bmatrix} \begin{bmatrix} \Delta x_1 \\ \Delta x_2 \end{bmatrix} = b \quad (3.54)$$

or

$$A\Delta x = b \quad (3.55)$$

in which

$$A_1 = \frac{\partial f}{\partial x_1} \quad (3.56)$$

is a  $2mn \times 3n$  submatrix derived in section 3.2, and

$$A_2 = \frac{\partial f}{\partial x_2} \quad (3.57)$$

is a  $2mn \times 6m$  submatrix derived in section 3.3.

The unknown parameters can then be estimated by the simultaneous least squares estimation provided that the number of observations is equal to, or more than, that of the unknown parameters and the starting values of these parameters are known. The corrections to the parameters are estimated by

$$\begin{aligned} \Delta x &= (A'W_1A)^{-1} A'W_1b \\ &= N^{-1} A'W_1b \end{aligned} \quad (3.58)$$

in which

$$\begin{aligned} N &= \begin{bmatrix} A_1'W_1A_1 & A_1'W_1A_2 \\ A_2'W_1A_1 & A_2'W_1A_2 \end{bmatrix} \\ &= \begin{bmatrix} A_{11} & A_{12} \\ A_{21} & A_{22} \end{bmatrix} \end{aligned} \quad (3.59)$$

Because of the special structure of the design matrix  $A$ , the structures of the matrices  $A_{11}$  and  $A_{22}$  are very special. Figure 3-7 illustrates the structures of the matrices  $A$ ,  $A_{11}$  and  $A_{22}$ .

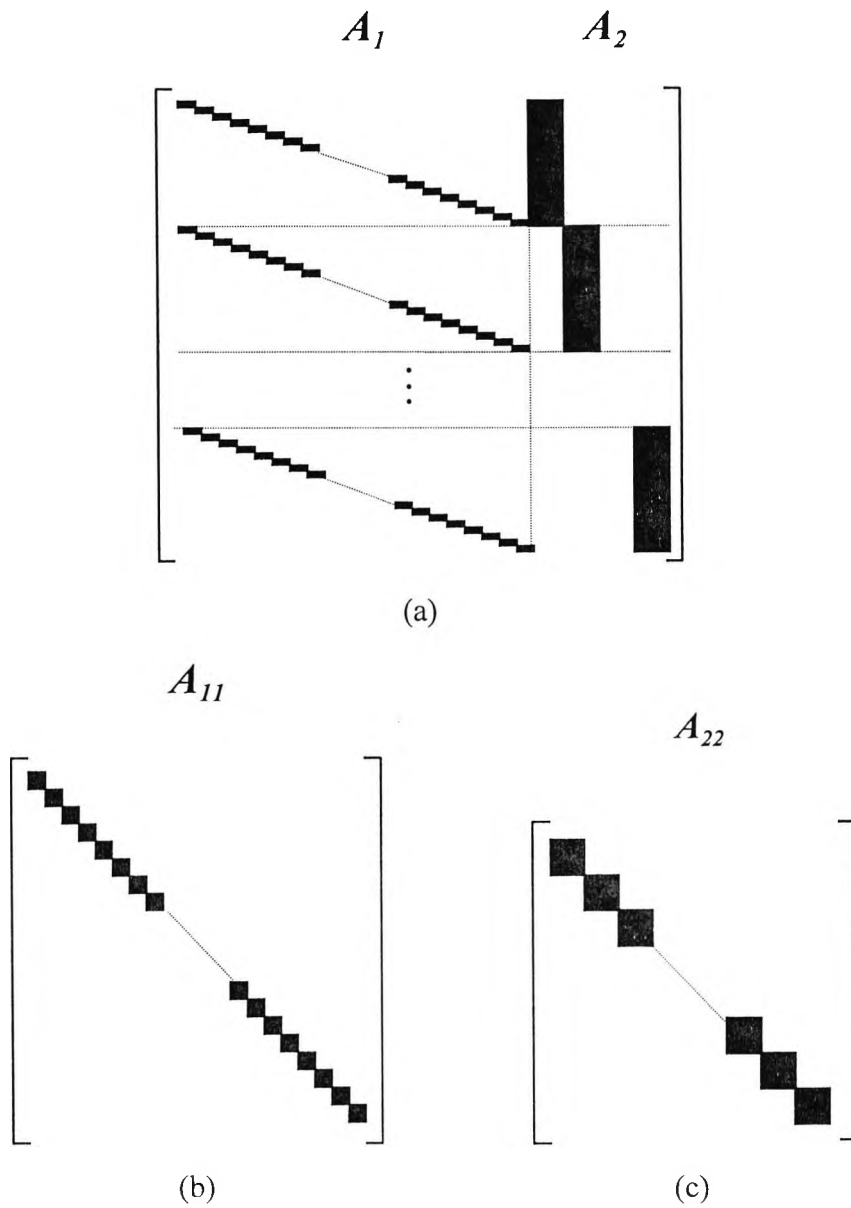


Figure 3-7

- (a) The structure of the design matrix  $A$  ( $A_1$  and  $A_2$ )
- (b) The structure of  $A_{11}$
- (c) The structure of  $A_{22}$

The small blocks in  $A_1$  are  $2 \times 3$  matrices and the big blocks in  $A_2$  are  $2n \times 6$  matrices. Both  $A_{11}$  and  $A_{22}$  are block diagonal matrices. The size of the blocks in  $A_{11}$  is  $3 \times 3$  and the size of the blocks in  $A_{22}$  is  $6 \times 6$ .

The submatrices in  $A_{12}$  are formed by the products of the transposes of the small blocks (size of  $2 \times 3$ ) in  $A_1$  and their corresponding blocks (size of  $2 \times 6$ ) in  $A_2$ . If an object point does not appear on a particular image, the corresponding submatrix (size of  $3 \times 6$ ) in  $A_{12}$  is null. This is the usual case in aerial photogrammetry which makes  $A_{12}$  regular and advantages can be taken from this fact (Brown 1976). But in close range photogrammetry, most of the object points appear on all the images. Matrices  $A_{12}$  and  $A_{21}$  are almost full. Not much can be done about this.

The least squares adjustment of the unknown parameters requires a series of matrix processes. The most difficult work in terms of speed and memory is to derive the inverse of the coefficient matrix  $N$ . The size of  $N$  could easily be hundreds or even thousands in close range photogrammetry. It is very expensive for a computer to calculate the inverse of such a big matrix. However, because of its special structure advantage can be taken when calculating the inverse of the matrix  $N$ . One of the methods is inversion by partitioning (Frank Ayres 1962, Brown 1976, Granshaw 1980), which gives

$$\begin{aligned}
 N^{-1} &= \begin{bmatrix} A_{11} & A_{12} \\ A_{21} & A_{22} \end{bmatrix}^{-1} \\
 &= \begin{bmatrix} B_{11} & B_{12} \\ B_{21} & B_{22} \end{bmatrix}
 \end{aligned} \tag{3.60}$$

in which

$$\begin{cases}
 B_{11} = A_{11}^{-1} + A_{11}^{-1} A_{12} K^{-1} A_{21} A_{11}^{-1} \\
 B_{12} = -A_{11}^{-1} A_{12} K^{-1} \\
 B_{12} = B_{21}' \\
 B_{22} = K^{-1}
 \end{cases} \tag{3.61}$$

and

$$\mathbf{K} = \mathbf{A}_{22} - \mathbf{A}_{21}\mathbf{A}_{11}^{-1}\mathbf{A}_{12} \quad (3.62)$$

Since  $\mathbf{A}_{11}$  is a block diagonal matrix, its inverse can be computed by inverting  $n \ 3 \times 3$  small matrices, which provides a big saving of time and memory. Matrix  $\mathbf{K}$  is generally full with a size of  $6m \times 6m$ . Therefore the inverse of  $\mathbf{K}$  becomes the main cost of processing the matrices.

An alternative to calculating the inverse of  $\mathbf{N}$  is to calculate the  $\mathbf{B}$  matrices by

$$\begin{cases} \mathbf{B}_{11} = \mathbf{K}^{-1} \\ \mathbf{B}_{12} = -\mathbf{K}^{-1}\mathbf{A}_{12}\mathbf{A}_{22}^{-1} \\ \mathbf{B}_{21} = \mathbf{B}_{12}^t \\ \mathbf{B}_{22} = \mathbf{A}_{22}^{-1} + \mathbf{A}_{22}^{-1}\mathbf{A}_{21}\mathbf{K}^{-1}\mathbf{A}_{12}\mathbf{A}_{22}^{-1} \end{cases} \quad (3.63)$$

and

$$\mathbf{K} = \mathbf{A}_{11} - \mathbf{A}_{12}\mathbf{A}_{22}^{-1}\mathbf{A}_{21} \quad (3.64)$$

This time the inverse of  $\mathbf{A}_{22}$  can easily be obtained by computing the inverse of a series of  $6 \times 6$  small matrices. However the size of  $\mathbf{K}$  is  $3n \times 3n$  and the matrix is generally full, hence the inverse of  $\mathbf{K}$  could be very expensive to calculate since  $3n$  is normally much larger than  $6m$  in close range photogrammetry (e.g. when 5 images are taken to measure 100 object points). But it could be possible that  $6m$  is larger than  $3n$  in some special cases such as when hundreds of images are taken to measure only a few object points. In this case Eq (3.63) and (3.64) are more suitable for calculating the inverse of  $\mathbf{N}$ .

In real 3D measurement applications, the coordinates of the object points  $\mathbf{x}_i$  are more important than the camera parameters  $\mathbf{x}_2$ . The corrections of  $\mathbf{x}_i$  can be obtained by

$$\begin{aligned} \Delta \mathbf{x}_i &= \begin{bmatrix} \mathbf{B}_{11} & \mathbf{B}_{12} \end{bmatrix} \begin{bmatrix} \mathbf{A}_1^t \\ \mathbf{A}_2^t \end{bmatrix} \mathbf{W}_1 \mathbf{b} \\ &= (\mathbf{B}_{11}\mathbf{A}_1^t + \mathbf{B}_{12}\mathbf{A}_2^t) \mathbf{W}_1 \mathbf{b} \end{aligned} \quad (3.65)$$

and the cofactor matrix of the estimated coordinates is given by

$$\begin{aligned}
 Q_{x_i} &= (B_{11}A_1' + B_{12}A_2')W_1Q_b((B_{11}A_1' + B_{12}A_2')W_1)' \\
 &= (B_{11}A_1' + B_{12}A_2')W_1(A_1B_{11} + A_2B_{21}) \\
 &= B_{11}A_{11}B_{11} + B_{11}A_{12}B_{21} + B_{12}A_{21}B_{11} + B_{12}A_{22}B_{21}
 \end{aligned} \tag{3.66}$$

The computational complexity of the last three terms is directly proportional to  $6m \times (3n)^2$  provided that the right order is applied when products of matrices are calculated. The computational complexity of the first term is directly proportional to  $(3n)^3$  if the products of the matrices are calculated directly. This is normally too expensive. The complexity can be reduced to  $6m \times (3n)^2$  when  $B_{11}$  is replaced by Eq (3.61) and the right order is considered.

The full cofactor (covariance) matrix is necessary during the network design stage which gives not only the standard deviations of the estimated parameters but also the correlations between them. However, in many cases only the standard deviations of the estimated parameters are of interest. These are obtained from the diagonal elements of the covariance matrix which can be approximately estimated by the inverse of  $A_{11}$  and are easy to calculate since  $A_{11}$  is a block diagonal matrix. Simulation tests show that this approximation is good enough for a strong network.

### 3.5 Bundle adjustment with constraints

The foregoing discussion of the bundle adjustment is based on the assumption that the coefficient matrix  $N$  is non-singular. However, photogrammetric observations are obtained from images which do not include any information in the object space to define a datum. If control points are involved in the bundle adjustment the datum problem may be solved. Otherwise constraints must be applied to remove the rank defects of  $N$  and make it possible to estimate the unknown parameters. Inner constraints are often used for the unbiased free network adjustment. Inner constraints can be applied to the object points or to the camera exterior parameters, or to both.

### 3.5.1 Inner constraints on the object points

When inner constraints are applied to the 3D coordinates of all the object points and treated as additional observations, the extended observation equations can be written as

$$\begin{bmatrix} A_1 & A_2 \\ G_1 & 0 \end{bmatrix} \begin{bmatrix} \Delta x_1 \\ \Delta x_2 \end{bmatrix} = \begin{bmatrix} b \\ 0 \end{bmatrix} \quad (3.67)$$

or

$$A_{g_1} \Delta x = b_{g_1} \quad (3.68)$$

where  $G_1$  is a  $7 \times 3n$  matrix which has been given in section 2.8.1. By applying inner constraints the unknown parameters can then be estimated. Noting that the last seven equations must be satisfied exactly, i.e., the residuals are zero, the unknown parameters are estimated by normal least square adjustment, i.e.,

$$\Delta x = (A_{g_1}' W_{g_1} A_{g_1})^{-1} A_{g_1}' W_{g_1} b_{g_1} \quad (3.69)$$

in which

$$W_{g_1} = \begin{bmatrix} W_1 & \\ & I_{7 \times 7} \end{bmatrix} \quad (3.70)$$

Therefore

$$\Delta x = \begin{bmatrix} A_1' W_1 A_1 + G_1' G_1 & A_1' W_1 A_2 \\ A_2' W_1 A_1 & A_2' W_1 A_2 \end{bmatrix}^{-1} \begin{bmatrix} A_1' G_1' \\ A_2' 0 \end{bmatrix} \begin{bmatrix} W_1 & \\ & I_{7 \times 7} \end{bmatrix} \begin{bmatrix} b \\ 0 \end{bmatrix} \quad (3.71)$$

$$\begin{aligned}
 &= \begin{bmatrix} A_{11} + G_1'G_1 & A_{12} \\ A_{21} & A_{22} \end{bmatrix}^{-1} \begin{bmatrix} A_1'W_1 G_1' \\ A_2'W_1 \ 0 \end{bmatrix} \begin{bmatrix} b \\ 0 \end{bmatrix} \\
 &= \begin{bmatrix} A_{11}' & A_{12}' \\ A_{21}' & A_{22}' \end{bmatrix}^{-1} \begin{bmatrix} A_1' \\ A_2' \end{bmatrix} W_1 b \\
 &= N_{g_1}^{-1} A' W_1 b
 \end{aligned}$$

With  $G_1'G_1$  added to  $A_{11}$ ,  $N_{g_1}$  becomes non-singular. The same procedures can then be carried out as discussed in section 3.4 to obtain the adjusted 3D coordinates of the object points and the cofactor matrix. But this time the computing of the inverse of  $A_{11}'$  is more difficult since the special structure of  $A_{11}$  (a block diagonal matrix) is spoiled due to the addition of  $G_1'G_1$ .

### 3.5.2 Inner constraints on the camera exterior parameters

Inner constraints can also be applied to the positions  $(X_L, Y_L, Z_L)$  of all the cameras and treated as additional observations. The extended observation equations may be written as

$$\begin{bmatrix} A_1 & A_2 \\ 0 & G_2 \end{bmatrix} \begin{bmatrix} \Delta x_1 \\ \Delta x_2 \end{bmatrix} = \begin{bmatrix} b \\ 0 \end{bmatrix} \tag{3.72}$$

or

$$A_{g_2} \Delta x = b_{g_2} \tag{3.73}$$

where  $G_2$  is a  $7 \times 6m$  matrix and is given by

$$\mathbf{G}_2 = \begin{bmatrix} 1 & 0 & 0 & 1 & 0 & 0 & \cdots & 1 & 0 & 0 \\ 0 & 1 & 0 & 0 & 1 & 0 & \cdots & 0 & 1 & 0 \\ 0 & 0 & 1 & 0 & 0 & 1 & \cdots & 0 & 0 & 1 \\ 0 & \mathbf{Z}_{L1} & -\mathbf{Y}_{L1} \mathbf{0}_{7 \times 3} & 0 & \mathbf{Z}_{L2} & -\mathbf{Y}_{L2} \mathbf{0}_{7 \times 3} & \cdots & 0 & \mathbf{Z}_{Lm} & -\mathbf{Y}_{Lm} \mathbf{0}_{7 \times 3} \\ -\mathbf{Z}_{L1} & 0 & \mathbf{X}_{L1} & -\mathbf{Z}_{L2} & 0 & \mathbf{X}_{L2} & \cdots & -\mathbf{Z}_{Lm} & 0 & \mathbf{X}_{Lm} \\ \mathbf{Y}_{L1} & -\mathbf{X}_{L1} & 0 & \mathbf{Y}_{L2} & -\mathbf{X}_{L2} & 0 & \cdots & \mathbf{Y}_{Lm} & -\mathbf{X}_{Lm} & 0 \\ \mathbf{X}_{L1} & \mathbf{Y}_{L1} & \mathbf{Z}_{L1} & \mathbf{X}_{L2} & \mathbf{Y}_{L2} & \mathbf{Z}_{L2} & \cdots & \mathbf{X}_{Lm} & \mathbf{Y}_{Lm} & \mathbf{Z}_{Lm} \end{bmatrix} \quad (3.74)$$

The  $\mathbf{0}$ s in  $\mathbf{G}_2$  are submatrices with a size of  $7 \times 3$ , which means the corresponding elements concerning camera rotational parameters are zero. By applying inner constraints to the positions of the cameras the unknown parameters can now be estimated. Again the last seven equations must be satisfied exactly, i.e., the residuals are zero, the unknown parameters are estimated by normal least squares adjustment, i.e.,

$$\Delta \mathbf{x} = (\mathbf{A}'_{g_2} \mathbf{W}_{g_2} \mathbf{A}_{g_2})^{-1} \mathbf{A}'_{g_2} \mathbf{W}_{g_2} \mathbf{b}_{g_2} \quad (3.75)$$

in which  $\mathbf{W}_{g_2}$  has the same format as  $\mathbf{W}_{g_1}$  given by (3.70). So

$$\begin{aligned} \Delta \mathbf{x} &= \begin{bmatrix} \mathbf{A}'_1 \mathbf{W}_1 \mathbf{A}_1 & \mathbf{A}'_1 \mathbf{W}_1 \mathbf{A}_2 \\ \mathbf{A}'_2 \mathbf{W}_1 \mathbf{A}_1 & \mathbf{A}'_2 \mathbf{W}_1 \mathbf{A}_2 + \mathbf{G}'_2 \mathbf{G}_2 \end{bmatrix}^{-1} \begin{bmatrix} \mathbf{A}'_1 \mathbf{0} \\ \mathbf{A}'_2 \mathbf{G}'_2 \end{bmatrix} \begin{bmatrix} \mathbf{W}_1 \\ \mathbf{I}_{7 \times 7} \end{bmatrix} \begin{bmatrix} \mathbf{b} \\ \mathbf{0} \end{bmatrix} \quad (3.76) \\ &= \begin{bmatrix} \mathbf{A}_{11} & \mathbf{A}_{12} \\ \mathbf{A}_{21} & \mathbf{A}_{22} + \mathbf{G}'_2 \mathbf{G}_2 \end{bmatrix}^{-1} \begin{bmatrix} \mathbf{A}'_1 \mathbf{W}_1 \mathbf{0} \\ \mathbf{A}'_2 \mathbf{W}_1 \mathbf{G}'_2 \end{bmatrix} \begin{bmatrix} \mathbf{b} \\ \mathbf{0} \end{bmatrix} \\ &= \begin{bmatrix} \mathbf{A}_{11} & \mathbf{A}_{12} \\ \mathbf{A}_{21} & \mathbf{A}'_{22} \end{bmatrix}^{-1} \begin{bmatrix} \mathbf{A}'_1 \\ \mathbf{A}'_2 \end{bmatrix} \mathbf{W}_1 \mathbf{b} \\ &= \mathbf{N}_{g_2}^{-1} \mathbf{A}' \mathbf{W}_1 \mathbf{b} \end{aligned}$$

The addition of  $\mathbf{G}'_2 \mathbf{G}_2$  to  $\mathbf{A}_{22}$  removes the rank defects of  $\mathbf{N}_{g_2}$  and makes it non-singular.

The adjusted 3D coordinates of the object points can then be obtained. Since the structure of  $\mathbf{A}_{11}$  remains unchanged, it is still a block diagonal matrix, the inverse of  $\mathbf{N}_{g_2}$  can be calculated by partitioning via Eq (3.61) and (3.62).

### 3.5.3 Discussion

Inner constraints can be applied in the bundle adjustment to remove the rank defects of the design matrix, so the unknown parameters can be estimated. The datum is defined by the starting values. Because the starting values are arbitrary, the estimated results are in an arbitrary datum. Different starting values lead to different results. But they are equivalent in the sense of least squares and the shape of the object remains unchanged.

With the additional seven constraint equations, the total number of equations used for the  $(3n+6m)$  parameters is  $(2mn+7)$ . The following conditions must be satisfied to enable the bundle adjustment to work, i.e.,

$$2mn + 7 \geq 3n + 6m \quad (3.77)$$

which gives

$$n \geq 3 + \frac{2}{2m - 3} \quad (3.78a)$$

and

$$m \geq 1.5 + \frac{1}{n - 3} \quad (3.78b)$$

This means that minimum of four object points are required generally (when  $m \geq 3$ ) and minimum of five object points are needed if only two photographs are used, and minimum of two cameras are required generally (when  $n \geq 5$ ) and minimum of three cameras are needed if only four object points are involved. Figure 3-8 illustrates the feasible area (in which the unknown parameters can be solved) of the bundle adjustment.

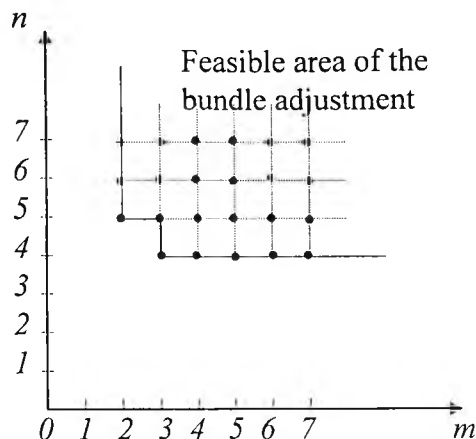


Figure 3-8 Feasible area of the bundle adjustment when applying inner constraints

But actually three object points are enough to determine the camera parameters (exterior parameters) provided that they all appear on the camera image plane and two images are adequate to solve the 3D coordinates of the object points. That implies enough information has been given to determine the unknown parameters with three object points and two cameras. But why can not these parameters be solved simultaneously by the bundle adjustment with inner constraints? Perhaps seven constraints are not enough.

When inner constraints are applied, the special structure of  $A_{11}$  or  $A_{22}$  is spoiled. This may make the computation of the inverse of the coefficient matrix  $N$  more complicated. An alternative method is to treat the coordinates of all object points as weighted observations which will keep  $A_{11}$  and  $A_{22}$  their special structure and take the advantages of the inverse by partitioning. This technique is termed the *unified bundle adjustment*.

### 3.6 The unified bundle adjustment

As mentioned in Chapter 2, in the unified least squares adjustment all the unknown parameters are treated as weighted observations. In the photogrammetric bundle adjustment these parameters are divided into two parts, the coordinates of the object points  $\mathbf{x}_1$  and the camera parameters  $\mathbf{x}_2$ . The weighted observations can be applied to the

object points or to the camera parameters. They can also be applied to object points and the camera parameters at the same time. But this is normally not necessary.

If the coordinates of the object points are treated as the observations, the additional observation equations are

$$x_i = x_i^0 \quad (3.79)$$

with associated weight matrix  $W_g$ . Since the coordinates of the object points are not measured beforehand they are treated as pseudo-observations.  $x_i^0$  will be the starting values and a unique weight  $g$  will be assigned to them. So the weight matrix is  $gI$ , where  $I$  is a  $3n \times 3n$  unit matrix. After linearization Eq (3.79) becomes

$$\Delta x_i = b_g \quad (3.80)$$

Therefore the extended observation equations are expressed as

$$\begin{bmatrix} A_1 & A_2 \\ I & 0 \end{bmatrix} \begin{bmatrix} \Delta x_1 \\ \Delta x_2 \end{bmatrix} = \begin{bmatrix} b \\ b_g \end{bmatrix} \quad (3.81)$$

or

$$A_u \Delta x = b_u \quad (3.82)$$

The unknown parameters are estimated by

$$\Delta x = (A_u^t W_u A_u)^{-1} A_u^t W_u b_u \quad (3.83)$$

where

$$W_u = \begin{bmatrix} W_l \\ gI \end{bmatrix} \quad (3.84)$$

So

$$\begin{aligned}
 \Delta \mathbf{x} &= \begin{bmatrix} \mathbf{A}'_1 \mathbf{W}_l \mathbf{A}_1 + g\mathbf{I} & \mathbf{A}'_1 \mathbf{W}_l \mathbf{A}_2 \\ \mathbf{A}'_2 \mathbf{W}_l \mathbf{A}_1 & \mathbf{A}'_2 \mathbf{W}_l \mathbf{A}_2 \end{bmatrix}^{-1} \begin{bmatrix} \mathbf{A}'_1 & \mathbf{I} \\ \mathbf{A}'_2 & \mathbf{0} \end{bmatrix} \begin{bmatrix} \mathbf{W}_l \\ g\mathbf{I} \end{bmatrix} \begin{bmatrix} \mathbf{b} \\ \mathbf{b}_g \end{bmatrix} \\
 &= \begin{bmatrix} \mathbf{A}_{11} + g\mathbf{I} & \mathbf{A}_{12} \\ \mathbf{A}_{21} & \mathbf{A}_{22} \end{bmatrix}^{-1} \begin{bmatrix} \mathbf{A}'_1 \\ \mathbf{A}'_2 \end{bmatrix} \mathbf{W}_l \mathbf{b} \\
 &= \mathbf{N}_u^{-1} \mathbf{A}' \mathbf{W}_l \mathbf{b}
 \end{aligned} \tag{3.85}$$

The addition of  $g\mathbf{I}$  to  $\mathbf{A}_{11}$  removes the column rank defects of  $\mathbf{N}$  and makes  $\mathbf{N}_u$  non-singular. Since  $g\mathbf{I}$  is a diagonal matrix, the structure of  $\mathbf{A}_{11}$  remains unchanged. The inverse of  $\mathbf{N}_u$  can easily be calculated by partitioning from Eq (3.61). The cofactor matrix of  $\mathbf{x}_l$  is obtained by Eq (3.66).

In the unified bundle adjustment, the weight factor  $g$  plays an important role. If  $g$  is assigned a big value, the parameters will be tied on their starting values, more iterations are required during the adjustment process and the results will be affected by these pseudo-observations, which is obviously not expected in the unified bundle adjustment. When  $g$  approaches infinity, the parameters will not be allowed to be adjusted at all. On the other hand if  $g$  is very small and approaches zero, which means the pseudo-observations are given a very large variance, the parameters are allowed to be adjusted freely by the real observations. It then becomes a free network adjustment. This is what is expected. But  $g$  cannot be zero. Otherwise  $\mathbf{N}_u$  will be singular. Theoretically the smaller  $g$  is the better. But practically  $g$  cannot be too small to make  $\mathbf{N}_u$  ill-conditioned otherwise the inverse of  $\mathbf{N}_u$  is unobtainable numerically due to the limitation of the computers.

Simulation tests show when an appropriate  $g$  (it is available in a very large range) is assigned the unified bundle adjustment will give numerically the same results as that obtained from the traditional bundle adjustment with inner constraints. However, the computational procedures are simplified and the speed is increased significantly.

With the unified bundle adjustment rank defects of the design matrix are removed. The datum is defined by the starting values of coordinates of the object points as in the

bundle adjustment with inner constraints. With additional  $3n$  pseudo-observations, the total number of the observation equations is  $2mn+3n$ , the inequality (3.77) becomes

$$2mn + 3n \geq 3n + 6m \quad (3.86)$$

which gives

$$n \geq 3 \quad \text{and} \quad m \geq 1 \quad (3.87)$$

This means that three is the minimum number of object points required for the unified bundle adjustment no matter how many cameras are used. This reflects the real situation of the simultaneous bundle adjustment. Figure 3-9 illustrates the feasible area of the unified bundle adjustment.

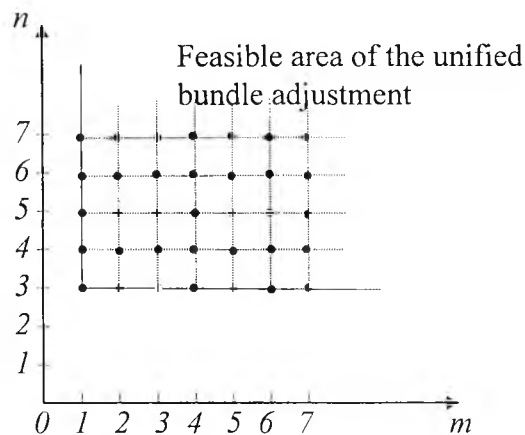


Figure 3-9 Feasible area of the unified bundle adjustment

### 3.7 Summary of the chapter

Close range photogrammetric 3D measurements are based upon image observations. The purpose is to obtain 3D coordinates of object points. The collinearity equations provide the basic functional model in close range photogrammetry which establish the relationship between the 2D image observations and the 3D coordinates to be estimated. The DLT is a modified model from the collinearity equations which encompasses some camera interior parameters in the 11 DLT parameters without additional consideration.

Once a functional model is defined, the least squares method can be used to estimate the unknown parameters from the known observations. Spatial control points may be required to define a datum and initialise camera exterior parameters. Resection is normally the first step to obtain the camera exterior parameters. It is usually followed by intersection to compute the 3D coordinates of the object points. This procedure provides the easiest method of 3D measurement, especially when the DLT model is used. However the results provided by this method are not likely to be precise. The precision of the estimated results is influenced not only by the 2D image observations but also by the control points. Furthermore when the unknown parameters are estimated by direct solution, rather than iterative solution, the least squares process is not applied to the sum of the squares of the residuals on the image planes (observations) and the precision of the estimated results cannot be evaluated. Therefore this method is not considered to be rigorous. The results may be used as the starting values of the bundle adjustment, a rigorous least squares estimation process.

In the bundle adjustment, the 3D coordinates of the object points and the camera parameters are all treated as unknowns. Least squares adjustment will adjust these unknown parameters according to the image observations. Constraints are required in the bundle adjustment to remove the rank defects of the design matrix; otherwise the unknown parameters are not estimable. Inner constraints are usually applied in the bundle adjustment for the free network solution. It is normal to apply inner constraints on the object points. In this case the full matrix  $A'_{II}$  (originally a block diagonal matrix) makes the computation process very expensive. However, the full covariance of the 3D

coordinates is available. Constraints can also be applied to the camera exterior parameters (positions only). It is useful when  $6m$  is less than  $3n$ , which is usual in close range photogrammetry, to save computation time. But the full covariance matrix of the 3D coordinates may not be available. The results from the inner constrained bundle adjustment are in an arbitrary coordinate system. A coordinate transformation may be required to relate the results to a given coordinate system. With spatial control points involved in the bundle adjustment, a datum can be defined properly and the results will be related to the controls. But the precision of the estimated results will be influenced by the controls. It is possible to include high precision controls to enhance the bundle adjustment results. However, it is often the case in close range photogrammetry that the precision of the controls may not be as good as that of the image observations. Therefore the results may be biased by the controls.

The structure of the coefficient matrix in the photogrammetric bundle adjustment is very special. Advantages can be taken by partitioning when calculating the inverse of the coefficient matrix. However with the inner constrained bundle adjustment the special structures of the matrices  $A_{11}$  and  $A_{22}$  are changed. The unified bundle adjustment is a method which can solve the problem. In the unified bundle adjustment, the 3D coordinates are treated as pseudo-observations with a small weight. In this way the datum is defined by the starting values of the 3D coordinates and the structure of the matrices  $A_{11}$  and  $A_{22}$  remain unchanged. When the weight of the pseudo-observations is small enough, its influence can be ignored. Therefore it is a free network adjustment process. The unified bundle adjustment method will give numerically the same results as the normal bundle adjustment with inner constraints, but with a significant saving of computation time.

The bundle adjustment is a simultaneous least squares process which is very expensive in terms of time and memory. But it is rigorous and the full covariance matrix is provided at the same time. If time and memory are not a concern, the bundle adjustment will provide satisfactory results. However, in the era of digital photogrammetry, when real-time 3D measurement is considered, more efficient methods have to be developed.

## Chapter 4

### Separate Least Squares Estimation

In Chapter 2, several methods of least squares were discussed. These methods have been widely used in surveying and photogrammetry for different purposes. However as far as speed is concern none of them are capable of dealing with real-time applications in close range photogrammetry. In this chapter an alternative method of least square estimation -- separate least squares estimation -- is introduced.

#### 4.1 Introduction

To introduce the method of the separate least squares estimation, let us first consider a set of linear equations with two variables

$$\begin{cases} 2x + y = 3 \\ x - 3y = -2 \end{cases} \quad (4.1)$$

The equations can be solved simultaneously by computing the inverse of the coefficient matrix (if it exists). Alternatively, the equations can be solved iteratively using the Jacobi method or the Gauss-Seidel method. Both methods are conditionally convergent as discussed in Chapter 2. In the Jacobi method and the Gauss-Seidel method, only one equation is used each time and one variable is solved (the other variable is considered as constant). Table 4-1 lists the iterative solution of  $x$  and  $y$  by the Gauss-Seidel method with  $(x, y) = (0, 0)$  as the starting values.

Table 4-1 The iterative solution by the Gauss-Seidel method

Iteration No.	$x$	$y$
0	0	0
1	1.5000	1.1667
2	0.9167	0.9722
3	1.0139	1.0046
4	0.9977	0.9992
5	1.0004	1.0001
6	0.9999	1.0000
7	1.0000	1.0000

Now consider another strategy. Instead of using one equation, both equations are used at the same time for each variable. Obviously this variable will be over-determined. This reminds us the redundant measurement. Another criterion is required for a unique solution. This criterion is least squares.

Firstly, suppose  $y$  is known (from a starting value). The terms with  $y$  are moved to the right hand sides of the equations. So Eq (4.1) becomes

$$\begin{cases} 2x = 3 - y \\ x = -2 + 3y \end{cases} \quad (4.2)$$

or

$$A_x x = b_x \quad (4.3)$$

where

$$A_x = \begin{bmatrix} 2 \\ 1 \end{bmatrix} \quad \text{and} \quad b_x = \begin{bmatrix} 3 - y \\ -2 + 3y \end{bmatrix}$$

The unknown parameter  $x$  is over-determined from above equations since  $y$  is known. Now least squares can be used to determine  $x$  uniquely, i.e.,

$$\begin{aligned}x &= (A'_x A_x)^{-1} A'_x b_x \\ &= \frac{1}{5}(y + 4)\end{aligned}\quad (4.4)$$

This suggests the iteration

$$x^{[k+1]} = \frac{1}{5}(y^{[k]} + 4) \quad (4.5)$$

After obtaining  $x$ , it is considered as known to determine  $y$ . So  $y$  can also be solved uniquely by least squares from Eq (4.1) after moving the terms with  $x$  to the right hand sides of the equations, i.e.,

$$\begin{aligned}y &= (A'_y A)^{-1} A'_y b_y \\ &= \frac{1}{10}(x + 9)\end{aligned}\quad (4.6)$$

This suggests the iteration

$$y^{[k+1]} = \frac{1}{10}(x^{[k+1]} + 9) \quad (4.7)$$

With Eq (4.5) and (4.7) the variables  $x$  and  $y$  are solved separately. Table 4-2 lists the separate solution by least squares with the starting values  $(x^{[0]}, y^{[0]}) = (0, 0)$ .

Table 4-2 The separate solution  
by least squares

Iteration No.	$X$	$y$
0	0	0
1	0.8000	0.9800
2	0.9960	0.9996
3	0.9999	1.0000
4	1.0000	1.0000

Now consider a general case

$$\begin{cases} a_{11}x + a_{12}y = b_1 \\ a_{21}x + a_{22}y = b_2 \end{cases} \quad (4.8)$$

Again solve  $x$  and  $y$  separately by least squares. The separate equations are given by

$$x^{[k+1]} = (A_x^t A_x)^{-1} A_x^t (b - A_y y^{[k]}) \quad (4.9)$$

$$y^{[k+1]} = (A_y^t A_y)^{-1} A_y^t (b - A_x x^{[k+1]}) \quad (4.10)$$

in which

$$A_x = \begin{bmatrix} a_{11} \\ a_{21} \end{bmatrix}, \quad A_y = \begin{bmatrix} a_{12} \\ a_{22} \end{bmatrix} \quad \text{and} \quad b = \begin{bmatrix} b_1 \\ b_2 \end{bmatrix}$$

Eq (4.9) and (4.10) can further be rearranged as

$$x^{[k+1]} = C y^{[k]} + D \quad (4.11)$$

$$y^{[k+1]} = E x^{[k+1]} + F \quad (4.12)$$

in which

$$\begin{cases} C = -(A_x^t A_x)^{-1} A_x^t A_y \\ D = (A_x^t A_x)^{-1} A_x^t b \\ E = -(A_y^t A_y)^{-1} A_y^t A_x \\ F = (A_y^t A_y)^{-1} A_y^t b \end{cases} \quad (4.13)$$

It is noticed that  $C$ ,  $D$ ,  $E$  and  $F$  are all  $1 \times 1$  matrices and they will remain unchanged during the separate process. After each iteration,  $x$  and  $y$  are re-estimated. So Eq (4.11) and (4.12) can be used successively to refine  $x$  and  $y$  until a convergent requirement is met.

If we further substitute  $x^{[k+1]}$  in Eq (4.12) from Eq (4.11), we have

$$y^{[k+1]} = CEy^{[k]} + DE + F \quad (4.14)$$

For convergence of  $y$ , the necessary and sufficient condition is (Jacques & Judd, 1987)

$$CE < 1 \quad (4.15)$$

i.e.,

$$(A_x^t A_y)(A_y^t A_x) < (A_x^t A_x)(A_y^t A_y) \quad (4.16)$$

Similarly, for convergence of  $x$ , the necessary and sufficient condition can also be obtained and it is found to be the same as given by the inequality (4.16). This condition can also be expressed as

$$(a_{11}a_{12} + a_{21}a_{22})^2 < (a_{11}^2 + a_{21}^2)(a_{12}^2 + a_{22}^2) \quad (4.17)$$

By expanding and eliminating the identical terms from both sides, the convergence condition becomes

$$(a_{11}a_{22} - a_{21}a_{12})^2 > 0 \quad (4.18)$$

which is equivalent to

$$\det A \neq 0 \quad (4.19)$$

It means that this separate least squares process will always converge with any starting values provided that the coefficient matrix of the linear system is non-singular. Although the conclusion is derived from a  $2 \times 2$  linear system, it should be possible to prove that it holds for any linear system. One thousand simulated linear system have

been tested. It is found that the solutions from the separate least squares estimation always converge to the right results even with ridiculous starting values. The method can also be used to solve non-linear equations.

This separate process is based on least squares and the unknown parameters are estimated separately. So this method is referred to as the *separate least squares estimation*. The term *separate LSE* is used afterwards.

If the functional model itself needs to be solved by least squares, the separate LSE method can be used directly.

## 4.2 Separate LSE

The separate LSE method is similar to the sequential LSE method since it is also a technique of division. However, instead of dividing the observations, the unknown parameters are divided into groups and estimated separately. When estimating one group of the unknown parameters, other parameters are considered as constants. These constants could either be the starting values or estimated results from the last iteration. The updated parameters are then used as constants in the functional model to estimate other unknown parameters. Each time only a part of the unknown parameters are estimated. So the size of the coefficient matrix is reduced.

Consider a measurement system with 1000 unknown parameters to be estimated by the least square estimation. With the simultaneous solution the computational complexities are:

$$\begin{aligned} & 1000^3 = 10^9 \quad (\text{time}) \\ \text{and} & \quad 1000^2 = 10^6 \quad (\text{memory}) \end{aligned}$$

Using the separate LSE, if the unknown parameters are divided into 100 groups with 10 parameters in each group, the computational complexities for one iteration are:

$$100 \times 10^3 = 10^5 \quad (\text{time})$$

and

$$10^2 \quad (\text{memory})$$

The separate LSE is an iterative process which estimates the unknown parameters iteratively and separately. But the iterations used here are different from the iterations used in the simultaneous LSE which are caused by the non-linear functional model. Even with a linear functional model iterations are still required by the separate LSE but not by the simultaneous method. The number of iterations required for the separate LSE is normally more than the simultaneous solution. But it is so quick for each iteration that the separate LSE is much faster, especially in close range photogrammetry.

#### 4.2.1 Linear case

For a linear system, the functional model may be expressed as

$$A\mathbf{x} = \mathbf{b} \quad (4.20)$$

in which

$\mathbf{x} = (x_1, x_2, \dots, x_u)^t$  is a vector of the unknown parameters,  
 $A$  is a  $m \times u$  coefficient matrix ( $m > u$ ), and  
 $\mathbf{b}$  is a  $m \times 1$  vector of the measured elements (observations).

To estimate the unknown parameters separately,  $\mathbf{x}$  may be divided into  $K$  groups, i.e.,  $\mathbf{x} = (\mathbf{X}_1, \mathbf{X}_2, \dots, \mathbf{X}_K)$  and  $A$  into  $A = (A_1, A_2, \dots, A_K)$  accordingly. Therefore Eq (4.20) becomes

$$A_1 X_1 + A_2 X_2 + \dots + A_K X_K = b \quad (4.21)$$

Suppose there are  $q$  parameters in  $\mathbf{X}_i$ , so  $A_i$  will be an  $m \times q$  matrix. When estimating  $\mathbf{X}_i$ , other parameters are considered as constants and the corresponding terms are moved to the right hand side of Eq (4.21), i.e.,

$$A_i X_i^{[k+1]} = b_i \quad (4.22)$$

in which

$$b_i = b - A_j X_j \quad (4.23)$$

and

$$A_j X_j = \sum_{\substack{j=1 \\ j \neq i}}^K A_j X_j^{[k]} \quad (4.24a)$$

or

$$A_j X_j = \sum_{j=1}^{i-1} A_j X_j^{[k+1]} + \sum_{j=i+1}^K A_j X_j^{[k]} \quad (4.24b)$$

The former is like the Jacobi iteration and the later is like the Gauss-seidel iteration in the sense of treating updated parameters. The superscripts  $[k]$  and  $[k+1]$  denotes the  $k$ th and  $(k+1)$ st iterations.

Since  $A_j X_j$  is non-stochastic, so  $W_b = W_b$ . By the linear least square estimation  $X_i$  is solved as

$$\begin{aligned} X_i^{[k+1]} &= (A_i' W_b A_i)^{-1} A_i' W_b b_i \\ &= (A_i' W_b A_i)^{-1} A_i' W_b (b - \sum_{\substack{j=1 \\ j \neq i}}^K A_j X_j^{[k]}) \end{aligned} \quad (4.25a)$$

or

$$X_i^{[k+1]} = (A_i' W_b A_i)^{-1} A_i' W_b (b - \sum_{j=1}^i A_j X_j^{[k+1]} - \sum_{j=i+1}^K A_j X_j^{[k]}) \quad (4.25b)$$

The size of  $A_i' W_b A_i$  is  $q \times q$ , much smaller than that of  $A' W_b A$ , which is  $m \times m$  for the simultaneous LSE. This is why time and memory are saved. After  $X_i$  is solved, it is considered as constant to solve other parameters. Since the constants assigned to the unknown parameters are starting values or the least squares estimates from previous iterations, based on these constants the least squares estimation of the current iteration

may not be the final results unless several iterations have been applied. The iterative process stops when the corrections for all the parameters are less than a given significant value.

By the general law of propagation of covariance, the cofactor matrix of the estimated parameters  $X_i$  is obtained by

$$Q_{X_i} = (A_i' W_b A_i)^{-1} A_i' W_b Q_{b_i} W_b A_i (A_i' W_b A_i)^{-1} \quad (4.26)$$

When estimating  $X_i$ , other parameters are considered as non-stochastic constants. But their stochastic models are introduced after the first iteration since their results can be estimated by the least squares process. From Eq(4.23) we have

$$Q_{b_i} = Q_b + A_J Q_J A_J' \quad (4.27)$$

in which

$$A_J = [A_1 \ A_2 \ \dots \ A_k]_{\text{without } A_i} \quad (4.28)$$

and

$$Q_J = \begin{bmatrix} Q_{X_1} & & & \\ & Q_{X_2} & & \\ & & \dots & \\ & & & Q_{X_k} \end{bmatrix}_{\text{without } Q_{X_i}} \quad (4.29)$$

Replacing  $Q_{b_i}$  in Eq (4.26) from Eq (4.27) and expressing  $(A_i' W_b A_i)^{-1}$  by  $N_i$  gives

$$Q_{X_i} = N_i + N_i A_i' A_J Q_J A_J' A_i N_i \quad (4.30)$$

After each iteration the estimated results (the solution and the cofactor matrix) for all the unknown parameters will be updated. The results will finally converge to the same solutions obtained from the simultaneous LSE.

It is noticed that the full cofactor (covariance) matrix is not available with separate LSE. The cofactor matrix of the estimated parameters is given by

$$Q_x = \begin{bmatrix} Q_{x_1} & & & \\ & Q_{x_2} & & \\ & & \dots & \\ & & & Q_{x_k} \end{bmatrix} \quad (4.31)$$

The correlation between the parameters, which are not in the same group, is not obtained.

If the separate LSE is compared with the iterative LSE it is found that the solution given by the separate LSE Eq (4.25) is identical to that given by LSE with block Jacobi iteration Eq (2.83) or block Gauss-Seidel iteration Eq (2.86) (Harley 1997). To show the equivalence of the two solutions, the least squares estimation of Eq (4.20) may be written as

$$(A'W_bA)x = A'W_b b \quad (4.32)$$

i.e.,

$$Nx = d \quad (4.33)$$

where

$$N = A'W_bA \quad \text{and} \quad d = A'W_b b .$$

In this case the solution of Eq (4.20) will be a least squares estimation. Dividing  $x$  into  $K$  groups as in Eq (4.21) and Eq (4.22),  $N$  and  $d$  become

$$N = \begin{bmatrix} A_1' W_b A_1 & A_1' W_b A_2 & \cdots & A_1' W_b A_k \\ A_2' W_b A_1 & A_2' W_b A_2 & \cdots & A_2' W_b A_k \\ \cdots & \cdots & \cdots & \cdots \\ A_k' W_b A_1 & A_k' W_b A_2 & \cdots & A_k' W_b A_k \end{bmatrix} \quad (4.34a)$$

and

$$d = \begin{bmatrix} A_1' W_b b \\ A_2' W_b b \\ \vdots \\ A_k' W_b b \end{bmatrix} \quad (4.34b)$$

so that  $N_{ij} = A_i' W_b A_j$  and  $d_i = A_i' W_b b$ .

If a Jacobi iteration Eq (2.83) is used, the solution of the linear equations (4.33) will be given by

$$X_i^{[k+1]} = (A_i' W_b A_i)^{-1} (A_i' W_b b - \sum_{\substack{j=1 \\ j \neq i}}^K A_i' W_b A_j X_j^{[k]}) \quad (4.35a)$$

This solution is identical to that given by Eq (4.25a). With the Gauss-seidel iteration of Eq (2.86), the solution will be

$$X_i^{[k+1]} = (A_i' W_b A_i)^{-1} (A_i' W_b b - \sum_{j=1}^{i-1} A_i' W_b A_j X_j^{[k+1]} - \sum_{j=i+1}^K A_i' W_b A_j X_j^{[k]}) \quad (4.35b)$$

This solution is identical to that given by Eq (4.25b).

Since matrix  $(A'WA)$  is symmetric and positive definite, this iterative process will always converge (Phillips & Cornelius 1986).

### 4.2.2 Non-linear case

For the non-linear functional models, the general observation equations can be expressed as

$$f(\mathbf{x}) = l \quad (4.36)$$

To estimate the unknown parameters separately,  $\mathbf{x}$  is divided into  $k$  groups, i.e.,  $\mathbf{x} = (X_1, X_2, \dots, X_k)$ . When estimating  $X_i$ , other parameters will be considered as constants. The linearized observation equations for estimating  $X_i$  become

$$A_i \Delta X_i = b_i \quad (4.37)$$

in which

$$A_i = \left( \frac{\partial f}{\partial X_i} \right)_0 \quad \text{and} \quad b_i = l - f(\mathbf{x}^0)$$

LSE can then be applied, i.e.,

$$\Delta X_i = (A_i^t W_i A_i)^{-1} A_i^t W_i b_i \quad (4.38)$$

and

$$X_i = (X_i)_0 + \Delta X_i \quad (4.39)$$

After  $X_i$  is adjusted, it is considered as constant to adjust other parameters. The iterative process terminates when the given stop criteria are met.

Unlike the iterative LSE discussed in section 2.5, which is applied to the inner iterations, the separate LSE combines the inner iteration and the outer iteration into one iteration. Instead of using one equation for each parameter all the equations are used. The separate LSE has the same advantage as the iterative LSE of saving memory. The size of  $A_i^t W_i A_i$  is  $q \times q$ , much smaller than that of  $A^t W_B A$ , which is  $m \times m$  for the

simultaneous LSE. The convergent speed of the separate LSE is very fast. It is much faster not only than that of the iterative LSE but also than that of the simultaneous LSE in some cases.

It is important to point out that  $A_i$  and  $b_i$  will change, and therefore have to be recomputed for each iteration.

By the general law of propagation of covariance, the cofactor matrix of the parameters  $X_i$  is obtained by

$$Q_{X_i} = Q_{\Delta X_i} = N_i A_i^t W_i Q_b W_i A_i N_i \quad (4.40)$$

Since  $b = l - f(x^0)$ , so

$$Q_b = Q_l + A_j Q_j A_j^t \quad (4.41)$$

in which

$$A_j = [A_1 \ A_2 \ \dots \ A_k]_{\text{without } A_i} \quad (4.42)$$

and

$$Q_j = \begin{bmatrix} Q_{X_1} & & & \\ & Q_{X_2} & & \\ & & \dots & \\ & & & Q_{X_k} \end{bmatrix}_{\text{without } Q_{X_i}} \quad (4.43)$$

Replacing  $Q_b$  in Eq(4.40) from Eq(4.41) and expressing  $(A_i^t W_i A_i)^{-1}$  by  $N_i$  gives

$$Q_{X_i} = N_i + N_i A_i^t A_j Q_j A_j^t A_i N_i \quad (4.44)$$

After each iteration the estimated results (the solution and the cofactor matrix) for all the unknown parameters are adjusted and refined. The results will finally converge at the same results obtained from the simultaneous LSE. Several numerical examples

(from simple surveying to complicated close range photogrammetry) are given in the thesis to verify this.

As with the linear case, the full cofactor (covariance) matrix is not available with separate LSE. The cofactor matrix of the parameters is given by

$$Q_x = \begin{bmatrix} Q_{x_1} & & & \\ & Q_{x_2} & & \\ & & \ddots & \\ & & & Q_{x_k} \end{bmatrix} \quad (4.45)$$

The correlations between the parameters which are not in the same group are not obtainable.

For a strong measurement network (which is normal in close range photogrammetry), the value of the second term in Eq (4.44) is much smaller than that of the first term. No significant difference is made by ignoring the second term in Eq (4.44). Based on this approximation, the block diagonal elements in the cofactor matrix can be adequately estimated by

$$Q_{x_i} = N_i = (A_i' W_i A_i)^{-1} \quad (4.46)$$

With the iterative LSE, two iterative loops are required as mentioned in 2.5. One is the outer iteration for linearization; the other is the inner iteration (Jacobi method or Gauss-Seidel method) which is used to solve the linearized equations. Therefore there are two convergence criteria, one for each iterative loop. The two criteria are checked during execution and the solution is reached when the convergence criterion of the outer iteration is met. With the separate LSE there is only one iterative loop, which is outer iteration, and one convergence criterion for the outer iteration. The inner iteration is merged with the outer iterative loop, since only one iteration is applied in the inner iteration. Therefore the separate LSE is a special case of the iterative LSE when it is used to solve non-linear equations.

### 4.3 Discussion

The separate LSE is a technique of division. Since the unknown parameters are divided into many groups and each time only some of the parameters are estimated, the size of the matrix to be inverted reduces, so the time and the memory required for each iteration is reduced. Normally more iterations are required for the separate LSE compared with the simultaneous LSE. However, the overall speed of convergence is much faster when the separate LSE is used in close range photogrammetry.

In the case of solving collinearity equations in close range photogrammetry, the unknown parameters can be divided into two groups, the coordinates of the object points and the camera parameters. Because of the block diagonal structure of the coefficient matrices, their inverses can be obtained by processing a series of small blocks with the size of  $3 \times 3$  and  $6 \times 6$ . The speed will be increased dramatically and the memory requirements reduced greatly.

The full covariance matrix is not available directly from the separate LSE. The cofactor matrix of the parameters  $Q_x$  is a block diagonal matrix given by Eq (4.44). The correlations between those parameters which are adjusted in the different groups are not provided. But those correlations may not be necessary in many cases. If they are required, the corresponding parameters need to be adjusted in the same group. The diagonal elements of the cofactor matrix are always available, which are enough to estimate the precision of the parameters. In close range photogrammetry, if the unknown parameters are divided into two groups as mentioned before, a full  $3 \times 3$  cofactor matrix for each object point is still available which is adequate to calculate the point error ellipsoid and a full  $6 \times 6$  cofactor matrix is also available for the camera parameters.

Correlations between the object points and the camera parameters may not be important. However if the full cofactor matrix is required, all the unknown parameters must be adjusted in one group, which leads to the traditional simultaneous LSE. In the situation of real-time, where fast 3D coordinates of the object points are required, the

cofactor matrix  $Q_x$  may not be necessary at all during the measurement process. It may be obtained by simulation. So the precision of the measurement system is actually known before the real measurement is carried out. In this case the separate LSE may well become a very useful method.

#### 4.4 A numerical example

The following example illustrates the use of the separate LSE for plane positioning of point  $P$  by measured distances to the base stations. Figure 4-1 illustrates the plane positioning measurement network.

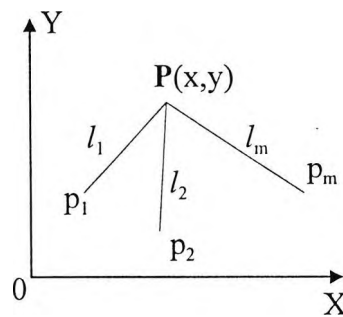


Figure 4-1 Plane positioning by measured distances to base stations

If  $m$  distances from  $m$  base stations are measured, the relationship between the measured elements  $l = (l_1, l_2, \dots, l_m)$  and the unknown parameters  $x$  and  $y$  is defined by

$$f_i(x, y) = ((x - x_i)^2 + (y - y_i)^2)^{\frac{1}{2}} = l_i \quad (4.47)$$

$$(i = 1, 2, \dots, m)$$

where  $x$  and  $y$ , the coordinates of the plane point  $P$ , are two unknown parameters to be estimated;  $x_i$  and  $y_i$  ( $i = 1, 2, \dots, m$ ) are coordinates of base stations whose values are known and assumed to be error-free.  $(l_1, l_2, \dots, l_m)$  are measured distances (observations from the point  $P$  to the base stations).

A minimum of two measured distances from base stations will give a unique solution for  $x$  and  $y$ . However for accurate positioning, more measured distances from base stations may be used. The LSE method is used to estimate the best solution. Since the functional model (4.47) is non-linear, linearization is needed for the subsequent LSE. Linearizing Eq (4.47) by Taylor series expansion to the first order accuracy gives the linearized observation equation

$$A \begin{bmatrix} \Delta x \\ \Delta y \end{bmatrix} = \mathbf{b} \quad (4.48)$$

where

$$A = \begin{bmatrix} \frac{\partial f_1}{\partial x} & \frac{\partial f_1}{\partial y} \\ \frac{\partial f_2}{\partial x} & \frac{\partial f_2}{\partial y} \\ \vdots & \vdots \\ \frac{\partial f_m}{\partial x} & \frac{\partial f_m}{\partial y} \end{bmatrix} \quad \text{and} \quad \mathbf{b} = \begin{bmatrix} l_1 - f_1(x^0, y^0) \\ l_2 - f_2(x^0, y^0) \\ \vdots \\ l_m - f_m(x^0, y^0) \end{bmatrix}$$

in which

$$\frac{\partial f_i}{\partial x} = \frac{2(x - x_i)}{((x - x_i)^2 + (y - y_i)^2)^{1/2}} \quad (4.49)$$

and 
$$\frac{\partial f_i}{\partial y} = \frac{2(y - y_i)}{((x - x_i)^2 + (y - y_i)^2)^{1/2}} \quad (4.50)$$

The unknown parameters  $x$  and  $y$  and their cofactor matrix can then be estimated by the simultaneous LSE or the separate LSE method.

A simulated numerical example is given as follows. Six distances are measured from base stations whose positions are known. The measured data are listed in Table 4-3.

Table 4-3 The measured distances from base stations

Base Station	$x$ (m)	$y$ (m)	Measured Distance (m)
1	799.4763	506.4013	199.5157
2	690.2819	649.0531	174.9510
3	504.9906	656.4831	184.5358
4	395.6187	505.3631	204.2132
5	514.2650	357.4463	167.1308
6	694.8844	352.0206	176.2120

The *a priori* standard deviation of each measured distance is given by

$$\sigma_i = 0.0001l_i$$

in which  $l_i$  is the measured distance. The reference variance  $\sigma_0^2$  is taken for  $l_0 = 100$  (m), i.e.,

$$\sigma_0^2 = (0.0001 \times 100)^2 = 0.0001(m^2)$$

In this simulation test,  $(\bar{x}, \bar{y}) = (600.0, 500.0)$  is the true position of the point **P**. Starting values of  $x$  and  $y$  can be obtained from any two measured distances. To simplify our discussion,  $(x, y) = (601.0, 499.0)$  is selected as the starting point for the LSE.

#### 4.4.1 Simultaneous solution

The simultaneous solution uses all six measurements to estimate  $x$  and  $y$  at the same time. From Eq (2.37) and (2.41)  $x$  and  $y$  are estimated. The results after each iteration are listed in Table 4-4.

Table 4-4 Estimated  $x$  and  $y$  by the simultaneous solution

Iteration No.	$x$ (m)	$y$ (m)	$\phi = v^T W_p v$ (m <sup>2</sup> )
0	601.000000	499.000000	2.513360
1	599.9649	500.3181	0.035075
2	599.9650	500.3173	0.035074
3	<b>599.9650</b>	<b>500.3173</b>	<b>0.035074</b>

The cofactor matrix of the estimated parameters  $x$  and  $y$  is

$$Q_{xy} = \begin{bmatrix} 1.1763 & -0.0354 \\ -0.0354 & 1.0566 \end{bmatrix}$$

So the covariance matrix of  $x$  and  $y$  is

$$C_{xy} = \sigma_0^2 Q_{xy} = 10^{-4} \times \begin{bmatrix} 1.1763 & -0.0354 \\ -0.0354 & 1.0566 \end{bmatrix} (m)$$

#### 4.4.2 Separate solution

The separate LSE uses six measurements all together, but adjusts  $x$  and  $y$  separately.

The observation equations  $x$  and  $y$  are expressed as

$$A_x \Delta x = b \quad (4.51)$$

and

$$A_y \Delta y = b \quad (4.52)$$

in which

$$A_x = \begin{bmatrix} \frac{\mathcal{F}_1}{\alpha} \\ \frac{\mathcal{F}_2}{\alpha} \\ \vdots \\ \frac{\mathcal{F}_6}{\alpha} \end{bmatrix} \quad \text{and} \quad A_y = \begin{bmatrix} \frac{\mathcal{F}_1}{\beta} \\ \frac{\mathcal{F}_2}{\beta} \\ \vdots \\ \frac{\mathcal{F}_6}{\beta} \end{bmatrix}$$

are two column vectors of the design matrix  $A$ . The cofactor matrices of the estimated parameters are given by

$$Q_x = N_x + N_x A_x' A_y Q_y A_y' A_x N_x \quad (4.53)$$

and

$$Q_y = N_y + N_y A_y' A_x Q_x A_x' A_y N_y \quad (4.54)$$

in which  $N_x = (A_x' W_l A_x)^{-1}$  and  $N_y = (A_y' W_l A_y)^{-1}$ . So

$$Q_{xy} = \begin{bmatrix} Q_x \\ Q_y \end{bmatrix} \quad (4.55)$$

The results after each iteration are listed in Table 4-5.

Table 4-5 Estimated results by the separate LSE

Iteration No.	$x$ (m)	$y$ (m)	$\phi = v' W_l v$ (m <sup>2</sup> )	$Q_x$	$Q_y$
0	601.0000	499.0000	2.513360	0.0000	0.0000
1	600.0096	500.3163	0.036763	1.1748	1.0568
2	599.9650	500.3173	0.035074	1.1763	1.0566
3	<b>599.9650</b>	<b>500.3173</b>	<b>0.035074</b>	<b>1.1763</b>	<b>1.0566</b>

Comparing Table 4-4 and 4-5, it can be seen that the results for the unknown parameters  $x$  and  $y$  from simultaneous solution and separate solution are identical. Both of these methods need three iterations to obtain  $x$  and  $y$  with their corrections less than  $10^{-4}$ . The

full cofactor matrix is not available with the separate solution, only the diagonal elements are obtained, i.e.,

$$\mathbf{Q}_{xy} = \begin{bmatrix} 1.1763 & \\ & 1.0566 \end{bmatrix}$$

The diagonal elements are identical with those obtained from simultaneous solution, and they are adequate to calculate the standard deviation of the estimated parameters  $x$  and  $y$ ,

$$\sigma_x = \sqrt{10^{-4} \times 1.1763} = 0.01085(m)$$

$$\sigma_y = \sqrt{10^{-4} \times 1.0566} = 0.01028(m)$$

Since this is a strong convergent measurement network, the diagonal elements of the cofactor matrix can be estimated approximately by

$$\mathbf{Q}_x = (\mathbf{A}_x^t \mathbf{W}_l \mathbf{A}_x)^{-1} \quad (4.56)$$

and

$$\mathbf{Q}_y = (\mathbf{A}_y^t \mathbf{W}_l \mathbf{A}_y)^{-1} \quad (4.57)$$

The results obtained from above equations after three iterations are

$$\mathbf{Q}_x = 1.1751 \quad \text{and} \quad \mathbf{Q}_y = 1.0555$$

which gives

$$\sigma_x = \sqrt{10^{-4} \times 1.1751} = 0.01084(m)$$

$$\sigma_y = \sqrt{10^{-4} \times 1.0555} = 0.01027(m)$$

It can be seen that the approximately estimated standard deviations of  $x$  and  $y$  are very close to their full estimation for this strong convergent network.

#### 4.5 Datum problem of the separate LSE

As mentioned in Chapter 2 constraints are required for the simultaneous LSE if datum is not defined. Otherwise it is not possible for the unknown parameters to be estimated. However the separate LSE does not always need additional constraints even if a datum is not defined. Since each time only a group of the unknown parameters are adjusted while all the observation equations are used. The column rank defects disappear provided that there are enough fixed parameters in other groups to define a datum. So the separate LSE is a real constraint free process.

Suppose the parameters are divided into two groups, the linearized observation equations can be expressed as

$$A\Delta x = A_1\Delta x_1 + A_2\Delta x_2 = b \quad (4.58)$$

in which the design matrix  $A$  is not of full rank if a datum is not defined. However the partitioned matrices  $A_1$  and  $A_2$  could be full rank if both  $x_1$  and  $x_2$  include enough information to define a datum. This is the case in close range photogrammetry where  $x_1$  refers to the 3D coordinate of the object points and  $x_2$  refers to the camera exterior parameters.

For the example given in section 2.9,  $A_1 = [-1]$  and  $A_2 = [1]$ , therefore  $x_1$  and  $x_2$  can be adjusted separately

$$\begin{aligned} \Delta x_1 &= (A_1^t A_1)^{-1} A_1^t b_1 \\ &= (1)(-1)(-2) \\ &= 2 \end{aligned}$$

so

$$\hat{x}_1 = x_1^0 + \Delta x_1 = 2$$

$$\begin{aligned}\Delta x_2 &= (A_2^t A_2)^{-1} A_2^t b_2 \\ &= (1)(1)(0) \\ &= 0\end{aligned}$$

so

$$\hat{x}_2 = x_2^0 + \Delta x_2 = 102$$

These results are equivalent to that obtained in section 2.9

In close range photogrammetry, the unknown parameters can be divided into two groups, the 3D coordinates of the object points and the camera parameters. Both  $A_1$  and  $A_2$  are full of rank. Therefore  $x_1$  and  $x_2$  can be estimated separately. When estimating the 3D coordinates of the object points datum will be held by the camera parameters. And When estimating the camera parameters datum will be held by of the object points.

Since all the parameters are equally treated with no bias, no distortion will be introduced. The estimated results by the separate LSE are equivalent to that obtained by the simultaneous LSE with inner constraints, but with a significant reduction of time and memory. Similar to the simultaneous LSE with inner constraints and the unified LSE, the datum of the separate LSE is defined by the starting values of the unknown parameters. The datum is actually arbitrary. The results can be transformed to a given coordinate system whenever necessary.

#### 4.6 Separate LSE with constraints

The purpose of including constraints in the separate LSE is not to remove the column defects from the design matrix but to relate the results to a given coordinate system so the subsequent coordinate transformation may be avoided. In close range photogrammetry, these constraints could be some fixed control points, control points with standard errors or scales (measured distances between control points).

### 4.6.1 With fixed control points

Suppose that the first  $p$  coordinates are fixed control points and expressed by  $\mathbf{x}_p$ . Other points are expressed by  $\mathbf{x}_q$ . So the linearized observation equations can be expressed as

$$A_p \Delta \mathbf{x}_p + A_q \Delta \mathbf{x}_q = \mathbf{b} + \mathbf{v} \quad (4.59)$$

Since  $\mathbf{x}_p$  is a constant, therefore  $\Delta \mathbf{x}_p = 0$ , the above equation becomes

$$A_q \Delta \mathbf{x}_q = \mathbf{b} + \mathbf{v} \quad (4.60)$$

In this case  $\mathbf{x}_p$  does not need to be estimated and its cofactor matrix  $\mathbf{Q}_{x_p} = \mathbf{0}$ .  $\mathbf{x}_q$  can be estimated by the separate LSE with the above equation and its cofactor matrix is given by

$$\mathbf{Q}_{x_q} = (A_q^T W_l A_q)^{-1} \quad (4.61)$$

The full cofactor matrix of the parameters is given by

$$\begin{aligned} \mathbf{Q}_X &= \begin{bmatrix} \mathbf{Q}_{x_p} & \\ & \mathbf{Q}_{x_q} \end{bmatrix} \\ &= \begin{bmatrix} \mathbf{0} & \\ & (A_q^T W_l A_q)^{-1} \end{bmatrix} \end{aligned} \quad (4.62)$$

### 4.6.2 With weighted control points

If the first  $p$  coordinates are previously estimated control points with the weight matrix  $W_g$ , the combined equations to estimate the unknown parameters are

$$\begin{cases} A_p \Delta \mathbf{x}_p + A_q \Delta \mathbf{x}_q = \mathbf{b} + \mathbf{v} \\ G \Delta \mathbf{x}_p = \mathbf{b}_g \end{cases} \quad (4.63)$$

where  $G$  and  $b_g$  were given by Eq (2.112) and (2.113) respectively. With the separate LSE, the unknown parameters are estimated in two groups,  $x_p$  and  $x_q$ . When estimating  $x_q$ , Eq (4.60) is used. When estimating  $x_p$ , Eq (4.63) becomes

$$\begin{cases} A_p \Delta x_p = b + v \\ G \Delta x_p = b_g \end{cases} \quad (4.64)$$

$x_p$  can be solved by the simultaneous LSE as discussed in section 4.2. It can also be solved by the separate LSE on a point by point basis. So the maximum size of matrices to be inverted is still  $3 \times 3$ .

#### 4.7 An application in surveying

The problem arises from a practical application when the plane positions of four control points are required for the camera resection purpose. Six distances between four control points in a plane are measured with given standard errors. The measured data are

$$\begin{aligned} l_1 &= 428.0 \pm 0.2mm & l_2 &= 430.6 \pm 0.2mm & l_3 &= 429.8 \pm 0.2mm \\ l_4 &= 427.3 \pm 0.2mm & l_5 &= 609.2 \pm 0.3mm & l_6 &= 603.5 \pm 0.3mm \end{aligned}$$

Figure 4-2 illustrates the measurement network.

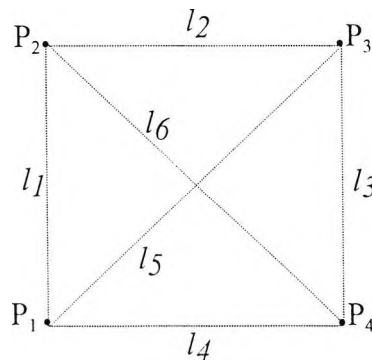


Figure 4-2 Plane positioning by measured distances

The functional model can be written as

$$\begin{cases} ((x_2 - x_1)^2 + (y_2 - y_1)^2)^{-1/2} = l_1 \\ ((x_3 - x_2)^2 + (y_3 - y_2)^2)^{-1/2} = l_2 \\ ((x_4 - x_3)^2 + (y_4 - y_3)^2)^{-1/2} = l_3 \\ ((x_1 - x_4)^2 + (y_1 - y_4)^2)^{-1/2} = l_4 \\ ((x_3 - x_1)^2 + (y_3 - y_1)^2)^{-1/2} = l_5 \\ ((x_4 - x_2)^2 + (y_4 - y_2)^2)^{-1/2} = l_6 \end{cases} \quad (4.65)$$

or simply

$$f(\mathbf{x}) = \mathbf{l} \quad (4.66)$$

in which  $\mathbf{l} = (l_1, l_2, \dots, l_6)$  is a vector of the measured elements and  $\mathbf{x} = (x_1, y_1, x_2, y_2, x_3, y_3, x_4, y_4)$  is a vector of the unknown parameters to be estimated. The linearized observation equations are expressed as

$$A\Delta\mathbf{x} = \mathbf{b} + \mathbf{v} \quad (4.67)$$

The weight matrix  $\mathbf{W}_l$  (let  $\sigma_0 = 1$ ) of the observations is

$$\mathbf{W}_l = \text{diag}(25.0 \ 25.0 \ 25.0 \ 25.0 \ 11.1 \ 11.1)$$

Suppose the starting values of the unknown parameters are estimated as

$$\begin{array}{cccc} x_1^0 = 0\text{mm} & x_2^0 = 0\text{mm} & x_3^0 = 430.6\text{mm} & x_4^0 = 427.3\text{mm} \\ y_1^0 = 0\text{mm} & y_2^0 = 428.0\text{mm} & y_3^0 = 429.8\text{mm} & y_4^0 = 0\text{mm} \end{array}$$

The design matrix  $\mathbf{A}$  is

$$A = \begin{bmatrix} 0.000 & -1.000 & 0.000 & 1.000 & 0.000 & 0.000 & 0.000 & 0.000 \\ 0.000 & 0.000 & -1.000 & -0.004 & 1.000 & 0.004 & 0.000 & 0.000 \\ 0.000 & 0.000 & 0.000 & 0.000 & 0.008 & 1.000 & -0.008 & -1.000 \\ -1.000 & 0.000 & 0.000 & 0.000 & 0.000 & 0.000 & 1.000 & 0.000 \\ -0.708 & -0.706 & 0.000 & 0.000 & 0.708 & 0.706 & 0.000 & 0.000 \\ 0.000 & 0.000 & -0.707 & 0.708 & 0.000 & 0.000 & 0.707 & -0.708 \end{bmatrix}$$

Since the measured elements do not include sufficient information to define the datum for the coordinates to be estimated in the functional model,  $A$  is column rank deficient. The scale of the datum is defined by the measured distances. But the position (two elements) and rotation (one element) of the datum are undefined. The column rank deficiency is three. Matrix  $(A'WA)$  is singular, the inverse of the matrix does not exist. The unknown parameters cannot be estimated by the simultaneous LSE unless the datum problem is solved.

With inner constraints (considering that the scale of the datum has been defined), the constraint equations can be expressed as

$$\begin{bmatrix} 1 & 0 & 1 & 0 & 1 & 0 & 1 & 0 \\ 0 & 1 & 0 & 1 & 0 & 1 & 0 & 1 \\ y_1 - x_1 & y_2 - x_2 & y_3 - x_3 & y_4 - x_4 \end{bmatrix} \begin{bmatrix} \Delta x_1 \\ \Delta y_1 \\ \Delta x_2 \\ \Delta y_2 \\ \Delta x_3 \\ \Delta y_3 \\ \Delta x_4 \\ \Delta y_4 \end{bmatrix} = G\Delta x = b_g = \begin{bmatrix} 0 \\ 0 \\ 0 \\ 0 \\ 0 \\ 0 \\ 0 \\ 0 \end{bmatrix}$$

The parameters can then be estimated by Eq (2.107) and (2.108). Table 4-6 lists the estimated results after each iteration.

Table 4-6 The estimated results by the simultaneous LSE with inner constraints

Iteration No.	$x_1$ (mm)	$y_1$ (mm)	$x_2$ (mm)	$y_2$ (mm)	$x_3$ (mm)	$y_3$ (mm)	$x_4$ (mm)	$y_4$ (mm)	$v^t W v$ (mm <sup>2</sup> )
1	-0.3448	-0.3449	0.3989	427.6043	430.9416	430.1359	426.9043	0.4047	0.8280
2	-0.3447	-0.3448	0.3992	427.6040	430.9415	430.1357	426.9040	0.4051	0.8280
3	-0.3447	-0.3448	0.3992	427.6040	430.9415	430.1357	426.9040	0.4051	0.8280

After three iterations the adjusted coordinates are stable to four decimal places. The cofactor matrix is

$$Q_x = \begin{bmatrix} 0.0148 & 0.0048 & -0.0064 & 0.0064 & -0.0048 & -0.0049 & -0.0036 & -0.0064 \\ & 0.0048 & -0.0064 & -0.0036 & -0.0049 & -0.0048 & 0.0064 & -0.0065 \\ & & 0.0149 & -0.0049 & -0.0036 & 0.0065 & -0.0049 & 0.0048 \\ & & & 0.0149 & -0.0063 & -0.0063 & 0.0048 & -0.0049 \\ & & & & 0.0148 & 0.0048 & -0.0064 & 0.0065 \\ & & & & & 0.0147 & -0.0063 & -0.0036 \\ & & & & & & 0.0149 & -0.0049 \\ & & & & & & & 0.0150 \end{bmatrix} \text{ (mm}^2\text{)}$$

*symmetric*

The trace of  $Q_x$  is 0.1188 (mm<sup>2</sup>).

With the unified LSE, an 8x8 diagonal matrix is added to the coefficient matrix  $A'WA$ , the diagonal elements of  $A'WA$  are incremented by a value of  $g$ . This will remove the rank defects of  $A'WA$  and make it non-singular. The unknown parameters can then be estimated. Table 4-7 shows the results of the unified LSE after each iteration, where  $g = 0.01$  (mm<sup>2</sup>) is chosen (which means the variances of the pseudo-observations are 100 mm<sup>2</sup>).

Table 4-7 The estimated results by the unified LSE

Iteration No.	$x_1$ (mm)	$y_1$ (mm)	$x_2$ (mm)	$y_2$ (mm)	$x_3$ (mm)	$y_3$ (mm)	$x_4$ (mm)	$y_4$ (mm)	$v^t W v$ (mm <sup>2</sup> )
1	-0.3447	-0.3447	0.3987	427.6045	430.9415	430.1357	426.9045	0.4046	0.8280
2	-0.3447	-0.3448	0.3992	427.6040	430.9415	430.1357	426.9040	0.4051	0.8280
3	-0.3447	-0.3448	0.3992	427.6040	430.9415	430.1357	426.9040	0.4051	0.8280

These results are identical (to four decimal places) with that obtained from the LSE with inner constraints.

From Eq (2.128) the cofactor matrix  $Q_x$  is calculated, i.e.,

$$Q_x = \begin{bmatrix} 0.0148 & 0.0048 & -0.0064 & 0.0064 & -0.0048 & -0.0049 & -0.0036 & -0.0064 \\ & 0.0048 & -0.0064 & -0.0036 & -0.0049 & -0.0048 & 0.0064 & -0.0065 \\ & & 0.0149 & -0.0049 & -0.0036 & 0.0065 & -0.0049 & 0.0048 \\ & & & 0.0149 & -0.0063 & -0.0063 & 0.0048 & -0.0049 \\ & & & & 0.0148 & 0.0048 & -0.0064 & 0.0065 \\ & & & & & 0.0147 & -0.0063 & -0.0036 \\ & & & & & & 0.0149 & -0.0049 \\ & & & & & & & 0.0150 \end{bmatrix} \text{ (mm}^2\text{)}$$

*symmetric*

It is also identical (to four decimal places) with that obtained from the LSE with inner constraints. The trace of  $Q_x$  is 0.1188 (mm<sup>2</sup>).

As mentioned before, for the intermediate parameters the cofactor matrix may not be necessary while the inverse of the cofactor matrix (the weight matrix) is more convenient to use. The weight matrix of the estimated parameters is gives as

$$W_x = A'W_1A$$

$$= \begin{bmatrix} 30.5659 & 5.6429 & 0.0001 & -0.0435 & -5.5659 & -5.5555 & -24.9999 & -0.0439 \\ & 30.5452 & -0.0435 & -24.9999 & -5.5555 & -5.5452 & -0.0439 & 0.0001 \\ & & 30.5457 & -5.3651 & -24.9991 & -0.1470 & -5.5465 & 5.5555 \\ & & & 30.5654 & -0.1470 & -0.0009 & 5.5555 & -5.5646 \\ & & & & 30.5673 & 5.9374 & -0.0022 & -0.2349 \\ & & & & & 30.5438 & -0.2349 & -24.9978 \\ & & & & & & 30.5487 & -5.2768 \\ & & & & & & & 30.5625 \end{bmatrix} \text{ (mm}^{-2}\text{)}$$

*symmetric*

The trace of  $W_x$  is 244.4444 (mm<sup>-2</sup>).

With the separate LSE the unknown parameters can be divided into two groups (two points in each group) or four groups (one point in each group). They can even be divided into eight groups (one coordinate in each group), but it not recommended in this example since too many iterations are required.

If the two group situation is considered, four points are divided into two groups with four coordinates in each group, i.e.,

$$X_1 = (x_1, y_1, x_2, y_2)$$

$$X_2 = (x_3, y_3, x_4, y_4)$$

The design matrix  $A$  is divided into two parts  $A_1$  and  $A_2$  accordingly.

$$A_1 = \begin{bmatrix} 0.000 & -1.000 & 0.000 & 1.000 \\ 0.000 & 0.000 & -1.000 & -0.004 \\ 0.000 & 0.000 & 0.000 & 0.000 \\ -1.000 & 0.000 & 0.000 & 0.000 \\ -0.708 & -0.706 & 0.000 & 0.000 \\ 0.000 & 0.000 & -0.707 & 0.708 \end{bmatrix} \text{ and } A_2 = \begin{bmatrix} 0.000 & 0.000 & 0.000 & 0.000 \\ 1.000 & 0.004 & 0.000 & 0.000 \\ 0.008 & 1.000 & -0.008 & -1.000 \\ 0.000 & 0.000 & 1.000 & 0.000 \\ 0.708 & 0.706 & 0.000 & 0.000 \\ 0.000 & 0.000 & 0.707 & -0.708 \end{bmatrix}$$

Observation equations are then constructed like Eq (4.37),  $X_1$  and  $X_2$  can be estimated separately. No constraints are required since  $A_1$  and  $A_2$  do not suffer the problem of column rank defects because both  $X_1$  and  $X_2$  include enough information to define the datum. In each iteration, instead of calculating the inverse of a 8x8 matrix (simultaneous adjustment) the inverses of two 4x4 matrices ( $A_1^T W_1 A_1$ ) and ( $A_2^T W_2 A_2$ ) are calculated. Three iterations are required before the parameters are stable to the fourth decimal point. Table 4-3 shows the results of the separate LSE.

Table 4-8 The estimated results by the separate LSE

Iteration No.	$x_1$ (mm)	$y_1$ (mm)	$x_2$ (mm)	$y_2$ (mm)	$x_3$ (mm)	$y_3$ (mm)	$x_4$ (mm)	$y_4$ (mm)	$v^T W v$ (mm <sup>2</sup> )
1	-0.0022	0.0248	-0.0021	427.9746	430.5355	431.2523	427.2449	1.5197	0.8976
2	-0.0022	0.0250	-0.0022	427.9744	430.5350	431.2545	427.2445	1.5175	0.8280
3	-0.0022	0.0250	-0.0022	427.9744	430.5350	431.2545	427.2445	1.5175	0.8280

These results are not identical with those obtained from the simultaneous adjustment since the datum is different, but they are equivalent. The shapes of the quadrilateral are same which can be verified by a coordinate transformation. The same  $v^T W v$  also implies

transformation may be required to related the results to a given coordinate system. Alternatively, control points can be included in the separate LSE process to avoid coordinate transformation.

The full covariance matrix is not provided in the separate LSE, only the block diagonal elements are given. The correlations between those parameters which are not estimated in the same group are not available.

Since the same functional model of measurements and the same target function of least squares minimisation are used in the separate least squares estimation as in the simultaneous least squares estimation, therefore their results must be the same. It is not easy to prove this theoretically. However many simulation and practical tests, both linear and non-linear, have been done to verify the fact. More results of the comparison of the two methods in close range photogrammetry will be given in Chapter 7.

this. The production of the full cofactor matrix is not possible because the unknown parameters are not solved simultaneously, but the weight matrix  $W_x$  can be calculated by

$$W_x = A'WA$$

$$= \begin{bmatrix} 30.5463 & 5.6429 & 0.0000 & -0.0000 & -5.5466 & -5.5555 & -24.9997 & -0.0873 \\ & 30.5648 & -0.0000 & -25.0000 & -5.5555 & -5.5645 & -0.0873 & 0.0003 \\ & & 30.5644 & -5.3651 & -24.9985 & -0.1905 & -5.5658 & 5.5555 \\ & & & 30.5467 & -0.1905 & -0.0015 & 5.5555 & -5.5453 \\ & & & & 30.5466 & 5.9374 & -0.0015 & -0.1914 \\ & & & & & 30.5645 & -0.1914 & -24.9985 \\ & & & & & & 30.5670 & -5.2768 \\ & & & & & & & 30.5441 \end{bmatrix} (\text{mm}^{-2})$$

*symmetric*

The trace of  $W_x$  is 244.4444 ( $\text{mm}^{-2}$ ). The difference of  $W_x$  from that obtained from the unified LSE is due to the change in datum. They are equivalent with respect to their datum. The same trace of  $W_x$  implies this. The difference will disappear after datum transformation. This will be verified in Chapter 6.

#### 4.8 Summary of the chapter

In this chapter, the method of the separate least squares estimation has been discussed. It divides the unknown parameters into groups and estimates them separately. Unlike the iterative LSE in which only one equation is used for each parameter in the inner iterations, the separate LSE uses all the equations for each group of the parameters and the inner iterations are combined with the outer iterations. Even with linear functional model iterations are still required and starting values of the unknown parameters are always needed.

Constraints are not always required in the separate LSE even if the column rank defects of the design matrix exists since the divided design matrices are normally of full rank provided that the datum can be defined by each group of the parameters. In this case, the datum will be defined by the starting values of the parameters. A coordinate

## Chapter 5

### Separate Adjustment of Photogrammetric Measurements

As discussed in the Chapter 4 the separate least squares estimation is a technique of division, which divides the unknown parameters into groups. In photogrammetry, the unknown parameters are naturally divided into two groups, the coordinates of the object points and the camera parameters. The coordinates of the object points are required eventually, while the camera parameters may not be necessary but have to be included as unknown parameters in the observation equations.

The term *separate adjustment* (or SA) can be used to describe the photogrammetric use of the separate LSE method (e.g. as the bundle adjustment is commonly used instead of the simultaneous LSE and the sequential adjustment instead of the sequential LSE).

#### 5.1 Free network separate adjustment

A free network adjustment means no constraints are involved in the adjustment process. The precision of the estimated results will be determined by the image observations only. The constraints are not necessary with the separate adjustment, but are normally required by the simultaneous bundle adjustment.

The separate adjustment is based on the same functional model used by the bundle adjustment, the collinearity equations. The linearized form is expressed as

$$A_1 \Delta x_1 + A_2 \Delta x_2 = b \quad (5.1)$$

where  $x_1$  denotes the coordinates of the object points and  $x_2$  the camera parameters.  $A_1$  and  $A_2$  are design matrices and have the same formats as described in Chapter 3.

The principle of the separate adjustment is to treat the unknown parameters  $x_1$  and  $x_2$  separately. The theory has been given in Chapter 4. In the separate adjustment process, only a part (group) of the parameters is adjusted in each step, either  $x_1$  or  $x_2$ . The adjustment iterates between the two steps and the results will be the same as those given by the simultaneous bundle adjustment. Figure 5-1 illustrates the procedure of the separate adjustment process.

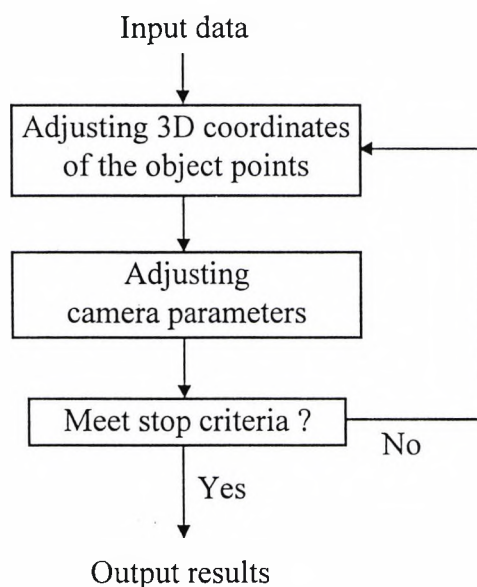


Figure 5-1 Separate adjustment process

### 5.1.1 Adjusting the object points

When adjusting the object points, the camera parameters are considered as constants. So  $\Delta x_2 = 0$ . Therefore the observation equations for estimating the coordinates of the object points become

$$A_1 \Delta x_1 = b \quad (5.2)$$

By least squares, the corrections of the 3D coordinates are estimated by

$$\begin{aligned} \Delta x_1 &= (A_1' W_1 A_1)^{-1} A_1' W_1 b \\ &= A_{11}^{-1} A_1' W_1 b \end{aligned} \quad (5.3)$$

Since  $A_{II}$  is a block diagonal matrix, the inverse of  $A_{II}$  can be calculated by inverting a series of  $3 \times 3$  matrices. The matrices  $A_I$  and  $A_{II}$  can be stored compactly as illustrated in Figure 5-2 and the products of the matrices are simplified. Each small block in  $A_I$  is a  $2 \times 3$  submatrix and each small block in  $A_{II}$  is a  $3 \times 3$  submatrix ( $n$  is the number of the object points and  $m$  is the number of the cameras).

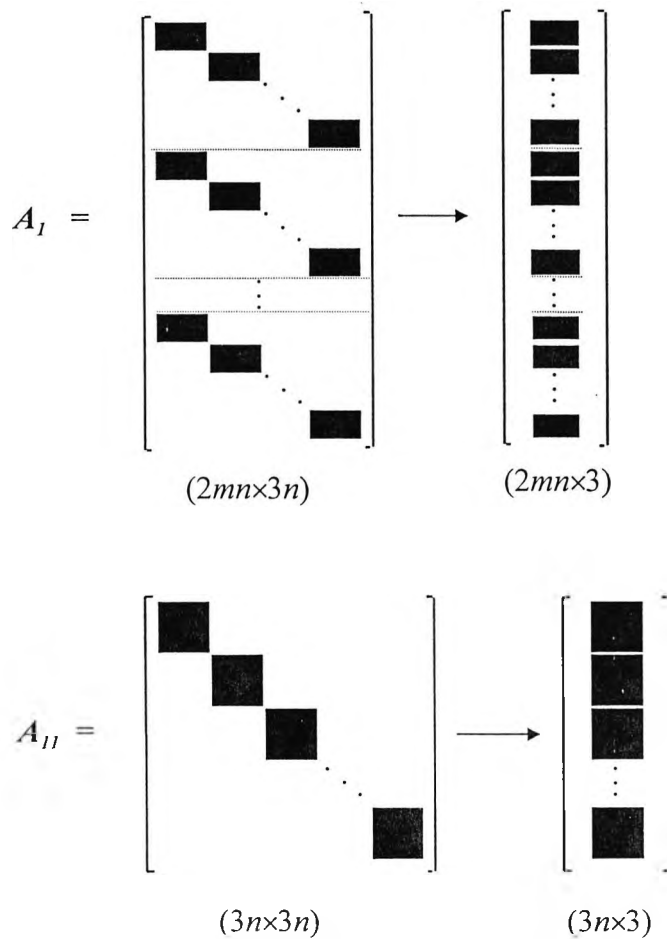


Fig 5-2 The structures of the matrices  $A_I$  and  $A_{II}$

Since the object points are independent of each other when the camera parameters are treated as constants, they can be adjusted separately. So the memory required can be reduced further. For the  $i$ th object point, the size of  $A_{Ii}$  is  $2m \times 3$  and the size of  $A_{IIi}$  is  $3 \times 3$ . The corrections of the 3D coordinates for the  $i$ th object point are given by

$$\Delta \mathbf{x}_{li} = A_{lli}^{-1} A_{li}' W_{li} \mathbf{b}_i \quad (5.4)$$

Matrix  $A_{lli}$  can be calculated by a further partitioning according to the cameras, i.e.,

$$\begin{aligned} A_{lli} &= A_{li}' W_{li} A_{li} \\ &= \sum_{j=1}^m A_{lij}' W_{lij} A_{lij} \\ &= \sum_{j=1}^m A_{llj} \end{aligned} \quad (5.5)$$

where  $A_{lij}$  is a  $2 \times 3$  matrix and  $W_{lij}$  is a  $2 \times 2$  matrix, which are contributed by the  $l$ th point on the  $j$ th camera. Similarly,  $A_{li}' W_{li} \mathbf{b}_i$  can also be calculated by partitioning, i.e.,

$$A_{li}' W_{li} \mathbf{b}_i = \sum_{j=1}^m A_{lij}' W_{lij} \mathbf{b}_{ij} \quad (5.6)$$

where  $\mathbf{b}_{ij}$  is a  $2 \times 1$  matrix attributed to the  $l$ th point on the  $j$ th camera. In this case, the maximum size of the matrix required to obtain the corrections for the 3D coordinates of the object point is  $3 \times 3$ .

It is obvious that the computational time is directly proportional to the number of the object points. The minimum number of the cameras required is two.

### 5.1.2 Adjusting the cameras

When adjusting the camera parameters, the coordinates of the object points are considered as constants. So  $\Delta \mathbf{x}_l = 0$ . Therefore the observation equations for estimating the camera parameters become

$$A_2 \Delta \mathbf{x}_2 = \mathbf{b} \quad (5.7)$$

By least squares, the corrections of the camera parameters are estimated by

$$\begin{aligned} \Delta x_2 &= (A_2^t W_1 A_2)^{-1} A_2^t W_1 b \\ &= A_{22}^{-1} A_2^t W_1 b \end{aligned} \tag{5.8}$$

where  $A_{22}$  is a block diagonal matrix, the inverse of  $A_{22}$  is calculated by inverting a series of  $6 \times 6$  matrices. Because of their special structures, the matrices  $A_2$  and  $A_{22}$  can be stored compactly as illustrated in Figure 5-3 and the products of the matrices are simplified. Each small blocks in  $A_2$  is a  $2n \times 6$  submatrix and each small blocks in  $A_{22}$  is a  $6 \times 6$  submatrix.

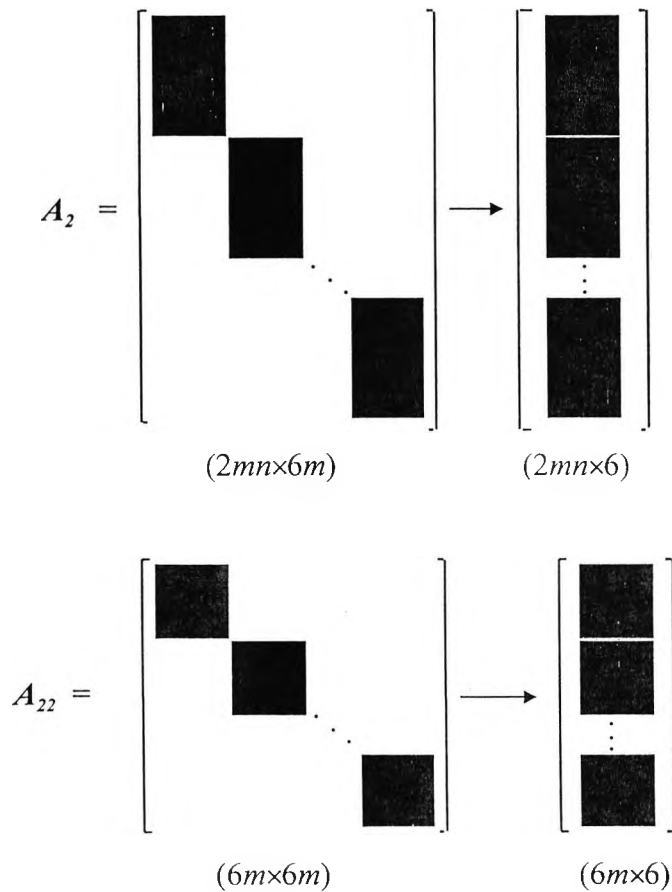


Figure 5-3 The structures of the matrices  $A_2$  and  $A_{22}$

Since the cameras are independent of each other, when the object points are fixed, the parameter of each individual camera can be adjusted separately. So the memory required can be reduced further. For the  $j$ th camera, the size of  $A_{2j}$  is  $2n \times 6$  and the size of  $A_{22j}$  is  $6 \times 6$ . The corrections of the parameters for the  $j$ th camera are given by

$$\Delta x_{2j} = A_{22j}^{-1} A_{2j}^t W_{lj} b_j \quad (5.9)$$

Matrix  $A_{22j}$  can be calculated by a further partitioning according to the object points, i.e.,

$$\begin{aligned} A_{22j} &= A_{2j}^t W_{lj} A_{2j} \\ &= \sum_{i=1}^n A_{2ji}^t W_{lji} A_{2ji} \\ &= \sum_{i=1}^n A_{22ji} \end{aligned} \quad (5.10)$$

where  $A_{2ji}$  is a  $2 \times 6$  matrix and  $W_{lji}$  is a  $2 \times 2$  matrix, which are contributed by the  $i$ th point on the  $j$ th camera. Similarly,  $A_{2j}^t W_{lj} b_j$  can also be calculated by partitioning, i.e.,

$$A_{2j}^t W_{lj} b_j = \sum_{i=1}^n A_{2ji}^t W_{lji} b_{ji} \quad (5.11)$$

where  $b_{ji}$  is a  $2 \times 1$  matrix attributed to the  $i$ th point on the  $j$ th camera. So the maximum size of the matrix required to obtain the corrections of the camera parameters is  $6 \times 6$ .

The computational time is directly proportional to the number of cameras. The minimum number of object points required is three.

### 5.1.3 Iteration between the two steps

The separate adjustment is an iterative process which is carried out between the two steps described above. After each iteration, the 3D coordinates and the camera

parameters are refined. The iterative process terminates when the stop criterion (e.g. the maximum adjustment of the 3D coordinates is less than a given value) is met.

#### **5.1.4 Datum definition**

A datum must be defined in the simultaneous bundle adjustment to remove the column rank defects of the design matrix so the unknown parameters can be estimated. However the pre-definition of the datum is generally not necessary in the separate adjustment. No constraints are required to make the unknown parameters estimable when the separate adjustment is applied. The datum is held either by the camera exterior parameters when the coordinates of the object points are adjusted or by the object points when the camera parameters are adjusted. Since both the coordinates of the object points and the camera exterior parameters are related to the same coordinate system, the datum is actually determined by the starting values of the parameters. If the coordinates of the object points are adjusted first, the datum will be determined by the starting values of the camera parameters, otherwise it will be determined by the starting values of the object points.

Because of the uncertainty of the starting values, the results from the separate adjustment are in an arbitrary coordinate system if spatial controls are not applied. The results from the separate adjustment may not be numerically identical with that obtained from the traditional bundle adjustment due to the different datum definition. However the shapes of the measured object are the same from both methods. So their results are equivalent. This can be verified by a rigid coordinate transformation of the object.

#### **5.1.5 Precision estimation**

The covariance (cofactor) matrix is a by-product which is normally produced directly by the simultaneous bundle adjustment at the same time when the unknown parameters are estimated. The square roots of the diagonal elements of the covariance matrix give the standard deviations to the corresponding parameters which are used to evaluate the precision of the measurement system. However, the full covariance matrix is not

available directly from the separate adjustment. It can be calculated when it is required from the design matrix and the computation is very expensive in terms of time and memory. In many cases the full covariance matrix is not necessary for the purpose of the standard deviations of the estimated parameters.

From the separate adjustment, the cofactor matrix of the coordinates of the object points is given approximately by

$$\mathbf{Q}_{x_i} = (\mathbf{A}_i^t \mathbf{W}_i \mathbf{A}_i)^{-1} = \mathbf{A}_{ii}^{-1} \quad (5.12)$$

For each object point a 3×3 cofactor matrix is given by

$$\mathbf{Q}_{x_{ii}} = (\mathbf{A}_{ii}^t \mathbf{W}_{ii} \mathbf{A}_{ii})^{-1} = \mathbf{A}_{iii}^{-1} \quad (5.13)$$

and the covariance matrix the 3D coordinates is

$$\mathbf{C}_{x_{ii}} = \hat{\sigma}_0^2 \mathbf{Q}_{x_{ii}} \quad (5.14)$$

The cofactor matrix of the camera parameters is given approximately by

$$\mathbf{Q}_{x_2} = (\mathbf{A}_2^t \mathbf{W}_2 \mathbf{A}_2)^{-1} = \mathbf{A}_{22}^{-1} \quad (5.15)$$

For each camera a 6×6 cofactor matrix is given by

$$\mathbf{Q}_{x_{2j}} = (\mathbf{A}_{2j}^t \mathbf{W}_{2j} \mathbf{A}_{2j})^{-1} = \mathbf{A}_{22j}^{-1} \quad (5.16)$$

and the covariance matrix of the camera parameters is

$$\mathbf{C}_{x_{2j}} = \hat{\sigma}_0^2 \mathbf{Q}_{x_{2j}} \quad (5.17)$$

For each object point the 3×3 covariance matrix  $C_{x_{ii}}$  is adequate to evaluate the precision of the estimated 3D coordinates and the error ellipsoid for each object point. And for each camera the covariance matrix  $C_{x_{2j}}$  is also available to analyse the precision and the correlations between the camera parameters.

The approximations are caused by the neglect of the variances of the camera parameters and the 3D coordinates of the object points when calculating  $C_{x_{ii}}$  and  $C_{x_{2j}}$  respectively. These approximations can be compensated for by including the variances into the iterative process as described in Chapter 4, however with more computational effort.

Simulation tests showed that the approximations were quite acceptable for a multi-camera strong network especially in close range photogrammetry. The differences caused by the approximations were normally less than one percent.

#### 5.1.6 Number of iterations

The number of iterations required for the separate adjustment process depends on the closeness of the starting values to their final results. However, more iterations are generally required for the separate adjustment than for the bundle adjustment. Normally four iterations are enough to give satisfactory results for the bundle adjustment with reasonable starting values, while for the separate adjustment ten or a few tens are required. Table 5-1 shows the maximum adjustment of the coordinates and the sum of squares of the residuals ( $\phi = v^t W v$ ) after each iteration for a close range photogrammetric measurement network with 100 object points and 4 cameras.

Table 5-1 The adjusted results by the bundle adjustment and the separate adjustment

No. of iteration	Bundle adjustment		Separate adjustment	
	Max. adjustment (mm)	$\phi = v^T W v$ (mm <sup>2</sup> )	Max. adjustment (mm)	$\phi = v^T W v$ (mm <sup>2</sup> )
1	19.7646	0.80576482	13.8760	1.24956487
2	0.3381	0.00375875	1.0679	0.12538475
3	0.0128	0.00011768	0.2812	0.02086453
4	0.0001	0.00011342	0.0778	0.00484658
5			0.0259	0.00103845
6			0.0125	0.00026584
7			0.0071	0.00011747
8			0.0042	0.00011375
9			0.0025	0.00011347
10			0.0014	0.00011344
11			0.0008	0.00011342
12			0.0005	0.00011342
13			0.0003	0.00011342
14			0.0001	0.00011342

### 5.1.7 Consistency with the bundle solution

The separate adjustment is based on the same functional model as the bundle adjustment. The target functions of the least squares from the two methods are also same, which are the sums of the weighted squares of residuals on the image planes. Simulation tests and practical tests show that the two methods always arrive at the same minimisation. Each individual residual for all the observations has also been checked and found to be the same for both methods. This means that their results are equivalent. The coordinates of their solution may not be numerically identical because of different datum definitions, but the shapes of the measured object from the two methods are always same. This has been verified by the rigid coordinate transformation and by including control points in the adjustment process. Some simulation test results will be given in Chapter 7.

### 5.1.8 Computational complexity

Least squares adjustment is an expensive computational process. Inverting the coefficient matrix  $A'WA$  is the main cost in terms of speed and memory. In the simultaneous bundle adjustment,  $A'WA$  is a symmetric positive definite matrix. Fast algorithms (for example, Cholesky) can be used to compute the inverse of  $A'WA$ . However even then the computational complexity is still high. If the size of  $A'WA$  is  $u \times u$ , the time required for computing the inverse of  $A'WA$  is directly proportional to  $u^3$  and the memory needed is directly proportional to  $u^2$ .

Suppose  $m$  images are used to measure  $n$  object points in a close range photogrammetric measurement system. If the bundle adjustment with inner constraints on the object points is used, the size of the coefficient matrix  $A'WA$  is  $(3n+6m) \times (3n+6m)$ . So the computational complexity for one iteration is

$$\begin{aligned} T(B) &\propto (3n+6m)^3 \\ \text{and} \quad M(B) &\propto (3n+6m)^2 \end{aligned}$$

With the separate adjustment, the computational complexity of time for one iteration is

$$T(S) \propto m \cdot n$$

and the maximum memory required is a  $6 \times 6$  unit no matter how many object points and cameras are involved. The time required for the separate adjustment can be expressed as

$$t_S = C_S \cdot m \cdot n \cdot I$$

where  $m$  is the number of the cameras,  $n$  is the number of the object points and  $I$  is the number of iterations.  $C_S$  is a coefficient which may vary according to the computers. It is found to be  $215 \mu\text{s}$  for a SUN Spark Classic and  $42 \mu\text{s}$  for a 120 MHz Pentium.

For the example given in section 4.7 (100 object points and 4 cameras). The time required by the separate adjustment (fourteen iterations) is about 1.4 seconds. For bundle adjustment for one iterations is 17 seconds. In total 68 seconds are needed for the whole adjustment process (four iterations). The simulation was conducted on SUN Sparc Classic. More tests were conducted and the results are given in Chapter 8.

### 5.1.9 Feasible area of the separate adjustment

In the separate adjustment process, the minimum numbers required for the object points and the camera are three and two respectively. Figure 5-4 illustrates the feasible area of the separate adjustment.

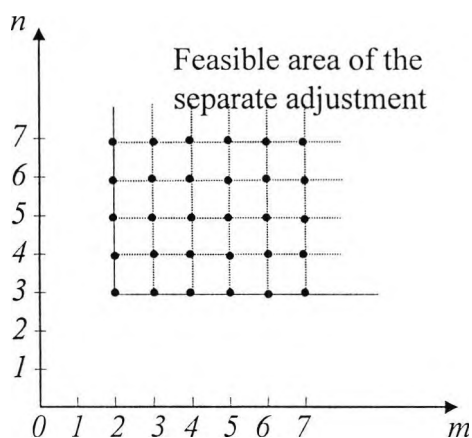


Figure 5-4 Feasible area of the separate adjustment

### 5.2 Continuous adjustment

The separate adjustment can produce the 3D coordinates much faster than the traditional bundle adjustment. Because of its high speed, it can be used in the measurement of moving object. It is often the case that the object points may move regularly while the cameras may be relatively stable. If the measurement process operates fast enough the object points could be tracked successfully. So the orientation of the object body can be measured in real-time.

To test the separate adjustment in a continuous measurement process a close range photogrammetric measurement network was simulated. Twelve sets of 3D data were created with a 2 mm linear movement between each set. These 3D data were imaged on four stationary cameras to get the 2D data. Random noise was added to these 2D data. The results from a measurement were used as the starting values for the next measurement. The results of twelve sets of ten iterations of the separate adjustment are illustrated in Figure 5-5 and Figure 5-6 for the maximum adjustment of the 3D coordinates and the standard deviation of the 3D coordinates respectively.

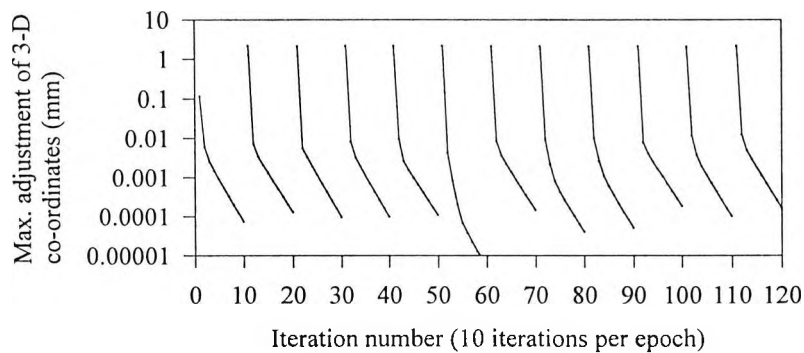


Figure 5-5 Graph of maximum adjustments for the 12 sets plotted for each iteration (note Log y axis)

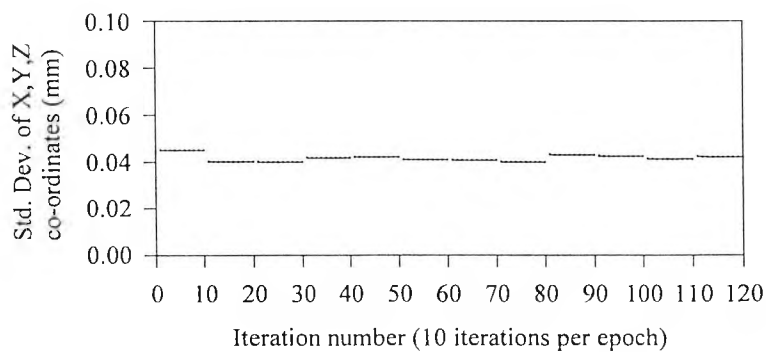
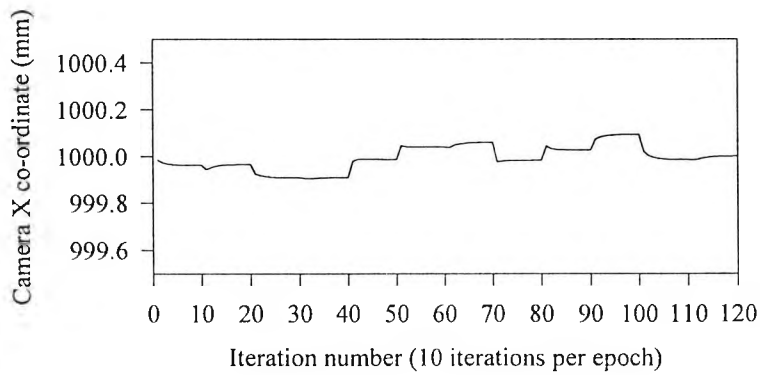
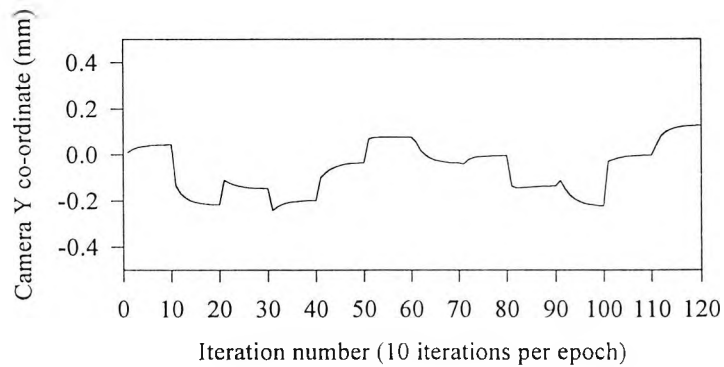


Figure 5-6 Graph of the standard deviation of the X, Y, Z coordinates for each iteration

Figure 5-5 illustrates that for each epoch after the first iteration which required a 2 mm adjustment, the maximum adjustment of the 3D coordinates rapidly approaches zero. Figure 5-6 illustrates that the *a posteriori* standard deviations of the 3D coordinates improve little after first iteration of each epoch. Therefore in the continuous measurement process, the separate adjustment will give satisfactory results with only a few iterations (two or three).

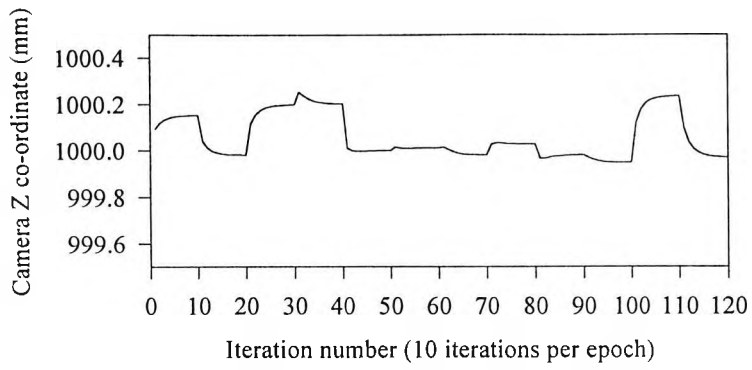


(a)

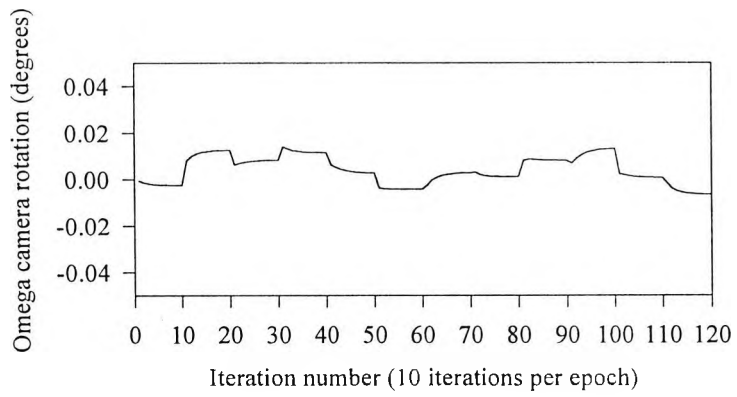


(b)

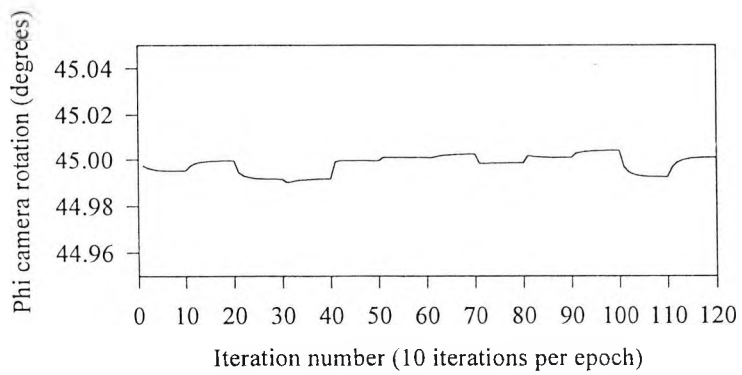
Figure 5-7 Stability of the Camera parameters



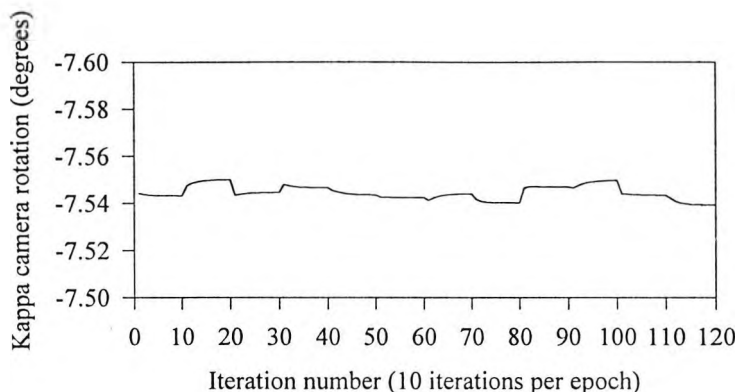
(c)



(d)



(e)



(f)

Figure 5-7 Stability of the Camera parameters

Figure 5-7 illustrates the stability of the camera parameters during the continuous measurement process by the separate adjustment. It can be seen that the camera parameters are not much influenced by the movement of the 3D coordinates of the object points.

In the real-time applications, the movement of an object is limited in 1/25 of a second, which means the starting values are not far away from the final solutions. In this case a satisfactory result can normally be obtained in a few iterations (two or three) by the separate adjustment. It is also possible to move and rotate the cameras to track the moving object. In this case a common datum becomes important to relate the measurement results to the same coordinate system.

### 5.3 Separate adjustment with controls

As mentioned in section 5.1.4, the coordinate datum will not cause problems in the separate adjustment. The purpose of including controls in the separate adjustment is to

relate the results to a given coordinate system so the coordinate transformation may be avoided.

Since controls are normally applied to the object points, the camera parameters are adjusted as usual, while the object points are divided into two parts: control points and normal points.

### 5.3.1 With fixed control points

It is often the case that some fixed ground control points are used to define a datum so that the measured results (the 3D coordinates of the object points) are related to the given coordinate system. In this case, the coordinates of the spatial points can be expressed as

$$\mathbf{x}_i = \begin{bmatrix} \mathbf{x}'_i \\ \mathbf{x}''_i \end{bmatrix} \quad (5.18)$$

where  $\mathbf{x}'_i$  is a vector of the coordinates of the control points and  $\mathbf{x}''_i$  is a vector of the coordinates of the normal object points. The normal object points will be adjusted as usual, while the control points will not be adjusted. The camera parameters will be adjusted as usual and all the spatial points (the control points and the normal object points) are used in this step. It has been verified that, with the same control points, the results from both simultaneous bundle adjustment and separate adjustment are numerically identical.

### 5.3.2 With weighted control points

If the control points are treated as weighted observations, they will be adjusted not only by the image observations but also by the survey observations. The survey observations of the control points can be expressed as

$$\mathbf{G}_i \Delta \mathbf{x}'_{ii} = \mathbf{c}_i \quad (5.19)$$

with associated weight matrix  $W_{gi}$ . So the combined observation equations for a control point become

$$\begin{bmatrix} A_{li} \\ G_i \end{bmatrix} \Delta x'_{li} = \begin{bmatrix} b_i \\ c_i \end{bmatrix} \quad (5.20)$$

Therefore the corrections of the 3D coordinates of the control points are given by

$$\Delta x'_{li} = (A_{li}' W_{li} A_{li} + G_i' W_{gi} G_i)^{-1} (A_{li}' W_{li} b_i + G_i' W_{gi} c_i) \quad (5.21)$$

Normal object points and the camera parameters are adjusted the same way as discussed before.

### 5.3.3 With scale

Scale is normally defined by the measured distances between control points. In this case, control point coordinates will be adjusted not only by the image observations but also by the measured distances between those control points. If the distance between the control points  $p_i$  and  $p_j$  is measured as  $d_{ij}$  with the standard deviation  $\sigma_{ij}$ , the additional observation equation is given by

$$((x_i - x_j)^2 + (y_i - y_j)^2 + (z_i - z_j)^2)^{1/2} = d_{ij} \quad (5.22)$$

with an associated weight  $\sigma_{ij}^{-2}$ . After linearization the observation equation becomes

$$G_{ij} \Delta x_{ij} = c_{ij} \quad (5.23)$$

in which

$$G_{ij} = \begin{bmatrix} \frac{x_i^0 - x_j^0}{d_{ij}^0} & \frac{y_i^0 - y_j^0}{d_{ij}^0} & \frac{z_i^0 - z_j^0}{d_{ij}^0} & \frac{x_j^0 - x_i^0}{d_{ij}^0} & \frac{y_j^0 - y_i^0}{d_{ij}^0} & \frac{z_j^0 - z_i^0}{d_{ij}^0} \end{bmatrix},$$

$$\Delta x_{ij} = [\Delta x_i \ \Delta y_i \ \Delta z_i \ \Delta x_j \ \Delta y_j \ \Delta z_j],$$

$$c_{ij} = d_{ij} - d_{ij}^0$$

and

$$d_{ij}^0 = ((x_i^0 - x_j^0)^2 + (y_i^0 - y_j^0)^2 + (z_i^0 - z_j^0)^2)^{1/2}$$

Because of the additional relationship between the control points  $x_i$  and  $x_j$ , they need to be adjusted together. Therefore the size of the matrices computed increases from  $3 \times 3$  to  $6 \times 6$ . Alternatively, all the control points can be adjusted together. So the maximum size of the matrix will be  $3n_c \times 3n_c$ , where  $n_c$  is the number of the control points.

### 5.3.4 Number of iterations

It has been seen from the above discussion that in the separate adjustment controls will not add too much computation in each iteration. However, simulation tests and practical tests show that with these additional constraints more iterations are required for the separate adjustment, especially when fixed controls are applied. This may influence the speed of the measurement process. To avoid this, an alternative method is a free network adjustment followed by a coordinate transformation.

## 5.4 Separate adjustment with DLT model

As mentioned in Chapter 3, the DLT model can be used to calculate the camera parameters directly with given control points in the object space. This is called resection. With the camera parameters as knowns the 3D coordinates of the object points can be calculated directly. This is called intersection. In this way the 3D coordinates of the object points and the camera parameters are estimated directly. No

starting values for the unknown parameters are required and no iterations are needed since the functional model appears to be linear after the rearrangements.

This measurement process (resection followed by intersection with DLT model) could be the easiest and fastest method for multi-camera photogrammetric 3D measurement. However, the precision from this measurement process is normally poorer than that from the simultaneous bundle adjustment or separate adjustment. The reasons are (i) the precision of the camera parameters are limited by a small number of control points, (ii) the degrees of freedom of the least squares from this measurement process are fewer than that of the simultaneous bundle adjustment and (iii) due to the rearrangements of the functional model the minimisations of the least squares are no longer the sums of the squares of the residuals on the image planes. The first two problems can be overcome by a series of separate adjustments with all the cameras and the object points involved in both steps and the third can be overcome by maintaining the non-linear functional model and applying the rigorous least squares adjustment in both steps to minimise the sums of the squares of the residuals on the image planes.

The collinearity equations after DLT have been given in Chapter 3. They are rewritten here and the subscripts are neglected for simplicity.

$$\begin{cases} f_x = \frac{D_1}{D_3} - x \\ f_y = \frac{D_2}{D_3} - y \end{cases} \quad (5.24)$$

where

$$\begin{cases} D_1 = L_1X + L_2Y + L_3Z + L_4 \\ D_2 = L_5X + L_6Y + L_7Z + L_8 \\ D_3 = L_9X + L_{10}Y + L_{11}Z + L_{11} \end{cases} \quad (5.25)$$

In general the functional model is expressed as

$$f(x_1, x_2, l) = 0 \quad (5.26)$$

where  $x_1$  is a vector of the 3D coordinates of the object points ( $X, Y, Z$ ) and  $x_2$  is a vector of the DLT parameters ( $L_1, L_2, \dots, L_{11}$ ) which involve six camera exterior parameters ( $X_L, Y_L, Z_L, \omega, \phi, \kappa$ ) and four camera interior parameters ( $x_p, y_p, c_x, c_y$ ). The linearized functional model is expressed as

$$A_1 \Delta x_1 + A_2 \Delta x_2 = b \quad (5.27)$$

where

$$A_1 = \begin{bmatrix} \frac{\partial x}{\partial X} & \frac{\partial x}{\partial Y} & \frac{\partial x}{\partial Z} \\ \frac{\partial y}{\partial X} & \frac{\partial y}{\partial Y} & \frac{\partial y}{\partial Z} \end{bmatrix} \quad (5.28)$$

and

$$A_2 = \begin{bmatrix} \frac{\partial x}{\partial L_1} & \frac{\partial x}{\partial L_2} & \dots & \frac{\partial x}{\partial L_{11}} \\ \frac{\partial y}{\partial L_1} & \frac{\partial y}{\partial L_2} & \dots & \frac{\partial y}{\partial L_{11}} \end{bmatrix} \quad (5.29)$$

The partial differentials in  $A_1$  are calculated as

$$\begin{aligned} \frac{\partial x}{\partial X} &= \frac{L_1 D_3 - L_9 D_1}{D_3^2} & \frac{\partial x}{\partial Y} &= \frac{L_2 D_3 - L_{10} D_1}{D_3^2} & \frac{\partial x}{\partial Z} &= \frac{L_3 D_3 - L_{11} D_1}{D_3^2} \\ \frac{\partial y}{\partial X} &= \frac{L_5 D_3 - L_9 D_2}{D_3^2} & \frac{\partial y}{\partial Y} &= \frac{L_6 D_3 - L_{10} D_2}{D_3^2} & \frac{\partial y}{\partial Z} &= \frac{L_7 D_3 - L_{11} D_2}{D_3^2} \end{aligned}$$

and the partial differentials in  $A_2$  are calculated as

$$\frac{\partial f_x}{\partial L_1} = \frac{X}{D_3} \quad \frac{\partial f_x}{\partial L_2} = \frac{Y}{D_3} \quad \frac{\partial f_x}{\partial L_3} = \frac{Z}{D_3} \quad \frac{\partial f_x}{\partial L_4} = \frac{1}{D_3}$$

$$\frac{\partial f_x}{\partial L_5} = \frac{\partial f_x}{\partial L_6} = \frac{\partial f_x}{\partial L_7} = \frac{\partial f_x}{\partial L_8} = 0$$

$$\frac{\partial f_x}{\partial L_9} = -\frac{D_1 X}{D_3^2} \quad \frac{\partial f_x}{\partial L_{10}} = -\frac{D_1 Y}{D_3^2} \quad \frac{\partial f_x}{\partial L_{11}} = -\frac{D_1 Z}{D_3^2}$$

$$\frac{\partial f_y}{\partial L_1} = \frac{\partial f_y}{\partial L_2} = \frac{\partial f_y}{\partial L_3} = \frac{\partial f_y}{\partial L_4} = 0$$

$$\frac{\partial f_y}{\partial L_5} = \frac{X}{D_3} \quad \frac{\partial f_y}{\partial L_6} = \frac{Y}{D_3} \quad \frac{\partial f_y}{\partial L_7} = \frac{Z}{D_3} \quad \frac{\partial f_y}{\partial L_8} = \frac{1}{D_3}$$

$$\frac{\partial f_y}{\partial L_9} = -\frac{D_2 X}{D_3^2} \quad \frac{\partial f_y}{\partial L_{10}} = -\frac{D_2 Y}{D_3^2} \quad \frac{\partial f_y}{\partial L_{11}} = -\frac{D_2 Z}{D_3^2}$$

The separate adjustment process can then be applied to the DLT model. In the step of adjusting 3D coordinates of the object points, the calculation process is similar as the usual case (collinearity equation based separate adjustment). The matrix  $A_{11}$  has the same structure as usual. The maximum size of the matrices processed is  $3 \times 3$  and the time required is directly proportional to the number of the object points. In the step of adjusting camera parameters, the number of unknowns for each camera is 11 rather than 6 this time. So the matrix  $A_{22}$  is a  $11 \times 11$  block diagonal matrix. This may increase the computation time slightly. However it is compensated by the simplified calculation of the linearization based on the DLT model.

The number of iterations of the separate adjustment with DLT model is usually fewer than the normal separate adjustment. Simulation tests show that the overall time required is roughly the same for the separate adjustment with DLT model and the normal collinearity equation model.

During the separate adjustment process, evaluation of the camera physical parameters is not necessary. They can be computed from the 11 DLT parameters at the end of adjustment process if they are required.

The precision of the results from the DLT model is better than that from the normal collinearity equation model. This is attributed to the inclusion of the camera interior parameters ( $x_p, y_p, c_x, c_y$ ) by the DLT model. However, the normal 11 parameter DLT model is not capable of dealing with other important camera interior parameters such as lens distortions.

For the same example given in section 5.1.6, a separate adjustment with DLT model is applied. After each iteration the maximum adjustment of the coordinates and the sum of squares of the residuals ( $\phi = v^t W v$ ) are calculated and listed in Table 5-2.

Table 5-2 The adjusted results by the separate adjustment with DLT model

No. of iteration	Max. adjustment (mm)	$\phi = v^t W v$ (mm <sup>2</sup> )
1	14.2325	1.13764872
2	1.0834	0.10237643
3	0.2046	0.01287485
4	0.0428	0.00387291
5	0.0103	0.00086748
6	0.0028	0.00022353
7	0.0006	0.00010948
8	0.0003	0.00010872
9	0.0001	0.00010872

It can be seen that the sum of the weighted squares of the residuals  $\phi$  from the DLT model is smaller than that from the normal collinearity equation model. More tests have been conducted and will be discussed in Chapter 7.

### 5.5 Self-calibration separate adjustment

In the foregoing discussion of photogrammetric measurement, systematic errors have not been considered (except for the DLT model). However, in close range digital photogrammetry, especially when non-metric CCD cameras are used, systematic errors are so significant that they cannot be neglected. These errors are mainly due to the

defects of the camera system and can be described by various of camera interior parameters. There are normally two ways of dealing with the systematic errors. One is to calibrate the cameras beforehand and correct the 2D coordinates on image planes accordingly. Another way is to treat the camera interior parameters as variables (unknown parameters or observations) and estimate them in the least squares adjustment. Therefore the camera interior parameters can be estimated together with other unknown parameters (3D coordinates of the object points and the camera exterior parameters). This method is called *self-calibration separate adjustment*.

In this section the separate adjustment will be used in place of the bundle adjustment. It is important to realise that the self-calibration technique does not require any object space control for the technique to be effective as a means of camera calibration (Atkinson 1996). Hence the benefits from the separate adjustment are more obvious.

For the modified functional model

$$f(\mathbf{x}_1, \mathbf{x}_2, \mathbf{x}'_2) = l \quad (5.30)$$

the linearized observation equations can be expressed as

$$A_1 \Delta \mathbf{x}_1 + A_2 \Delta \mathbf{x}_2 + A'_2 \Delta \mathbf{x}'_2 = b \quad (5.31)$$

where  $\mathbf{x}_1 = (X, Y, Z)$  denotes a vector of the 3D coordinates of the object points,  $\mathbf{x}_2 = (X_L, Y_L, Z_L, \omega, \phi, \kappa)$  denotes a vector of the camera exterior parameters,  $\mathbf{x}'_2 = (c, x_p, y_p, k_1, k_2, k_3, p_1, p_2)$  denotes a vector of the camera interior parameters, and

$$A_1 = \frac{\partial f}{\partial \mathbf{x}_1}, \quad A_2 = \frac{\partial f}{\partial \mathbf{x}_2}, \quad A'_2 = \frac{\partial f}{\partial \mathbf{x}'_2}$$

The derivation of  $A_1$  and  $A_2$  has been discussed in Chapter 3. The derivation of  $A'_2$  is given in Appendix I.

### 5.5.1 Three step separate adjustment

When the camera interior parameters are considered, the unknown parameters may be divided into three groups as indicated in Eq (5.31). With the separate adjustment each group of unknown parameters is adjusted individually. When adjusting any group of parameters the other two groups are treated as constants. So the separate adjustment procedure could be:

Step I : Adjusting 3D coordinates of the object points

$$\Delta x_1 = (A_1' W_1 A_1)^{-1} A_1' W_1 b \quad (5.32)$$

Step II : Adjusting camera exterior parameters

$$\Delta x_2 = (A_2' W_1 A_2)^{-1} A_2' W_1 b \quad (5.33)$$

Step III : Adjusting camera interior parameters

$$\Delta x_2' = (A_2'^t W_1 A_2')^{-1} A_2'^t W_1 b \quad (5.34)$$

Steps I and II are the same as discussed in section 4.7. In Step III the matrix  $A_2'$  has a structure shown in Figure 5-8 (a). Hence the coefficient matrix  $A_2'^t W_1 A_2'$  is a block diagonal matrix (Figure 5-8 (b)), Each sub-block is a  $8 \times 8$  matrix. So the inverse of  $A_2'^t W_1 A_2'$  is calculated by inverting  $m$   $8 \times 8$  matrices, which will save both computation time and memory. If several images are taken by only one camera in the measurement process, which is usual in close range photogrammetry for camera calibration, there is only one set of camera interior parameters. So  $A_2'^t W_1 A_2'$  will be a  $8 \times 8$  matrix.

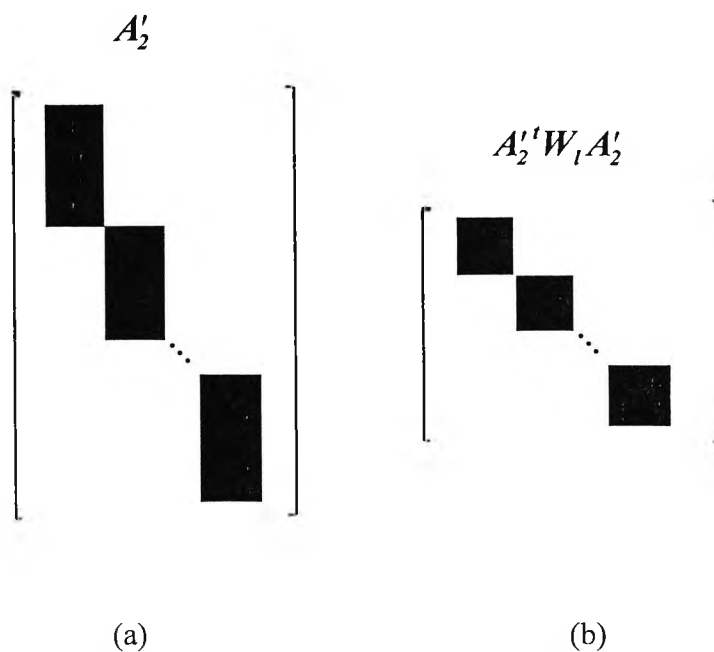


Figure 5-8 (a) Structure of  $A'_2$   
 (b) Structure of  $A'_2{}^t W_1 A'_2$

With the separate adjustment discussed above, the maximum sizes of the matrices need to be inverted in each step are  $3 \times 3$ ,  $6 \times 6$  and  $8 \times 8$  respectively. The correlations between the camera exterior and interior parameters are not available.

### 5.5.2 Two step separate adjustment

Another possible way of using separate adjustment is to put the camera interior and exterior parameters in the same group. So the iterations are between two groups. One group is the 3D coordinates of the object points and the other group is the camera parameters. For each camera there will be 14 parameters, 6 exterior parameters and 8 interior parameters. The size of the matrices to be inverted is  $14 \times 14$ . In this case the correlations between the camera exterior and interior parameters are available.

### 5.5.3 A simulation test

To test the self-calibration separate adjustment, a simulation network of close range photogrammetric measurement is constructed. Eight images are taken from four stations (with a 90° axial camera rotation) by one camera to measure 100 object points. Camera interior parameters are generated and listed in Table 5-3. Random noise with a standard deviation of  $\sigma_0 = 0.0004$  mm is added to the 2D image coordinates.

Table 5-3 Generated camera interior parameters

$\Delta x_p(\text{mm})$	$\Delta y_p(\text{mm})$	$\Delta c(\text{mm})$	$k_1(\text{mm}^{-2})$	$k_2(\text{mm}^{-4})$	$k_3(\text{mm}^{-6})$	$p_1(\text{mm}^{-1})$	$p_2(\text{mm}^{-1})$
1.00e-2	1.00e-2	3.52e-2	5.36e-3	-1.33e-4	7.35e-6	5.00e-4	5.00e-4

The separate adjustment with camera interior parameters considered is applied. The resulting *a posteriori* standard deviation of the observations was  $\hat{\sigma}_0 = 0.000397$  mm, which is very close to the *a priori* value. This means that systematic errors are well compensated and the measured results are mainly influenced by random errors. Figure 5-10 shows an error map from one image. No significant systematic error can be seen. However, if camera interior parameters are not considered in the adjustment process, the resulting *a posteriori* standard deviation will be  $\hat{\sigma}_0 = 0.001670$  mm. Significant systematic errors can be observed in the error map shown in Figure 5-11. More tests were conducted and the results are given in Chapter 7.

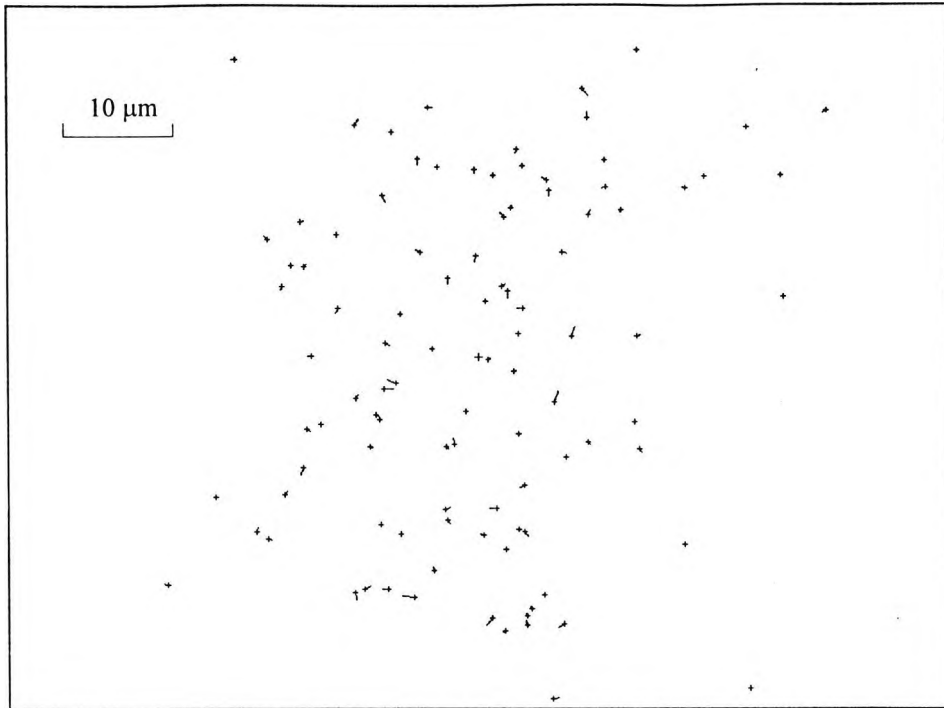


Figure 5-9 An error map with systematic errors compensated

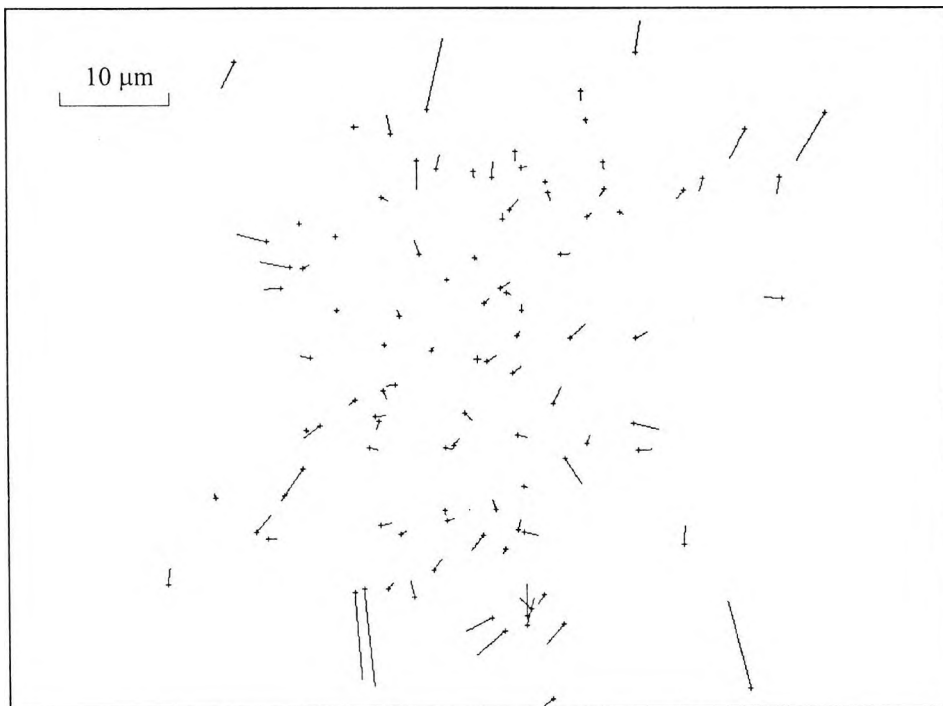


Figure 5-10 An error map with systematic errors uncompensated

## 5.6 Summary of the chapter

In this chapter, the method of the separate adjustment of the photogrammetric measurement is discussed. It is based upon the theory of the separate least squares adjustment discussed in Chapter 4. In the separate adjustment process, the 3D coordinates of the object points and the camera parameters are adjusted separately and iteratively. Since the datum can always be determined in both adjustment steps, constraints may not be necessary in the separate adjustment. A free network adjustment without any constraints becomes feasible and can be easily applied. Because the same functional model and the same target function of the least squares are used, the same results can be expected from the separate adjustment as from the simultaneous bundle adjustment.

The adjusted 3D coordinates of the object points from the free network separate adjustment are in an arbitrary coordinate system. A coordinate transformation is necessary if these 3D coordinates are required in a given coordinate system. It is also possible to include controls in the separate adjustment process to relate the estimated results to a given datum. In this case, the coordinate transformation can be avoided. But it is found that with controls involved in the separate adjustment process the convergent speed is slowed down significantly. Therefore for the fast 3D measurement it is better to use free network separate adjustment followed by a coordinate transformation. A fast coordinate transformation method (linear transformation), which is especially suitable for the results from the free network separate adjustment, will be discussed in Chapter 6.

The number of iterations required for the separate adjustment may be more than that for the bundle adjustment. However, due to the simple computation and the linear computational complexity, the speed of convergence of the separate adjustment is much faster than that of the bundle adjustment, especially for large data sets. The maximum memory required by the separate adjustment is limited to a  $6 \times 6$  unit (or  $14 \times 14$  when camera interior parameters are considered) no matter how many cameras and object

points are involved. Because of the high speed and low memory requirements, the separate adjustment can be used in real-time measurement to track moving objects.

The separate adjustment can also be applied to the self-calibration adjustment or for camera calibration. A three step separate adjustment (with camera interior and exterior parameters divided) or a two step separate adjustment (with camera interior and exterior parameters integrated) can be used.

The disadvantage of the separate adjustment is that the full covariance matrix of the estimated results is not provided directly. To evaluate the precision of the 3D coordinates a  $3 \times 3$  covariance matrix for each object point and a  $6 \times 6$  (or  $14 \times 14$ ) covariance matrix for each camera are given. These may be adequate in most cases. A full weight matrix of the estimated results is always available from the design matrix, from which the full covariance matrix can be derived whenever it is required.

## Chapter 6

### Coordinate Transformation

In surveying and photogrammetric measurement it is sometimes necessary to transform estimated coordinates from one coordinate system to another. The former could be an arbitrary coordinate system (e.g. the results from the simultaneous LSE with inner constraints or from the separate LSE with no specific constraints). The latter could be a specific pre-defined coordinate system. The transformation parameters can be obtained by knowing some coordinates (a minimum of four for 2D transformation and seven for 3D transformation) of common points in both systems. This transformation is named as *conformal transformation* or *similarity transformation* since no deformation of geometric shape is introduced by this transformation. The only change that may happen is a uniform scaling. After obtaining the transformation parameters all the coordinates of the object points (together with their cofactor matrix) in one coordinate system can be transformed to the other system.

#### 6.1 Two dimensional transformation

The relationship between the two sets of coordinates  $(x, y)$  and  $(x', y')$  for a common point  $i$  can generally be described as

$$\begin{cases} x'_i = ax_i + by_i + c \\ y'_i = -bx_i + ay_i + d \end{cases} \quad (6.1)$$

for a 2D similarity transformation. In this transformation,  $(x_i, y_i)$  could be the coordinates obtained from the simultaneous LSE with inner constraints or from the separate LSE with no specific constraints. So the datum defined by the starting values is arbitrary.  $(x'_i, y'_i)$  could be the pre-measured coordinates of some control points. To fulfil the coordinate transformation, the first step is to estimate the four transformation parameters  $a$ ,  $b$ ,  $c$  and  $d$  from the given coordinates of the common points in both coordinate systems. The second step is to transform the coordinates of all other points

from the arbitrary coordinate system to the pre-defined coordinate system via the estimated transformation parameters.

### 6.1.1 Estimation of the transformation parameters

If  $n$  common points are known in both coordinates system, Eq (6.1) may be written as

$$\begin{cases} x_1 a + y_1 b + c + 0 = x'_1 \\ y_1 a - x_1 b + 0 + d = y'_1 \\ x_2 a + y_2 b + c + 0 = x'_2 \\ y_2 a - x_2 b + 0 + d = y'_2 \\ \vdots \\ x_n a + y_n b + c + 0 = x'_n \\ y_n a - x_n b + 0 + d = y'_n \end{cases} \quad (6.2)$$

In matrix form it is

$$At = E \quad (6.3)$$

where

$$A = \begin{bmatrix} x_1 & y_1 & 1 & 0 \\ y_1 & -x_1 & 0 & 1 \\ x_2 & y_2 & 1 & 0 \\ y_2 & -x_2 & 0 & 1 \\ \vdots & \vdots & \vdots & \vdots \\ x_n & y_n & 1 & 0 \\ y_n & -x_n & 0 & 1 \end{bmatrix}, \quad t = \begin{bmatrix} a \\ b \\ c \\ d \end{bmatrix} \quad \text{and} \quad E = \begin{bmatrix} x'_1 \\ y'_1 \\ x'_2 \\ y'_2 \\ \vdots \\ x'_n \\ y'_n \end{bmatrix}$$

A minimum of two common points will determine the four parameters. If more points are available, least squares can be used for the best solution. Four cases are considered, they are: (i) both  $(x, y)$  and  $(x', y')$  are fixed; (ii)  $(x, y)$  are fixed while  $(x', y')$  are the observations with the weight matrix  $W_{x'}$ ; (iii)  $(x', y')$  are fixed while  $(x, y)$  are the

observations with the weight matrix  $W_x$ ; and (iv) both  $(x, y)$  and  $(x', y')$  are observations with the weight matrices  $W_x$  and  $W_x'$  respectively. For different cases the transformation parameters  $t$  may be estimated differently.

### Case I

The transformation parameters are obtained directly by linear least squares estimation, i.e.,

$$t = (A'A)^{-1} A'E \quad (6.4)$$

### Case II

The transformation parameters can also be obtained directly by linear least squares estimation, but taking the weight of the observations into account. So the cofactor matrix and the weight matrix of the transformation parameters are also available.

$$t = (A'W_x'A)^{-1} A'W_x'E \quad (6.5)$$

The cofactor matrix and weight matrix of the transformation parameters are estimated by

$$Q_t = (A'W_x'A)^{-1} \quad (6.6)$$

and

$$W_t = (A'W_x'A) \quad (6.7)$$

### Case III

Eq (6.1) can be rearranged as

$$\begin{aligned} \begin{bmatrix} x_i \\ y_i \end{bmatrix} &= \begin{bmatrix} a & b \\ -b & a \end{bmatrix}^{-1} \begin{bmatrix} x'_i - c \\ y'_i - d \end{bmatrix} \\ &= \frac{1}{a^2 + b^2} \begin{bmatrix} ax'_i - by'_i + (bd - ac) \\ bx'_i + ay'_i + (-bc - ad) \end{bmatrix}. \end{aligned}$$

Let  $a' = \frac{a}{a^2 + b^2}$ ,  $b' = \frac{b}{a^2 + b^2}$ ,  $c' = \frac{bd - ac}{a^2 + b^2}$  and  $d' = \frac{-bc - ad}{a^2 + b^2}$

So Eq (6.1) becomes

$$\begin{aligned} x_i &= a'x'_i - b'y'_i + c' \\ y_i &= b'x'_i + a'y'_i + d' \end{aligned} \tag{6.8}$$

or

$$A't' = E' \tag{6.9}$$

where

$$A' = \begin{bmatrix} x'_1 - y'_1 & 1 & 0 \\ y'_1 & x'_1 & 0 & 1 \\ x'_2 - y'_2 & 1 & 0 \\ y'_2 & x'_2 & 0 & 1 \\ \vdots & \vdots & \vdots & \vdots \\ x'_n - y'_n & 1 & 0 \\ y'_n & x'_n & 0 & 1 \end{bmatrix}, \quad t' = \begin{bmatrix} a' \\ b' \\ c' \\ d' \end{bmatrix} \quad \text{and} \quad E' = \begin{bmatrix} x_1 \\ y_1 \\ x_2 \\ y_2 \\ \vdots \\ x_n \\ y_n \end{bmatrix}$$

The parameters  $a'$ ,  $b'$ ,  $c'$  and  $d'$  are obtained directly by linear squares estimation, i.e.,

$$t' = (A'^t W_x A')^{-1} A'^t W_x E' \tag{6.10}$$

$$Q_{t'} = (A'^t W_x A')^{-1} \tag{6.11}$$

$$W_{t'} = (A'^t W_x A') \tag{6.12}$$

Least squares estimates for the original parameters  $a$ ,  $b$ ,  $c$  and  $d$  can then be obtained by

$$a = \frac{a'}{a'^2 + b'^2}, \quad b = \frac{b'}{a'^2 + b'^2}, \quad c = \frac{a'c' - b'd'}{a'^2 + b'^2} \quad \text{and} \quad d = \frac{a'd' - b'c'}{a'^2 + b'^2}$$

The cofactor matrix of  $t$  is obtained by

$$Q_t = JQ_r J^t \tag{6.13}$$

in which  $J$  is given by

$$J = \begin{bmatrix} \frac{\partial a}{\partial a'} & \frac{\partial a}{\partial b'} & \frac{\partial a}{\partial c'} & \frac{\partial a}{\partial d'} \\ \frac{\partial b}{\partial a'} & \frac{\partial b}{\partial b'} & \frac{\partial b}{\partial c'} & \frac{\partial b}{\partial d'} \\ \frac{\partial c}{\partial a'} & \frac{\partial c}{\partial b'} & \frac{\partial c}{\partial c'} & \frac{\partial c}{\partial d'} \\ \frac{\partial d}{\partial a'} & \frac{\partial d}{\partial b'} & \frac{\partial d}{\partial c'} & \frac{\partial d}{\partial d'} \end{bmatrix}$$

The weight matrix of  $t$  can be obtained by

$$\begin{aligned} W_t &= Q_t^{-1} && (6.14) \\ &= (JQ_r J^t)^{-1} \\ &= J^{t^{-1}} Q_r^{-1} J^{-1} \\ &= J^{t^{-1}} W_r J^{-1} \end{aligned}$$

#### Case IV

In this general case, both  $(x, y)$  and  $(x', y')$  are observations with weight matrix  $W_x$  and  $W_{x'}$  respectively. The functional model (6.1) is no longer linear since both  $(x, y)$  and  $t (= (a, b, c, d)^t)$  are variables.

Let  $l = (x_1 \ y_1 \ x_2 \ y_2 \ \dots \ x_n \ y_n \ x'_1 \ y'_1 \ x'_2 \ y'_2 \ \dots \ x'_n \ y'_n)'$ , the linearized functional model becomes

$$A\Delta t + Bv = C \tag{6.15}$$

in which  $\Delta t = (\Delta a \ \Delta b \ \Delta c \ \Delta d)'$  is a vector of corrections to the parameters,  $v$  is a vector of residuals of the observations, the cofactor matrix of the observations is given by

$$Q_l = \begin{bmatrix} Q_x \\ Q_x' \end{bmatrix}$$

assuming that  $(x, y)$  and  $(x', y')$  are uncorrelated. In Eq (6.15)

$$A = \left(\frac{\partial f}{\partial a}\right)_0 = \begin{bmatrix} x_1 & y_1 & 1 & 0 \\ y_1 & -x_1 & 0 & 1 \\ x_2 & y_2 & 1 & 0 \\ y_2 & -x_2 & 0 & 1 \\ \vdots & \vdots & & \\ x_n & y_n & 1 & 0 \\ y_n & -x_n & 0 & 1 \end{bmatrix}_{2n \times 4} \quad C = -(f)_0 = \begin{bmatrix} x'_1 - ax_1 - by_1 - c \\ y'_1 + bx_1 - ay_1 - d \\ x'_2 - ax_2 - by_2 - c \\ y'_2 + bx_2 - ay_2 - d \\ \vdots \\ x'_n - ax_n - by_n - c \\ y'_n + bx_n - ay_n - d \end{bmatrix}_{2n \times 1}$$

$$B = \left(\frac{\partial f}{\partial a}\right)_0 = \begin{bmatrix} a & b & 0 & 0 & \dots & 0 & 0 & -1 & 0 & 0 & 0 & \dots & 0 & 0 \\ -b & a & 0 & 0 & \dots & 0 & 0 & 0 & -1 & 0 & 0 & \dots & 0 & 0 \\ 0 & 0 & a & b & \dots & 0 & 0 & 0 & 0 & -1 & 0 & \dots & 0 & 0 \\ 0 & 0 & -b & a & \dots & 0 & 0 & 0 & 0 & 0 & -1 & \dots & 0 & 0 \\ & & & \vdots & & & & & & & \vdots & & & \\ 0 & 0 & 0 & 0 & \dots & a & b & 0 & 0 & 0 & 0 & \dots & -1 & 0 \\ 0 & 0 & 0 & 0 & \dots & -b & a & 0 & 0 & 0 & 0 & \dots & 0 & -1 \end{bmatrix}_{2n \times 4n}$$

$$= [B_1 \ B_2]_{2n \times 4n}$$

where

$$B_1 = \begin{bmatrix} a & b & 0 & 0 & \cdots & 0 & 0 \\ -b & a & 0 & 0 & \cdots & 0 & 0 \\ 0 & 0 & a & b & \cdots & 0 & 0 \\ 0 & 0 & -b & a & \cdots & 0 & 0 \\ & & & & \vdots & & \\ 0 & 0 & 0 & 0 & \cdots & a & b \\ 0 & 0 & 0 & 0 & \cdots & -b & a \end{bmatrix}_{2n \times 2n}$$

and

$$B_2 = -I_{2n \times 2n}$$

By generalized least squares estimation (Mikhail 1976) the unknown parameters are estimated by

$$\Delta t = (A'(BQ_1B')^{-1}A)^{-1}A'(BQ_1B')^{-1}C \quad (6.16)$$

$$Q_t = (A'(BQ_1B')^{-1}A)^{-1} \quad (6.17)$$

$$W_t = (A'(BQ_1B')^{-1}A) \quad (6.18)$$

in which

$$(BQ_1B')^{-1} = \left( \begin{bmatrix} B_1 & B_2 \end{bmatrix} \begin{bmatrix} Q_x & \\ & Q_x' \end{bmatrix} \begin{bmatrix} B_1' \\ B_2' \end{bmatrix} \right)^{-1} \quad (6.19a)$$

$$= (B_1Q_xB_1' + Q_x')^{-1} \quad (6.19b)$$

$$= Q_x'^{-1} - Q_x'^{-1}B_1(Q_x^{-1} + B_1'Q_x'^{-1}B_1)^{-1}B_1'Q_x'^{-1} \quad (6.19c)$$

$$= W_x' - W_x'B_1(W_x + B_1'W_x'B_1)^{-1}B_1'W_x' \quad (6.19d)$$

If the cofactor matrices  $Q_x$  and  $Q_x'$  of the coordinates  $(x, y)$  and  $(x', y')$  are available Eq (6.19b) should be used. But if the cofactor matrices are not obtainable (e.g. the

results from separate LSE), the weight matrices (which are easily obtained) can be used in Eq (6.19d) to calculate  $(BQ_i B^t)^{-1}$ . Therefore the transformation parameters can be estimated without knowing the cofactor matrices of the coordinates which are difficult to obtain by separate LSE.

The parameters  $a$ ,  $b$ ,  $c$  and  $d$  in  $B$  and  $C$  are initially given as starting values. After each iteration  $B$  and  $C$  should be updated and another iteration applied. The iterative procedure terminates when the given stop criteria are met.

The estimates for the third special case (Case III) can also be derived from the estimates of the general case (Case IV). In Case III, the coordinates  $(x', y')$  are fixed, so

$$W'_x \rightarrow \infty \quad \text{or} \quad Q'_x \rightarrow 0$$

Therefore

$$\begin{aligned} (BQ_i B^t)^{-1} &= (B_1 Q_x B_1^t)^{-1} \\ &= B_1^{t-1} Q_x^{-1} B_1^{-1} \\ &= \left( \frac{B_1}{a^2 + b^2} \right) W_x \left( \frac{B_1^t}{a^2 + b^2} \right) \\ &= (a^2 + b^2)^{-2} (B_1 W_x B_1^t) \end{aligned} \tag{6.20}$$

The transformation parameters are estimated by

$$\begin{aligned} \Delta t &= (A^t (BQ_i B^t)^{-1} A)^{-1} A^t (BQ_i B^t)^{-1} C \\ &= (a^2 + b^2)^2 (A^t B_1 W_x B_1^t A)^{-1} A^t (a^2 + b^2)^{-2} B_1 W_x B_1^t C \\ &= (A^t B_1 W_x B_1^t A)^{-1} A^t B_1 W_x B_1^t C \end{aligned} \tag{6.21}$$

$$\begin{aligned} Q_i &= (A^t (BQ_i B^t)^{-1} A)^{-1} \\ &= (a^2 + b^2)^2 (A^t B_1 W_x B_1^t A)^{-1} \end{aligned} \tag{6.22}$$

$$\begin{aligned} W_t &= (A'(BQ_t B')^{-1}A) \\ &= (a^2 + b^2)^{-2} (A' B_1 W_x B_1' A) \end{aligned} \quad (6.23)$$

$s = \sqrt{a^2 + b^2}$  is the scale factor of the transformation. If the scale is to remain constant after transformation, i.e.,  $s = 1$ , the cofactor matrix and the weight matrix are then obtained by

$$Q_t = (A' B_1 W_x B_1' A)^{-1} \quad (6.24)$$

and

$$W_t = A' B_1 W_x B_1' A \quad (6.25)$$

Another special case is that all the  $(x, y)$  coordinates are uncorrelated and have the same weight  $w_1$ , and all the  $(x', y')$  coordinates are uncorrelated and have the same weight  $w_2$ . Under these assumptions, the weight matrices of the coordinates become

$$\begin{aligned} W_x &= \text{diag}(w_1, w_1, \dots, w_1)_{2n \times 2n} \\ W_x' &= \text{diag}(w_2, w_2, \dots, w_2)_{2n \times 2n} \end{aligned}$$

So

$$\begin{aligned} (B W_t B)^{-1} &= W_x' - W_x' B_1 (W_x + B_1' W_x' B_1)^{-1} B_1' W_x' \\ &= w_2 I_{2n \times 2n} - w_2^2 (a^2 + b^2) (w_1 + (a^2 + b^2) w_2)^{-1} I_{2n \times 2n} \\ &= \left( w_2 - \frac{w_2^2 (a^2 + b^2)}{w_1 + (a^2 + b^2) w_2} \right) I_{2n \times 2n} \\ &= \frac{w_1 w_2}{w_1 + (a^2 + b^2) w_2} I_{2n \times 2n} \end{aligned}$$

Considering that the cofactor matrices are also diagonal matrices and the diagonal elements  $q = 1/w$ , so

$$\begin{aligned}
 (\mathbf{B}\mathbf{W}_t\mathbf{B})^{-1} &= \frac{\frac{1}{q_1q_2}}{\frac{1}{q_1} + (a^2 + b^2)\frac{1}{q_2}} I_{2n \times 2n} \\
 &= \frac{1}{q_2 + (a^2 + b^2)q_1} I_{2n \times 2n}
 \end{aligned}$$

This is the same result as given in Mikhail (1981) where only this special case was discussed.

The transformation parameters can then be estimated by Eq (6.21) to (6.23). If the shape of the object remains unchanged in both coordinate systems, the transformation parameters can be estimated perfectly, i.e., the cofactor matrix of the transformation parameters will be null ( $\mathbf{Q}_t = \mathbf{0}$ ) and the weight matrix approaches infinity ( $\mathbf{W}_t \rightarrow \infty$ ). The transformation parameters can simply be estimated by Eq (6.4).

### 6.1.2 Estimation of transformed coordinates

With the estimated transformation parameters all the coordinates can then be transformed from one coordinate system to another coordinate system by Eq (6.1). The coordinates transformed from  $(x, y)$  system to  $(x', y')$  system can easily be obtained. However the cofactor matrix or weight matrix also need to be estimated. For this purpose Eq (6.1) is expressed as

$$\mathbf{x}' = \mathbf{f}(\mathbf{x}, t) \quad (6.26)$$

If  $m$  points are transformed, then

$$\mathbf{x}' = \begin{bmatrix} x'_1 \\ y'_1 \\ x'_2 \\ y'_2 \\ \vdots \\ x'_m \\ y'_m \end{bmatrix} \quad \mathbf{x} = \begin{bmatrix} x_1 \\ y_1 \\ x_2 \\ y_2 \\ \vdots \\ x_m \\ y_m \end{bmatrix} \quad \mathbf{t} = \begin{bmatrix} a \\ b \\ c \\ d \end{bmatrix}$$

By the general law of propagation of the cofactor matrices

$$\mathbf{Q}_{x'} = \mathbf{J}\mathbf{Q}_{xt}\mathbf{J}' \quad (6.27)$$

in which

$$\mathbf{Q}_{xt} = \begin{bmatrix} \mathbf{Q}_x \\ \mathbf{Q}_t \end{bmatrix} \quad (6.28)$$

and

$$\mathbf{J} = [\mathbf{J}_x \ \mathbf{J}_t] = \begin{bmatrix} \frac{\partial}{\partial x} & \frac{\partial}{\partial t} \end{bmatrix} \quad (6.29)$$

where

$$\mathbf{J}_x = \begin{bmatrix} a & b & 0 & 0 & \cdots & 0 & 0 \\ -b & a & 0 & 0 & \cdots & 0 & 0 \\ 0 & 0 & a & b & \cdots & 0 & 0 \\ 0 & 0 & -b & a & \cdots & 0 & 0 \\ & & & & \vdots & & \\ 0 & 0 & 0 & 0 & \cdots & a & b \\ 0 & 0 & 0 & 0 & \cdots & -b & a \end{bmatrix}_{2n \times 2n} \quad (6.30)$$

and

$$J_t = \begin{bmatrix} x_t & y_t & 1 & 0 \\ y_t & -x_t & 0 & 1 \\ x_2 & y_2 & 1 & 0 \\ y_2 & -x_2 & 0 & 1 \\ \vdots & \vdots & & \\ x_n & y_n & 1 & 0 \\ y_n & -x_n & 0 & 1 \end{bmatrix}_{2n \times 4} \quad (6.31)$$

So the cofactor matrix of the transformed coordinates is obtained by

$$\begin{aligned} Q'_x &= [J_x \ J_t] \begin{bmatrix} Q_x \\ Q_t \end{bmatrix} \begin{bmatrix} J'_x \\ J'_t \end{bmatrix} \\ &= J_x Q_x J'_x + J_t Q_t J'_t \end{aligned} \quad (6.32)$$

and the weight matrix is obtained by

$$\begin{aligned} W'_x &= Q_x'^{-1} \\ &= (J_x Q_x J'_x + J_t Q_t J'_t)^{-1} \end{aligned} \quad (6.33)$$

Let  $U = J_x Q_x J'_x$ , therefore

$$W'_x = U^{-1} - U^{-1} J_t (W_t + J'_t U^{-1} J_t)^{-1} J'_t U^{-1} \quad (6.34)$$

and

$$\begin{aligned} U^{-1} &= (J_x Q_x J'_x)^{-1} \\ &= J_x'^{-1} Q_x^{-1} J_x^{-1} \\ &= (a^2 + b^2)^{-2} (J_x W_x J'_x) \end{aligned} \quad (6.35)$$

In the special case when  $Q_t = 0$ , Eq (6.34) becomes

$$\begin{aligned} W'_x &= U^{-1} \\ &= (a^2 + b^2)^{-2} (J_x W_x J'_x) \end{aligned} \quad (6.36)$$

For the example discussed in section 4.7, the results (the coordinates of four plane points and their weight matrix) estimated from the inner constrained LSE (or the unified LSE) and the separate LSE can be compared after a coordinate transformation. The eight coordinates from the separate LSE, expressed as  $x$ , are

$x_1$ (mm)	$y_1$ (mm)	$x_2$ (mm)	$y_2$ (mm)	$x_3$ (mm)	$y_3$ (mm)	$x_4$ (mm)	$y_4$ (mm)
-0.0022	0.0250	-0.0022	427.9744	430.5350	431.2545	427.2445	1.5175

and the weight matrix is

$$W_x = \begin{bmatrix} 30.5463 & 5.6429 & 0.0000 & -0.0000 & -5.5466 & -5.5555 & -24.9997 & -0.0873 \\ & 30.5648 & -0.0000 & -25.0000 & -5.5555 & -5.5645 & -0.0873 & 0.0003 \\ & & 30.5644 & -5.3651 & -24.9985 & -0.1905 & -5.5658 & 5.5555 \\ & & & 30.5467 & -0.1905 & -0.0015 & 5.5555 & -5.5453 \\ & & & & 30.5466 & 5.9374 & -0.0015 & -0.1914 \\ & & & & & 30.5645 & -0.1914 & -24.9985 \\ & & & & & & 30.5670 & -5.2768 \\ & & & & & & & 30.5441 \end{bmatrix} \text{ (mm}^{-2}\text{)}$$

*symmetric*

The eight coordinates from the inner constrained LSE (or the unified LSE), expressed as  $x'$ , are

$x_1'$ (mm)	$y_1'$ (mm)	$x_2'$ (mm)	$y_2'$ (mm)	$x_3'$ (mm)	$y_3'$ (mm)	$x_4'$ (mm)	$y_4'$ (mm)
-0.3447	-0.3448	0.3992	427.6040	430.9415	430.1357	426.9040	0.4051

With any two points (e.g. the first two points) in  $x$  and  $x'$  the transformation parameters  $t$  (from  $x$  to  $x'$ ) are estimated, they are

$$a = 1.0000, \quad b = 0.0017, \quad c = -0.3425, \quad d = -0.3698$$

The other points can then be transformed from  $x$  to  $x'$ . It was found that the transformed coordinates perfectly agreed with the coordinates from the inner

constrained LSE (or the unified LSE). Therefore the shapes of the quadrilateral were same. The cofactor matrix of the matrix of the transformation parameters is null ( $Q_t = 0$ ).

To compare the weight matrices of the estimated coordinates from the two methods, the matrix  $J_x$  is constructed with  $a$  and  $b$  by Eq (6.30). The weight matrix of the estimated coordinates after coordinate transformation is calculated by Eq (6.36). The result is

$$W'_x = \begin{bmatrix} 30.5659 & 5.6429 & 0.0001 & -0.0435 & -5.5659 & -5.5555 & -24.9999 & -0.0439 \\ & 30.5452 & -0.0435 & -24.9999 & -5.5555 & -5.5452 & -0.0439 & 0.0001 \\ & & 30.5457 & -5.3651 & -24.9991 & -0.1470 & -5.5465 & 5.5555 \\ & & & 30.5654 & -0.1470 & -0.0009 & 5.5555 & -5.5646 \\ & & & & 30.5673 & 5.9374 & -0.0022 & -0.2349 \\ & & & & & 30.5438 & -0.2349 & -24.9978 \\ & & & & & & 30.5487 & -5.2768 \\ & & & & & & & 30.5625 \end{bmatrix} (mm^{-2})$$

*symmetric*

This is exactly the same (to 4 decimal places) as that obtained from the inner constrained LSE (or the unified LSE).

## 6.2 Three dimensional transformation

### 6.2.1 Conventional method

In the 3D case, similarity transformation can be described by seven parameters, one in scale, three in rotation and three in translation. In matrix form, the transformation can be expressed as

$$x' = sRx + T \quad (6.37)$$

where  $x$  and  $x'$  are vectors of coordinates (3D positions) before and after transformation respectively,  $s$  is a scale factor,  $R$  is a  $3 \times 3$  orthogonal matrix with three

$\kappa$ ), and  $T$  is a vector with three translations ( $x_0, y_0, z_0$ ). The seven transformation parameters are expressed by  $u = [s \ \omega \ \phi \ \kappa \ x_0 \ y_0 \ z_0]$ . The functional model for one point with coordinates in both systems is

$$f_i = sR x_i + T - x'_i = 0 \quad (6.38)$$

and the linearized functional model for one point is

$$A_i \Delta u + B_i v_i = C_i \quad (6.39)$$

where  $A_i$  is a Jacobian matrix

$$A_i = \left( \frac{\partial f_i}{\partial u} \right)_0 = \begin{bmatrix} R x_i & sR_\omega x_i & sR_\phi x_i & sR_\kappa x_i & I \\ (3 \times 1) & (3 \times 1) & (3 \times 1) & (3 \times 1) & (3 \times 3) \end{bmatrix}$$

in which

$$R_\omega = \frac{\partial R}{\partial \omega} = R \begin{bmatrix} 0 & 0 & 0 \\ 0 & 0 & 1 \\ 0 & -1 & 0 \end{bmatrix}$$

$$R_\phi = \frac{\partial R}{\partial \phi} = R \begin{bmatrix} 0 & \sin w & \cos w \\ -\sin w & 0 & 0 \\ \cos w & 0 & 0 \end{bmatrix} = \begin{bmatrix} 0 & 0 & -\cos k \\ 0 & 0 & \sin k \\ \cos k & -\sin k & 0 \end{bmatrix} R$$

$$R_\kappa = \frac{\partial R}{\partial \kappa} = \begin{bmatrix} 0 & 1 & 0 \\ -1 & 0 & 0 \\ 0 & 0 & 0 \end{bmatrix} R$$

$B_i$  is also a Jacobian matrix

$$B_i = \left( \frac{\partial f_i}{\partial a} \right)_0 = \begin{bmatrix} sR & -I \\ (3 \times 3) & (3 \times 3) \end{bmatrix}$$

For  $n$  points the linearized functional model becomes

$$A\Delta u + Bv = C \quad (6.40)$$

where

$$A = \begin{bmatrix} A_1 \\ A_2 \\ \vdots \\ A_n \end{bmatrix} \quad \text{and} \quad B = \begin{bmatrix} B_1 & 0 & \cdots & 0 \\ 0 & B_2 & \cdots & 0 \\ \cdots & \cdots & \cdots & \cdots \\ 0 & 0 & \cdots & B_n \end{bmatrix}$$

Conventionally, the seven transformation parameters can be estimated by least squares using Eq (6.40). The coordinates before and after transformation are treated as observations and the sum of weighted squares of the residuals at the control points is minimised. The seven parameters are estimated by

$$\Delta u = (A'(BQ_i B')^{-1} A)^{-1} A'(BQ_i B')^{-1} C \quad (6.41)$$

This is a general case of least squares process which requires sophisticated computation. After obtaining the transformation parameters, all the coordinates of the object points in one coordinate system can be transformed to the other system. The cofactor matrix of the transformed coordinates can be calculated by the S-transformation (Strang van Hees 1982). This conventional method of coordinate transformation is rigorous, but very complicated. It has been well understood and will not be discussed in detail here.

In this section a method of linear coordinate transformation is discussed. The computation of the transformation parameters is significantly simplified and it is especially suitable for the 3D coordinates obtained by separate least squares adjustment with no constraints. The full covariance matrix of the 3D coordinates is not necessary in this case, whilst the inverse of the covariance matrix (the weight matrix) which is available from the design matrix can be used instead.

## 6.2.2 Linear coordinate transformation

### 6.2.2.1 Estimation of the transformation parameters

If  $n$  common points are known in both coordinates system, the transformation equations can be expressed in a linear form with twelve transformation parameters, i.e.,

$$At = b \tag{6.42}$$

where

$$A = \begin{bmatrix} x_1 & y_1 & z_1 & 0 & 0 & 0 & 0 & 0 & 0 & 1 & 0 & 0 \\ 0 & 0 & 0 & x_1 & y_1 & z_1 & 0 & 0 & 0 & 0 & 1 & 0 \\ 0 & 0 & 0 & 0 & 0 & 0 & x_1 & y_1 & z_1 & 0 & 0 & 1 \\ x_2 & y_2 & z_2 & 0 & 0 & 0 & 0 & 0 & 0 & 1 & 0 & 0 \\ 0 & 0 & 0 & x_2 & y_2 & z_2 & 0 & 0 & 0 & 0 & 1 & 0 \\ 0 & 0 & 0 & 0 & 0 & 0 & x_2 & y_2 & z_2 & 0 & 0 & 1 \\ & & & \vdots & & \vdots & & & & & & \\ x_n & y_n & z_n & 0 & 0 & 0 & 0 & 0 & 0 & 1 & 0 & 0 \\ 0 & 0 & 0 & x_n & y_n & z_n & 0 & 0 & 0 & 0 & 1 & 0 \\ 0 & 0 & 0 & 0 & 0 & 0 & x_n & y_n & z_n & 0 & 0 & 1 \end{bmatrix},$$

$$t = \begin{bmatrix} t_1 \\ t_2 \\ \vdots \\ t_{12} \end{bmatrix} \quad \text{and} \quad b = \begin{bmatrix} x'_1 \\ y'_1 \\ z'_1 \\ x'_2 \\ y'_2 \\ z'_2 \\ \vdots \\ x'_n \\ y'_n \\ z'_n \end{bmatrix}$$

A minimum of four common points in both system will determine the twelve transformation parameters uniquely. However if more points are given, least squares estimation is used for the best solution. Four situations are considered, and they are

- (i) both  $(x, y, z)$  and  $(x', y', z')$  are fixed;
- (ii)  $(x, y, z)$  are fixed while  $(x', y', z')$  are the observations with weight matrix  $W_x'$ ;
- (iii)  $(x', y', z')$  are fixed while  $(x, y, z)$  are the observations with weight matrix  $W_x$ ;
- (iv) both  $(x, y, z)$  and  $(x', y', z')$  are observations with weight matrix  $W_x$  and  $W_x'$  respectively.

### Case I

The twelve transformation parameters can be obtained directly by linear least squares estimation, i.e.,

$$t = (A'A)^{-1} A'b \quad (6.43)$$

### Case II

The twelve transformation parameters can also be obtained directly by linear least squares estimation, but with the weight of the observations taking into account. So the cofactor matrix and the weight matrix of the transformation parameters are also available.

$$t = (A'W_x'A)^{-1} A'W_x'b \quad (6.44)$$

The cofactor matrix and weight matrix of the parameters are estimated by

$$Q_t = (A'W_x'A)^{-1} \quad (6.45)$$

and

$$W_t = (A'W_x'A) \quad (6.46)$$

**Case III and IV**

Considered the general case (case IV) first and then treat case III as a special case. In case IV, both  $(x, y, z)$  and  $(x', y', z')$  are observations with weight matrix  $W_x$  and  $W_x'$  respectively. The functional model is no longer linear. Rearranging Eq (6.42) to give

$$\begin{cases} f_x = t_1 x_i + t_2 y_i + t_3 z_i + t_{10} - x'_i = 0 \\ f_y = t_4 x_i + t_5 y_i + t_6 z_i + t_{11} - x'_i = 0 \\ f_z = t_7 x_i + t_8 y_i + t_9 z_i + t_{12} - x'_i = 0 \end{cases} \quad (6.47)$$

Let  $t = [t_1 \ t_2 \ \dots \ t_{12}]'$  and  $l = [l_1 \ l_2]'$ , where

$$\begin{aligned} l_1 &= (x_1 \ y_1 \ z_1 \ x_2 \ y_2 \ z_2 \ \dots \ x_n \ y_n \ z_n) \\ l_2 &= (x'_1 \ y'_1 \ z'_1 \ x'_2 \ y'_2 \ z'_2 \ \dots \ x'_n \ y'_n \ z'_n) \end{aligned}$$

The linearized functional model becomes

$$A\Delta t + Bv = C \quad (6.48)$$

in which  $\Delta t = [\Delta t_1 \ \Delta t_2 \ \dots \ \Delta t_{12}]'$  is a vector of the corrections of the parameters,  $v$  is a vector of the residuals of the observations. The weight matrix and cofactor matrix of the observations are given by

$$W_l = \begin{bmatrix} W_x & \\ & W_x' \end{bmatrix} \quad \text{and} \quad Q_l = \begin{bmatrix} Q_x & \\ & Q_x' \end{bmatrix}$$

considering that  $(x, y, z)$  and  $(x', y', z')$  are generally uncorrelated. In Eq (6.48)



$$C = -(f)^0 = \begin{bmatrix} x'_1 - t_1 x_1 - t_2 y_1 - t_3 z_1 - t_{10} \\ y'_1 - t_4 x_1 - t_5 y_1 - t_6 z_1 - t_{11} \\ z'_1 - t_7 x_1 - t_8 y_1 - t_9 z_1 - t_{12} \\ x'_2 - t_1 x_2 - t_2 y_2 - t_3 z_2 - t_{10} \\ y'_2 - t_4 x_2 - t_5 y_2 - t_6 z_2 - t_{11} \\ z'_2 - t_7 x_2 - t_8 y_2 - t_9 z_2 - t_{12} \\ \vdots \\ x'_n - t_1 x_n - t_2 y_n - t_3 z_n - t_{10} \\ y'_n - t_4 x_n - t_5 y_n - t_6 z_n - t_{11} \\ z'_n - t_7 x_n - t_8 y_n - t_9 z_n - t_{12} \end{bmatrix}$$

By the general least squares estimation the unknown parameters are estimated by

$$\Delta t = (A^t (BQ_l B^t)^{-1} A)^{-1} A^t (BQ_l B^t)^{-1} C \quad (6.49)$$

$$Q_l = (A^t (BQ_l B^t)^{-1} A)^{-1} \quad (6.50)$$

$$W_l = (A^t (BQ_l B^t)^{-1} A) \quad (6.51)$$

in which

$$\begin{aligned} (BQ_l B^t)^{-1} &= \left( \begin{bmatrix} B_1 & B_2 \end{bmatrix} \begin{bmatrix} Q_x & \\ & Q'_x \end{bmatrix} \begin{bmatrix} B_1^t \\ B_2^t \end{bmatrix} \right)^{-1} \\ &= (B_l Q_x B_l^t + Q'_x)^{-1} \end{aligned} \quad (6.52)$$

If both  $Q_x$  and  $Q'_x$  are not obtained,  $(BQ_l B^t)^{-1}$  can be calculated by

$$\begin{aligned} (BQ_l B^t)^{-1} &= Q_x'^{-1} - Q_x'^{-1} B_l (Q_x^{-1} + B_l^t Q_x'^{-1} B_l)^{-1} B_l^t Q_x'^{-1} \\ &= W_x' - W_x' B_l (W_x + B_l^t W_x' B_l)^{-1} B_l^t W_x' \end{aligned} \quad (6.53)$$

If the cofactor matrices  $Q_x$  and  $Q'_x$  of the coordinates  $(x, y, z)$  and  $(x', y', z')$  are available Eq (6.52) should be used. If these cofactor matrices are not obtainable (e.g. the

results from the separate LSE) the weight matrices, which are always available from the design matrix, can be used in Eq (6.53) to calculate  $(BQ_iB)^{-1}$ . Therefore the transformation parameters can be estimated without the cofactor matrices of the coordinates which are difficult to obtain by the LSE.

The parameters  $t_1$  to  $t_{12}$  in  $B$  and  $C$  are starting values initially. After each iteration  $B$  and  $C$  should be updated and another iteration applied. The iterative procedure terminates when the required precision is obtained.

### 6.2.2.2 Estimation of the transformed coordinates

With the estimated transformation parameters  $t_1$  to  $t_{12}$ , all the coordinates can then be transformed from one coordinate system to another coordinate system. The transformation equations can be expressed as

$$\begin{cases} x'_i = t_1x_i + t_2y_i + t_3z_i + t_{10} \\ y'_i = t_4x_i + t_5y_i + t_6z_i + t_{11} \\ z'_i = t_7x_i + t_8y_i + t_9z_i + t_{12} \end{cases} \quad (6.54)$$

The coordinates transformed from  $(x, y, z)$  to  $(x', y', z')$  can easily be obtained from above equations. To estimate the cofactor matrix and the weight matrix of the transformed coordinates, Eq (6.54) are expressed as

$$x' = f(x, t) \quad (6.55)$$

If  $m$  points are transformed, then

$$\mathbf{x}' = \begin{bmatrix} x'_1 \\ y'_1 \\ z'_1 \\ x'_2 \\ y'_2 \\ z'_2 \\ \vdots \\ x'_m \\ y'_m \\ z'_m \end{bmatrix} \quad \mathbf{x} = \begin{bmatrix} x_1 \\ y_1 \\ z_1 \\ x_2 \\ y_2 \\ z_2 \\ \vdots \\ x_m \\ y_m \\ z_m \end{bmatrix} \quad \mathbf{t} = \begin{bmatrix} t_1 \\ t_2 \\ \vdots \\ t_{12} \end{bmatrix}$$

By the general law of propagation of the cofactor matrices

$$\mathbf{Q}_{x'} = \mathbf{J} \mathbf{Q}_{xt} \mathbf{J}' \tag{6.56}$$

in which

$$\mathbf{Q}_{xt} = \begin{bmatrix} \mathbf{Q}_x \\ \mathbf{Q}_t \end{bmatrix} \tag{6.57}$$

and

$$\mathbf{J} = [\mathbf{J}_x \ \mathbf{J}_t] = \left[ \frac{\partial \mathbf{f}}{\partial \mathbf{x}} \ \frac{\partial \mathbf{f}}{\partial \mathbf{t}} \right] \tag{6.58}$$

where

$$\mathbf{J}_x = \frac{\partial \mathbf{f}}{\partial \mathbf{x}} = \begin{bmatrix} t_1 & t_2 & t_3 & & & \\ t_4 & t_5 & t_6 & 0 & 0 & 0 \\ t_7 & t_8 & t_9 & & & \\ & t_1 & t_2 & t_3 & & \\ 0 & t_4 & t_5 & t_6 & 0 & 0 \\ & t_7 & t_8 & t_9 & \dots & \\ 0 & 0 & & & & 0 \\ & & & & & t_1 & t_2 & t_3 \\ 0 & 0 & 0 & & & t_4 & t_5 & t_6 \\ & & & & & t_7 & t_8 & t_9 \end{bmatrix}_{3m \times 3m} \tag{6.59}$$

and

$$J_t = \frac{\partial f}{\partial a} = \begin{bmatrix} x_1 & y_1 & z_1 & 0 & 0 & 0 & 0 & 0 & 0 & 0 & 1 & 0 & 0 \\ 0 & 0 & 0 & x_1 & y_1 & z_1 & 0 & 0 & 0 & 0 & 0 & 1 & 0 \\ 0 & 0 & 0 & 0 & 0 & 0 & x_1 & y_1 & z_1 & 0 & 0 & 0 & 1 \\ x_2 & y_2 & z_2 & 0 & 0 & 0 & 0 & 0 & 0 & 0 & 1 & 0 & 0 \\ 0 & 0 & 0 & x_2 & y_2 & z_2 & 0 & 0 & 0 & 0 & 0 & 1 & 0 \\ 0 & 0 & 0 & 0 & 0 & 0 & x_2 & y_2 & z_2 & 0 & 0 & 0 & 1 \\ & & & \vdots & & & \vdots & & & & & & \\ x_m & y_m & z_m & 0 & 0 & 0 & 0 & 0 & 0 & 0 & 1 & 0 & 0 \\ 0 & 0 & 0 & x_m & y_m & z_m & 0 & 0 & 0 & 0 & 0 & 1 & 0 \\ 0 & 0 & 0 & 0 & 0 & 0 & x_m & y_m & z_m & 0 & 0 & 0 & 1 \end{bmatrix}_{3m \times 12} \quad (6.60)$$

So the cofactor matrix and the weight matrix of the transformed coordinates are obtained by

$$\begin{aligned} Q_{x'} &= [J_x \ J_t] \begin{bmatrix} Q_x \\ Q_t \end{bmatrix} \begin{bmatrix} J_x' \\ J_t' \end{bmatrix} \\ &= J_x Q_x J_x' + J_t Q_t J_t' \end{aligned} \quad (6.61)$$

and

$$\begin{aligned} W_{x'} &= Q_{x'}^{-1} \\ &= (J_x Q_x J_x' + J_t Q_t J_t')^{-1} \end{aligned} \quad (6.62)$$

Let  $U = J_x Q_x J_x'$ , therefore

$$W_{x'} = U^{-1} - U^{-1} J_t (W_t + J_t' U^{-1} J_t)^{-1} J_t' U^{-1} \quad (6.63)$$

and

$$\begin{aligned} U^{-1} &= (J_x Q_x J_x')^{-1} \\ &= J_x'^{-1} Q_x^{-1} J_x^{-1} \end{aligned} \quad (6.64)$$

Since  $J_x$  is an orthogonal matrix (when the scale factor  $s$  is extracted),  $J^{-1} = J^t$ , therefore

$$U^{-1} = J_x W_x J_x^t \quad (6.65)$$

In the special case when  $Q_t = 0$ , Eq (6.63) becomes

$$\begin{aligned} W_x' &= U^{-1} \\ &= (J_x W_x J_x^t) \end{aligned} \quad (6.66)$$

For the estimated 3D coordinates from the bundle adjustment and the separate adjustment, the weight matrix  $W_x$  is a block diagonal matrix in which each block is a  $3 \times 3$  square matrix. If the 3D coordinates are required to transform into another coordinate system  $x'$ , a block diagonal matrix  $J_x$  can be constructed from Eq (6.59) and the weight matrix  $W_x'$  (after transformation) can be calculated by Eq (6.66). Because of the special structures of the matrices  $W_x$  and  $J_x$ , the products of the matrices are calculated between  $3 \times 3$  square matrices. Time and memory are saved significantly.

### 6.2.3 Estimation of seven parameters from twelve parameters

It is necessary sometimes to know the seven transformation parameters ( $s, \alpha, \beta, \gamma, x_0, y_0, z_0$ ) instead of the twelve parameters ( $t_1, t_2, \dots, t_{12}$ ). In this case the pre-estimated twelve parameters  $t$  (together with their weight matrix) are treated as observations and the seven parameters need to be estimated. The relationships between these parameters are expressed as

$$\begin{cases}
 s(\cos \beta \cos \gamma) & = t_1 \\
 s(\sin \alpha \sin \beta \cos \gamma + \cos \alpha \sin \gamma) & = t_2 \\
 s(-\cos \alpha \sin \beta \cos \gamma + \sin \alpha \sin \gamma) & = t_3 \\
 s(-\cos \beta \sin \gamma) & = t_4 \\
 s(-\sin \alpha \sin \beta \sin \gamma + \cos \alpha \cos \gamma) & = t_5 \\
 s(\cos \alpha \sin \beta \sin \gamma + \sin \alpha \cos \gamma) & = t_6 \\
 s(\sin \beta) & = t_7 \\
 s(-\sin \alpha \cos \beta) & = t_8 \\
 s(\cos \alpha \cos \beta) & = t_9 \\
 x_0 & = t_{10} \\
 y_0 & = t_{11} \\
 z_0 & = t_{12}
 \end{cases} \quad (6.67)$$

These equations are typical observation equations with twelve measured elements and seven unknown parameters to be estimated. The seven parameters can be estimated by least squares, i.e.,

$$\Delta x = (A'W_tA)^{-1} A'W_t b \quad (6.68)$$

$$x = (x)_0 + \Delta x \quad (6.69)$$

$$W_x = A'W_tA \quad (6.70)$$

$$Q_x = (A'W_tA)^{-1} \quad (6.71)$$

in which

$$A = \left( \frac{\partial f}{\partial x} \right)_0 = \begin{bmatrix} \frac{\partial f_1}{\partial s} & \frac{\partial f_1}{\partial \alpha} & \frac{\partial f_1}{\partial \beta} & \frac{\partial f_1}{\partial \gamma} & \frac{\partial f_1}{\partial x_0} & \frac{\partial f_1}{\partial y_0} & \frac{\partial f_1}{\partial z_0} \\ \frac{\partial f_2}{\partial s} & \frac{\partial f_2}{\partial \alpha} & \frac{\partial f_2}{\partial \beta} & \frac{\partial f_2}{\partial \gamma} & \frac{\partial f_2}{\partial x_0} & \frac{\partial f_2}{\partial y_0} & \frac{\partial f_2}{\partial z_0} \\ \vdots & \vdots & \vdots & \vdots & \vdots & \vdots & \vdots \\ \frac{\partial f_{12}}{\partial s} & \frac{\partial f_{12}}{\partial \alpha} & \frac{\partial f_{12}}{\partial \beta} & \frac{\partial f_{12}}{\partial \gamma} & \frac{\partial f_{12}}{\partial x_0} & \frac{\partial f_{12}}{\partial y_0} & \frac{\partial f_{12}}{\partial z_0} \end{bmatrix}_{12 \times 7}$$

$$\Delta \mathbf{x} = \begin{bmatrix} \Delta s \\ \Delta \alpha \\ \Delta \beta \\ \Delta \gamma \\ \Delta x_0 \\ \Delta y_0 \\ \Delta z_0 \end{bmatrix} \quad \text{and} \quad \mathbf{b} = \begin{bmatrix} t_1 - (f_1)_0 \\ t_2 - (f_2)_0 \\ \vdots \\ t_{12} - (f_{12})_0 \end{bmatrix}$$

The elements in  $\mathbf{A}$  are derived in Appendix I.

### 6.3 Applications

#### 6.3.1 Datum transformation

It is sometimes necessary to transform a set of coordinates from one coordinate system to another coordinate system especially when results in an arbitrary datum are obtained from a bundle adjustment without control or from the separate adjustment in close range photogrammetry.

With the conventional coordinate transformation method, based on Eq (6.37), the seven transformation parameters can be estimated by Eq (6.42) with control points in both systems. After this, other coordinates can be transformed. This is followed by a S-transformation to calculate the cofactor matrix of the transformed coordinates. The full cofactor matrix of the original coordinates is required and the computation is very complicated.

With a linear transformation, the twelve transformation parameters can be estimated by Eqs (6.49) to (6.53) using control points before and after transformation. The coordinates (after transformation) of other points together with their cofactor matrix and weight matrix are calculated by Eqs (6.54) and (6.66). In this case, the full cofactor

matrix of the coordinates is not necessary. The inverse of the cofactor matrix, which is always available from the design matrix, can be used instead. The computation process is much simplified.

### 6.3.2 Relative positioning of a moving object

In industrial environments, it is sometimes required to monitor the position of a moving object relative to a given coordinate system, which is usually defined by the ground control points. Using close range photogrammetry, the coordinates of the targeted points on the object and the control points can be measured in a common coordinate system. In the case of free network adjustment (bundle adjustment or separate adjustment) the whole system, the object points and the control points (treated as normal object points in the adjustment process), may shift in the object space. Under this situation, the estimated 3D coordinates need to be transformed into the pre-defined coordinate system (defined by the control points). Firstly, the control points are used to estimate the transformation parameters. Then the other object points can be transformed into the pre-defined coordinate system. After each movement of the object, its relative position to the pre-defined coordinate system can be estimated via coordinate transformations. A numerical example will be given in Chapter 7.

### 6.3.3 Relative positioning of two rigid objects

It is sometimes required to monitor the relative position of two rigid objects. Using close range photogrammetry, the coordinates of the targeted points on the objects can be measured in a common coordinate system  $S_0$ . In this case the coordinates of the targeted points on both objects need to be measured in their local coordinate systems  $S_1$  and  $S_2$ , the relative position of the two objects can be determined by a series of coordinate transformations. Figure 6-1 illustrates the configuration.

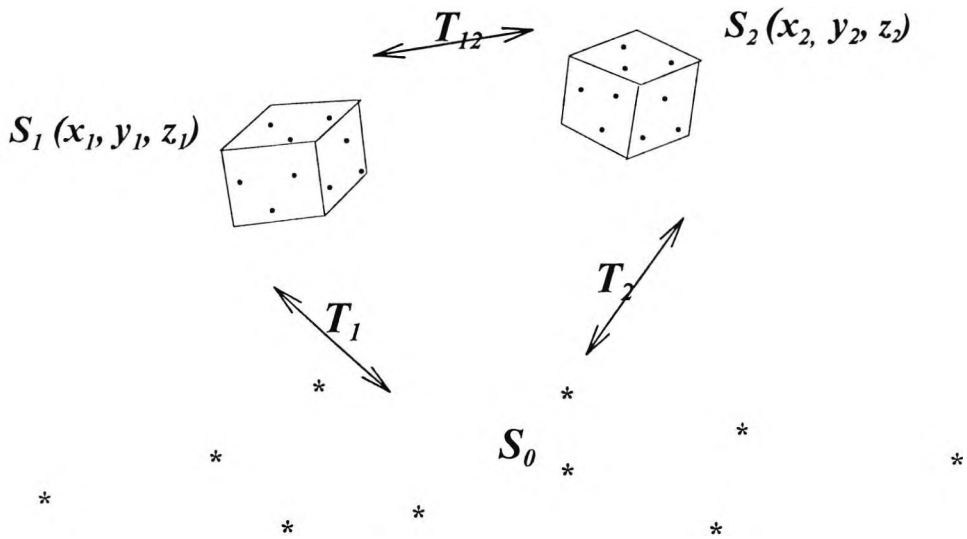


Figure 6-1 Relative position of two objects

The coordinates of the targeted points on the two objects  $S_0(x_1, y_1, z_1)$  and  $S_0(x_2, y_2, z_2)$  are measured by close range photogrammetry in a common coordinate system  $S_0$  which is defined by the control points. These points are also measured in the two local coordinate systems at  $S_1(x_1, y_1, z_1)$  and  $S_2(x_2, y_2, z_2)$ . The transformation parameters  $T_1$  are determined from all points on object I in system  $S_0$  and  $S_1$ , and the transformation parameters  $T_2$  are determined from all points on object II in system  $S_0$  and  $S_2$ . After that, the relative position of the two objects  $T_{12}$  can be determined from  $T_1$  and  $T_2$ . In this application of coordinate transformation, the position of the ground control points are not required, the distances between them may be needed to define the scale.

#### 6.4 Summary of the chapter

Photogrammetric methods provide estimations of the 3D coordinates of the spatial points on objects. It is often necessary to relate these points to a given coordinate system. In another situation, the relative position of the two objects may be required. This chapter describes a linear coordinate transformation to solve these problems. Compared with the conventional coordinate transformation methods, the method of linear transformation is simple and easy to apply. The size of the matrix to be inverted is  $12 \times 12$  rather than  $3n \times 3n$  (for the conventional method) when the transformation parameters are estimated. This is a significant saving in terms of time and memory. Using the twelve transformation parameters all the coordinates can be transformed from one coordinate system to another system together with their cofactor matrix and the weight matrix. The computational process is very simple. Hence the computationally expensive S-transformation can be avoided. The linear coordinate transformation is especially suitable for the 3D coordinates obtained by the separate least squares adjustment with no constraints, since the full cofactor matrix of the 3D coordinates is not required in this case. The inverse of the cofactor matrix (the weight matrix) which is always available from the design matrix can be used instead. The coordinate transformation is also useful for relative position of a moving object and between two objects.

## Chapter 7

### Simulation tests

In this chapter the results of some simulation tests are given which were conducted to test the theories discussed in the previous chapters. A simulation network is constructed and its configuration is illustrated in Figure 7-1. The object points are uniformly distributed in a  $400 \times 400 \times 200$  mm box, with one control point on each of the eight corners. These control points are used to initialise the camera parameters and define the coordinate system. The cameras are uniformly located on a circle at a distance of about 1500 mm from the centre of the box. The principal distance of the cameras is 8.5 mm.

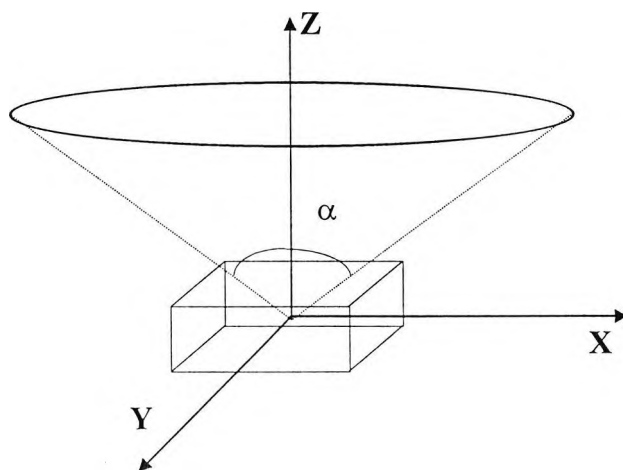


Figure 7-1 The simulation test network

#### 7.1 Test of resection with the 2D DLT model

To test the 2D DLT resection method a simulated test field with four control points on the corners of a square was constructed in object space as shown in Figure 7-2. The four control points are supposed to be in the same plane and their coordinates are shown in the Table 7-1.

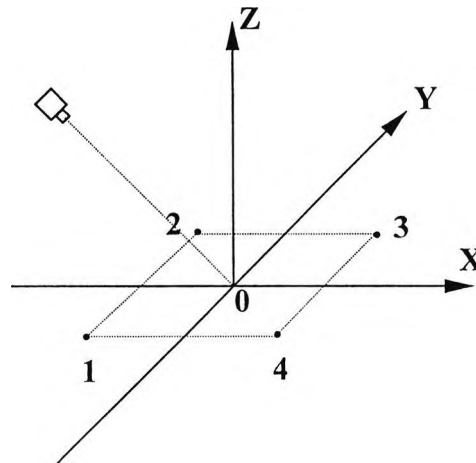


Figure 7-2 Four control points in a same plane

Table 7-1 Coordinates of the four control points

control pts	X (mm)	Y (mm)	Z (mm)
1	-200.0	-200.0	0.0
2	-200.0	200.0	0.0
3	200.0	200.0	0.0
4	200.0	-200.0	0.0

### 7.1.1 Test for camera positions

A simulation test program was written to test the 2D DLT method for space resection. Cameras to be resected were randomly distributed in the object space above the control point plane aiming to the centre of the four control points. Table 7-2 shows the camera parameters for six positions (focal length  $f = 8.5$  mm). The four control points were projected onto the image planes of the cameras and the 2D coordinates are listed in Table 7-3.

Table 7-2 Camera parameters of six examples

Camera	$X_L$ (mm)	$Y_L$ (mm)	$Z_L$ (mm)	$\omega$ (deg)	$\varphi$ (deg)	$\kappa$ (deg)
1	-45.4	1062.6	1011.3	-48.4170	-1.7727	-12.2935
2	-1468.7	1075.7	2301.0	-25.0557	-30.0036	97.4457
3	17.2	1229.8	274.9	-77.3997	0.7820	39.3152
4	730.0	432.4	3222.5	-7.6424	12.6542	-12.5978
5	-870.5	-479.9	2513.7	10.8085	-18.7862	-99.8043
6	-1058.2	1140.6	2049.5	-29.0971	-24.2830	68.0109

Table 7-3 2D coordinates of the control points

Camera	Control pts	$x$ (mm)	$y$ (mm)
1	1	-0.901427	-0.943204
1	2	-1.422228	0.601111
1	3	1.089468	1.139969
1	4	1.156880	-0.488956
2	1	-0.443716	0.693742
2	2	0.605550	0.327285
2	3	0.435713	-0.681255
2	4	-0.537972	-0.290767
3	1	-1.051026	0.531994
3	2	-1.027941	1.290710
3	3	1.442593	-0.730187
3	4	0.755609	-0.948755
4	1	-0.353593	-0.586493
4	2	-0.607309	0.379611
4	3	0.368714	0.611579
4	4	0.613853	-0.383699
5	1	0.730657	-0.461137
5	2	-0.506284	-0.737210
5	3	-0.678564	0.428257
5	4	0.495576	0.721608
6	1	-0.823921	0.435122
6	2	0.360228	0.711443
6	3	0.828037	-0.437286
6	4	-0.315354	-0.622818

With the 3D coordinates of the control points and their 2D coordinates on the image planes as known parameters the 2D DLT method was used and the eight DLT parameters  $L_1$  to  $L_8$  were computed directly. The eight DLT parameters for the six cameras are listed in Table 7-4.

Table 7-4 The eight DLT parameters for the six cameras

Camera	$L_1$	$L_2$	$L_3$	$L_4$	$L_5$	$L_6$	$L_7$	$L_8$
1	-8.65e-4	8.51e-5	1.45e-7	-1.45e-4	-4.62e-4	-3.30e-7	2.10e-5	-4.93e-4
2	3.83e-5	-2.97e-4	5.66e-7	2.92e-4	1.11e-4	8.91e-7	1.70e-4	-1.25e-4
3	-8.14e-4	-1.01e-4	-3.00e-7	5.02e-4	-1.40e-4	-1.24e-7	-1.08e-5	-7.74e-5
4	-2.86e-4	7.34e-5	1.20e-7	-8.38e-5	-2.88e-4	-1.89e-7	-8.57e-5	-3.89e-5
5	5.96e-5	3.54e-4	-2.01e-7	-3.45e-4	8.38e-5	2.77e-7	1.19e-4	8.56e-5
6	-1.44e-4	-3.41e-4	-2.53e-7	3.23e-4	-8.70e-5	-4.31e-7	1.59e-4	-1.72e-4

The camera physical parameters ( $X_L$ ,  $Y_L$ ,  $Z_L$ ,  $\omega$ ,  $\varphi$ ,  $\kappa$ ) were calculated from the eight DLT parameters. Since no errors were introduced in either 3D or 2D coordinates, the reconstructed camera parameters were identical with the generated data. Table 7-5 shows the results.

Table 7-5 The recovered camera parameters

Camera	$X_L$ (mm)	$Y_L$ (mm)	$Z_L$ (mm)	$\omega$ (deg)	$\varphi$ (deg)	$\kappa$ (deg)
1	-45.40	1062.60	1011.3	-48.4170	-1.7727	-12.2935
2	-1468.70	1075.70	2301.0	-25.0557	-30.0036	97.4457
3	17.20	1229.80	274.9	-77.3997	0.7820	39.3152
4	730.00	432.40	3222.5	-7.6424	12.6542	-12.5978
5	-870.50	-479.90	2513.7	10.8085	-18.7862	-99.8043
6	-1058.20	1140.60	2049.5	-29.0971	-24.2830	68.0109

If the 2D or 3D coordinates have no errors, there will be no error for the reconstructed camera parameters. Five hundred tests with cameras randomly distributed in the object space above the control point plane were performed by simulation. The resulting camera parameters were always the same as the generated data. However, random errors are inevitable in practice. The following tests investigated the influence of 3D and 2D errors on the results of the camera parameters.

### 7.1.2 Error propagation from 3D to cameras

To test the influence of the 3D observation errors on the camera parameters, random errors (normally distributed) were added to the 3D coordinates of the control points. With these control points, camera parameters were calculated and statistically analysed. One thousand sets of control points were tested. Table 7-6 lists an example of the generated camera parameters and reconstructed camera parameters. Figure 7-3 and 7-4 illustrates the influence of the 3D errors on the camera position parameters and rotation parameters.

Table 7-6 An example of the generated camera parameters and reconstructed camera parameters with errors on the control points

	$X_L$ (mm)	$Y_L$ (mm)	$Z_L$ (mm)	$\omega$ (deg)	$\phi$ (deg)	$\kappa$ (deg)
generated	707.0	0.0	707.0	0.0	45.0	-67.2385
reconstructed	704.059	5.6787	702.666	-0.1826	44.0238	-68.0924

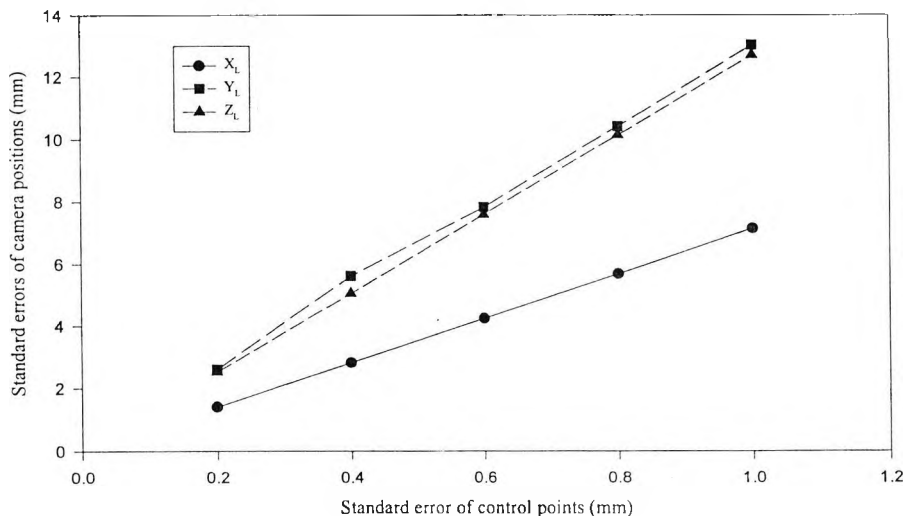


Figure 7-3 The influence of 3D errors on camera position parameters

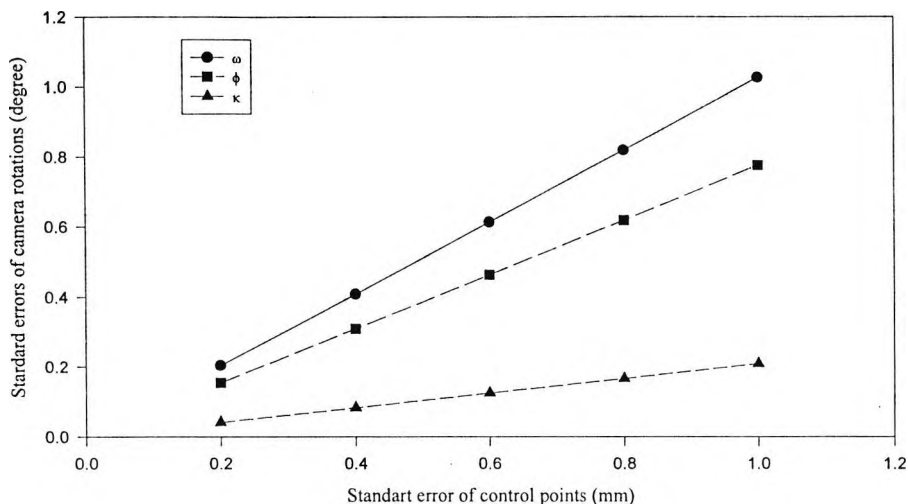


Figure 7-4 The influence of 3D errors on camera rotation parameters

It was found that the 3D errors on the control points show a linear influence on the camera parameters. The camera parameters are very sensitive to the 3D errors of the control points. A one millimetre standard error on the control points could cause a ten millimetre error on the camera position parameters and one degree error on the camera rotation parameters. However, with this accuracy the camera parameters are likely to be good enough to be used as the starting values in the bundle adjustment or the separate adjustment.

### 7.1.3 Error propagation from 2D to cameras

To test the influence of 2D observation errors on the camera parameters, random errors (normally distributed) were added to the 2D coordinates on the image plane. With these 2D image data, the camera parameters were calculated and statistically analysed. One thousand tests were performed with error added 2D data. Table 7-7 shows an example of the generated camera parameters and reconstructed camera parameters. Figure 7-5 and 7-6 illustrates the influence of the 3D errors on the camera position parameters and rotation parameters.

Table 7-7 An example of the generated camera parameters and reconstructed camera parameters with errors on the 2D coordinates

	$X_L$ (mm)	$Y_L$ (mm)	$Z_L$ (mm)	$\omega$ (deg)	$\phi$ (deg)	$\kappa$ (deg)
generated	707.0	0.0	707.0	0.0	45.0	128.488
reconstructed	708.958	0.7788	707.074	-0.0614	44.996	128.505

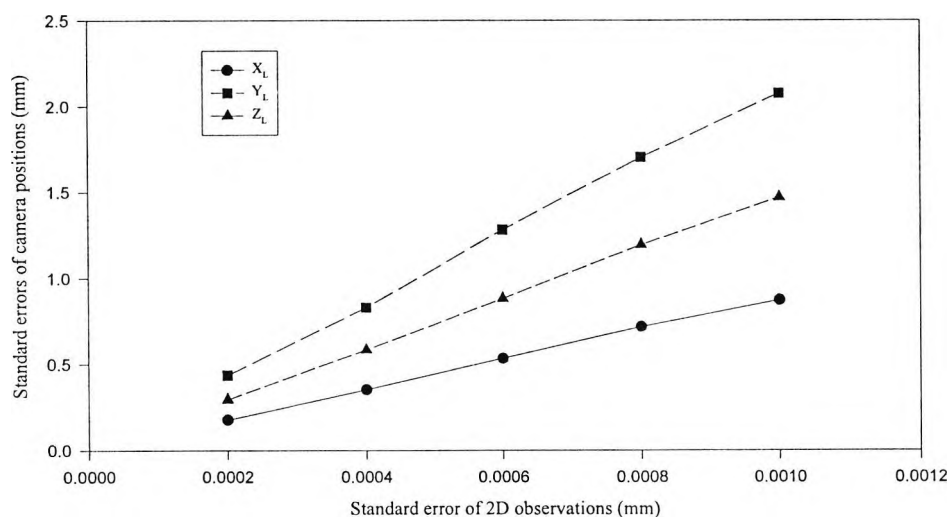


Figure 7-5 The influence of 2D errors on camera position parameters

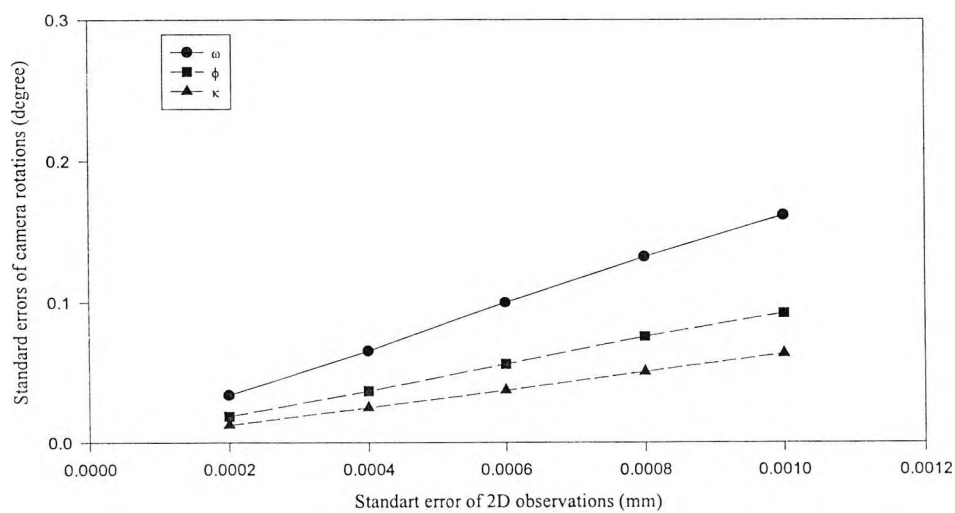


Figure 7-6 The influence of 2D errors on camera rotation parameters

## 7.2 Test of resection followed by intersection with the DLT model

In this simulation test four cameras were used and uniformly distributed on a circle with a 90 degree interval between each camera. Their true position and rotation parameters are shown in Table 7-8.

Table 7-8 The parameters of four cameras on a circle

Camera	$X_L$ (mm)	$Y_L$ (mm)	$Z_L$ (mm)	$\omega$ (deg)	$\phi$ (deg)	$\kappa$ (deg)
1	1000.0	0.0	1000.0	0.0	45.0	-7.54
2	0.0	1000.0	1000.0	-45.0	0.0	92.18
3	-1000.0	0.0	1000.0	0.0	-45.0	52.98
4	0.0	-1000.0	1000.0	45.0	0.0	-13.64

Eight control points were computed in the object space with a standard deviation of 1 mm. The true positions of these control points are given in Table 7-9.

Table 7-9 Eight Control points

control pts	X (mm)	Y (mm)	Z (mm)
1	200.0	200.0	100.0
2	-200.0	200.0	100.0
3	-200.0	-200.0	100.0
4	200.0	-200.0	100.0
5	200.0	200.0	-100.0
6	-200.0	200.0	-100.0
7	-200.0	-200.0	-100.0
8	200.0	-200.0	-100.0

The 2D coordinates of the control points on the camera image planes were computed. Errors with a standard deviation of 0.0004 mm were added to the 2D data. Using these known 2D coordinates of the control points on the camera image planes and their 3D coordinates (errors added), the camera parameters were estimated using the DLT model and the results are given in Table 7-10.

Table 7-10 Estimated camera parameters using DLT model

Camera	$X_L$ (mm)	$Y_L$ (mm)	$Z_L$ (mm)	$\omega$ (deg)	$\varphi$ (deg)	$\kappa$ (deg)
1	997.24	-3.69	1001.40	0.91	44.72	-8.53
2	-2.68	998.14	998.26	-44.96	-0.87	91.47
3	-998.97	2.04	1002.27	-0.53	-44.72	52.00
4	2.14	-1003.42	997.41	45.53	0.73	-14.20

With these approximately estimated camera parameters the coordinates of the object points were located directly by spatial intersection. In this simulation test, 100 object points were randomly distributed in the volume of the box. Their 2D coordinates on camera image planes were computed. Normally distributed errors ( $\sigma_0 = 0.0004$  mm) were added to these 2D coordinates deliberately. The space intersection method was then used to estimate the 3D coordinates of these object points. Table 7-11 shows the root mean square (RMS) of the standard deviations of the estimated 3D coordinates of the object points.

Table 7-11 The RMS standard deviations of the estimated 3D coordinates from the method of resection followed by intersection with DLT model

$\sigma_x$ (mm)	$\sigma_y$ (mm)	$\sigma_z$ (mm)	$\sigma_{xyz}$ (mm)
0.0773	0.0812	0.1739	0.1195

The relative precision of the estimated 3D coordinates from this measurement process was found to be 1:5,023.

More tests were conducted with different 3D and 2D errors. Figure 7-7 and 7-8 show the influence of 3D and 2D errors on the precision of the estimated 3D coordinates.

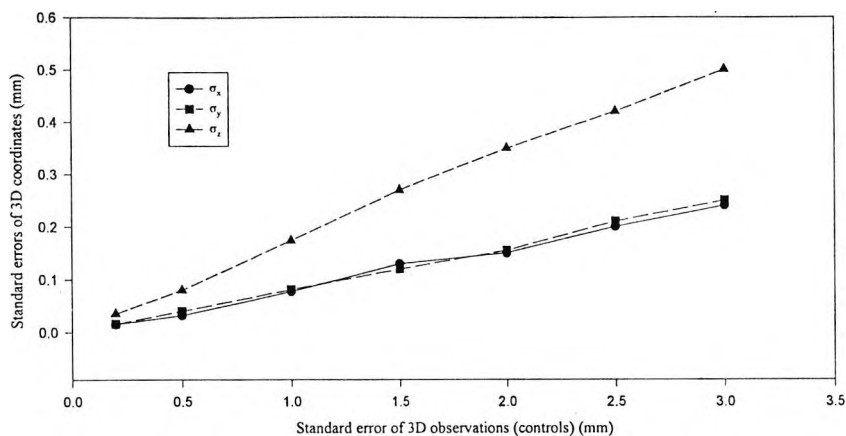


Figure 7-7 The influence of the precision of control observations on the precision of the 3D coordinates of interested points

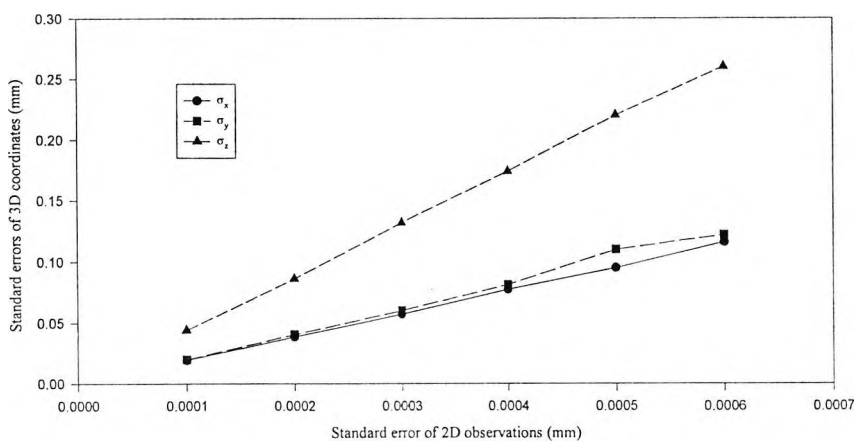


Figure 7-8 The influence of image coordinate error on the precision of the 3D coordinates of interested points

It was found, as expected, that the precisions of the estimated 3D coordinates were linearly affected by the 3D errors on control points and 2D errors on the image observations. The influence of the 2D errors is inevitable. But the influence of the 3D errors on control points should be avoided.

### 7.3 Test of the bundle adjustment

With the 3D coordinates of the object points and the camera parameters obtained above as the starting values, a photogrammetric bundle adjustment with inner constraints was applied to adjust these known parameters. After each iteration, the sum of the squares of the residuals on the observations ( $\phi = v^t W v$ ) and the maximum adjustment of the 3D coordinates were calculated. Table 7-12 shows the results after each iteration. The iterative process terminated when the maximum adjustment on the 3D coordinates was less than 0.0001 mm.

Table 7-12 The bundle adjustment process

Iteration	$\phi = v^t W v$ (mm <sup>2</sup> )	max. adjustment (mm)
1	0.0000736237	0.25996
2	0.0000734231	0.00112
3	0.0000734190	0.00001

From the covariance matrix provided by the bundle adjustment the root mean squares (RMS) of the standard deviations of the estimated 3D coordinates were obtained. Table 7-13 shows the results from the bundle adjustment.

Table 7-13 The RMS standard deviations of the estimated  
3D coordinates from the bundle adjustment

$\sigma_x$ (mm)	$\sigma_y$ (mm)	$\sigma_z$ (mm)	$\sigma_{xyz}$ (mm)
0.0370	0.0370	0.0458	0.0402

The relative precision of the estimated 3D coordinates from this measurement process was found to be 1:14,945.

More tests were conducted with different 2D errors. Figure 7-9 shows the influence of 2D errors on the precision of the estimated 3D coordinates.

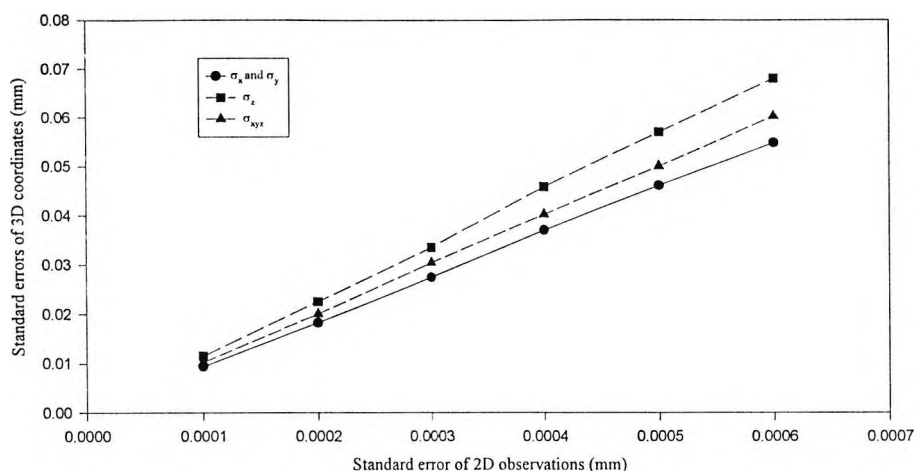


Figure 7-9 The influence of 2D error on the precision of 3D coordinates

## 7.4 Tests of the separate adjustment

### 7.4.1 Free network adjustment

With same starting values as used in the bundle adjustment, the separate adjustment was applied. Firstly perfect observations (2D coordinates on image plane without errors) were used in the separate least squares adjustment. After each iteration, the 3D coordinates of the object points and the camera parameters were adjusted. The sum of the squares of the residuals on the observations ( $\phi = v^t W v$ ) and the maximum adjustment of the 3D coordinates were calculated. Table 7-14 shows the results after each iteration. The iterative process terminated when the maximum adjustment was less than 0.0001 mm.

It is not surprising to observe that  $\phi$  can be reduced to zero. Without observation errors, the object points can be reconstructed perfectly in the 3D space. The whole body of the object points may move in the 3D space. But after the coordinate transformation they perfectly agree with their true values.

Table 7-14 The separate adjustment process  
without observation errors

Iteration	$\phi = v^t W v (\text{mm}^2)$	max. adjustment
1	0.0000003212	0.12124
2	0.0000000881	0.00866
3	0.0000000307	0.00354
4	0.0000000116	0.00161
5	0.0000000045	0.00095
6	0.0000000018	0.00075
7	0.0000000007	0.00035
8	0.0000000003	0.00021
9	0.0000000001	0.00013
10	0.0000000000	0.00008

The second test used errors added to image coordinates ( $\sigma_0 = 0.0004$  mm) in the separate adjustment process. Again after each iteration, the sum of the squares of the residuals on the observations ( $\phi = v^t W v$ ) and the maximum adjustment of the 3D coordinates were calculated. Table 7-15 shows the results after each iteration. The iterative process terminated when the maximum adjustment was less than 0.0001 mm.

Table 7-15 The separate adjustment process  
with observation errors

Iteration	$\phi = v^t W v (\text{mm}^2)$	max. adjustment (mm)
1	0.0000737445	0.12101
2	0.0000735089	0.00867
3	0.0000734504	0.00354
4	0.0000734309	0.00162
5	0.0000734236	0.00096
6	0.0000734208	0.00058
7	0.0000734197	0.00035
8	0.0000734192	0.00021
9	0.0000734191	0.00013
10	0.0000734190	0.00008

The separate adjustment process terminated after 10 iterations. Comparing the sum of the squares of the residuals on the image planes ( $\phi = v^t W v$ ) from both the bundle

adjustment and the separate adjustment it can be seen that they both converge to the same minimum. This implies that the estimated results from the two methods are equivalent. The resulting 3D coordinates of the object points are compared with those obtained from the simultaneous bundle adjustment. They agree perfectly after the coordinate transformation.

From the sum of squares of the residuals on the observations the *a posteriori* reference variance  $\hat{\sigma}_0$  was calculated, i.e.,

$$\hat{\sigma}_0 = \sqrt{\frac{v'Wv}{r}} = 0.000393(\text{mm})$$

This is very close to the *a priori* reference variance  $\sigma_0 = 0.0004$  mm. From the 3×3 covariance matrices of each object point, the RMS values of the standard deviations of the estimated 3D coordinates were calculated. Table 7-16 shows the results from the separate adjustment.

Table 7-16 The standard deviations of the estimated  
3D coordinates from the separate adjustment

$\sigma_x$ (mm)	$\sigma_y$ (mm)	$\sigma_z$ (mm)	$\sigma_{xyz}$ (mm)
0.0373	0.0373	0.0461	0.0404

The relative precision of the estimated 3D coordinates from this measurement process is found to be 1:14,834. It should be pointed out that the standard deviations of the 3D coordinates were estimated approximately from the 3×3 covariance matrices of each object points. That is why the results shown in Table 7-16 are slightly different from that shown in Table 7-13. For this strong convergent network the approximation is quite acceptable.

### 7.4.2 With control points

To verify the results from the separate adjustment, further tests were conducted for the bundle adjustment and the separate adjustment with eight fixed control points. It was found that their resulting 3D coordinates and the camera parameters were identical even with different starting values.

### 7.5 Speed of the separate adjustment

To test the speed of the separate adjustment process object points were generated and their 2D locations calculated. Errors were added to the 2D image coordinates. The starting values of the 3D coordinates of the object points and the camera parameters were estimated by resection followed by intersection with eight control points. The computation time of the separate adjustment was found, as expected, to be directly proportional to the numbers of object points, cameras and iterations. The coefficient  $C_s$  was found to be 215  $\mu$ s for a SUN Sparc Classic and 42  $\mu$ s for a 120 MHz Pentium. A comparison with a simultaneous bundle adjustment (GAP 1992) developed at City University is performed for a four camera network and the results are listed in Table 7-17.

Table 7-17 Comparison of speed between the bundle adjustment and the separate adjustment for a four camera network

Number of pts	BA(seconds)	SA(seconds)
50	8	0.43
100	45	0.86
150	152	1.29
200	389	1.72
250	748	2.15
300	1269	2.58
350	2116	3.01
400	2967	3.44
:	:	:
1000	Not measured	8.60

## 7.6 More comparisons between BA and SA

The minimisation of the sum of squares of the residuals ( $\mathbf{v}^t\mathbf{W}\mathbf{v}$ ) on the image planes is the objective of the least squares process. Table 7-18 shows some simulation test results of the bundle adjustment and the separate adjustment for a four camera network. The values of  $\mathbf{v}^t\mathbf{W}\mathbf{v}$  calculated from both methods are always same (the small differences in the eighth decimal place is caused by the round off of input data), and each individual residual on the image planes is also the same for the two methods. A further check was made by comparing the difference between 3D coordinates of the object points obtained from both methods after a 3D transformation. The results indicated no differences to the level of precision used.

Table 7-18 Comparison of the sum of the squares of residuals on image planes between the bundle adjustment and the separate adjustment for a four camera network

Number of points	BA $\mathbf{v}^t\mathbf{W}\mathbf{v}$ (mm <sup>2</sup> )	SA $\mathbf{v}^t\mathbf{W}\mathbf{v}$ (mm <sup>2</sup> )
50	0.00024738	0.00024739
100	0.00047313	0.00047313
150	0.00079095	0.00079093
200	0.00094817	0.00094816
250	0.00119077	0.00119079
300	0.00150056	0.00150054
350	0.00168301	0.00168300
400	0.00192340	0.00192340

The accuracy of the 3D coordinates of the object points estimated by the two methods is the same since their results are same. In the separate adjustment method, the full covariance matrix is not calculated, the accuracy of the 3D coordinates of the object points estimated can be evaluated approximately by the method discussed in Chapter 5. Table 7-19 shows these approximate values and the values calculated from the full covariance matrix with a six camera network. It can be seen that the results are very

close especially when the number of targets increases. So the approximately evaluated standard deviations of the 3D coordinates appear to be acceptable.

Table 7-19 Comparison between the standard deviations of the 3D coordinates estimated from the full covariance matrix and the approximations

Number of targets	$\sigma_x$ (mm)		$\sigma_y$ (mm)		$\sigma_z$ (mm)	
	BA	SA	BA	SA	BA	SA
50	0.04653	0.04677	0.04644	0.04678	0.05614	0.05738
100	0.04678	0.04689	0.04677	0.04689	0.05696	0.05763
150	0.04685	0.04693	0.04685	0.04693	0.05724	0.05770
200	0.04680	0.04685	0.04680	0.04686	0.05716	0.05752

### 7.7 More tests with separate adjustment

It is well known that increasing the number of images at each camera station will increase the accuracy of 3D coordinates of the object points measured in photogrammetry. Table 7-20 illustrates the results of the simulation test with six camera stations and 200 targets. When the number of images increases, the standard deviations of the 3D coordinates decreases and they are inversely proportional to the square root of the number of images as reported by Fraser (1992).

Table 7-20 The effects of increasing the number of images

Number of images	$\sigma_x$ (mm)	$\sigma_y$ (mm)	$\sigma_z$ (mm)
1	0.04686	0.04686	0.05752
2	0.03313	0.03313	0.04067
4	0.02343	0.02343	0.02876
6	0.01913	0.01913	0.02348
8	0.01657	0.01657	0.02034
$k$	$0.04686k^{-1/2}$	$0.04686k^{-1/2}$	$0.05752k^{-1/2}$

Changing the network geometry gives a different accuracy for the estimated 3D coordinates. Table 7-21 and Figure 7-10 illustrates the influence of the network geometry on the accuracy of 3D coordinates by changing the convergence angle  $\alpha$ . A large angle will cause the accuracy to worsen in  $x$  and  $y$ , and get better in  $z$ . It can be seen that theoretically a convergent angle of about  $110^\circ$  will give the best accuracy for  $\sigma_{xyz}$  (RMS value) and angles between  $100^\circ$  and  $120^\circ$  are reasonable. The  $q$ -value is equal to 0.5 in this situation as reported by Fraser (1984).

Table 7-21 The effects of changing network geometry

Convergent angle (deg)	$\sigma_x$ (mm)	$\sigma_y$ (mm)	$\sigma_z$ (mm)	$\sigma_{xyz}$ (mm)
60	0.04351	0.04351	0.08145	0.05893
80	0.04558	0.04559	0.06330	0.05217
100	0.04826	0.04827	0.05307	0.04992
108	0.04943	0.04944	0.05023	0.04970
110	0.04973	0.04974	0.04960	0.04969
112	0.05004	0.05005	0.04901	0.04970
120	0.05127	0.05128	0.04690	0.04986
140	0.05420	0.05421	0.04317	0.05080
160	0.05642	0.05643	0.04117	0.05184

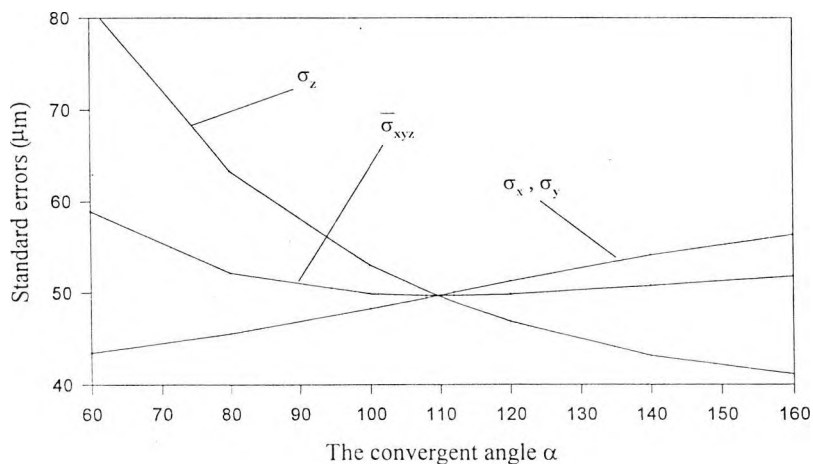


Figure 7-10 3D precision of different network geometry

### 7.8 Tests of separate adjustment with DLT models

A separate adjustment program based on the DLT model was written and tested. The same input data as used for the bundle adjustment and the separate adjustment were used again. After each iteration, the sum of the squares of the residuals on the observations ( $\phi = v^t W v$ ) and the maximum adjustment of the 3D coordinates were calculated. Table 7-22 lists the results after each iteration. The iterative process terminated when the maximum adjustment was less than 0.0001 mm.

Table 7-22 The separate adjustment process with the DLT model

Iteration	$\phi = v^t W v$ (mm <sup>2</sup> )	max. adjustment (mm)
1	0.0000920333	0.22662
2	0.0000727032	0.02924
3	0.0000722330	0.00529
4	0.0000722170	0.00115
5	0.0000722162	0.00032
6	0.0000722161	0.00011
7	0.0000722161	0.00004

The separate adjustment process terminated after 7 iterations. Comparing the sum of the squares of the residuals on the image planes ( $\phi = v^t W v$ ) from the normal separate adjustment it can be seen that the results are slightly improved. This is because that DLT model encompasses some camera interior parameters which the normal collinearity equations do not. However, since these interior parameters are highly correlated with the camera exterior parameters, the improvement is not significant.

From the sum of squares of the residuals on the observations the *a posteriori* reference variance  $\hat{\sigma}_0^2$  was calculated, i.e.,

$$\hat{\sigma}_0 = \sqrt{\frac{v^t W v}{r}} = 0.000389(\text{mm})$$

From the 3×3 covariance matrices of each object points, the RMS values of the standard deviations of the estimated 3D coordinates were calculated. Table 7-23 shows the results from the separate adjustment with the DLT model.

Table 7-23 The standard deviations of the estimated 3D coordinates from the separate adjustment with DLT model

$\sigma_x(\text{mm})$	$\sigma_y(\text{mm})$	$\sigma_z(\text{mm})$	$\sigma_{xyz}(\text{mm})$
0.0369	0.0369	0.0456	0.0400

The relative precision of the estimated 3D coordinates from this measurement process was found to be 1:15,000.

### 7.9 Tests of self calibration adjustment

In these simulation tests the camera interior parameters were generated. These parameters are: principal point shift ( $\Delta x_p$ ,  $\Delta y_p$ ), principal distance shift  $\Delta c$ , radial lens distortion parameters  $k_1$ ,  $k_2$ ,  $k_3$ , and decentring lens distortion parameters  $p_1$  and  $p_2$ . 100 object points were used. Eight images were taken by the same camera from four stations with a 90 degree axial rotation. 2D image coordinates were calculated taking into account those camera interior parameters. Realistic camera interior parameters were used and are listed in Table 7-24.

Table 7-24 Generated camera interior parameters

$\Delta x_p(\text{mm})$	$\Delta y_p(\text{mm})$	$\Delta c(\text{mm})$	$k_1(\text{mm}^{-2})$	$k_2(\text{mm}^{-4})$	$k_3(\text{mm}^{-6})$	$p_1(\text{mm}^{-1})$	$p_2(\text{mm}^{-1})$
1.00e-2	1.00e-2	3.52e-2	5.36e-3	-1.33e-4	7.35e-6	5.00e-4	5.00e-4

A separate adjustment process was conducted and it is found that without random noise involved on the 2D observations the camera interior parameters could be recovered perfectly. With random noise ( $\sigma_0 = 0.0001 \text{ mm}$ ) added the camera interior parameters

were estimated and listed in Table 7-25 (the second row lists the standard deviations of the estimates).

Table 7-25 Recovered camera interior parameters from simulated 2D observation errors

	$\Delta x_p$ (mm)	$\Delta y_p$ (mm)	$\Delta c$ (mm)	$k_1$ (mm <sup>-2</sup> )	$k_2$ (mm <sup>-4</sup> )	$k_3$ (mm <sup>-6</sup> )	$p_1$ (mm <sup>-1</sup> )	$p_2$ (mm <sup>-1</sup> )
Value	1.02e-2	1.05e-2	3.52e-2	5.33e-3	-1.55e-4	1.43e-5	4.99e-4	5.01e-4
STDV	1.13e-3	1.14e-3	5.55e-4	4.97e-5	3.25e-5	8.14e-6	2.09e-6	2.08e-6

More tests were conducted with different 2D observation errors  $\sigma_0$ . The results from ten test sets were plotted for the recovered camera interior parameters from Figure 7-11 to 7-18. The true values of the camera parameters were listed in Table 7-24. From Figure 7-11 and 7-12 it can be seen that the principal point offset  $x_p$  and  $y_p$  are very sensitive to the 2D observation errors. The principal distance offset  $\Delta c$  is relatively stable and can be recovered reasonably well (this can be seen from Figure 7-13). The recovered radial lens distortion parameters  $k_1$ ,  $k_2$  and  $k_3$  are shown in Figures 7-14, 7-15 and 7-16 respectively. It can be seen that  $k_1$  can be recovered well, but  $k_2$  and  $k_3$  are sensitive to the 2D observation errors. The high correlations between the radial lens distortion parameters can be seen clearly from the plotted curves. The recovered parameters  $k_1$ ,  $k_2$  and  $k_3$  could be very different, but their contributions to the radial lens distortion were almost the same. This can be seen from the lens distortion curves illustrated in Figure 7-19. The ten curves were plotted using the different sets of parameters. The reason that these curves differ when the radius is over 2 mm is that most of the 2D observations on the image planes are in the range the 2 mm radius. Therefore the radial distortion out of this range can not be recovered properly. The decentring lens distortion parameters  $p_1$  and  $p_2$  are the most stable parameters in the self calibration procedure and can be recovered very well. This can be seen in Figure 7-17 and 7-18.

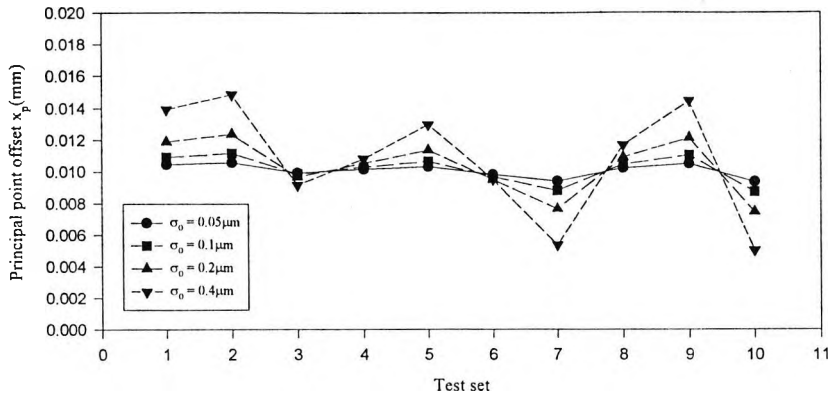


Figure 7-11 The recovered principal point offset  $x_p$

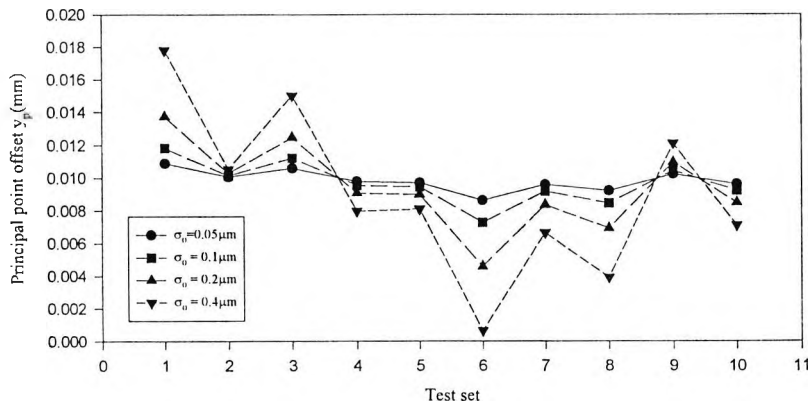


Figure 7-12 The recovered principal point offset  $y_p$

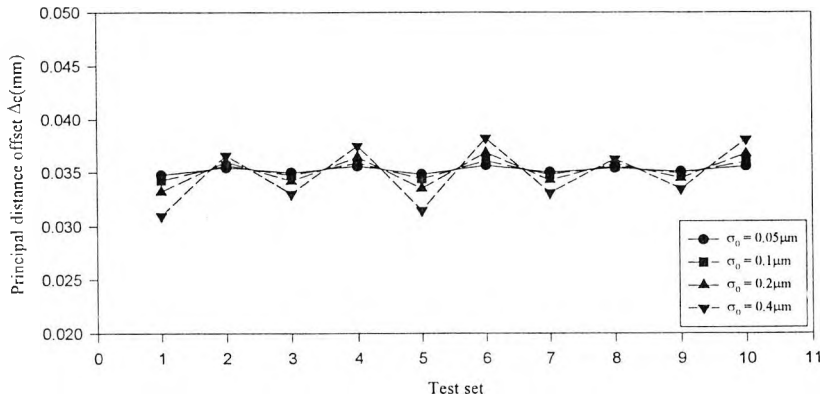


Figure 7-13 The recovered principal distance offset  $\Delta_c$

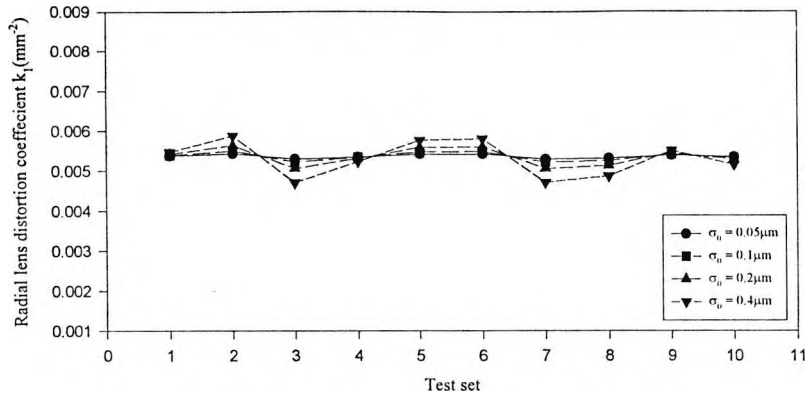


Figure 7-14 The recovered radial lens distortion parameter  $k_1$

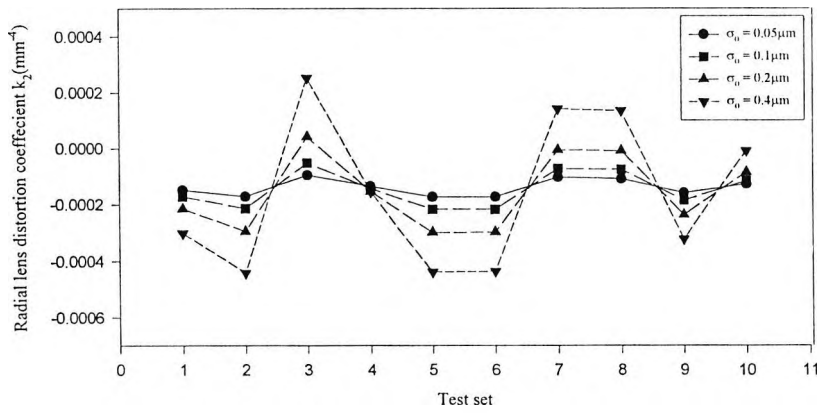


Figure 7-15 The recovered radial lens distortion parameter  $k_2$

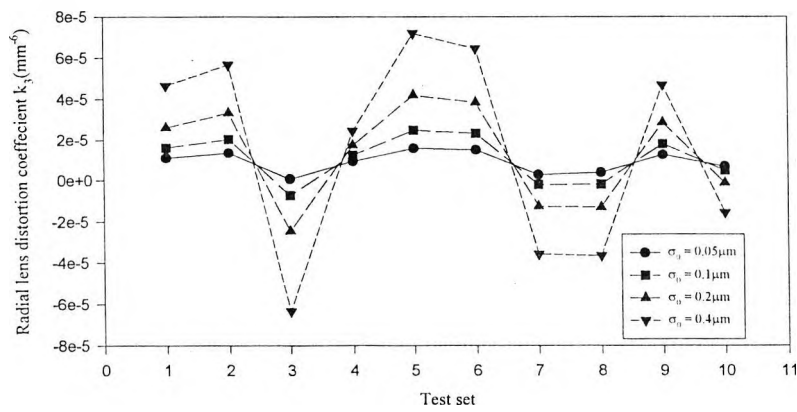


Figure 7-16 The recovered radial lens distortion parameter  $k_3$

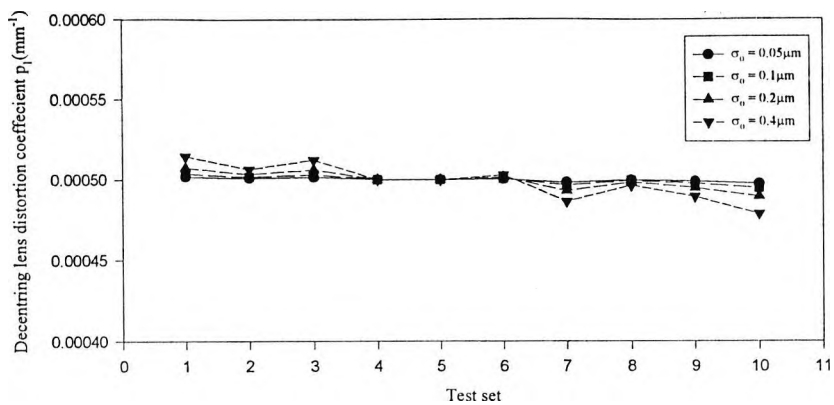


Figure 7-17 The recovered decentring lens distortion parameter  $p_1$

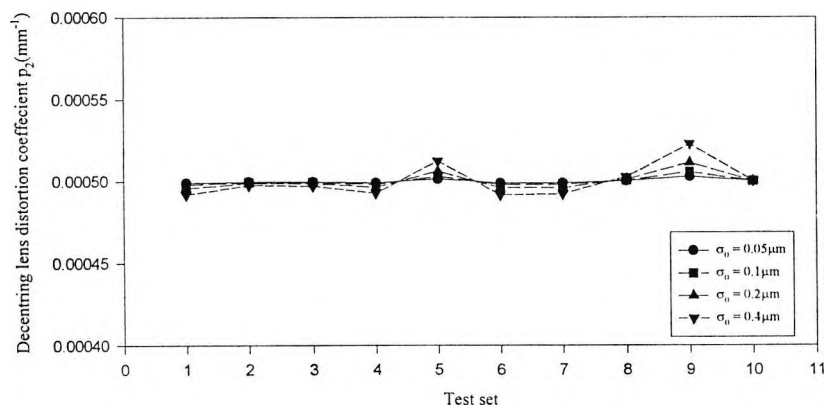


Figure 7-18 The recovered decentring lens distortion parameter  $p_2$

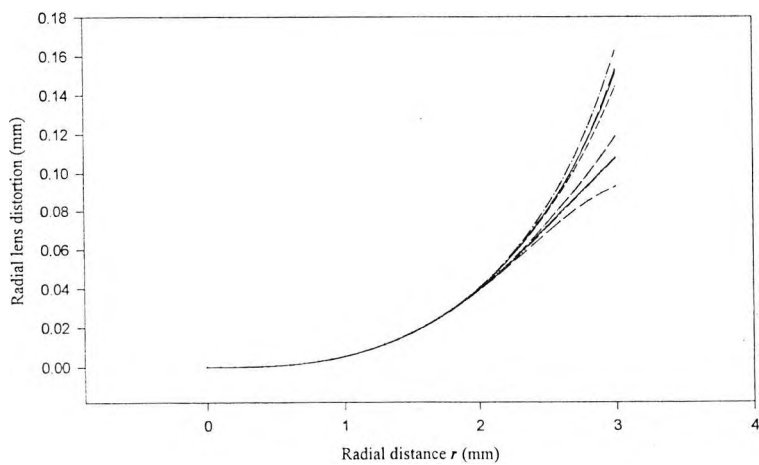


Figure 7-19 The radial lens distortion with different set of parameters

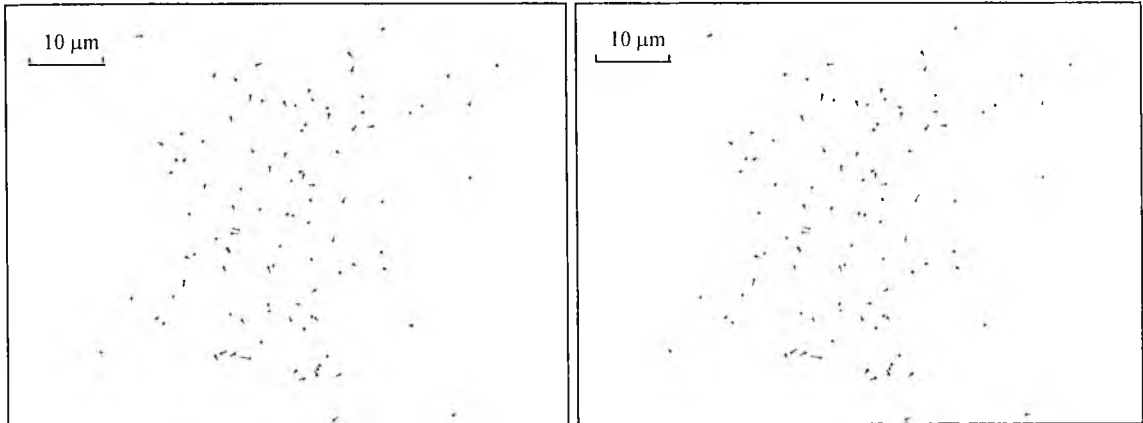
When the camera interior parameters were taken into account in the separate adjustment process, the *a posteriori*  $\hat{\sigma}_0$  calculated from the sum of the squares of the residuals on image planes was very close to the *a priori*  $\sigma_0$ . This implies that the precisions of the estimated results are mainly influenced by the random errors of the observations and the systematic errors are well compensated. Table 7-26 shows some results from the separate adjustment process.

Table 7-26 The *a posteriori*  $\hat{\sigma}_0$  and the standard deviations of the estimated 3D coordinates with and without calibration of the camera interior parameters

$\sigma_0$	with self-calibration		without calibration	
	$\hat{\sigma}_0$	$\sigma_{xy}$	$\hat{\sigma}_0$	$\sigma_{xy}$
0.000010	0.000010	0.000075	0.001530	0.11180
0.000100	0.000101	0.000746	0.001534	0.11181
0.000200	0.000202	0.001492	0.001540	0.11224
0.000300	0.000302	0.002239	0.001552	0.11313
0.000400	0.000403	0.002985	0.001571	0.11448

To visualise the effect of self-calibration, image residuals from one of the image planes were plotted from the results of the separate adjustment with and without self-calibration respectively. Random errors with a standard deviation of  $\sigma_0 = 0.0004$  mm were added to the 2D image observations. It can be seen from Figure 7-20 that the influence of the principal point offset  $x_p$  and  $y_p$  is not significant even without self-calibration. This is because that the principal point offset  $x_p$  and  $y_p$  are highly correlated with the camera exterior parameters (Clarke 1996), and therefore can be compensated. The principal distance offset  $\Delta c$  is also correlated with the camera exterior parameters, but not as highly as the principal point offset. Systematic errors may not be clearly seen in Figure 7-21 without self-calibration. But from the resultant  $\hat{\sigma}_0$  and RMS  $\sigma_{xy}$ , it can be seen that the 3D precision is about ten percent worse than it would be when self-calibration is used. Radial lens distortion and decentring lens distortion may have significant effects on the 3D precision if they are not modelled. Significant systematic errors can be seen in Figure 7-22 and 7-23 without self-calibration. The 3D precision

can be many times worse than it would be when self-calibration is used. The *a posteriori*  $\hat{\sigma}_\theta$  from the self-calibration adjustment is very close to the *a priori*  $\sigma_\theta$ . This implies that systematic errors are well compensated and the precision of the measurement results is mainly influenced by the random errors on the 2D observations.



(a) without calibration

(b) with self-calibration

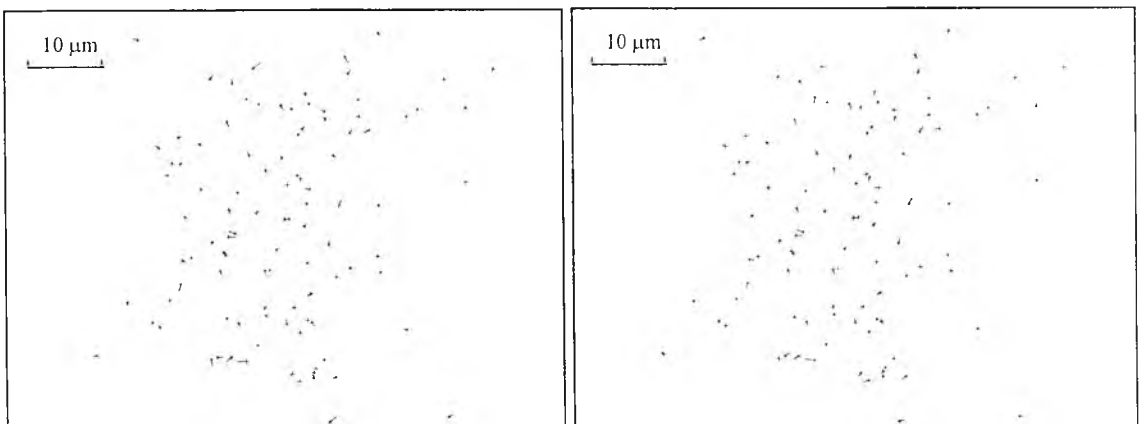
$$\hat{\sigma}_\theta = 0.000405 \text{ mm}$$

$$\hat{\sigma}_\theta = 0.000395 \text{ mm}$$

$$\sigma_{xyz} = 0.029547 \text{ mm}$$

$$\sigma_{xyz} = 0.029398 \text{ mm}$$

Figure 7-20 Image residuals ( $x_p = 0.01 \text{ mm}$ ,  $y_p = 0.01 \text{ mm}$ ,  $\sigma_\theta = 0.0004 \text{ mm}$ )



(a) without calibration

(b) with self-calibration

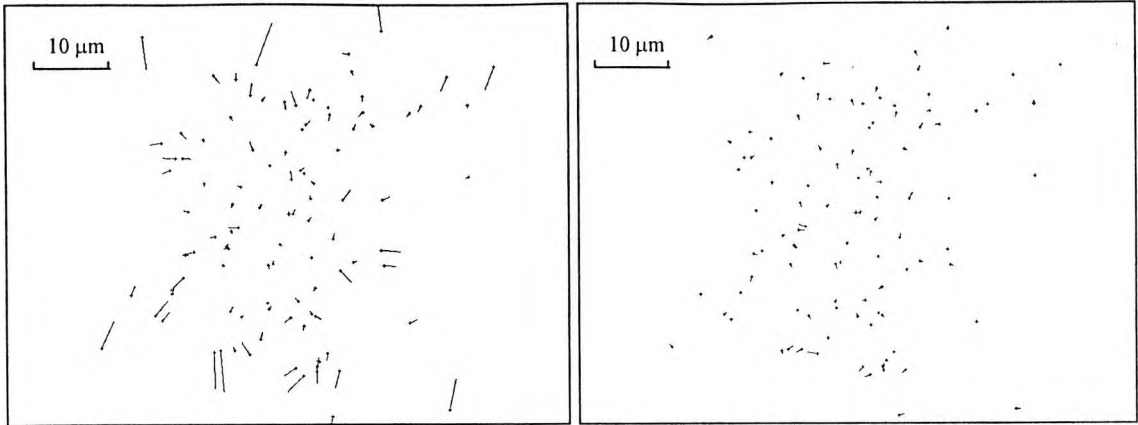
$$\hat{\sigma}_\theta = 0.000436 \text{ mm}$$

$$\hat{\sigma}_\theta = 0.000395 \text{ mm}$$

$$\sigma_{xyz} = 0.031764 \text{ mm}$$

$$\sigma_{xyz} = 0.029277 \text{ mm}$$

Figure 7-21 Image residuals ( $\Delta c = 0.0352 \text{ mm}$ ,  $\sigma_\theta = 0.0004 \text{ mm}$ )



(a) without calibration

$$\hat{\sigma}_\theta = 0.001247 \text{ mm}$$

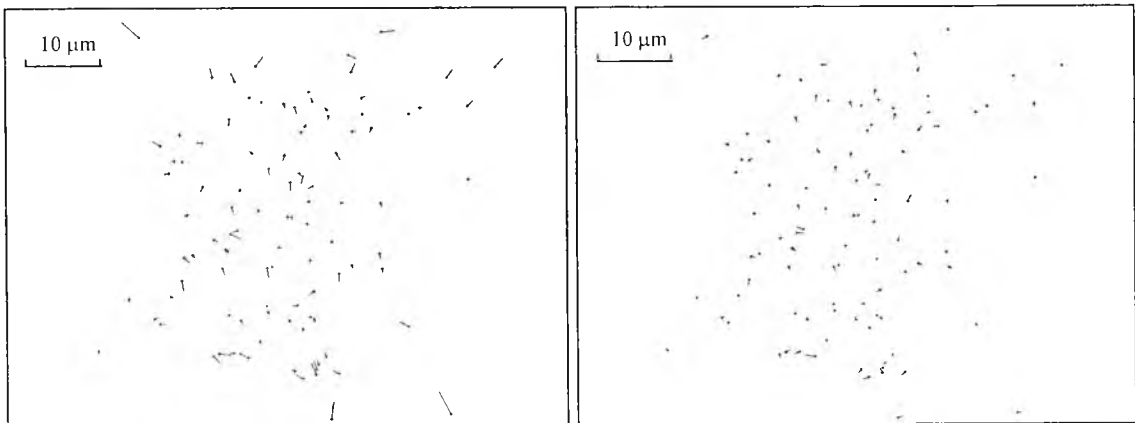
$$\sigma_{xyz} = 0.090809 \text{ mm}$$

(b) with self-calibration

$$\hat{\sigma}_\theta = 0.000399 \text{ mm}$$

$$\sigma_{xyz} = 0.029647 \text{ mm}$$

Figure 7-22 Image residuals ( $k_1 = 5.36e-3 \text{ mm}^{-2}$ ,  $k_2 = -1.33e-4 \text{ mm}^{-4}$ ,  $k_3 = 7.35e-6 \text{ mm}^{-6}$ )



(a) without calibration

$$\hat{\sigma}_\theta = 0.000941 \text{ mm}$$

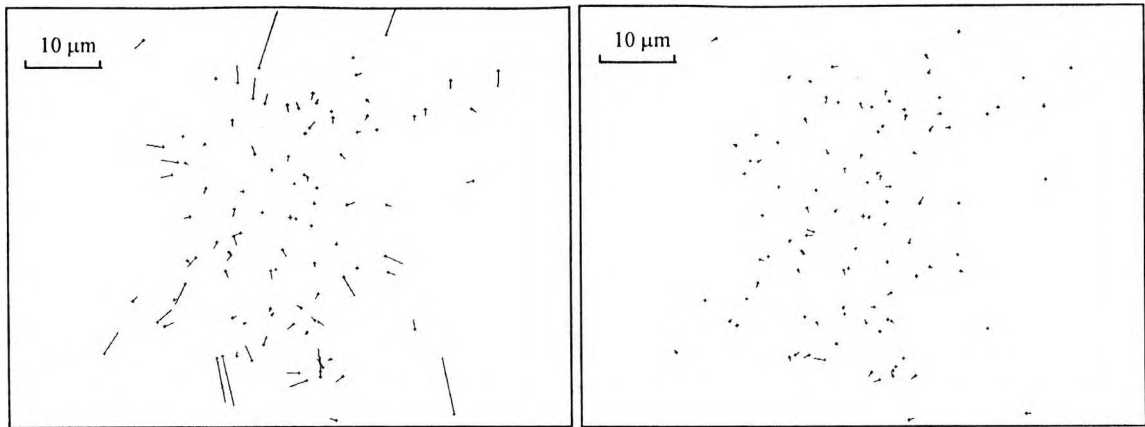
$$\sigma_{xyz} = 0.068514 \text{ mm}$$

(b) with self-calibration

$$\hat{\sigma}_\theta = 0.000395 \text{ mm}$$

$$\sigma_{xyz} = 0.029374 \text{ mm}$$

Figure 7-23 Image residuals ( $p_1 = 5.0e-4 \text{ mm}^{-1}$ ,  $p_2 = 5.0e-4 \text{ mm}^{-1}$ ,  $\sigma_\theta = 0.0004 \text{ mm}$ )



(a) without calibration

$$\hat{\sigma}_\theta = 0.001586 \text{ mm}$$

$$\sigma_{xyz} = 0.115607 \text{ mm}$$

(b) with self-calibration

$$\hat{\sigma}_\theta = 0.000399 \text{ mm}$$

$$\sigma_{xyz} = 0.029506 \text{ mm}$$

Figure 7-24 Image residuals ( $x_p = 0.01 \text{ mm}$ ,  $y_p = 0.01 \text{ mm}$ ,  $\Delta c = 0.0352 \text{ mm}$ ,  
 $k_1 = 5.36e-3 \text{ mm}^{-2}$ ,  $k_2 = -1.33e-4 \text{ mm}^{-4}$ ,  $k_3 = 7.35e-6 \text{ mm}^{-6}$ ,  
 $p_1 = 5.0e-4 \text{ mm}^{-1}$ ,  $p_2 = 5.0e-4 \text{ mm}^{-1}$ ,  $\sigma_\theta = 0.0004 \text{ mm}$ )

### 7.10 Test of continuous measurement of a moving object

In this simulation test a rigid object (a cube) was created and moved continuously in the object space with rotations and translations with respect to a given datum. The purpose of the test was to measure the movement of the object by multi-camera close range photogrammetry and coordinate transformation discussed in previous chapters. Figure 7-26 illustrates the measurement network.

The datum was defined by sixteen control points. The 3D coordinates of the control points are listed in Table 7-27, numbered from 1000 to 1015. Forty two targets were put on the six faces of the cube. The 3D coordinates of these object points on the cube (the initial position) are also listed in Table 7-27, numbered from 1016 to 1057.

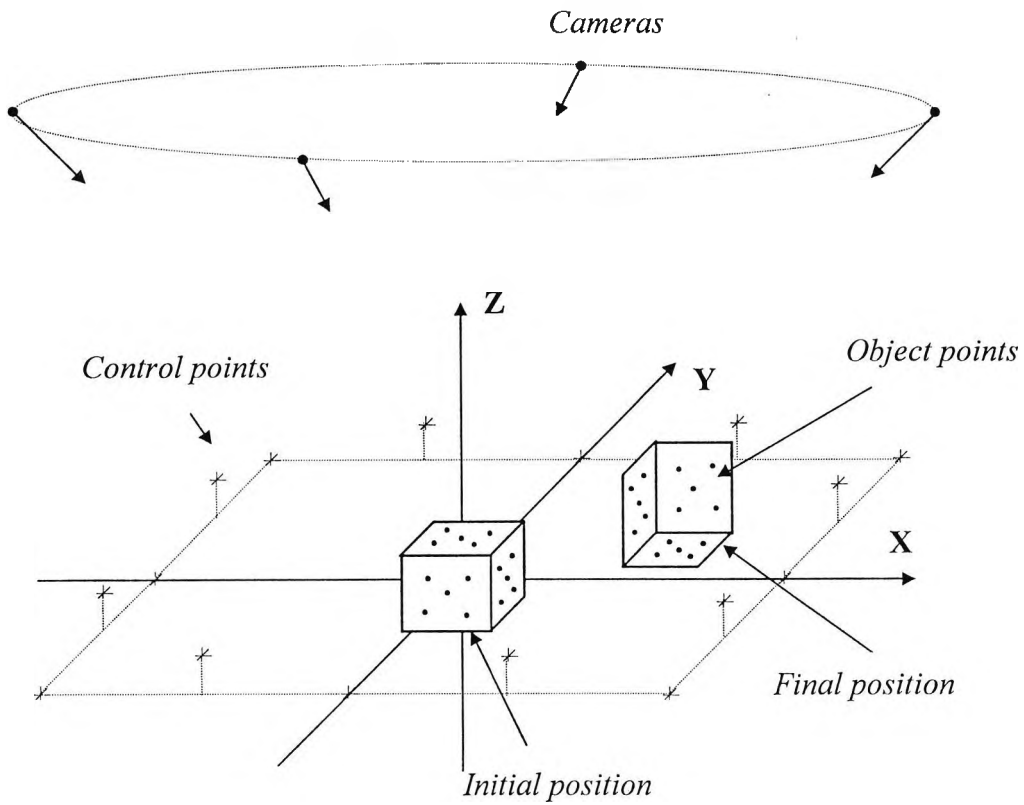


Figure 7-26 The measurement network

Table 7-27 The 3D coordinates of the control points and the object points

Point No.	X (mm)	Y (mm)	Z (mm)
1000	0.0	500.0	0.0
1001	250.0	500.0	100.0
1002	500.0	500.0	0.0
1003	500.0	250.0	100.0
1004	500.0	0.0	0.0
1005	500.0	-250.0	100.0
1006	500.0	-500.0	0.0
1007	250.0	-500.0	100.0
1008	0.0	-500.0	0.0
1009	-250.0	-500.0	100.0
1010	-500.0	-500.0	0.0
1011	-500.0	-250.0	100.0
1012	-500.0	0.0	0.0

1013	-500.0	250.0	100.0
1014	-500.0	500.0	0.0
1015	-250.0	500.0	100.0
1016	100.0	100.0	100.0
1017	100.0	-100.0	100.0
1018	-100.0	-100.0	100.0
1019	-100.0	100.0	100.0
1020	100.0	100.0	0.0
1021	100.0	-100.0	0.0
1022	-100.0	-100.0	0.0
1023	-100.0	100.0	0.0
1024	100.0	100.0	-100.0
1025	100.0	-100.0	-100.0
1026	-100.0	-100.0	-100.0
1027	-100.0	100.0	-100.0
1028	0.0	0.0	100.0
1029	50.0	50.0	100.0
1030	50.0	-50.0	100.0
1031	-50.0	-50.0	100.0
1032	-50.0	50.0	100.0
1033	0.0	0.0	-100.0
1034	50.0	50.0	-100.0
1035	50.0	-50.0	-100.0
1036	-50.0	-50.0	-100.0
1037	-50.0	50.0	-100.0
1038	100.0	0.0	0.0
1039	100.0	50.0	50.0
1040	100.0	50.0	-50.0
1041	100.0	-50.0	-50.0
1042	100.0	-50.0	50.0
1043	-100.0	0.0	0.0
1044	-100.0	50.0	50.0
1045	-100.0	50.0	-50.0
1046	-100.0	-50.0	-50.0
1047	-100.0	-50.0	50.0
1048	0.0	100.0	0.0
1049	50.0	100.0	50.0
1050	50.0	100.0	-50.0
1051	-50.0	100.0	-50.0
1052	-50.0	100.0	50.0
1053	0.0	-100.0	0.0
1054	50.0	-100.0	50.0
1055	50.0	-100.0	-50.0
1056	-50.0	-100.0	-50.0
1057	-50.0	-100.0	50.0

The cube was moved fifty small steps with translations and rotations. The translation and rotation parameters with respect to the datum are listed in Table 7-28.

Table 7-28 Movement of the cube

Step No.	Translations			Rotations		
	$X_i$ (mm)	$Y_i$ (mm)	$Z_i$ (mm)	$\alpha$ (deg)	$\beta$ (deg)	$\gamma$ (deg)
1	1.50	0.50	0.80	0.20	0.10	0.30
2	3.00	1.00	1.60	0.40	0.20	0.60
3	4.50	1.50	2.40	0.60	0.30	0.90
4	6.00	2.00	3.20	0.80	0.40	1.20
5	7.50	2.50	4.00	1.00	0.50	1.50
6	9.00	3.00	4.80	1.20	0.60	1.80
7	10.50	3.50	5.60	1.40	0.70	2.10
8	12.00	4.00	6.40	1.60	0.80	2.40
9	13.50	4.50	7.20	1.80	0.90	2.70
10	15.00	5.00	8.00	2.00	1.00	3.00
11	16.50	5.50	8.80	2.20	1.10	3.30
12	18.00	6.00	9.60	2.40	1.20	3.60
13	19.50	6.50	10.40	2.60	1.30	3.90
14	21.00	7.00	11.20	2.80	1.40	4.20
15	22.50	7.50	12.00	3.00	1.50	4.50
16	24.00	8.00	12.80	3.20	1.60	4.80
17	25.50	8.50	13.60	3.40	1.70	5.10
18	27.00	9.00	14.40	3.60	1.80	5.40
19	28.50	9.50	15.20	3.80	1.90	5.70
20	30.00	10.00	16.00	4.00	2.00	6.00
21	31.50	10.50	16.80	4.20	2.10	6.30
22	33.00	11.00	17.60	4.40	2.20	6.60
23	34.50	11.50	18.40	4.60	2.30	6.90
24	36.00	12.00	19.20	4.80	2.40	7.20
25	37.50	12.50	20.00	5.00	2.50	7.50
26	39.00	13.00	20.80	5.20	2.60	7.80
27	40.50	13.50	21.60	5.40	2.70	8.10
28	42.00	14.00	22.40	5.60	2.80	8.40
29	43.50	14.50	23.20	5.80	2.90	8.70
30	45.00	15.00	24.00	6.00	3.00	9.00
31	46.50	15.50	24.80	6.20	3.10	9.30
32	48.00	16.00	25.60	6.40	3.20	9.60
33	49.50	16.50	26.40	6.60	3.30	9.90
34	51.00	17.00	27.20	6.80	3.40	10.20
35	52.50	17.50	28.00	7.00	3.50	10.50
36	54.00	18.00	28.80	7.20	3.60	10.80

37	55.50	18.50	29.60	7.40	3.70	11.10
38	57.00	19.00	30.40	7.60	3.80	11.40
39	58.50	19.50	31.20	7.80	3.90	11.70
40	60.00	20.00	32.00	8.00	4.00	12.00
41	61.50	20.50	32.80	8.20	4.10	12.30
42	63.00	21.00	33.60	8.40	4.20	12.60
43	64.50	21.50	34.40	8.60	4.30	12.90
44	66.00	22.00	35.20	8.80	4.40	13.20
45	67.50	22.50	36.00	9.00	4.50	13.50
46	69.00	23.00	36.80	9.20	4.60	13.80
47	70.50	23.50	37.60	9.40	4.70	14.10
48	72.00	24.00	38.40	9.60	4.80	14.40
49	73.50	24.50	39.20	9.80	4.90	14.70
50	75.00	25.00	40.00	10.00	5.00	15.00

In this measurement network, four cameras were used with a convergence angle of 90 degrees. The starting values of the camera parameters were estimated by space resection using the ground control points. After each movement of the cube, images were taken by the four cameras and the 2D coordinates were computed (it was assumed that all the object points could be seen by all the cameras). A separate adjustment (free network) process was then applied with results of the last measurement as the starting values of the 3D coordinates. Since no constraints were using in the separate adjustment process, the resulting 3D coordinates of the object points were in an arbitrary datum. A linear coordinate transformation was then used to bring these object points back to the pre-defined datum. The theory of the linear coordinate transformation was discussed in chapter seven. Firstly, the 3D coordinates of the sixteen controls in both datums (pre-defined and arbitrary) were used to compute the twelve transformation parameters. With these transformation parameters all the object points on the cube were then transformed into the pre-defined datum. The movement of the cube, the translation and rotation parameters, was estimated with the 3D coordinates of the object points on the cube before and after movement.

It was found, as expected, that without 2D observation errors the estimated movement of the cube was exactly the same as it moved. When errors with a standard deviation of 0.0004 mm were added to the 2D observations, the translation and rotation parameters

(together with their full covariance matrix) were estimated. The estimated translation and rotation parameters of the cube are listed in Table 7-29.

Table 7-29 The estimated translation and rotation parameters of the moving cube

Step No.	Translations			Rotations		
	$X_i$ (mm)	$Y_i$ (mm)	$Z_i$ (mm)	$\alpha$ (deg)	$\beta$ (deg)	$\gamma$ (deg)
1	1.5162	0.4770	0.806	0.1878	0.0833	0.3072
2	2.9698	1.0207	1.629	0.3755	0.1979	0.6041
3	4.5029	1.4991	2.4082	0.5956	0.3071	0.8964
4	5.9852	1.9756	3.2383	0.8040	0.3981	1.2003
5	7.5100	2.5362	4.0008	0.9915	0.4837	1.5057
6	8.9949	2.9793	4.8255	1.1778	0.5989	1.8081
7	10.5015	3.4896	5.6248	1.3901	0.6981	2.1073
8	11.9675	3.9896	6.4109	1.6128	0.7922	2.4136
9	13.5173	4.4871	7.2037	1.7776	0.8967	2.7117
10	15.0419	5.0440	7.9794	1.9736	0.9945	3.0007
11	16.5049	5.5319	8.8562	2.1847	1.0976	3.3083
12	17.9710	5.9747	9.6256	2.3927	1.1928	3.6065
13	19.5130	6.5295	10.3956	2.5688	1.2860	3.9066
14	20.9834	7.0031	11.1739	2.7882	1.3912	4.2019
15	22.4844	7.5083	12.0084	2.9882	1.4838	4.5031
16	23.9867	7.9967	12.8223	3.1944	1.5963	4.8090
17	25.4926	8.5307	13.6292	3.3830	1.7137	5.1090
18	26.9900	9.0116	14.4382	3.5790	1.7879	5.4045
19	28.4600	9.5188	15.2511	3.7830	1.8806	5.7015
20	29.9781	9.9995	15.9625	4.0011	1.9969	6.0039
21	31.5158	10.5111	16.8136	4.1896	2.0825	6.3080
22	32.9740	11.0093	17.6085	4.3880	2.1872	6.6008
23	34.4839	11.4646	18.4158	4.6078	2.2949	6.9046
24	35.9964	11.9840	19.1736	4.7966	2.3898	7.2120
25	37.4699	12.5247	19.9989	4.9903	2.4993	7.5077
26	38.9934	13.0136	20.8158	5.1906	2.5991	7.8164
27	40.4836	13.4951	21.6106	5.3979	2.6954	8.1057
28	42.0273	14.0220	22.4509	5.5861	2.8159	8.4010
29	43.4935	14.5041	23.1944	5.7914	2.9076	8.7052
30	44.9749	14.9671	24.0223	5.9985	3.0064	8.9956
31	46.5040	15.5272	24.7670	6.1960	3.1065	9.3145
32	48.0123	16.0097	25.5920	6.3810	3.1923	9.5986
33	49.5175	16.4897	26.3878	6.6027	3.3032	9.9020
34	51.0017	16.9709	27.1802	6.7953	3.3944	10.2164
35	52.4960	17.4530	28.0303	6.9884	3.5065	10.5008

36	54.0086	17.9806	28.8098	7.2084	3.5989	10.8038
37	55.4999	18.4888	29.6044	7.3904	3.6966	11.1023
38	56.9912	19.0036	30.4179	7.6015	3.7915	11.4015
39	58.4902	19.5170	31.1810	7.7770	3.8896	11.7034
40	59.9809	20.0282	31.9538	7.9850	4.0014	12.0046
41	61.4707	20.5002	32.8067	8.1809	4.0713	12.3089
42	62.9786	20.9721	33.6195	8.3814	4.1923	12.6008
43	64.5143	21.4809	34.3861	8.5836	4.3029	12.9063
44	65.9811	22.0148	35.2135	8.7816	4.3841	13.2038
45	67.4843	22.5027	36.0118	9.0028	4.4731	13.5136
46	68.9862	22.9836	36.8123	9.1914	4.5744	13.8016
47	70.4639	23.5049	37.6221	9.3955	4.6940	14.1002
48	72.0170	24.0058	38.3717	9.5938	4.7741	14.3996
49	73.5023	24.4943	39.2151	9.7774	4.8957	14.7035
50	74.9755	24.9864	39.9771	9.9986	5.0001	15.0028

Error propagation from the 2D observations to the movement parameters of the cube was estimated as follows:

- (i) The  $3 \times 3$  weight matrices of the estimated 3D coordinates of each object point (control points and the points on the cube) were obtained from the design matrix in the separate adjustment process.
- (ii) The weight matrix of the twelve linear transformation parameters was computed from the sixteen pairs of control points in the two datums by Eq (6-51) and (6-53).
- (iii) After datum transformation the weight matrix of the 3D coordinates of the object points on the cube was computed by Eq (6-63).
- (iv) The weight matrix of the twelve transformation parameters of the cube was computed from the forty two pairs of object points on the cube by Eq (6-51) and (6-53).
- (v) The full covariance matrix of the six movement parameters (three translation and three rotations) was computed from the twelve linear transformation parameters and the weight matrix by Eq (6-71).

The standard deviations of the six movement parameters were computed from their covariance. The mean standard deviations was computed and they are listed in Table 7-30.

Table 7-30 The mean standard deviation of the six movement parameters

$\sigma_x$ (mm)	$\sigma_y$ (mm)	$\sigma_z$ (mm)	$\sigma_\alpha$ ( $^\circ$ )	$\sigma_\beta$ ( $^\circ$ )	$\sigma_\gamma$ ( $^\circ$ )
0.0185	0.0196	0.0236	0.0121	0.0114	0.0086

## Chapter 8

### A Practical Test

In this chapter, a close range photogrammetric measurement process of a test field is discussed. Ninety targets (retro-reflected material) were put on the test field. The measurement was conducted in a laboratory environment. Figure 8-1 illustrates the test field.

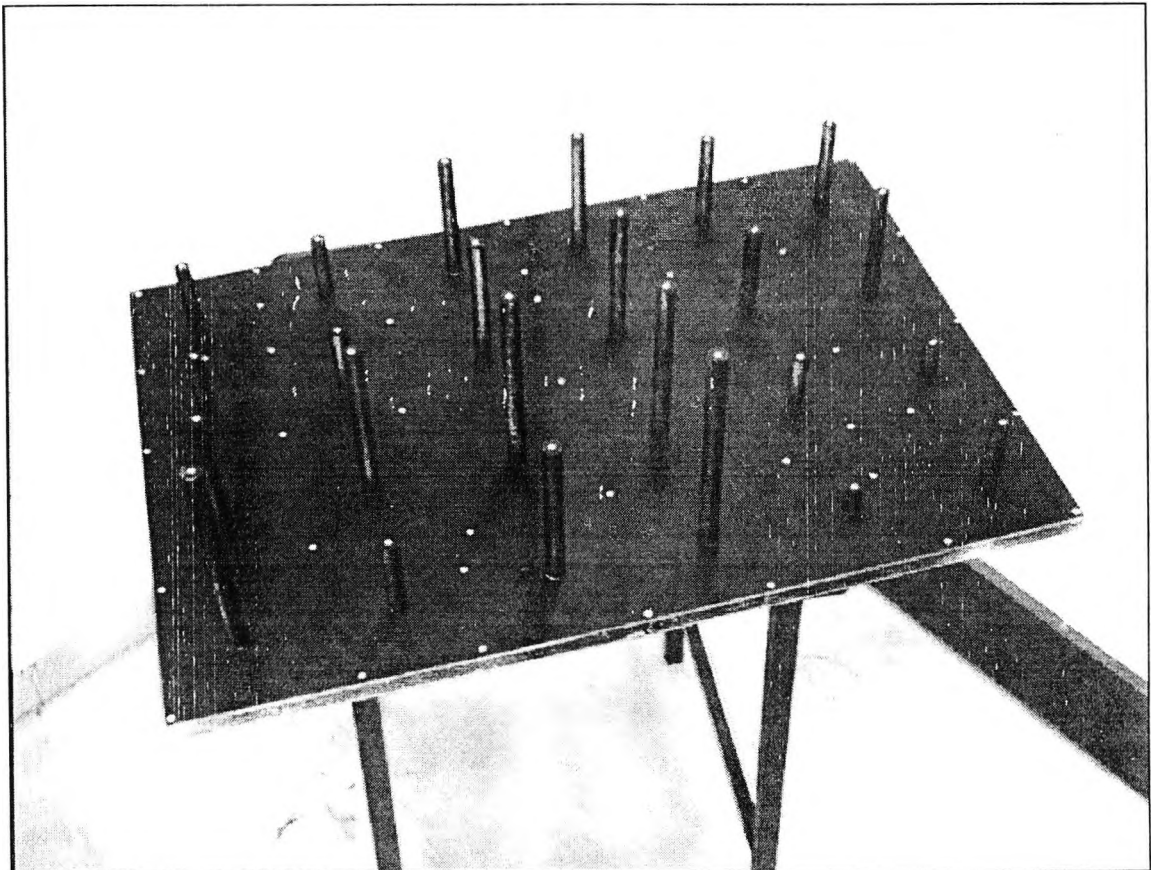


Figure 8-1 The test field

A close range photogrammetric 3D measurement network was constructed. Eight images were taken from four stations, two images at each station with a 90 degree (approximately) axial rotation. The eight images (negative images numbered 1001 to 1008, size of 744x568 pixels) are illustrated in Figure 8-2 to 8-9.

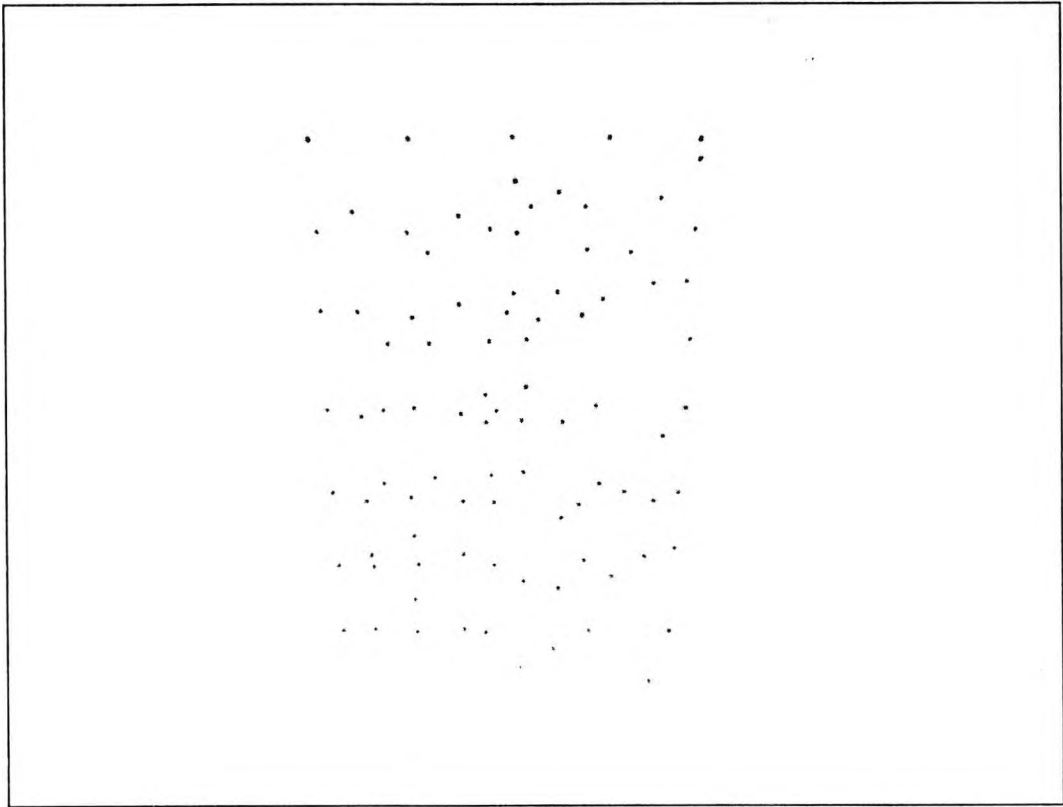


Figure 8-2 Image No. 1001

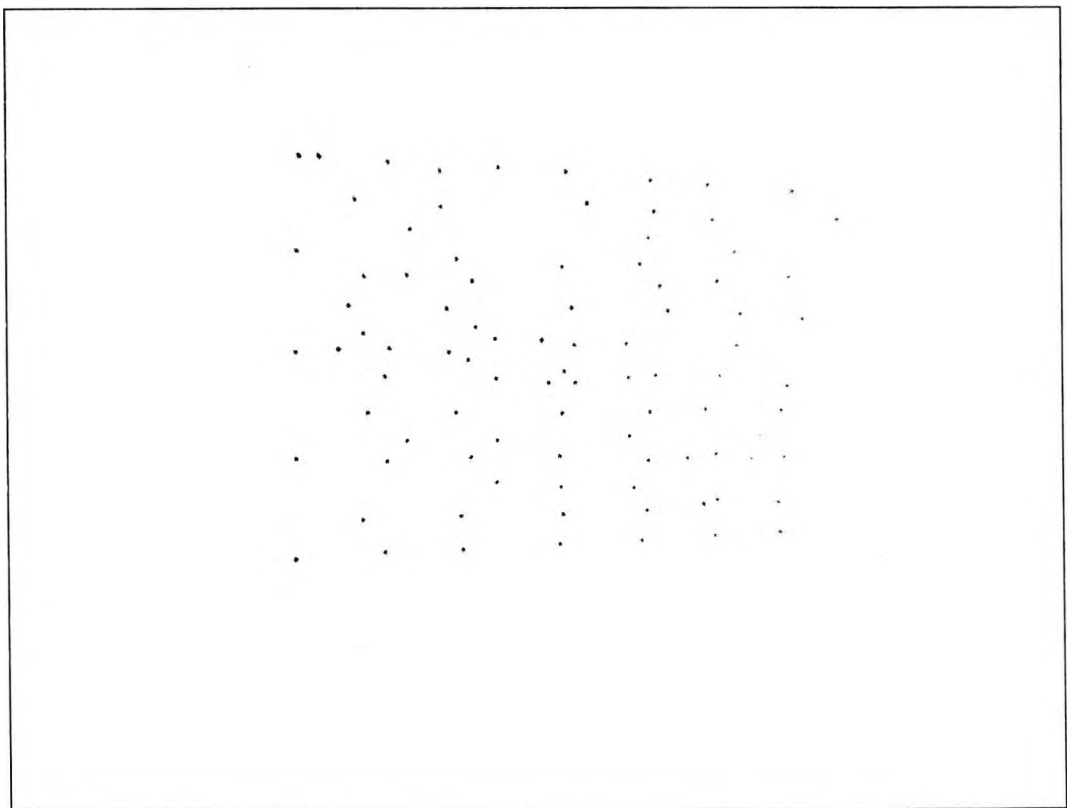


Figure 8-3 Image No. 1002

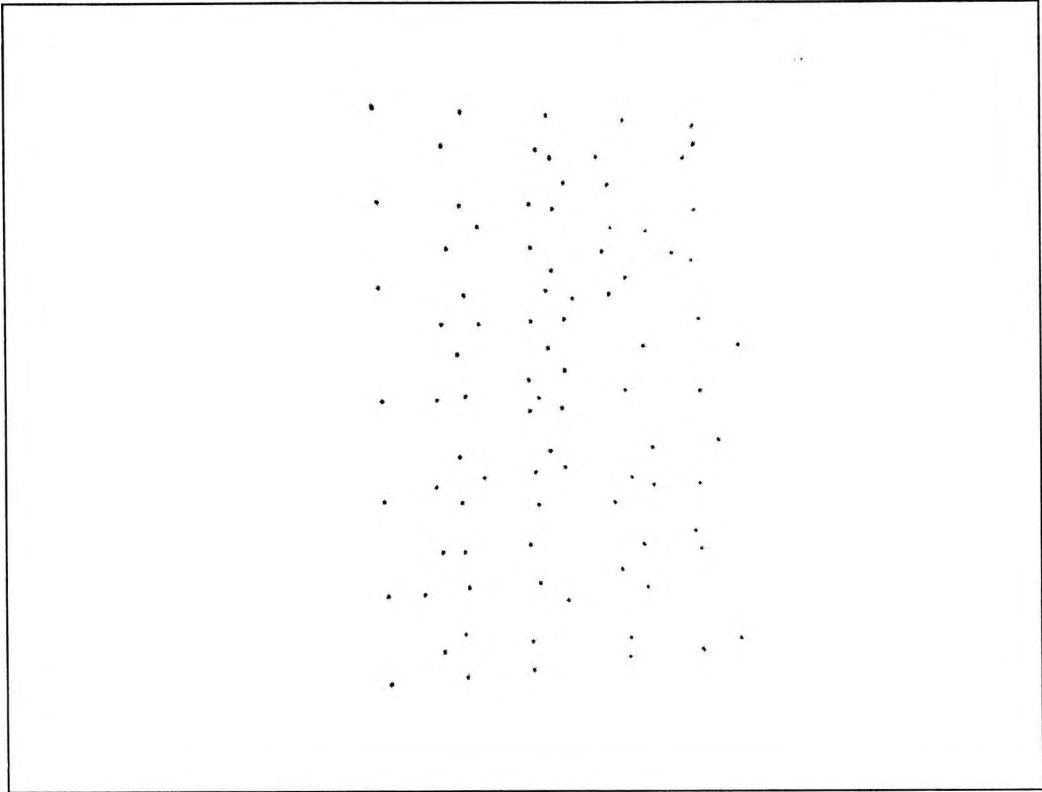


Figure 8-4 Image No. 1003

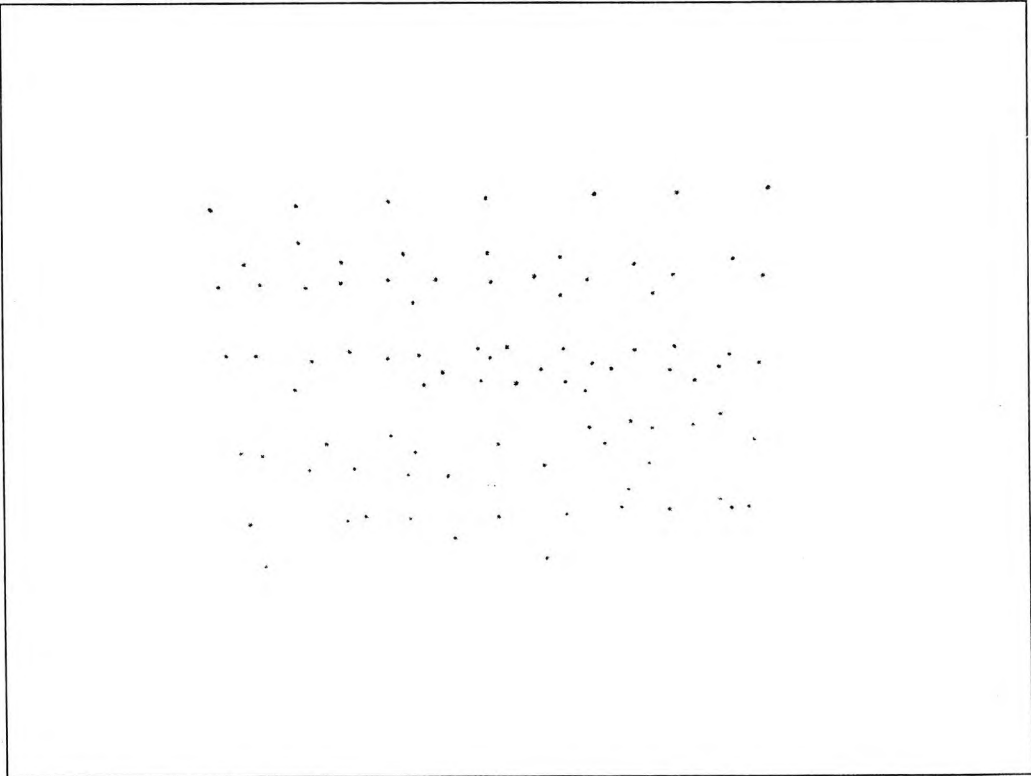


Figure 8-5 Image No. 1004

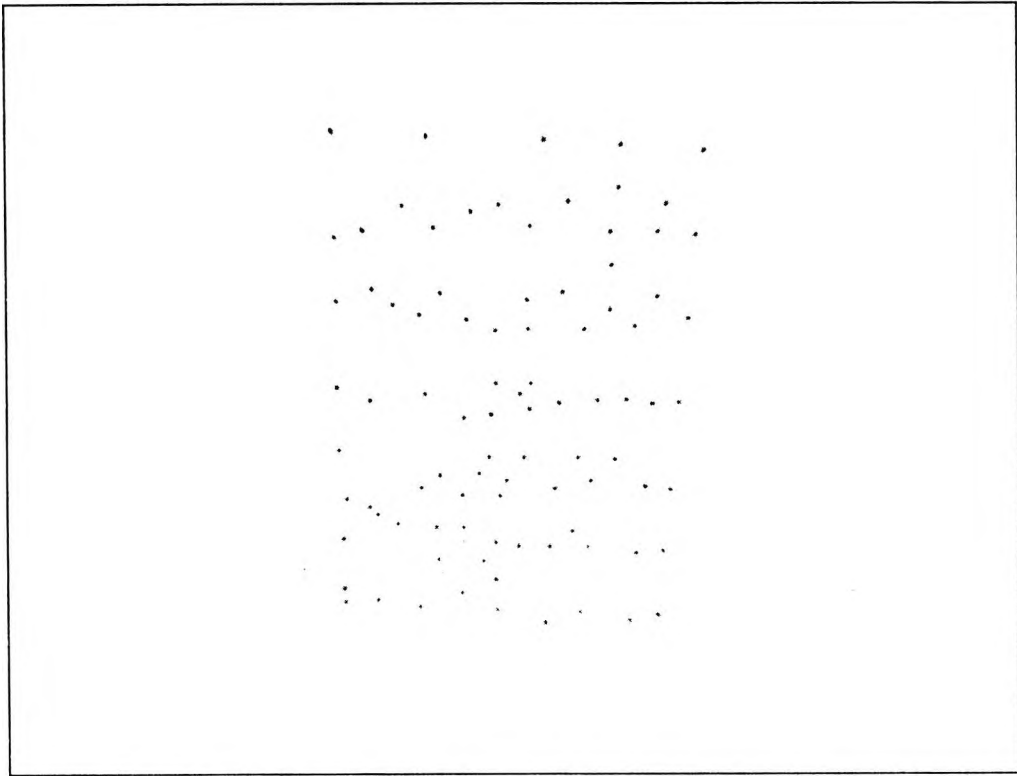


Figure 8-6 Image No. 1005

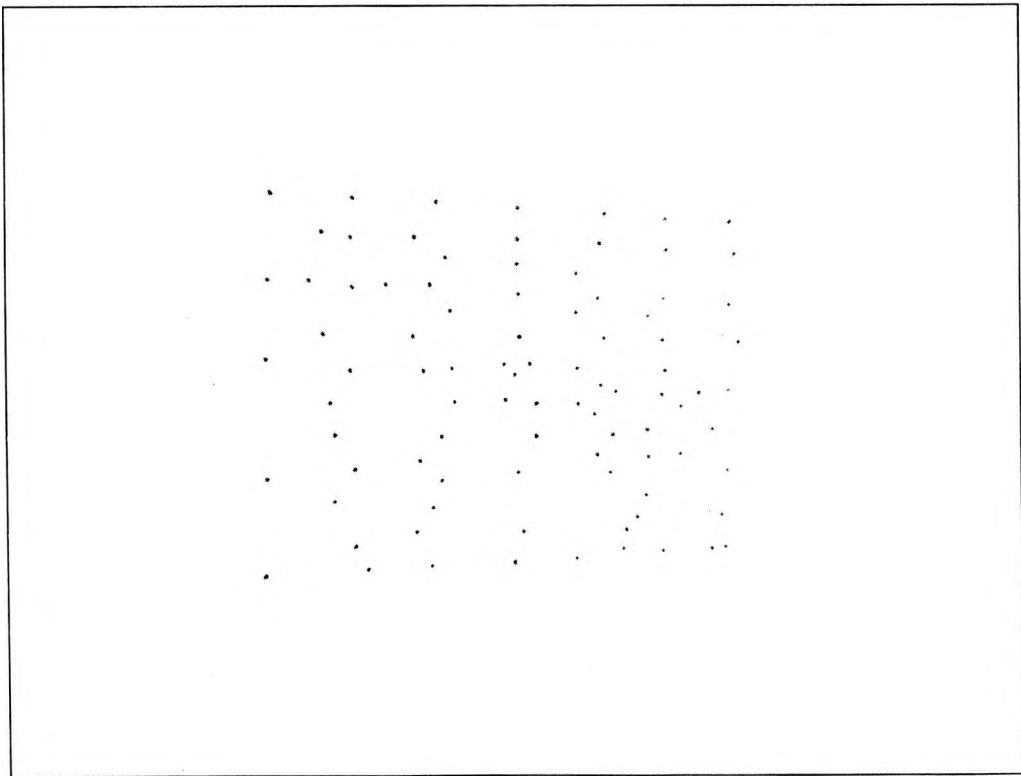


Figure 8-7 Image No. 1006

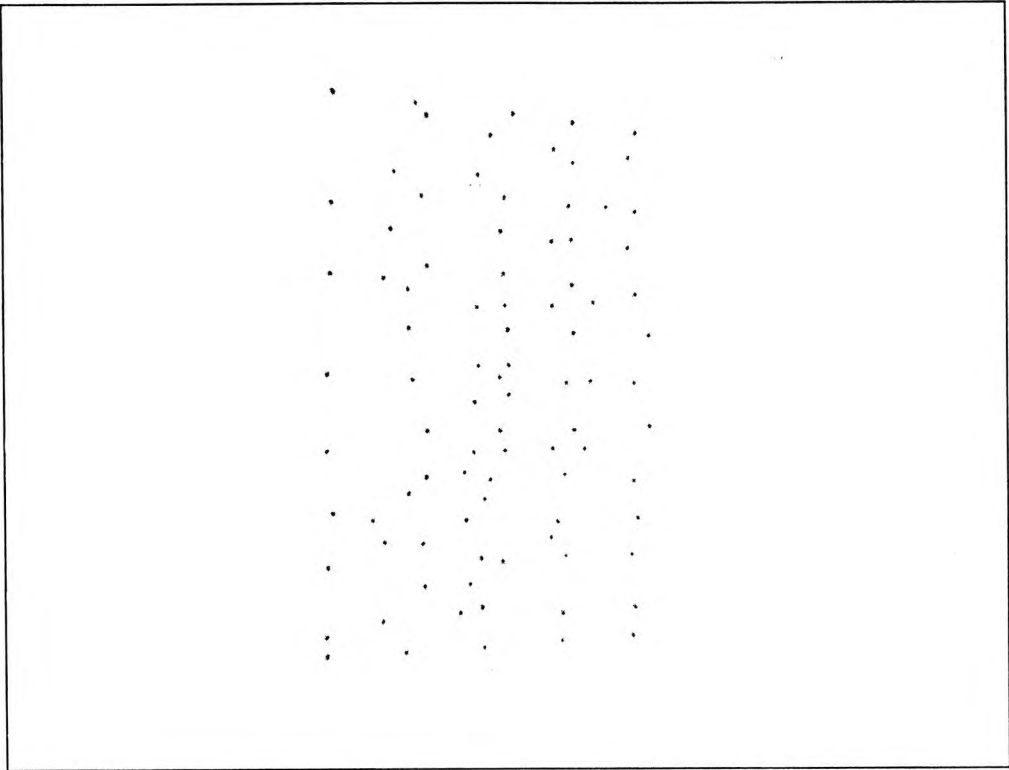


Figure 8-8 Image No. 10007

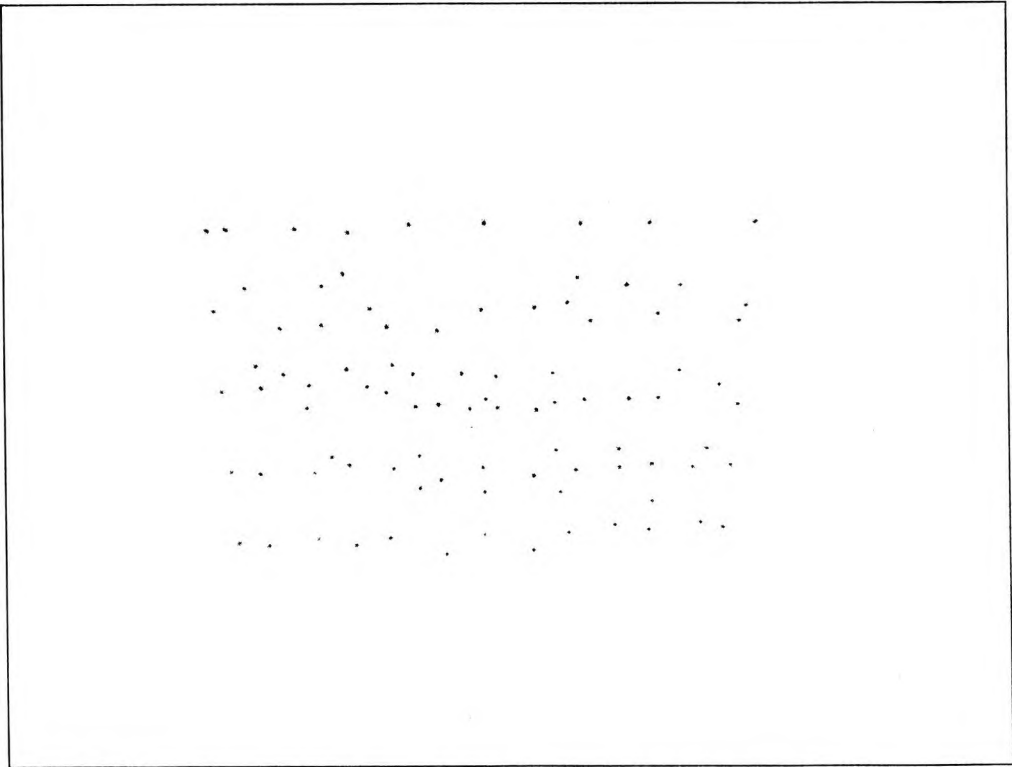


Figure 8-9 Image No. 1008

### 8.1 Measurement of the control points in the object space

The four points on the corners of the board were used as the control points. They were assumed to be in the same plane (the XY plane) for resection purposes. Figure 8-10 illustrates the configuration of the control points.

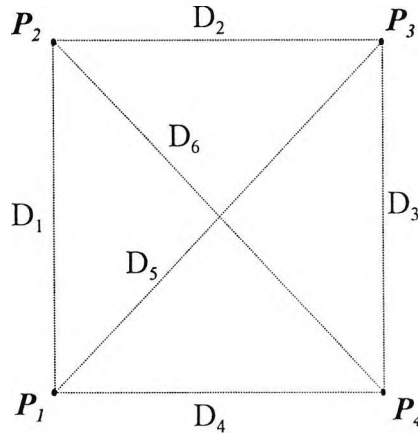


Figure 8-10 The configuration of the control points

The distances between the control points were measured with a steel tape. They are listed as follows:

$$\begin{aligned}
 D_1 &= 600.5 \pm 0.2 \text{ mm} \\
 D_2 &= 395.2 \pm 0.2 \text{ mm} \\
 D_3 &= 595.8 \pm 0.2 \text{ mm} \\
 D_4 &= 397.7 \pm 0.2 \text{ mm} \\
 D_5 &= 712.2 \pm 0.3 \text{ mm} \\
 D_6 &= 723.1 \pm 0.3 \text{ mm}
 \end{aligned}$$

A separate least squares adjustment was used to estimate the positions of the control points. The theory was discussed in chapter 4. Realistic starting values were used, i.e.,  $P_1(x, y) = (0, 0)$ ,  $P_2(x, y) = (0, 600.5)$ ,  $P_3(x, y) = (395.2, 600.5)$  and  $P_4(x, y) = (397.7, 0)$ . The estimated coordinates of the control points after least squares adjustment are listed in Table 8-1.

Table 8-1 The estimated coordinates of the control points

Control pts	X (mm)	Y (mm)	Z (mm)
1	1.303	1.982	0.0
2	-1.288	602.494	0.0
3	393.873	596.160	0.0
4	399.012	0.364	0.0

## 8.2 Initialisation of the camera exterior parameters

Starting values of the camera exterior parameters were estimated by space resection using the 2D DLT model. The theory was discussed in Chapter 3. From the eight images the control points were recognised and their 2D coordinates were computed. Table 8-2 lists the 2D coordinates of the control points on the image planes.

Table 8-2 The 2D coordinates of the control points on the image planes

Image No.	Control pts	$x$ (mm)	$y$ (mm)
1001	101	0.82634	1.66025
1001	102	0.80221	-1.40195
1001	103	-1.24096	-1.47524
1001	104	-1.60159	1.54994
1002	101	-1.74148	1.31663
1002	102	1.35723	0.99625
1002	103	1.18834	-1.05476
1002	104	-1.88283	-1.10697
1003	101	0.82933	1.58837
1003	102	0.80469	-1.61559
1003	103	-1.22282	-1.76566
1003	104	-1.22624	1.76176
1004	101	1.51860	-0.91649
1004	102	-1.67440	-0.90893
1004	103	-1.81908	1.10539
1004	104	1.71778	1.11054
1005	101	-1.18269	-1.33647
1005	102	-1.18817	1.71453
1005	103	1.21717	1.53035
1005	104	0.86415	-1.48188
1006	101	1.61229	-0.82419
1006	102	-1.45340	-1.00621
1006	103	-1.40823	1.39274

1006	104	1.66687	1.24815
1007	101	-1.15198	-1.75338
1007	102	-1.27826	1.83438
1007	103	0.82907	1.72391
1007	104	0.92524	-1.50587
1008	101	-1.91209	1.17528
1008	102	1.69382	1.25529
1008	103	1.52801	-0.82070
1008	104	-1.68980	-0.89740

With the 2D coordinates of the control points on image planes and their 3D coordinates in the object space as knowns, space resection with 2D DLT model was used to estimate the camera exterior parameters. The estimated camera exterior parameters are listed in Table 8-3.

Table 8-3 The starting values of the camera exterior parameters

Image No.	$X_L$ (mm)	$Y_L$ (mm)	$Z_L$ (mm)	$\omega$ (deg)	$\phi$ (deg)	$\kappa$ (deg)
1001	250.711	-441.797	1370.251	28.325	3.092	179.334
1002	194.103	-394.432	1382.789	25.569	-2.140	90.862
1003	882.860	224.905	1386.405	3.128	25.187	177.543
1004	910.320	263.011	1375.768	0.501	28.345	-92.091
1005	165.233	1057.872	1367.458	-28.780	-1.349	1.943
1006	206.090	1026.756	1381.629	-27.610	0.594	-89.558
1007	-501.022	297.184	1386.155	-0.270	-27.385	0.893
1008	-532.936	257.120	1370.779	2.853	-27.904	90.235

### 8.3 Starting values of the 3D coordinates

With camera exterior parameters as knowns, an intersection method was used to estimate the 3D coordinates of the object points. The theory of intersection method was discussed in Chapter 3. The estimated 3D coordinates are listed in Table 8-4.

Table 8-4 Starting values of the 3D coordinates obtained from intersection

Point No.	X (mm)	Y (mm)	Z (mm)
100	45.2920	555.3751	149.4480
101	148.7276	554.6239	90.4114
102	223.7562	599.7040	-0.8328
103	306.0528	597.4143	-1.7467
104	-0.4722	601.4213	1.6679
105	394.8677	594.0176	-2.3364
106	98.2244	599.1891	0.2669
107	352.7524	554.3839	48.7721
108	249.5625	554.2962	52.4732
109	307.1642	551.1034	-1.5278
110	146.7505	451.6116	120.5256
111	178.2786	527.4297	-0.7159
112	72.8184	522.6147	-0.1436
113	395.5496	501.4948	-1.7760
114	353.9312	503.8002	-1.6520
115	213.3062	504.6696	-0.9304
116	301.6727	501.6118	-1.4086
117	106.6698	499.1602	-0.3311
118	44.6350	453.3604	60.2282
119	352.3077	452.1226	50.8464
120	249.2901	453.2312	50.5767
121	-0.7234	484.9015	-0.3375
122	305.6685	462.8434	-1.2598
123	146.5401	350.1362	140.6307
124	114.5765	423.2506	-0.6927
125	213.3829	418.7704	-0.8726
126	350.8387	351.1256	99.7065
127	249.0462	350.7768	103.8980
128	45.6016	349.7703	110.5176
129	307.5134	410.4782	-1.2630
130	397.0967	403.1283	-1.2361
131	-0.7644	409.2594	-0.3365
132	62.0242	407.2622	-0.5804
133	337.5034	391.7127	-1.0860
134	91.4455	396.4933	-0.6673
135	279.9158	385.4562	-1.1800
136	216.3162	383.3759	-0.9704
137	178.9848	380.2455	-0.9140
138	47.4614	247.7378	155.1124
139	221.8266	315.6481	-0.8941
140	146.3861	246.3285	125.4436
141	181.5239	314.0301	-0.8689
142	351.5115	250.0266	102.5540
143	249.9056	246.2324	106.2096
144	396.9248	298.0049	-0.8175

145	334.6599	299.1238	-0.8420
146	210.1080	301.7747	-0.9229
147	-2.8141	301.8348	-1.0605
148	300.9423	296.8985	-0.8720
149	98.3000	297.5441	-0.9683
150	222.2644	282.2129	-0.8633
151	176.9941	273.3545	-0.8423
152	327.2278	220.0722	-0.5534
153	282.6603	220.4782	-0.6525
154	217.9764	218.5412	-0.7940
155	176.4666	217.0136	-0.8680
156	-2.5094	219.4215	-1.2140
157	164.5436	194.2223	-1.0570
158	299.8894	189.9130	-0.5499
159	116.7984	189.9184	-1.1110
160	351.5999	145.7826	80.2202
161	198.7079	185.7239	-0.8748
162	397.4640	181.1312	0.0118
163	250.2405	143.7181	70.0433
164	94.8377	171.9393	-1.1804
165	191.2782	163.9894	-0.7891
166	147.3929	145.2415	39.9365
167	44.0464	145.9598	19.0627
168	5.4585	152.7537	-1.3937
169	281.4705	117.7617	-0.2449
170	66.5630	119.8839	-1.3316
171	113.2695	116.6570	-1.1640
172	302.3937	95.7736	-0.0520
173	187.8699	97.5664	-0.6181
174	396.0863	93.6868	0.4454
175	216.5906	92.9009	-0.5535
176	0.3141	95.3946	-1.4462
177	249.4709	45.8347	85.4522
178	352.0740	44.6833	75.5404
179	173.3537	69.2177	-0.6657
180	116.2640	69.7485	-1.0345
181	45.5316	43.4593	48.4497
182	146.8900	43.4262	29.4848
183	189.8113	42.4347	-0.4304
184	-0.4146	21.1817	-1.5000
185	398.5203	-2.5089	1.5888
186	0.6110	0.4923	-1.7157
187	298.3324	-2.3076	0.7376
188	193.2333	-2.9955	-0.2054
189	93.7947	-1.9388	-1.0564

### 8.4 Self-calibration separate adjustment

With the camera exterior parameters and the 3D coordinates of the object points obtained in section 8.2 and 8.3 as starting values, a self-calibration separate adjustment was used to estimate the locations of the object points. The distances measured between the control points were used as scales in the adjustment process. Camera interior parameters were also obtained. The theory was discussed in chapter 6. Table 8-5 lists the estimated 3D coordinates and the standard deviations of the object points.

Table 8-5 The 3D coordinates and the standard deviations of the object points estimated from the self-calibration separate adjustment

Points No.	X (mm)	Y (mm)	Z (mm)	$\sigma_X$ (mm)	$\sigma_Y$ (mm)	$\sigma_Z$ (mm)
100	44.8946	555.6872	151.0539	0.0205	0.0209	0.0379
101	148.6848	554.4676	91.1520	0.0212	0.0217	0.0408
102	223.8240	600.0465	-0.3790	0.0222	0.0229	0.0455
103	306.3379	598.0050	-1.3492	0.0223	0.0229	0.0456
104	-1.4062	602.6913	2.1822	0.0223	0.0227	0.0454
105	395.7798	595.2234	-2.0436	0.0224	0.0228	0.0457
106	98.0234	599.7151	0.7572	0.0222	0.0228	0.0454
107	352.9746	554.6835	49.3644	0.0218	0.0222	0.0430
108	249.5333	554.1406	52.9998	0.0217	0.0221	0.0428
109	307.2372	551.0950	-1.2168	0.0223	0.0228	0.0456
110	146.8569	450.9985	120.4294	0.0210	0.0212	0.0394
111	178.3312	526.9614	-0.4061	0.0223	0.0227	0.0455
112	72.8831	522.3692	0.1966	0.0223	0.0227	0.0455
113	395.7461	501.5642	-1.5539	0.0224	0.0226	0.0457
114	353.9188	503.6385	-1.4261	0.0224	0.0227	0.0456
115	213.2977	504.0751	-0.6806	0.0223	0.0227	0.0455
116	301.5502	501.2016	-1.1832	0.0224	0.0227	0.0456
117	106.8521	498.6520	-0.0493	0.0223	0.0226	0.0455
118	44.8763	452.9060	60.5159	0.0217	0.0218	0.0424
119	352.0476	451.7644	51.0145	0.0218	0.0220	0.0429
120	249.1130	452.5782	50.5780	0.0218	0.0220	0.0429
121	-0.7848	484.7853	-0.0097	0.0224	0.0225	0.0455
122	305.4253	462.3108	-1.0953	0.0224	0.0226	0.0456
123	146.7450	349.7460	139.8805	0.0208	0.0209	0.0385
124	114.9334	422.6088	-0.5464	0.0224	0.0225	0.0455
125	213.3476	418.0833	-0.7822	0.0224	0.0226	0.0456
126	350.3700	350.8733	99.5324	0.0213	0.0213	0.0406
127	248.8092	350.4055	103.2887	0.0212	0.0213	0.0403
128	46.0422	349.4074	110.3981	0.0211	0.0211	0.0399

129	307.1404	409.9481	-1.1656	0.0224	0.0225	0.0456
130	396.8226	402.8768	-1.0747	0.0225	0.0225	0.0457
131	-0.4706	408.9297	-0.0956	0.0224	0.0224	0.0455
132	62.4878	406.7493	-0.4095	0.0224	0.0225	0.0455
133	337.0626	391.2911	-0.9852	0.0224	0.0225	0.0457
134	91.9071	395.9421	-0.5382	0.0224	0.0225	0.0456
135	279.5755	384.9374	-1.1222	0.0224	0.0225	0.0456
136	216.2616	382.8013	-0.9290	0.0224	0.0225	0.0456
137	179.1271	379.6765	-0.8677	0.0224	0.0225	0.0456
138	47.8490	247.6683	154.8793	0.0206	0.0206	0.0378
139	221.7397	315.4320	-0.9041	0.0224	0.0225	0.0456
140	146.6586	246.4118	124.7264	0.0209	0.0210	0.0393
141	181.6744	313.8145	-0.8771	0.0224	0.0224	0.0456
142	351.0560	250.1250	102.4006	0.0212	0.0212	0.0405
143	249.7045	246.3770	105.5867	0.0212	0.0212	0.0403
144	396.4600	297.9454	-0.6559	0.0225	0.0224	0.0457
145	334.1186	299.0403	-0.7667	0.0224	0.0224	0.0457
146	210.0914	301.6405	-0.9370	0.0224	0.0224	0.0456
147	-2.3237	301.6767	-0.8885	0.0225	0.0223	0.0456
148	300.4765	296.8164	-0.8345	0.0224	0.0224	0.0457
149	98.8465	297.4129	-0.9246	0.0224	0.0224	0.0456
150	222.1794	282.2018	-0.8747	0.0224	0.0224	0.0457
151	177.1762	273.3865	-0.8524	0.0224	0.0224	0.0456
152	326.7610	220.3284	-0.4365	0.0224	0.0224	0.0457
153	282.3088	220.7820	-0.5853	0.0224	0.0224	0.0457
154	217.9326	218.8797	-0.7666	0.0224	0.0224	0.0457
155	176.6455	217.3463	-0.8451	0.0224	0.0224	0.0457
156	-2.1182	219.4382	-1.0586	0.0225	0.0223	0.0457
157	164.7716	194.6335	-1.0086	0.0224	0.0224	0.0457
158	299.5278	190.2975	-0.4287	0.0224	0.0224	0.0457
159	117.2056	190.2769	-1.0452	0.0224	0.0224	0.0457
160	351.3597	146.0402	80.4711	0.0214	0.0214	0.0416
161	198.7691	186.1828	-0.8137	0.0223	0.0224	0.0457
162	397.1978	181.2893	0.2611	0.0224	0.0223	0.0458
163	250.1245	144.1750	69.9915	0.0215	0.0215	0.0421
164	95.2592	172.2827	-1.0871	0.0224	0.0224	0.0457
165	191.3715	164.4934	-0.6995	0.0223	0.0224	0.0457
166	147.6395	145.6821	39.9216	0.0219	0.0219	0.0436
167	44.3653	146.1190	19.2028	0.0222	0.0221	0.0447
168	5.6520	152.7706	-1.2322	0.0224	0.0223	0.0457
169	281.2962	118.1947	-0.0261	0.0223	0.0224	0.0458
170	66.8250	120.0830	-1.1761	0.0224	0.0224	0.0457
171	113.5296	117.0106	-1.0105	0.0223	0.0224	0.0458
172	302.2562	96.0799	0.2215	0.0223	0.0223	0.0458
173	187.9489	98.0006	-0.4174	0.0223	0.0224	0.0458
174	396.2177	93.5739	0.7945	0.0223	0.0223	0.0458

175	216.5970	93.3262	-0.3300	0.0223	0.0224	0.0458
176	0.1580	95.1233	-1.2553	0.0224	0.0223	0.0458
177	249.5056	45.8654	86.0432	0.0212	0.0214	0.0414
178	352.2663	44.3899	76.3574	0.0214	0.0214	0.0419
179	173.4362	69.4893	-0.4187	0.0223	0.0224	0.0458
180	116.3840	69.8854	-0.8104	0.0223	0.0224	0.0458
181	45.3520	42.9867	48.9643	0.0217	0.0218	0.0432
182	146.9538	43.4247	29.8495	0.0219	0.0220	0.0442
183	189.8510	42.5122	-0.1243	0.0222	0.0224	0.0458
184	-1.1520	20.0908	-1.2690	0.0223	0.0224	0.0458
185	399.3724	-3.8043	2.0273	0.0222	0.0223	0.0459
186	-0.3139	-0.9414	-1.4774	0.0223	0.0224	0.0459
187	298.5322	-2.9347	1.1824	0.0222	0.0224	0.0458
188	193.2391	-3.4633	0.1906	0.0222	0.0224	0.0458
189	93.5616	-2.7026	-0.7306	0.0222	0.0224	0.0458

The mean standard deviations of the 3D coordinates were found to be

$$\bar{\sigma}_x = 0.0221mm \quad \bar{\sigma}_y = 0.0222mm \quad \bar{\sigma}_z = 0.0445mm$$

which gave a relative precision of 1:25,462. The resulting 3D coordinates of the object points on the test field were in an arbitrary datum, which was defined by the starting values of the control points. However, the relative positions of the object points or the shape of the test field were not related to the datum.

Camera interior parameters were also obtained with the separate adjustment process. They are listed in Table 8-6 (the second row lists the standard deviations of the parameters).

Table 8-6 Camera interior parameters and their standard deviations

$\Delta x_p$ (mm)	$\Delta y_p$ (mm)	$\Delta c$ (mm)	$k_1$ (mm <sup>-2</sup> )	$k_2$ (mm <sup>-4</sup> )	$k_3$ (mm <sup>-6</sup> )	$p_1$ (mm <sup>-1</sup> )	$p_2$ (mm <sup>-1</sup> )
2.21e-1	3.52e-3	1.53e-2	3.76e-3	-3.19e-4	3.74e-5	2.79e-4	-1.88e-4
8.83e-3	8.71e-3	7.42e-4	2.80e-4	1.22e-4	1.59e-5	2.34e-5	2.36e-5

Figure 8-11 illustrates the image residuals plotted for one of the images (image No. 1001), and Figure 8-12 illustrates the reconstructed 3D test field.

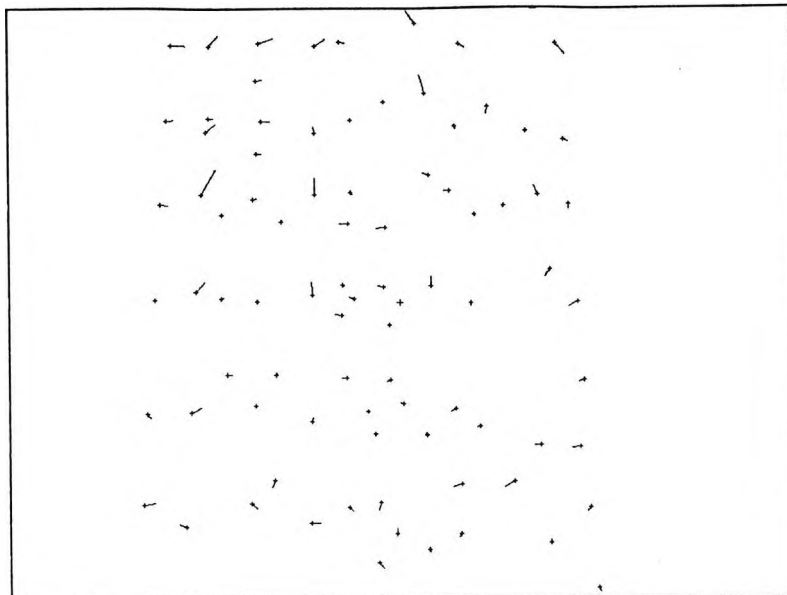


Figure 8-11 Image residuals on image No. 1001

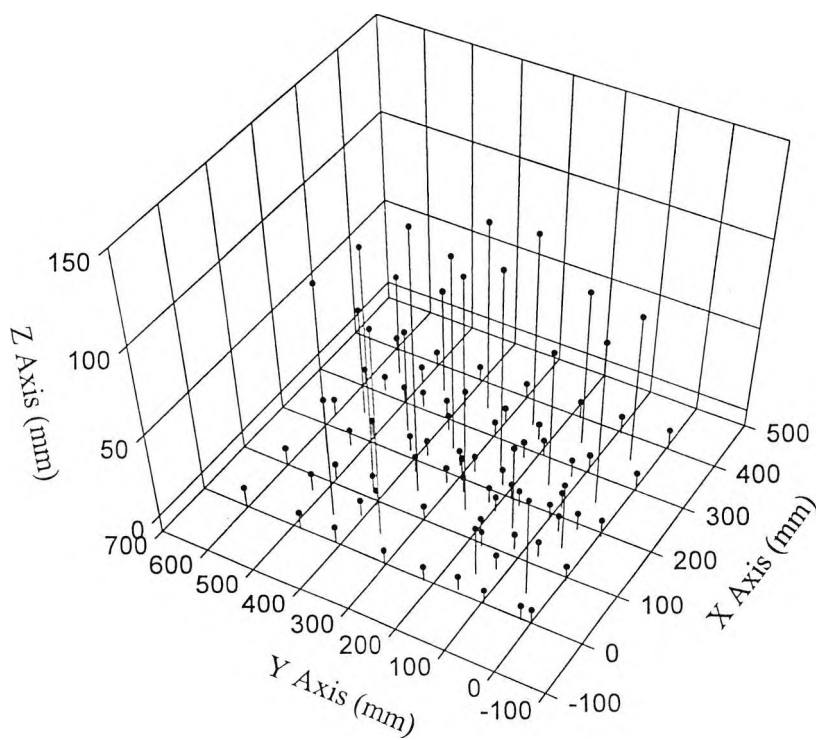


Figure 8-12 Reconstructed test field

To verify that the results from the separate adjustment are the same as that from the bundle adjustment, a self-calibrated bundle adjustment (CUBA 1996) was applied with the same starting values. It was found that same minimisation of the sum of the squares of the residuals on image planes was obtained and the resulting camera interior parameters were identical. This is because that the sum of the squares of the residuals on image planes and the camera interior parameters are datum independent. Therefore the calibrated camera interior parameters can be used for the subsequent measurement purpose provided that the physical configuration of the camera remains unchanged. 3D coordinates of the object points (after coordinate transformation) were also checked and found to be identical with that obtained from the separate adjustment.

## Chapter 9

### Conclusions

Photogrammetry has been widely used in the areas where 3D coordinates are required. Least squares estimation methods have been successfully used to deal with redundant measurements. Conventionally, all the unknown parameters were estimated simultaneously in the least squares process. This leads to the bundle adjustment in close range photogrammetry, which is very expensive in terms of computation time and memory requirements. Methods such as sequential adjustment, unified bundle adjustment and Block Successive Over Relaxation (BSOR) can be use in some cases to improve the conventional bundle adjustment. But none of them have the capability to deal with real-time measurement.

In this thesis, an alternative method of least squares estimation, named *separate least squares estimation*, is introduced. It divides the unknown parameters into groups and estimates them separately. The separate least squares estimation uses all the equations for each group of the parameters and the inner iterations are merged in the outer iterations. Even with linear functional model iterations are still required and starting values of the unknown parameters are always needed. Constraints are not always required in the separate least squares estimation even when column rank defects of the design matrix exist since the divided design matrices are normally of full rank provided that datum can be defined by each group of the parameters. In this case, the datum will be defined by the starting values of the parameters. A coordinate transformation may be required to relate the results to a given coordinate system. Alternatively, control points can be included in the separate least squares estimation process to avoid coordinate transformation. The separate least squares estimation will give the same results as the simultaneous least squares estimation, but with a significant saving in time and memory.

Based on the theory of the separate least squares estimation, an alternative method, named *separate adjustment*, was developed and successfully used in close range

photogrammetry to replace the conventional bundle adjustment. In the separate adjustment process, the 3D coordinates of the object points and the camera parameters are adjusted separately and iteratively. Since the datum can always be determined in both adjustment steps, constraints may not be necessary in the separate adjustment. Free network adjustment without any constraints becomes feasible and can be easily applied. Because the same functional model and the same target function of the least squares are used, the same results can be expected from the separate adjustment as from the simultaneous bundle adjustment. Several simulation tests and practical tests verified this.

The number of iterations required for the separate adjustment may be more than that for the bundle adjustment. However, due to the simple computation and the linear computational complexity, the speed of convergence of the separate adjustment is much faster than that of the bundle adjustment, especially for large data sets. The maximum memory required by the separate adjustment is limited to a  $6 \times 6$  (or  $14 \times 14$  when camera interior parameters are considered) unit no matter how many cameras and object points are involved. Because of the high speed and low memory requirements, the separate adjustment can be used in the real-time measurement to track moving objects.

The separate adjustment can also be applied to the self-calibration adjustment. A three step separate adjustment (divide camera interior and exterior parameters) or a two step separate adjustment (integrate camera interior and exterior parameters) can be used.

The disadvantage of the separate adjustment is that the full covariance matrix of the estimated results is not provided directly. To evaluate the precision of the 3D coordinates a  $3 \times 3$  covariance matrix for each object point and a  $6 \times 6$  (or  $14 \times 14$ ) covariance matrix for each camera are given. These may be adequate in most cases. A full weight matrix (block diagonal matrix) of the estimated results is always available from the design matrix, from which the full covariance matrix can be derived whenever it is required.

For the intermediate parameters the full covariance matrix may not be necessary, whilst the weight matrix (the inverse of the cofactor matrix), which is easy to obtain from the design matrix, is more convenient to use. When coordinate transformation is required, the weight matrix can be transformed easily.

## Appendix I

## Derivations of some partial derivatives

To derive the partial derivatives in Chapter 3 and Chapter 5, the collinearity equations are rewritten as follows

$$\begin{cases} f_x = x + c \frac{M_1}{M_3} \\ f_y = y + c \frac{M_2}{M_3} \end{cases} \quad (\text{A1.1})$$

in which

$$\begin{cases} M_1 = m_{11}(X - X_L) + m_{12}(Y - Y_L) + m_{13}(Z - Z_L) \\ M_2 = m_{21}(X - X_L) + m_{22}(Y - Y_L) + m_{23}(Z - Z_L) \\ M_3 = m_{31}(X - X_L) + m_{32}(Y - Y_L) + m_{33}(Z - Z_L) \end{cases} \quad (\text{A1.2})$$

and

$$\begin{cases} m_{11} = \cos \phi \cos \kappa \\ m_{12} = \sin \omega \sin \phi \cos \kappa + \cos \omega \sin \kappa \\ m_{13} = -\cos \omega \sin \phi \cos \kappa + \sin \omega \sin \kappa \\ m_{21} = -\cos \phi \sin \kappa \\ m_{22} = -\sin \omega \sin \phi \sin \kappa + \cos \omega \cos \kappa \\ m_{23} = \cos \omega \sin \phi \cos \kappa + \sin \omega \cos \kappa \\ m_{31} = \sin \phi \\ m_{32} = -\sin \omega \cos \phi \\ m_{33} = \cos \omega \cos \phi \end{cases} \quad (\text{A1.3})$$

The subscripts  $i$  and  $j$  are neglected for simplicity.

Linearized functional model is expressed as

$$A_1 \Delta x_1 + A_2 \Delta x_2 = b \quad (\text{A1.4})$$

in which  $x_1 = (X, Y, Z)$  is a vector of the 3D coordinates of the object points and  $x_2 = (X_L, Y_L, Z_L, \omega, \phi, \kappa)$  is a vector of the camera exterior parameters.

#### A1.1 Derivation of $A_1$ (partial derivatives with respect to 3D coordinates)

$$A_1 = \begin{bmatrix} \frac{\partial f_x}{\partial X} & \frac{\partial f_x}{\partial Y} & \frac{\partial f_x}{\partial Z} \\ \frac{\partial f_y}{\partial X} & \frac{\partial f_y}{\partial Y} & \frac{\partial f_y}{\partial Z} \end{bmatrix} \quad (\text{A1.5})$$

in which

$$\frac{\mathcal{J}_x}{\partial X} = c(m_{11} - m_{31}M_1 / M_3) / M_3 \quad (\text{A1.6a})$$

$$\frac{\mathcal{J}_x}{\partial Y} = c(m_{12} - m_{32}M_1 / M_3) / M_3 \quad (\text{A1.6b})$$

$$\frac{\mathcal{J}_x}{\partial Z} = c(m_{13} - m_{33}M_1 / M_3) / M_3 \quad (\text{A1.6c})$$

$$\frac{\mathcal{J}_y}{\partial X} = c(m_{21} - m_{31}M_2 / M_3) / M_3 \quad (\text{A1.6d})$$

$$\frac{\mathcal{J}_y}{\partial Y} = c(m_{22} - m_{32}M_2 / M_3) / M_3 \quad (\text{A1.6e})$$

$$\frac{\mathcal{J}_y}{\partial Z} = c(m_{23} - m_{33}M_2 / M_3) / M_3 \quad (\text{A1.6f})$$

**A1.2 Derivation of  $A_2$**  (partial derivatives with respect to camera exterior parameters)

$$A_2 = \begin{bmatrix} \frac{\mathcal{J}_x}{\partial X_L} & \frac{\mathcal{J}_x}{\partial Y_L} & \frac{\mathcal{J}_x}{\partial Z_L} & \frac{\mathcal{J}_x}{\partial \omega} & \frac{\mathcal{J}_x}{\partial \phi} & \frac{\mathcal{J}_x}{\partial \kappa} \\ \frac{\mathcal{J}_y}{\partial X_L} & \frac{\mathcal{J}_y}{\partial Y_L} & \frac{\mathcal{J}_y}{\partial Z_L} & \frac{\mathcal{J}_y}{\partial \omega} & \frac{\mathcal{J}_y}{\partial \phi} & \frac{\mathcal{J}_y}{\partial \kappa} \end{bmatrix} \quad (\text{A1.7})$$

in which

$$\frac{\mathcal{J}_x}{\partial X_L} = -c(m_{11} - m_{31}M_1 / M_3) / M_3 = -\frac{\mathcal{J}_x}{\partial X} \quad (\text{A1.8a})$$

$$\frac{\mathcal{J}_x}{\partial Y_L} = -c(m_{12} - m_{32}M_1 / M_3) / M_3 = -\frac{\mathcal{J}_x}{\partial Y} \quad (\text{A1.8b})$$

$$\frac{\mathcal{J}_x}{\partial Z_L} = -c(m_{13} - m_{33}M_1 / M_3) / M_3 = -\frac{\mathcal{J}_x}{\partial Z} \quad (\text{A1.8c})$$

$$\frac{\mathcal{J}_x}{\partial \omega} = c\left(\frac{\partial M_1}{\partial \omega} - \frac{\partial M_3}{\partial \omega} M_1 / M_3\right) / M_3 \quad (\text{A1.8d})$$

$$\frac{\partial \mathcal{F}_x}{\partial \phi} = c \left( \frac{\partial M_1}{\partial \phi} - \frac{\partial M_3}{\partial \phi} M_1 / M_3 \right) / M_3 \quad (\text{A1.8e})$$

$$\frac{\partial \mathcal{F}_x}{\partial \kappa} = c \left( \frac{\partial M_1}{\partial \kappa} - \frac{\partial M_3}{\partial \kappa} M_1 / M_3 \right) / M_3 \quad (\text{A1.8f})$$

$$\frac{\partial \mathcal{F}_y}{\partial X_L} = -c(m_{21} - m_{31} M_2 / M_3) / M_3 = -\frac{\partial \mathcal{F}_y}{\partial X} \quad (\text{A1.9a})$$

$$\frac{\partial \mathcal{F}_y}{\partial Y_L} = -c(m_{22} - m_{32} M_2 / M_3) / M_3 = -\frac{\partial \mathcal{F}_y}{\partial Y} \quad (\text{A1.9b})$$

$$\frac{\partial \mathcal{F}_y}{\partial Z_L} = -c(m_{23} - m_{33} M_2 / M_3) / M_3 = -\frac{\partial \mathcal{F}_y}{\partial Z} \quad (\text{A1.9c})$$

$$\frac{\partial \mathcal{F}_y}{\partial \omega} = c \left( \frac{\partial M_2}{\partial \omega} - \frac{\partial M_3}{\partial \omega} M_2 / M_3 \right) / M_3 \quad (\text{A1.9d})$$

$$\frac{\partial \mathcal{F}_y}{\partial \phi} = c \left( \frac{\partial M_2}{\partial \phi} - \frac{\partial M_3}{\partial \phi} M_2 / M_3 \right) / M_3 \quad (\text{A1.9e})$$

$$\frac{\partial \mathcal{F}_y}{\partial \kappa} = c \left( \frac{\partial M_2}{\partial \kappa} - \frac{\partial M_3}{\partial \kappa} M_2 / M_3 \right) / M_3 \quad (\text{A1.9f})$$

in which

$$\frac{\partial M_1}{\partial \omega} = -m_{13}(Y - Y_L) + m_{12}(Z - Z_L) \quad (\text{A1.10a})$$

$$\begin{aligned} \frac{\partial M_1}{\partial \phi} = & -\sin \phi \cos \kappa (X - X_L) + \sin \omega \cos \phi \cos \kappa (Y - Y_L) \\ & - \cos \omega \cos \phi \cos \kappa (Z - Z_L) \end{aligned} \quad (\text{A1.10b})$$

$$\frac{\partial M_1}{\partial \kappa} = M_2 \quad (\text{A1.10c})$$

$$\frac{\partial M_2}{\partial \omega} = -m_{23}(Y - Y_L) + m_{22}(Z - Z_L) \quad (\text{A1.11a})$$

$$\begin{aligned} \frac{\partial M_2}{\partial \phi} = & \sin \phi \sin \kappa (X - X_L) - \sin \omega \cos \phi \sin \kappa (Y - Y_L) \\ & + \cos \omega \cos \phi \sin \kappa (Z - Z_L) \end{aligned} \quad (\text{A1.11b})$$

$$\frac{\partial M_2}{\partial \kappa} = -M_1 \quad (\text{A1.11c})$$

$$\frac{\partial M_3}{\partial \omega} = -m_{33}(Y - Y_L) + m_{32}(Z - Z_L) \quad (\text{A1.12a})$$

$$\begin{aligned} \frac{\partial M_3}{\partial \phi} = & \cos \phi (X - X_L) + \sin \omega \sin \phi (Y - Y_L) \\ & - \cos \omega \sin \phi (Z - Z_L) \end{aligned} \quad (\text{A1.12b})$$

$$\frac{\partial M_3}{\partial \kappa} = 0 \quad (\text{A1.12c})$$

### A1.3 Derivation of $A_2'$ (partial derivatives with respect to camera interior parameters)

The modified functional model when camera interior parameters are considered are expressed as

$$\begin{cases} f_x = (x - x_p) + \Delta x_r + \Delta x_d + c_x \frac{M_1}{M_3} \\ f_y = (y - y_p) + \Delta y_r + \Delta y_d + c_y \frac{M_2}{M_3} \end{cases} \quad (\text{A1.12})$$

where

$$\begin{aligned} \Delta x_r &= (x - x_p) \Delta r / r \\ &= (x - x_p) (k_1 r^2 + k_2 r^4 + k_3 r^6) \end{aligned} \quad (\text{A1.13})$$

$$\begin{aligned} \Delta y_r &= (y - y_p) \Delta r / r \\ &= (y - y_p) (k_1 r^2 + k_2 r^4 + k_3 r^6) \end{aligned} \quad (\text{A1.14})$$

$$\begin{aligned} \Delta x_d &= p_1 (r^2 + 2(x - x_p)^2) + 2p_2 (x - x_p) (y - y_p) \\ &= 2(x - x_p) (p_1 (x - x_p) + p_2 (y - y_p)) + p_1 r^2 \end{aligned} \quad (\text{A1.15})$$

$$\begin{aligned} \Delta y_d &= p_2 (r^2 + 2(y - y_p)^2) + 2p_1 (x - x_p) (y - y_p) \\ &= 2(y - y_p) (p_1 (x - x_p) + p_2 (y - y_p)) + p_2 r^2 \end{aligned} \quad (\text{A1.16})$$

in which

$$r^2 = (x - x_p)^2 + (y - y_p)^2 \quad (\text{A1.17})$$

Replacing  $\Delta x_r, \Delta y_r, \Delta x_d, \Delta y_d$  in (A1.12) from (A1.13) to (A1.16) gives

$$\begin{cases} f_x = (x - x_p)H + p_1 r^2 + c_x \frac{M_1}{M_3} \\ f_y = (y - y_p)H + p_2 r^2 + c_y \frac{M_2}{M_3} \end{cases} \quad (\text{A1.18})$$

in which

$$H = 1 + k_1 r^2 + k_2 r^4 + k_3 r^6 + 2p_1(x - x_p) + 2p_2(y - y_p) \quad (\text{A1.19})$$

The elements of  $A'_2$  are given by

$$A'_2 = \begin{bmatrix} \frac{\partial f_x}{\partial x} & \frac{\partial f_x}{\partial y} & \frac{\partial f_x}{\partial x_p} & \frac{\partial f_x}{\partial y_p} & \frac{\partial f_x}{\partial k_1} & \frac{\partial f_x}{\partial k_2} & \frac{\partial f_x}{\partial k_3} & \frac{\partial f_x}{\partial p_1} & \frac{\partial f_x}{\partial p_2} \\ \frac{\partial f_y}{\partial x} & \frac{\partial f_y}{\partial y} & \frac{\partial f_y}{\partial x_p} & \frac{\partial f_y}{\partial y_p} & \frac{\partial f_y}{\partial k_1} & \frac{\partial f_y}{\partial k_2} & \frac{\partial f_y}{\partial k_3} & \frac{\partial f_y}{\partial p_1} & \frac{\partial f_y}{\partial p_2} \end{bmatrix} \quad (\text{A1.20})$$

where

$$\frac{\partial f_x}{\partial x} = \frac{M_1}{M_3} \quad (\text{A1.21a})$$

$$\frac{\partial f_x}{\partial y} = 0 \quad (\text{A1.21b})$$

$$\frac{\partial f_x}{\partial x_p} = -H + (x - x_p) \left( \frac{\partial H}{\partial x_p} - 2p_1 \right) \quad (\text{A1.21c})$$

$$\frac{\partial f_x}{\partial y_p} = (x - x_p) \frac{\partial H}{\partial y_p} - 2p_2(y - y_p) \quad (\text{A1.21d})$$

$$\frac{\partial f_x}{\partial k_1} = (x - x_p) r^2 \quad (\text{A1.21e})$$

$$\frac{\partial f_x}{\partial k_2} = (x - x_p) r^4 \quad (\text{A1.21f})$$

$$\frac{\partial f_x}{\partial k_3} = (x - x_p) r^6 \quad (\text{A1.21g})$$

$$\frac{\partial \mathcal{F}_x}{\partial p_1} = 2(x - x_p)^2 + r^2 \quad (\text{A1.21h})$$

$$\frac{\partial \mathcal{F}_x}{\partial p_2} = 2(x - x_p)(y - y_p) \quad (\text{A1.21i})$$

$$\frac{\partial \mathcal{F}_y}{\partial x} = 0 \quad (\text{A1.22a})$$

$$\frac{\partial \mathcal{F}_y}{\partial x} = \frac{M_2}{M_3} \quad (\text{A1.22b})$$

$$\frac{\partial \mathcal{F}_y}{\partial x_p} = (y - y_p) \frac{\partial H}{\partial x_p} - 2p_2(x - x_p) \quad (\text{A1.22c})$$

$$\frac{\partial \mathcal{F}_y}{\partial y_p} = -H + (y - y_p) \left( \frac{\partial H}{\partial y_p} - 2p_2 \right) \quad (\text{A1.22d})$$

$$\frac{\partial \mathcal{F}_y}{\partial k_1} = (y - y_p)r^2 \quad (\text{A1.22e})$$

$$\frac{\partial \mathcal{F}_y}{\partial k_2} = (y - y_p)r^4 \quad (\text{A1.22f})$$

$$\frac{\partial \mathcal{F}_y}{\partial k_3} = (y - y_p)r^6 \quad (\text{A1.22g})$$

$$\frac{\partial \mathcal{F}_y}{\partial p_1} = 2(x - x_p)(y - y_p) \quad (\text{A1.22h})$$

$$\frac{\partial \mathcal{F}_y}{\partial p_2} = 2(y - y_p)^2 + r^2 \quad (\text{A1.22i})$$

in which

$$\frac{\partial H}{\partial x_p} = -2(x - x_p)(k_1 + 2k_2r^2 + 3k_3r^4) - 2p_1 \quad (\text{A1.23})$$

$$\frac{\partial H}{\partial y_p} = -2(y - y_p)(k_1 + 2k_2r^2 + 3k_3r^4) - 2p_2 \quad (\text{A1.24})$$

### A1.4 Derivation of partial derivatives when estimating seven transformation parameters from the twelve

The relationship between the seven parameters ( $s, \alpha, \beta, \gamma, x_0, y_0, z_0$ ) and the twelve parameters ( $t_1, t_2, \dots, t_{12}$ ) is expressed as

$$\begin{cases} s(\cos \beta \cos \gamma) & = t_1 \\ s(\sin \alpha \sin \beta \cos \gamma + \cos \alpha \sin \gamma) & = t_2 \\ s(-\cos \alpha \sin \beta \cos \gamma + \sin \alpha \sin \gamma) & = t_3 \\ s(-\cos \beta \sin \gamma) & = t_4 \\ s(-\sin \alpha \sin \beta \sin \gamma + \cos \alpha \cos \gamma) & = t_5 \\ s(\cos \alpha \sin \beta \sin \gamma + \sin \alpha \cos \gamma) & = t_6 \\ s(\sin \beta) & = t_7 \\ s(-\sin \alpha \cos \beta) & = t_8 \\ s(\cos \alpha \cos \beta) & = t_9 \\ x_0 & = t_{10} \\ y_0 & = t_{11} \\ z_0 & = t_{12} \end{cases}$$

With  $x = (s, \alpha, \beta, \gamma, x_0, y_0, z_0)$  as the unknown parameters and  $t = (t_1, t_2, \dots, t_{12})$  as the observations, the functional model can be expressed as

$$f(x, t) = 0$$

The Jacobian **matrix** is obtained by

$$A = \left( \frac{\partial f}{\partial x} \right)_0 = \begin{bmatrix} \frac{\partial f_1}{\partial s} & \frac{\partial f_1}{\partial \alpha} & \frac{\partial f_1}{\partial \beta} & \frac{\partial f_1}{\partial \gamma} & \frac{\partial f_1}{\partial x_0} & \frac{\partial f_1}{\partial y_0} & \frac{\partial f_1}{\partial z_0} \\ \frac{\partial f_2}{\partial s} & \frac{\partial f_2}{\partial \alpha} & \frac{\partial f_2}{\partial \beta} & \frac{\partial f_2}{\partial \gamma} & \frac{\partial f_2}{\partial x_0} & \frac{\partial f_2}{\partial y_0} & \frac{\partial f_2}{\partial z_0} \\ \vdots & \vdots & \vdots & \vdots & \vdots & \vdots & \vdots \\ \frac{\partial f_{12}}{\partial s} & \frac{\partial f_{12}}{\partial \alpha} & \frac{\partial f_{12}}{\partial \beta} & \frac{\partial f_{12}}{\partial \gamma} & \frac{\partial f_{12}}{\partial x_0} & \frac{\partial f_{12}}{\partial y_0} & \frac{\partial f_{12}}{\partial z_0} \end{bmatrix}_{12 \times 7}$$

$$= \begin{bmatrix} m_{11} \frac{\mathcal{F}_1}{\partial \alpha} \frac{\mathcal{F}_1}{\partial \beta} \frac{\mathcal{F}_1}{\partial \gamma} 0 0 0 \\ m_{12} \frac{\mathcal{F}_2}{\partial \alpha} \frac{\mathcal{F}_2}{\partial \beta} \frac{\mathcal{F}_2}{\partial \gamma} 0 0 0 \\ \vdots \\ m_{33} \frac{\mathcal{F}_9}{\partial \alpha} \frac{\mathcal{F}_9}{\partial \beta} \frac{\mathcal{F}_9}{\partial \gamma} 0 0 0 \\ 0 0 0 0 1 0 0 \\ 0 0 0 0 0 1 0 \\ 0 0 0 0 0 0 1 \end{bmatrix}$$

in which

$$\frac{\mathcal{F}_1}{\partial \alpha} = 0, \frac{\mathcal{F}_1}{\partial \beta} = s(-\sin \beta \cos \gamma), \frac{\mathcal{F}_1}{\partial \gamma} = s(-\cos \beta \sin \gamma)$$

$$\frac{\mathcal{F}_2}{\partial \alpha} = s(\cos \alpha \sin \beta \cos \gamma - \sin \alpha \sin \gamma), \frac{\mathcal{F}_2}{\partial \beta} = s(\sin \alpha \cos \beta \cos \gamma), \frac{\mathcal{F}_2}{\partial \gamma} = s(-\sin \alpha \sin \beta \sin \gamma + \cos \alpha \cos \gamma)$$

$$\frac{\mathcal{F}_3}{\partial \alpha} = s(\sin \alpha \sin \beta \cos \gamma + \cos \alpha \sin \gamma), \frac{\mathcal{F}_3}{\partial \beta} = s(-\cos \alpha \cos \beta \cos \gamma), \frac{\mathcal{F}_3}{\partial \gamma} = s(\cos \alpha \sin \beta \sin \gamma + \sin \alpha \cos \gamma)$$

$$\frac{\mathcal{F}_4}{\partial \alpha} = 0, \frac{\mathcal{F}_4}{\partial \beta} = s(\sin \beta \sin \gamma), \frac{\mathcal{F}_4}{\partial \gamma} = s(-\cos \beta \cos \gamma)$$

$$\frac{\mathcal{F}_5}{\partial \alpha} = s(-\cos \alpha \sin \beta \sin \gamma - \sin \alpha \cos \gamma), \frac{\mathcal{F}_5}{\partial \beta} = s(-\sin \alpha \cos \beta \sin \gamma), \frac{\mathcal{F}_5}{\partial \gamma} = s(-\sin \alpha \sin \beta \cos \gamma - \cos \alpha \sin \gamma)$$

$$\frac{\mathcal{F}_6}{\partial \alpha} = s(-\sin \alpha \sin \beta \sin \gamma + \cos \alpha \cos \gamma), \frac{\mathcal{F}_6}{\partial \beta} = s(\cos \alpha \cos \beta \sin \gamma), \frac{\mathcal{F}_6}{\partial \gamma} = s(\cos \alpha \sin \beta \cos \gamma - \sin \alpha \sin \gamma)$$

$$\frac{\mathcal{F}_7}{\partial \alpha} = 0, \frac{\mathcal{F}_7}{\partial \beta} = s(\cos \beta), \frac{\mathcal{F}_7}{\partial \gamma} = 0$$

$$\frac{\mathcal{F}_8}{\partial \alpha} = s(-\cos \alpha \cos \beta), \frac{\mathcal{F}_8}{\partial \beta} = s(\sin \alpha \sin \beta), \frac{\mathcal{F}_8}{\partial \gamma} = 0$$

$$\frac{\mathcal{F}_9}{\partial \alpha} = s(-\sin \alpha \cos \beta), \frac{\mathcal{F}_9}{\partial \beta} = s(-\cos \alpha \sin \beta), \frac{\mathcal{F}_9}{\partial \gamma} = 0$$

## Appendix II

### Some Results From The Simulation Tests

#### A2.1 The 3D coordinates of 100 generated object points (the first 8 are control points)

Point No.	X (mm)	Y (mm)	Z (mm)
1000	200.0000	200.0000	100.0000
1001	-200.0000	200.0000	100.0000
1002	-200.0000	-200.0000	100.0000
1003	200.0000	-200.0000	100.0000
1004	200.0000	200.0000	-100.0000
1005	-200.0000	200.0000	-100.0000
1006	-200.0000	-200.0000	-100.0000
1007	200.0000	-200.0000	-100.0000
1008	10.4750	-128.0250	-36.7937
1009	18.9375	188.1375	-64.8313
1010	87.6250	-107.2625	1.3249
1011	-148.9250	-165.6375	-20.2063
1012	-86.4500	-49.2500	101.4062
1013	19.2875	113.6125	32.3937
1014	114.2125	119.5750	68.5376
1015	-137.7750	56.1875	-35.5562
1016	-57.9125	175.6750	6.4437
1017	-35.6875	48.5250	60.8500
1018	181.5500	156.3125	77.4625
1019	76.2750	110.6375	19.1688
1020	-40.5750	-54.3375	-58.9937
1021	138.7000	-29.6500	-5.0750
1022	201.0625	-148.2125	-56.4562
1023	192.5750	102.0625	-16.2312
1024	119.5251	110.4250	95.9562
1025	-188.5000	-69.4500	55.0188
1026	-100.4750	41.4750	-91.1125
1027	191.5875	-69.2875	-87.8437
1028	-19.0125	174.7875	17.1937
1029	-151.3250	33.3750	-48.3812
1030	3.1000	-103.0375	-2.3187
1031	-33.6750	157.5750	-12.5625
1032	-53.2750	-43.5500	-91.1626
1033	-134.2250	13.9500	42.6561
1034	-160.2375	-35.8250	58.3937
1035	-99.7250	-59.5875	-52.8999
1036	-78.0000	-75.2625	81.6937

## Appendix II

1037	-184.9875	66.7000	-18.3687
1038	77.0000	100.0625	92.0562
1039	-104.4500	143.4375	98.0813
1040	118.9250	-23.2626	38.0500
1041	131.5125	-134.9750	-42.6811
1042	-144.5750	153.9625	53.6375
1043	-114.8125	-142.6750	-39.6688
1044	128.8250	-110.3250	15.3188
1045	93.1000	-119.0875	102.7125
1046	-97.5875	-23.6250	54.6750
1047	152.6250	166.5000	100.3062
1048	-38.0500	-22.9750	-73.9625
1049	-12.5374	-102.5875	101.9375
1050	67.3875	47.4875	-50.4625
1051	-13.6875	123.5625	-83.8625
1052	-4.8750	-137.5000	-49.6750
1053	187.0625	51.5000	102.3750
1054	-4.5125	127.5500	52.4062
1055	-44.0625	-3.4375	7.9061
1056	-159.8250	43.3875	-28.9000
1057	-141.2875	119.2875	45.6062
1058	-17.2625	88.5876	-80.4813
1059	194.3625	25.8125	51.5999
1060	37.1625	61.2625	60.0812
1061	-123.0375	-76.2625	-42.0812
1062	80.1625	-80.0250	15.7875
1063	-28.6124	-74.4250	-8.9625
1064	31.7000	-0.1500	24.2375
1065	-29.6750	-146.5875	-47.5813
1066	-185.3625	200.2125	-76.5500
1067	-45.1500	64.8875	-28.2312
1068	26.5250	-53.2000	15.8000
1069	-5.1875	-132.9625	25.9937
1070	-129.4875	27.2000	-40.1562
1071	157.2250	142.0375	73.0312
1072	166.8000	43.6125	10.7062
1073	-131.1125	68.2625	41.4125
1074	-91.9375	-156.3000	66.8937
1075	-121.6250	-26.6250	-27.9438
1076	143.7375	-143.7500	-46.2063
1077	-127.4000	-3.4375	-22.1438
1078	6.7750	5.9250	-27.9313
1079	15.2750	-150.6000	6.4000
1080	48.6750	100.1875	14.0436
1081	-59.0500	128.4750	21.0312
1082	-90.6750	74.7000	13.0750
1083	123.1375	163.6000	82.2687
1084	-172.1125	127.9125	85.8250

Appendix II

1085	63.8250	-132.3625	-38.2875
1086	-131.9000	-83.2000	72.4313
1087	19.6750	-185.1125	-57.5687
1088	-191.3125	-53.3125	27.2750
1089	13.0000	23.6500	-68.5311
1090	137.2375	-186.3500	-94.6875
1091	-45.1250	52.4375	-95.8249
1092	56.6375	174.8625	-23.2437
1093	98.7750	-37.8750	101.1625
1094	44.6375	-154.0000	-54.6188
1095	127.3375	156.6125	51.1875
1096	-194.4250	102.9125	-14.3250
1097	-51.7125	-116.4875	-62.4938
1098	-168.7625	-152.6750	-67.4124
1099	122.8625	-183.4750	61.9188

**A2.2 The starting values of the 3D coordinates obtained by resection followed by intersection**

Point No.	X (mm)	Y (mm)	Z (mm)
1000	204.0991	202.8445	101.3254
1001	-195.7463	203.5645	99.9212
1002	-202.9014	-195.9590	98.8392
1003	197.5738	-196.3199	99.2827
1004	204.4320	203.5470	-98.5635
1005	-195.6471	204.0223	-99.9517
1006	-202.9323	-195.2381	-101.1813
1007	197.5523	-195.5598	-100.7851
1008	9.1848	-123.7341	-37.4500
1009	23.0507	191.8472	-64.0883
1010	86.7006	-103.2835	0.8933
1011	-151.1659	-161.2033	-21.1604
1012	-86.6341	-45.4829	100.9858
1013	22.0725	117.1718	32.7698
1014	116.9780	122.8961	69.1767
1015	-135.9672	60.3426	-35.7355
1016	-54.0473	179.2963	6.8963
1017	-34.0673	52.2298	60.8905
1018	184.9936	159.3657	78.4042
1019	78.9944	114.1775	19.6713
1020	-40.7581	-50.0964	-59.5420
1021	139.1070	-25.8114	-5.0922
1022	199.4811	-144.0395	-56.9108
1023	195.1809	105.5788	-15.4445
1024	122.1336	113.7038	96.5812

Appendix II

1025	-189.0345	-65.4361	54.3002
1026	-98.9030	45.6426	-91.2261
1027	191.4048	-65.1115	-87.9582
1028	-15.1373	178.4032	17.6566
1029	-150.0284	37.6018	-48.7510
1030	2.2491	-98.8895	-2.9133
1031	-30.1314	161.3032	-12.1605
1032	-53.2355	-39.1467	-91.6071
1033	-133.2600	17.9095	42.2754
1034	-160.1532	-31.8207	57.8318
1035	-100.0333	-55.3068	-53.4316
1036	-78.5861	-71.4218	81.0678
1037	-183.0650	70.7337	-18.7715
1038	79.5207	103.4122	92.5740
1039	-101.2999	146.9601	98.1934
1040	119.2849	-19.4927	38.0660
1041	130.2073	-130.7629	-43.1879
1042	-141.1327	157.6737	53.6692
1043	-116.6439	-138.3284	-40.5037
1044	127.8069	-106.3662	14.9202
1045	91.9169	-115.3536	102.1905
1046	-97.2928	-19.6783	54.3050
1047	156.1353	169.5352	101.3288
1048	-37.6008	-18.7076	-74.2632
1049	-13.4860	-98.7774	101.3472
1050	69.1171	51.4240	-50.2576
1051	-10.6293	127.5928	-83.4706
1052	-6.5004	-133.1850	-50.3109
1053	188.7227	54.7205	102.8860
1054	-1.5293	131.1244	52.8481
1055	-43.3448	0.6142	7.6273
1056	-158.3547	47.4860	-29.2725
1057	-138.4731	122.9991	45.5005
1058	-14.8599	92.7303	-80.1959
1059	195.6350	29.3054	51.9998
1060	39.0271	64.8707	60.2775
1061	-123.5790	-71.9439	-42.7579
1062	79.6424	-76.0927	15.4543
1063	-29.0845	-70.2796	-9.5397
1064	32.5031	3.7743	24.1942
1065	-31.3923	-142.1206	-48.3227
1066	-180.9713	204.1812	-76.5208
1067	-43.2086	68.8875	-28.2871
1068	26.4420	-49.2169	15.4569
1069	-6.7417	-128.8931	25.3292
1070	-128.2456	31.3839	-40.4642
1071	160.4604	145.2030	73.8742
1072	168.4512	47.2022	11.1524

Appendix II

1073	-129.1818	72.1484	41.2768
1074	-93.9119	-152.1794	66.0531
1075	-121.3916	-22.4589	-28.3744
1076	142.2212	-139.5319	-46.7230
1077	-126.6849	0.6171	-22.4969
1078	7.7315	10.0180	-28.0473
1079	13.4950	-146.3886	5.5994
1080	51.1645	103.8358	14.3794
1081	-56.0214	132.1354	21.3050
1082	-88.6195	78.6205	13.0258
1083	126.6481	166.7444	83.0630
1084	-169.1147	131.5787	85.7104
1085	62.3477	-128.1883	-38.8876
1086	-132.5914	-79.2530	71.8099
1087	17.3698	-180.6644	-58.4102
1088	-191.5632	-49.2211	26.6195
1089	14.3013	27.8147	-68.6050
1090	134.9642	-181.9145	-95.4153
1091	-43.2937	56.7168	-95.7609
1092	60.4460	178.4791	-22.4585
1093	98.9605	-34.2996	101.0677
1094	42.8543	-149.5887	-55.3675
1095	130.8430	159.8594	52.0430
1096	-191.8785	106.8421	-14.5530
1097	-52.8993	-111.9516	-63.2272
1098	-170.7538	-148.1710	-68.3220
1099	120.6113	-179.6011	61.1751

**A2.3 Adjusted 3D coordinates by the bundle adjustment (inner constraints)**

Point No.	X (mm)	Y (mm)	Z (mm)	$\sigma_x$ (mm)	$\sigma_y$ (mm)	$\sigma_z$ (mm)
1000	202.4055	201.5421	100.8341	0.0389	0.0390	0.0459
1001	-197.3337	205.2520	100.2438	0.0390	0.0390	0.0459
1002	-200.9916	-194.5849	98.7392	0.0389	0.0390	0.0459
1003	198.7972	-198.1705	99.3667	0.0390	0.0389	0.0459
1004	202.6618	202.2861	-99.0185	0.0418	0.0419	0.0562
1005	-197.0859	205.8989	-99.5467	0.0418	0.0418	0.0562
1006	-200.7506	-193.7900	-101.0548	0.0418	0.0418	0.0562
1007	198.9787	-197.4314	-100.6247	0.0419	0.0418	0.0562
1008	10.2574	-124.0462	-37.3909	0.0419	0.0418	0.0528
1009	21.5219	191.9196	-64.2142	0.0420	0.0419	0.0543
1010	87.4639	-104.1980	0.8996	0.0413	0.0413	0.0509
1011	-149.5059	-160.2092	-21.0940	0.0411	0.0411	0.0520
1012	-86.1997	-44.9795	100.9795	0.0400	0.0400	0.0459
1013	21.1204	117.0609	32.6602	0.0410	0.0409	0.0493
1014	115.9128	122.0631	68.9149	0.0402	0.0402	0.0475

## Appendix II

1015	-136.2578	61.4642	-35.5631	0.0417	0.0418	0.0528
1016	-55.4418	179.8977	6.9086	0.0410	0.0409	0.0506
1017	-34.4648	52.4449	60.8668	0.0407	0.0407	0.0479
1018	183.6135	158.1090	77.9987	0.0396	0.0397	0.0470
1019	78.0276	113.6335	19.4843	0.0411	0.0411	0.0500
1020	-40.2001	-49.9039	-59.4728	0.0424	0.0424	0.0540
1021	139.2028	-27.0283	-5.1892	0.0413	0.0414	0.0512
1022	200.4717	-145.8612	-56.8412	0.0414	0.0415	0.0539
1023	194.1898	104.1619	-15.7677	0.0410	0.0412	0.0518
1024	121.1320	112.8056	96.3161	0.0398	0.0399	0.0462
1025	-188.2247	-64.0429	54.3715	0.0402	0.0403	0.0482
1026	-99.0660	46.4647	-91.0792	0.0427	0.0427	0.0557
1027	191.8019	-66.7726	-87.9920	0.0421	0.0423	0.0555
1028	-16.5461	178.6942	17.5886	0.0409	0.0408	0.0501
1029	-150.0872	38.8214	-48.5576	0.0419	0.0420	0.0535
1030	3.0965	-99.1275	-2.8856	0.0415	0.0415	0.0511
1031	-31.3889	161.6996	-12.1845	0.0414	0.0413	0.0516
1032	-52.7229	-38.8236	-91.5100	0.0428	0.0428	0.0557
1033	-133.2515	18.9099	42.3730	0.0407	0.0408	0.0488
1034	-159.6894	-30.6505	57.9109	0.0403	0.0404	0.0480
1035	-99.3444	-54.6259	-53.3238	0.0421	0.0422	0.0537
1036	-77.9300	-71.0027	81.0660	0.0403	0.0403	0.0469
1037	-183.4067	72.2588	-18.5240	0.0412	0.0413	0.0519
1038	78.6248	102.8129	92.3754	0.0401	0.0401	0.0464
1039	-102.4450	147.8174	98.2694	0.0398	0.0397	0.0461
1040	119.3271	-20.5623	37.9567	0.0408	0.0409	0.0490
1041	131.1698	-132.0393	-43.1398	0.0417	0.0417	0.0532
1042	-142.3261	158.9014	53.8452	0.0402	0.0402	0.0482
1043	-115.2259	-137.6045	-40.4138	0.0417	0.0416	0.0530
1044	128.5323	-107.6042	14.9140	0.0409	0.0410	0.0502
1045	92.6701	-116.3499	102.1602	0.0398	0.0398	0.0458
1046	-97.0171	-19.0319	54.3437	0.0407	0.0407	0.0482
1047	154.7071	168.4982	100.9550	0.0394	0.0394	0.0459
1048	-37.3024	-18.4934	-74.1948	0.0426	0.0426	0.0548
1049	-12.7231	-98.9312	101.3182	0.0400	0.0400	0.0459
1050	68.6848	50.8777	-50.3533	0.0422	0.0422	0.0536
1051	-11.5999	127.8197	-83.4893	0.0426	0.0425	0.0553
1052	-5.3131	-133.3783	-50.2365	0.0420	0.0420	0.0535
1053	188.1106	53.2317	102.6054	0.0395	0.0396	0.0458
1054	-2.5809	131.2065	52.7621	0.0406	0.0406	0.0483
1055	-43.2678	0.8634	7.6477	0.0415	0.0415	0.0506
1056	-158.5093	48.7772	-29.0752	0.0415	0.0416	0.0524
1057	-139.3704	124.1669	45.6596	0.0404	0.0404	0.0486
1058	-15.5343	92.9290	-80.1922	0.0426	0.0426	0.0551
1059	195.2238	27.7361	51.7638	0.0402	0.0403	0.0483
1060	38.4675	64.5314	60.1641	0.0407	0.0407	0.0479
1061	-122.7163	-71.0850	-42.6452	0.0418	0.0419	0.0531
1062	80.1879	-76.9242	15.4311	0.0412	0.0412	0.0501

Appendix II

1063	-28.4198	-70.2275	-9.5049	0.0416	0.0416	0.0514
1064	32.4583	3.4124	24.1367	0.0413	0.0413	0.0497
1065	-30.0906	-142.1187	-48.2411	0.0420	0.0419	0.0534
1066	-182.4443	205.9153	-76.1691	0.0416	0.0416	0.0549
1067	-43.6823	69.2497	-28.2590	0.0419	0.0419	0.0524
1068	26.8382	-49.5969	15.4392	0.0413	0.0413	0.0502
1069	-5.6707	-129.1028	25.3562	0.0410	0.0409	0.0496
1070	-128.2867	32.4056	-40.3116	0.0419	0.0419	0.0530
1071	159.1998	144.0951	73.5253	0.0399	0.0399	0.0473
1072	167.9364	45.8733	10.9321	0.0409	0.0410	0.0504
1073	-129.6463	73.1785	41.3972	0.0407	0.0407	0.0489
1074	-92.5530	-151.7066	66.0530	0.0402	0.0401	0.0476
1075	-120.9806	-21.5687	-28.2576	0.0417	0.0418	0.0524
1076	143.2394	-140.9113	-46.6633	0.0416	0.0416	0.0533
1077	-126.4746	1.5777	-22.3701	0.0416	0.0417	0.0521
1078	7.6960	9.8841	-28.0601	0.0420	0.0420	0.0524
1079	14.6952	-146.7734	5.6447	0.0412	0.0411	0.0506
1080	50.3021	103.4875	14.2408	0.0412	0.0412	0.0502
1081	-57.0369	132.6660	21.3225	0.0410	0.0410	0.0499
1082	-89.1575	79.3412	13.1014	0.0412	0.0412	0.0503
1083	125.2538	165.9202	82.7440	0.0398	0.0398	0.0468
1084	-170.0934	132.9806	85.9174	0.0397	0.0397	0.0466
1085	63.3769	-128.9327	-38.8352	0.0418	0.0418	0.0529
1086	-131.7758	-78.3778	71.8313	0.0402	0.0402	0.0473
1087	18.9074	-181.1013	-58.3059	0.0420	0.0418	0.0539
1088	-190.8613	-47.7763	26.7343	0.0405	0.0407	0.0496
1089	14.1350	27.6716	-68.6137	0.0425	0.0425	0.0545
1090	136.3669	-183.2866	-95.2841	0.0422	0.0421	0.0559
1091	-43.6195	57.0971	-95.6939	0.0429	0.0429	0.0559
1092	58.9949	178.2157	-22.6554	0.0415	0.0414	0.0521
1093	99.0970	-35.2552	100.9605	0.0400	0.0400	0.0459
1094	44.1009	-150.1985	-55.2872	0.0420	0.0419	0.0538
1095	129.4918	159.0032	51.7273	0.0403	0.0403	0.0484
1096	-192.5376	108.4820	-14.2639	0.0410	0.0411	0.0517
1097	-51.7935	-111.7318	-63.1372	0.0422	0.0422	0.0542
1098	-169.1027	-146.9727	-68.2012	0.0418	0.0418	0.0544
1099	121.8458	-180.8656	61.2308	0.0400	0.0399	0.0478

*a posteriori* :  $\hat{\sigma}_0 = 0.000433$  (mm)

RMS standard deviations:  $\bar{\sigma}_x = 0.0411$  (mm)

$\bar{\sigma}_y = 0.0411$  (mm)

$\bar{\sigma}_z = 0.0509$  (mm)

**A2.4 Adjusted camera parameters by the bundle adjustment**

Camera No.	$X_L$ (mm)	$Y_L$ (mm)	$Z_L$ (mm)	$\omega$ (deg)	$\phi$ (deg)	$\kappa$ (deg)
1001	999.0877	-8.9771	1000.3989	0.7355	44.9328	-8.2762
1002	8.7136	999.5503	1002.8703	-44.7895	0.3194	91.7613
1003	-999.8688	9.0991	998.0143	-0.3007	-45.0727	52.2496
1004	-9.6634	-999.2358	995.4040	45.2165	-0.4251	-13.9555

**A2.5 Adjusted 3D coordinates by the separate adjustment (free network)**

Point No.	$X$ (mm)	$Y$ (mm)	$Z$ (mm)	$\sigma_x$ (mm)	$\sigma_y$ (mm)	$\sigma_z$ (mm)
1000	202.4422	201.5940	100.7536	0.0390	0.0390	0.0459
1001	-197.3347	205.2795	100.2830	0.0390	0.0390	0.0459
1002	-200.9693	-194.5951	98.8504	0.0390	0.0390	0.0459
1003	198.8572	-198.1563	99.3579	0.0390	0.0390	0.0459
1004	202.6382	202.3026	-99.1179	0.0418	0.0419	0.0562
1005	-197.1473	205.8911	-99.5263	0.0419	0.0418	0.0562
1006	-200.7885	-193.8356	-100.9624	0.0418	0.0419	0.0562
1007	198.9784	-197.4526	-100.6523	0.0419	0.0418	0.0562
1008	10.2541	-124.0610	-37.3686	0.0419	0.0418	0.0529
1009	21.4925	191.9302	-64.2538	0.0420	0.0419	0.0543
1010	87.4782	-104.1994	0.8986	0.0413	0.0413	0.0509
1011	-149.5170	-160.2343	-21.0156	0.0411	0.0411	0.0520
1012	-86.1751	-44.9684	101.0297	0.0400	0.0400	0.0459
1013	21.1247	117.0816	32.6429	0.0410	0.0409	0.0493
1014	115.9366	122.0966	68.8716	0.0402	0.0402	0.0475
1015	-136.2854	61.4580	-35.5294	0.0417	0.0418	0.0528
1016	-55.4562	179.9151	6.9009	0.0410	0.0409	0.0506
1017	-34.4533	52.4613	60.8804	0.0407	0.0407	0.0479
1018	183.6442	158.1517	77.9294	0.0396	0.0397	0.0470
1019	78.0334	113.6552	19.4492	0.0411	0.0411	0.0500
1020	-40.2193	-49.9188	-59.4506	0.0424	0.0424	0.0540
1021	139.2154	-27.0204	-5.2200	0.0413	0.0414	0.0512
1022	200.4816	-145.8698	-56.8743	0.0414	0.0415	0.0539
1023	194.1964	104.1835	-15.8393	0.0410	0.0412	0.0518
1024	121.1651	112.8435	96.2754	0.0398	0.0399	0.0462
1025	-188.2224	-64.0481	54.4516	0.0402	0.0403	0.0482
1026	-99.1060	46.4496	-91.0592	0.0427	0.0427	0.0557
1027	191.7968	-66.7798	-88.0394	0.0421	0.0423	0.0556
1028	-16.5536	178.7157	17.5704	0.0409	0.0408	0.0501
1029	-150.1186	38.8100	-48.5170	0.0419	0.0420	0.0535
1030	3.1014	-99.1343	-2.8624	0.0415	0.0415	0.0511
1031	-31.4057	161.7133	-12.1980	0.0414	0.0413	0.0516

## Appendix II

1032	-52.7535	-38.8439	-91.4889	0.0428	0.0428	0.0557
1033	-133.2527	18.9138	42.4206	0.0407	0.0408	0.0488
1034	-159.6855	-30.6502	57.9767	0.0403	0.0404	0.0480
1035	-99.3669	-54.6438	-53.2823	0.0421	0.0422	0.0537
1036	-77.9090	-70.9969	81.1164	0.0403	0.0403	0.0469
1037	-183.4342	72.2538	-18.4764	0.0412	0.0413	0.0519
1038	78.6533	102.8465	92.3489	0.0401	0.0401	0.0464
1039	-102.4343	147.8450	98.2900	0.0398	0.0397	0.0461
1040	119.3505	-20.5473	37.9348	0.0408	0.0409	0.0490
1041	131.1766	-132.0484	-43.1531	0.0417	0.0417	0.0532
1042	-142.3332	158.9198	53.8717	0.0402	0.0402	0.0482
1043	-115.2410	-137.6288	-40.3516	0.0417	0.0416	0.0530
1044	128.5549	-107.6009	14.9026	0.0409	0.0410	0.0502
1045	92.7161	-116.3341	102.1692	0.0398	0.0398	0.0458
1046	-97.0091	-19.0272	54.3882	0.0407	0.0407	0.0482
1047	154.7413	168.5441	100.8947	0.0394	0.0394	0.0459
1048	-37.3276	-18.5078	-74.1803	0.0426	0.0426	0.0548
1049	-12.6882	-98.9205	101.3558	0.0400	0.0400	0.0459
1050	68.6725	50.8805	-50.3809	0.0422	0.0422	0.0536
1051	-11.6343	127.8189	-83.5095	0.0426	0.0425	0.0553
1052	-5.3211	-133.3972	-50.2091	0.0420	0.0420	0.0535
1053	188.1554	53.2692	102.5557	0.0395	0.0396	0.0458
1054	-2.5737	131.2307	52.7514	0.0406	0.0406	0.0483
1055	-43.2700	0.8649	7.6681	0.0415	0.0415	0.0506
1056	-158.5363	48.7696	-29.0319	0.0415	0.0416	0.0524
1057	-139.3776	124.1808	45.6907	0.0404	0.0404	0.0486
1058	-15.5660	92.9253	-80.2046	0.0426	0.0426	0.0551
1059	195.2555	27.7627	51.7116	0.0402	0.0403	0.0484
1060	38.4848	64.5532	60.1535	0.0407	0.0407	0.0479
1061	-122.7367	-71.1040	-42.5928	0.0419	0.0419	0.0531
1062	80.2042	-76.9209	15.4289	0.0412	0.0412	0.0502
1063	-28.4215	-70.2347	-9.4779	0.0416	0.0416	0.0514
1064	32.4680	3.4218	24.1354	0.0413	0.0413	0.0497
1065	-30.0998	-142.1396	-48.2045	0.0420	0.0419	0.0534
1066	-182.4972	205.9126	-76.1509	0.0416	0.0416	0.0549
1067	-43.6996	69.2512	-28.2540	0.0419	0.0419	0.0524
1068	26.8479	-49.5943	15.4482	0.0413	0.0413	0.0502
1069	-5.6563	-129.1079	25.3900	0.0410	0.0409	0.0496
1070	-128.3132	32.3963	-40.2756	0.0419	0.0419	0.0530
1071	159.2277	144.1342	73.4655	0.0399	0.0399	0.0473
1072	167.9521	45.8926	10.8812	0.0409	0.0410	0.0504
1073	-129.6508	73.1874	41.4340	0.0407	0.0407	0.0489
1074	-92.5331	-151.7120	66.1208	0.0402	0.0401	0.0476
1075	-120.9996	-21.5804	-28.2131	0.0417	0.0418	0.0524
1076	143.2468	-140.9212	-46.6790	0.0416	0.0416	0.0533
1077	-126.4937	1.5689	-22.3275	0.0416	0.0417	0.0521
1078	7.6872	9.8833	-28.0600	0.0420	0.0420	0.0524
1079	14.7067	-146.7824	5.6736	0.0412	0.0411	0.0506

Appendix II

1080	50.3043	103.5056	14.2154	0.0412	0.0412	0.0502
1081	-57.0443	132.6814	21.3250	0.0410	0.0410	0.0499
1082	-89.1671	79.3482	13.1223	0.0412	0.0412	0.0503
1083	125.2799	165.9609	82.6913	0.0398	0.0398	0.0468
1084	-170.0919	133.0005	85.9599	0.0397	0.0397	0.0466
1085	63.3785	-128.9449	-38.8283	0.0418	0.0418	0.0529
1086	-131.7622	-78.3777	71.8984	0.0402	0.0402	0.0473
1087	18.9020	-181.1246	-58.2781	0.0420	0.0418	0.0539
1088	-190.8686	-47.7849	26.8096	0.0405	0.0407	0.0496
1089	14.1135	27.6656	-68.6224	0.0426	0.0426	0.0545
1090	136.3615	-183.3095	-95.2948	0.0422	0.0421	0.0559
1091	-43.6564	57.0856	-95.6930	0.0429	0.0429	0.0560
1092	58.9824	178.2347	-22.7001	0.0415	0.0414	0.0522
1093	99.1383	-35.2317	100.9531	0.0400	0.0400	0.0459
1094	44.0970	-150.2168	-55.2722	0.0420	0.0419	0.0538
1095	129.5094	159.0379	51.6717	0.0403	0.0403	0.0484
1096	-192.5669	108.4805	-14.2196	0.0410	0.0411	0.0517
1097	-51.8111	-111.7538	-63.1008	0.0423	0.0422	0.0542
1098	-169.1306	-147.0061	-68.1237	0.0418	0.0418	0.0545
1099	121.8861	-180.8613	61.2387	0.0400	0.0399	0.0478

*a posteriori* :  $\hat{\sigma}_0 = 0.000433$  (mm)

RMS standard deviations:  $\bar{\sigma}_x = 0.0411$  (mm)

$\bar{\sigma}_y = 0.0411$  (mm)

$\bar{\sigma}_z = 0.0509$  (mm)

### A2.6 Adjusted camera parameters by the separate adjustment

Camera No.	$X_L$ (mm)	$Y_L$ (mm)	$Z_L$ (mm)	$\omega$ (deg)	$\phi$ (deg)	$\kappa$ (deg)
1001	999.4827	-8.7356	1000.1991	0.7220	44.9501	-8.2715
1002	8.9565	999.8248	1002.7908	-44.7998	0.3293	91.7760
1003	-999.6622	9.2176	998.4140	-0.3072	-45.0554	52.2547
1004	-9.3049	-999.1503	995.6839	45.2063	-0.4105	-13.9653

### A2.7 Transformation parameters from the 3D coordinates of BA to SA

$$\begin{bmatrix} t_1 & t_2 & t_3 & t_{10} \\ t_4 & t_5 & t_6 & t_{11} \\ t_7 & t_8 & t_9 & t_{12} \end{bmatrix} = \begin{bmatrix} 0.9999 & 0.0001 & -0.0003 & 0.0005 \\ -0.0001 & 0.9999 & -0.0002 & -0.0028 \\ 0.0003 & 0.0002 & 0.9999 & -0.0068 \end{bmatrix}$$

### A2.8 Comparison between the 3D coordinates of BA and SA after transformation

$\sigma_x(\text{mm})$	$\sigma_y(\text{mm})$	$\sigma_z(\text{mm})$
0.0000	0.0000	0.0000

### A2.8 Adjusted 3D coordinates by BA and SA with 8 control points fixed

Point No.	$X(\text{mm})$	$Y(\text{mm})$	$Z(\text{mm})$	$\sigma_x(\text{mm})$	$\sigma_y(\text{mm})$	$\sigma_z(\text{mm})$
1000	200.0000	200.0000	100.0000	0.0000	0.0000	0.0000
1001	-200.0000	200.0000	100.0000	0.0000	0.0000	0.0000
1002	-200.0000	-200.0000	100.0000	0.0000	0.0000	0.0000
1003	200.0000	-200.0000	100.0000	0.0000	0.0000	0.0000
1004	200.0000	200.0000	-100.0000	0.0000	0.0000	0.0000
1005	-200.0000	200.0000	-100.0000	0.0000	0.0000	0.0000
1006	-200.0000	-200.0000	-100.0000	0.0000	0.0000	0.0000
1007	200.0000	-200.0000	-100.0000	0.0000	0.0000	0.0000
1008	10.5453	-128.0458	-36.8120	0.0425	0.0425	0.0536
1009	18.8964	188.0949	-64.8515	0.0427	0.0425	0.0551
1010	87.6633	-107.3393	1.3223	0.0419	0.0419	0.0516
1011	-148.9540	-165.6238	-20.1528	0.0418	0.0417	0.0528
1012	-86.5052	-49.2960	101.4765	0.0406	0.0406	0.0466
1013	19.3047	113.5548	32.3628	0.0416	0.0415	0.0501
1014	114.1512	119.5601	68.4918	0.0408	0.0408	0.0482
1015	-137.7415	56.2367	-35.4793	0.0424	0.0424	0.0536
1016	-57.9069	175.6312	6.4643	0.0416	0.0415	0.0514
1017	-35.6841	48.5026	60.9043	0.0413	0.0413	0.0486
1018	181.5723	156.2773	77.3539	0.0402	0.0402	0.0477
1019	76.2574	110.5951	19.1143	0.0417	0.0417	0.0507
1020	-40.6457	-54.4061	-59.1167	0.0430	0.0430	0.0548
1021	138.7184	-29.6786	-5.1298	0.0420	0.0420	0.0520
1022	201.0385	-148.2119	-56.4508	0.0420	0.0421	0.0547
1023	192.5246	102.0453	-16.2815	0.0417	0.0418	0.0526
1024	119.4935	110.4479	95.9372	0.0404	0.0405	0.0469
1025	-188.4727	-69.4748	55.0505	0.0408	0.0409	0.0489
1026	-100.4651	41.3599	-91.0235	0.0433	0.0434	0.0565
1027	191.6013	-69.2758	-87.9055	0.0428	0.0429	0.0564
1028	-18.9650	174.8218	17.1024	0.0415	0.0414	0.0508
1029	-151.3887	33.4067	-48.3781	0.0425	0.0426	0.0543
1030	3.1982	-103.0493	-2.3696	0.0421	0.0421	0.0518
1031	-33.6996	157.5709	-12.6048	0.0420	0.0420	0.0524
1032	-53.3184	-43.5542	-91.1979	0.0434	0.0434	0.0565
1033	-134.2428	13.9793	42.6593	0.0413	0.0414	0.0495
1034	-160.2222	-35.7909	58.4282	0.0409	0.0410	0.0487

Appendix II

1035	-99.7712	-59.6468	-52.8659	0.0428	0.0428	0.0545
1036	-78.0195	-75.3326	81.6373	0.0409	0.0409	0.0476
1037	-184.9923	66.6713	-18.4063	0.0418	0.0419	0.0527
1038	77.0489	100.0473	92.0893	0.0407	0.0407	0.0471
1039	-104.5234	143.4475	98.0645	0.0403	0.0403	0.0467
1040	118.8290	-23.2284	38.0450	0.0414	0.0415	0.0498
1041	131.5899	-134.9627	-42.6987	0.0423	0.0423	0.0539
1042	-144.5857	154.0073	53.6262	0.0408	0.0408	0.0490
1043	-114.8870	-142.7668	-39.6155	0.0423	0.0423	0.0538
1044	128.8038	-110.3204	15.3022	0.0416	0.0416	0.0509
1045	93.1156	-119.0702	102.6826	0.0404	0.0404	0.0465
1046	-97.6265	-23.6079	54.7302	0.0413	0.0413	0.0489
1047	152.5848	166.4946	100.3244	0.0400	0.0400	0.0466
1048	-38.0524	-23.0073	-73.9693	0.0432	0.0432	0.0556
1049	-12.4954	-102.6059	101.9179	0.0406	0.0406	0.0466
1050	67.3911	47.4576	-50.5176	0.0428	0.0428	0.0544
1051	-13.6837	123.5854	-83.8530	0.0432	0.0431	0.0562
1052	-4.9653	-137.5732	-49.6093	0.0427	0.0426	0.0543
1053	187.0613	51.4756	102.3626	0.0401	0.0402	0.0465
1054	-4.5125	127.5675	52.4562	0.0412	0.0412	0.0490
1055	-44.0906	-3.3871	7.8583	0.0421	0.0421	0.0513
1056	-159.8808	43.3642	-28.9097	0.0422	0.0423	0.0532
1057	-141.3219	119.2500	45.5618	0.0410	0.0411	0.0494
1058	-17.2974	88.6521	-80.4177	0.0433	0.0432	0.0560
1059	194.3448	25.8402	51.5761	0.0408	0.0409	0.0491
1060	37.1769	61.2579	60.0567	0.0413	0.0413	0.0487
1061	-122.9916	-76.2879	-42.0874	0.0425	0.0425	0.0539
1062	80.1533	-80.0624	15.7703	0.0418	0.0418	0.0509
1063	-28.6079	-74.4457	-9.0584	0.0423	0.0422	0.0522
1064	31.6754	-0.0844	24.2448	0.0419	0.0419	0.0505
1065	-29.6740	-146.5367	-47.5463	0.0426	0.0425	0.0542
1066	-185.3255	200.1932	-76.5884	0.0422	0.0422	0.0558
1067	-45.1768	64.8980	-28.3259	0.0425	0.0425	0.0532
1068	26.5247	-53.2064	15.7484	0.0420	0.0419	0.0509
1069	-5.2632	-133.0148	26.0136	0.0416	0.0416	0.0504
1070	-129.5069	27.2171	-40.1326	0.0425	0.0426	0.0538
1071	157.2671	142.0162	72.9635	0.0405	0.0405	0.0480
1072	166.8235	43.5854	10.6888	0.0416	0.0417	0.0512
1073	-131.1325	68.3065	41.4746	0.0413	0.0413	0.0496
1074	-91.9334	-156.2700	66.9376	0.0408	0.0407	0.0483
1075	-121.6882	-26.6747	-27.8790	0.0424	0.0424	0.0532
1076	143.7425	-143.7428	-46.2075	0.0423	0.0423	0.0541
1077	-127.3888	-3.5437	-22.0672	0.0423	0.0423	0.0529
1078	6.7721	5.9692	-27.9743	0.0426	0.0426	0.0532
1079	15.2494	-150.5833	6.3287	0.0418	0.0417	0.0514
1080	48.6024	100.1710	13.9435	0.0418	0.0418	0.0510
1081	-59.0528	128.4132	21.0661	0.0416	0.0416	0.0506
1082	-90.7149	74.7356	13.0836	0.0418	0.0418	0.0510

Appendix II

1083	123.1150	163.5783	82.1521	0.0404	0.0404	0.0475
1084	-172.0894	127.9394	85.8527	0.0403	0.0403	0.0473
1085	63.7368	-132.4561	-38.3111	0.0425	0.0424	0.0537
1086	-131.8394	-83.2373	72.4978	0.0408	0.0408	0.0480
1087	19.6935	-185.1317	-57.5375	0.0426	0.0424	0.0548
1088	-191.2956	-53.3272	27.3392	0.0412	0.0413	0.0503
1089	12.9992	23.6729	-68.6279	0.0432	0.0432	0.0553
1090	137.1894	-186.3864	-94.6896	0.0428	0.0427	0.0567
1091	-45.0913	52.4863	-95.7563	0.0435	0.0435	0.0568
1092	56.5696	174.8810	-23.2671	0.0421	0.0420	0.0529
1093	98.8041	-37.8773	101.1694	0.0406	0.0406	0.0466
1094	44.6227	-153.9711	-54.6671	0.0427	0.0426	0.0546
1095	127.3780	156.5798	51.1368	0.0409	0.0408	0.0491
1096	-194.4534	102.8469	-14.2668	0.0416	0.0417	0.0525
1097	-51.6858	-116.3871	-62.5358	0.0429	0.0428	0.0550
1098	-168.7442	-152.7357	-67.3115	0.0424	0.0424	0.0553
1099	122.8429	-183.5088	61.9308	0.0406	0.0406	0.0485

*a posteriori* :  $\hat{\sigma}_0 = 0.000440$  (mm)

RMS standard deviations:  $\bar{\sigma}_x = 0.0418$  (mm)

$\bar{\sigma}_y = 0.0418$  (mm)

$\bar{\sigma}_z = 0.0516$  (mm)

**References and Bibliography**

Abdel-Aziz, Y. & Karara, H.M. 1971

**Direct Linear Transformation From Comparator Coordinates into Object Space Coordinates in Close Range Photogrammetry**

Papers from the American Society of Photogrammetry Symposium on Close Range Photogrammetry, Urbana, Illinois. 433, pp. 1-18.

Abdel-Aziz, Y.I. 1979

**An Application of Photogrammetric Techniques to Building Construction**

Photogrammetric Engineering and Remote Sensing, Vol. 45, No. 4, pp. 539-544.

Abdel-Aziz, Y.I. 1982

**The Accuracy of Control Points For Close Range Photogrammetry**

International Archives of Photogrammetry, Vol. 24, Part V/1, pp. 1-11.

Anderson, J.M. & Mikhail, E.M. 1985

**Introduction to Surveying**

McGraw-Hill Publishing Company, London, 703 pages.

Ashkenazi, V. 1974

**The Adjustment and Analysis of Very Large Networks**

The Canadian Surveyor, Vol. 28, No. 5, December 1974, pp. 653-663.

Atkinson, K.B. (Ed), 1996

**Close Range Photogrammetry and Machine Vision**

Whittles Publishing, UK. 371 pages.

Baarda, W. 1973

**S-transformation and Criterion Matrices**

Netherlands Geodetic Commission Publications on Geodesy, New Series, 5(1). 168 pages

Balce, A.E. 1988

**Comparison of Block Adjustment Methods And Accuracies of Photogrammetric Point Determination**

CISM Journal ACSGC, Vol. 42, No. 3, Autumn 1988, pp. 217- 225.

Bevington, P.R. 1969

**Data Reduction and Error Analysis For The Physical Sciences**

McGraw-Hill Book Company. pp. 336.

Beyer, B.A. 1992

**Automated Dimensional Inspection with Real-time Photogrammetry**

International Archive of Photogrammetry and Remote Sensing, Vol. XXIX, Part B5, pp. 722-727.

References and Bibliography

- Blais, J.A.R. 1972  
**Three-Dimensional Similarity**  
The Canadian Surveyor, Vol. 26, No. 1, March 1972.
- Blais, J.A.R. & Chapman, M.A. 1984  
**The Use of Auxiliary Airborne Sensor Data in SPACE-M Photogrammetric Block Adjustment**  
The Canadian Surveyor, Vol. 38, No. 1, Spring 1984, pp. 3-14.
- Blais, J.A.R. & Chapman, M.A. 1984  
**The Use of Relative Terrestrial Control Data in SPACE-M Photogrammetric Block Adjustment**  
The Canadian Surveyor, Vol. 38, No. 4, Winter 1984, pp. 299-310.
- Boge, W.E. 1965  
**Resection Using Iterative Least Squares**  
Photogrammetric Engineering, Vol. XXXI, No. 4, July 1965, pp. 701-715.
- Brown, D.C. 1960.  
**Results in Geodetic Photogrammetry**  
Photogrammetric Engineering, 26(3): pp. 444-452.
- Brown, D.C., Davis, R.G. and Johnson, F.C. 1964  
**Research in Mathematical Targetting, The Practical and Rigorous Adjustment of Large Photogrammetric Nets.**  
Rome Air Development Centre Report RADC - TDR - 353. Rome, New York.
- Brown, D.C. 1971  
**Close-Range Camera Calibration**  
Photogrammetric Engineering, 1971. pp. 855-866.
- Brown, D.C. 1976  
**The Bundle Method -- Progress and Prospects**  
International Archives of Photogrammetry, 21(3) Paper 303: 33 pages
- Brown, D.C. 1989  
**A Strategy for Multi-Camera On-The-Job Self-Calibration**  
Institut fur Photogrammetrie Stuttgart, Stuttgart 1989, pp. 1-13.
- Bunch, J.R. & Parlett, B.N. 1971  
**Direct Methods for Solving Symmetric Indefinite Systems of Linear Equations.**  
SIMA Journal of Numerical Analysis. Vol. 8. No. 4, December 1971.
- Caspary, W. 1987  
**Concepts of Network and Deformation Analysis**  
Univ. of New South Wales, Monograph No. 11, Kensington, N.S.W.

- Chen, J. 1995  
**The Use of Multiple Cameras and Geometric Constraints for 3-D Measurement**  
PhD Thesis, City University, UK, 245 pages.
- Clarke, T.A. 1995  
**An Analysis of the Prospects for Digital Close Range Photogrammetry**  
ISPRS Journal of Photogrammetry and Remote Sensing, 50(3): pp. 4-7.
- Clarke, T.A., Cooper, M.A.R., Chen, J. and Robson, S. 1995  
**Automatic Three Dimensional Measurement Using Multiple CCD Camera Views**  
Photogrammetric Record, Vol. 15, No. 85, pp. 27-42.
- Clarke, T.A. & Wang, X. 1995  
**An Analysis of Subpixel Target Location Accuracy Using Fourier Transform Based Models**  
Videometrics IV, SPIE Vol. 2598.
- Clarke, T.A., Fryer, J.G., Wang, X. 1996  
**The Principal Point for CCD Cameras**  
Photogrammetric Record. In press.
- Cooper, M.A.R. 1980  
**A Singular Braced Quadrilateral**  
Survey Review XXV, 198, October 1980. pp. 351-359.
- Cooper, M.A.R. 1987  
**Control Surveys in Civil Engineering**  
William Collins Sons & Co. Ltd, London. 381 pages.
- Cooper, M.A.R. & Cross, P.A. 1988  
**Statistical Concepts and Their Application in Photogrammetry and Surveying**  
Photogrammetric Record, Vol. 12, No. 71, pp. 637-663.
- Cooper, M.A.R. & Cross, P.A. 1991  
**Statistical Concepts and Their Application in Photogrammetry and Surveying (Continued)**  
Photogrammetric Record, Vol. 13, No. 77, pp. 645-678.
- Cox, M.G. 1981  
**The Least Squares Solution of Overdetermined Linear Equations Having Band or Augmented Band Structure.**  
SIMA Journal of Numerical Analysis (1981) 1, pp. 3-22.

References and Bibliography

- Cross, P.A. 1983  
**Advanced Least Squares Applied to Position-Fixing**  
Working Paper No. 6, Department of Land Surveying, North East London Polytechnic.
- CUBA 1996  
**The City University Bundle Adjustment**  
By Tim Short, City University, London
- Deakin, R.E., Collier, P.A. & Leahy, F.J. 1994  
**Transformation of Coordinates Using Least Squares Collocation**  
The Australian Surveyor, Vol. 39, No. 1, March 1994, pp. 6-20.
- Dermanis, A. 1994  
**The Photogrammetric Inner Constraints**  
ISPRS Journal of Photogrammetry And Remote Sensing, Vol. 49, No. 1, pp. 25-39.
- Edmundson, K. & Fraser, C.S. 1995  
**Sequential Estimation in Single-Sensor Vision Metrology for Industrial Photogrammetry.**  
Presented Paper, 1995 ACSM/ASPRS Annual Convention, Charlotte, NC.
- Edmundson, K. & Fraser, C.S. 1996  
**Implementation of Sequential Estimation for Single-Sensor Vision Metrology**  
International Archives of Photogrammetry and Remote Sensing.  
Vol. XXXI, Part B5. Vienna 1996, pp. 133-139.
- El-Hakim, S.F. & Faig, W. 1981  
**A Combined Adjustment of Geodetic and Photogrammetric Observations**  
Photogrammetric Engineering and Remote Sensing, Vol. 47, No. 1, pp. 93-99.
- Faig, W. 1975  
**Calibration of Close Range Photogrammetric Systems: Mathematical Formulation**  
Photogrammetric Engineering and Remote Sensing, Vol. 42(12), pp. 1479-1486.
- Faig, W. & Shih, T.Y. 1986  
**Critical Configuration of Object Space Control Points for The Direct Linear Transformation**  
Real-Time Photogrammetry- A New Challenge, ISPRS, Vol. 26, Part 5, pp. 23-29.
- Frank Ayres, JR. 1974  
**Theory and Problems of Matrices**  
McGraw-Hill International Book Company, New York. 219 pages.

References and Bibliography

- Fraser, C.S. 1982  
**Multiple Focal Setting Self-Calibration of Close-Range Metric Cameras**  
Photogrammetric Engineering and Remote Sensing, Vol. 46(9), pp. 1161-1171.
- Fraser, C.S. 1982  
**Self-Calibration of a Fixed-Frame Multiple Camera System**  
Photogrammetric Engineering and Remote Sensing, Vol. 46(11), pp. 1439-1445.
- Fraser, C.S. 1982  
**Optimisation of Precision in Close Range Photogrammetry**  
Photogrammetric Engineering and Remote Sensing, Vol. 48, pp. 561-570.
- Fraser, C.S. 1984  
**Network Design Considerations for Non-topographic Photogrammetry**  
Photogrammetric Engineering and Remote Sensing, Vol. 50, No. 8,  
pp. 1115-1126
- Fraser, C.S. & Gruendig, L. 1985  
**The Analysis of Photogrammetric Deformation Measurement on Turtle Mountain**  
Photogrammetric Engineering and Remote Sensing, Vol. 51, No. 2, pp. 207-216.
- Fraser, C.S. & Brown, D.C. 1986  
**Industrial Photogrammetry: New Developments and Recent Applications**  
Photogrammetric Record, Vol. 12, No. 68, pp. 197-216.
- Fraser, C.S. 1992  
**Photogrammetric Measurement to One Part in a Million**  
Photogrammetric Engineering & Remote Sensing, Vol 58. No 3. pp. 305-310.
- Fryer, J.G. & Brown, D.C. 1986  
**Lens Distortion for Close Range Photogrammetry**  
Photogrammetric Engineering and Remote Sensing, Vol. 52, No. 1, pp. 51-58.
- Fryer, J.G. & Mason, S.O. 1989  
**Rapid Lens Calibration of a Video Camera**  
Photogrammetric Engineering and Remote Sensing, Vol. 55, No. 4, pp. 437-442.
- Fryer, J.G. 1996  
**Single Station Self-Calibration Techniques**  
International Archives of Photogrammetry and Remote Sensing.  
Vol. XXXI, Part B5. Vienna 1996, pp. 178-181.
- GAP 1992  
**General Adjustment Program -- User Manual**  
Dept. of Civil Engineering, City University, London, 19 pages.

References and Bibliography

- Gill, P.E., Murray, W., Wright, M.H. 1993  
**Practical Optimization**  
Academic Press Limited, London, 401 pages.
- Granshaw, S.I. 1980  
**Bundle Adjustment Methods in Engineering Photogrammetry**  
Photogrammetric Record, Vol. 10, No. 56, pp. 181-207.
- Gruen, A., 1978  
**Accuracy, Reliability and Statistics in Close-Range Photogrammetry**  
ISP., Commission V Inter-Congress symposium, Photogrammetry for Industry.  
Stockholm.
- Gruen, A. 1985  
**Algorithmic Aspects in On-Line Triangulation**  
Photogrammetric Engineering and Remote Sensing. Vol. 51, pp. 419-436.
- Gruen, A., Kersten, T.P. 1992  
**Sequential Estimation in Robot Vision**  
International Archives of Photogrammetry and Remote Sensing, Vol. XXIX,  
Part B5, Commission V, pp. 923-931.
- Hades, I. 1981  
**Bundle Adjustment in Industrial Photogrammetry**  
Photogrammetria, Vol. 37, No. 2, December 1981, pp. 45-60
- Hageman, L.A. & Young, D.M. 1981.  
**Applied Iterative Methods.**  
Academic Press. 386 pages.
- Harley, I. A. 1997  
Comments given in thesis examination.
- Hill, A., Cootes, T.F. & Taylor, C.J. 1995.  
**Active shape models and the shape approximation problem.**  
British Machine Vision Conference, 1995. pp. 157-166.
- Holm, K.R. 1984  
**Test of Algorithms for Sequential Adjustment in Close Range  
Photogrammetry**  
International Archives of Photogrammetry and Remote Sensing, ISPRS,  
Vol. XXV, Part A5, pp. 383-390.
- Hultquist, P.F. 1988  
**Numerical Methods for Engineers and Computer Scientists**  
The Benjamin/Cummings Publishing Company, Inc. 326 pages.

References and Bibliography

- Jacoby, S.L.S., Kowalik, J.S. & Pizzo, J.T. 1972.  
**Iterative Methods for Nonlinear Optimisation Problems.**  
Prentice-Hall, Inc., Englewood Cliffs, New Jersey. 277 pages.
- Jacques, I. & Judd, C. 1987  
**Numerical Analysis**  
Chapman and Hall, London and New York. 326 pages.
- Jones, A., 1970  
**Spiral -- A New Algorithm for Non-linear Parameter Estimation Using Least Squares**  
Computer Journal, Vol. 13, 1970.
- Kailath, T. (Ed) 1977  
**Linear Least-Squares Estimation**  
Dowden, Hutchinson & Ross, Inc. pp. 318.
- Karara, H.M. (Ed), 1989  
**Non-topographic Photogrammetry.**  
American Society for Photogrammetry and Remote Sensing, Falls Church, Virginia, 445 pages.
- Kenefick, J.F., Gyer, M.S. & Harp, B.F. 1972  
**Analytical Self-Calibration**  
Photogrammetric Engineering, November 1972, pp. 1117-1126.
- Kissam, P 1956  
**Surveying For Civil Engineers**  
McGraw-Hill Book Company, INC. 716 pages.
- Kok, J.J 1984  
**Some Notes on Numerical Methods and Techniques for Least Squares Adjustments**  
Surveying Science in Finland, (1984) (2), pp. 1-35.
- Kreyszig, E. 1993  
**Advanced Engineering Mathematics--Seventh Edition**  
John Willy & Sons, INC. pp. 1271.
- Kuang, S. 1996  
**Geodetic Network Analysis and Optimal Design.**  
Ann Arbor Press, Inc. 368 pages.
- Kubik, K., Merchant, D. & Schenk, T. 1987  
**Robust Estimation in Photogrammetry**  
Photogrammetric Engineering and Remote Sensing, Vol. 53, No. 2, pp. 167-169.

References and Bibliography

- Lee, C.K. & Faig, W. 1996  
**Vibration Monitoring with Video Cameras**  
International Archives of Photogrammetry and Remote Sensing.  
Vol. XXXI, Part B5. Vienna 1996, pp. 152-159.
- Marel, H. van der 1989  
**Algorithm Aspects of Solving Large Systems of Equations**  
"Mathematical Aspects of Data Analysis"  
ISPRS, Pisa, 1-2 June 1989.
- Methley, B.D.F. 1986  
**Computational Models in Surveying And Photogrammetry**  
Blackie & Sons Limited, Glasgow and London. 346 pages.
- Mikhail, E.D. 1976  
**Observations and Least Squares**  
IEP--A Dun-Donnelley Publisher, New York. 497 pages.
- Mikhail, E.D. & Gracie, G. 1981  
**Analysis and Adjustment of Survey Measurements**  
Van Nostrand Reinhold Company, New York. 340 pages.
- Miles, M.J. 1963  
**Methods of solution of the adjustment of a block of aerial triangulation.**  
Photogrammetric Record. Vol. IV. No 22. pp. 287-298.
- Nossiter, B.S. & Fryer, J.G. 1995  
**An Analytical And Digital Photogrammetric Study of The 'SIRIUS'**  
The Australian Surveyor, Vol. 40, No. 1, March 1995, pp. 29-34.
- Obidowski, R.M. & Chapman, M.A. 1993  
**Processing Theodolite Observations With A Photogrammetric Bundle Adjustment: An Industrial Survey Application**  
Geomatica, Vol. 47, No. 3&4, Autumn 1993, pp. 245-259.
- Papo, H.B. & Perelmuter, A. 1985  
**Control Network Analysis by a Dynamic Model**  
The Canadian Surveyor, Vol. 39, No. 1, Spring 1985, pp. 3-10.
- Papo, H.B. & Perelmuter, A. 1988  
**Datum Definition In The GPS Era**  
CISM Journal ACAGC, Vol. 42, No. 2, Summer 1988, pp. 127-132.

- Peckham, G. 1970  
**A New Method for Minimising a Sum of Squares Without Calculating Gradients**  
Computer Journal, Vol. 13, 1970.
- Peters, G. & Wilkinson, J. H. 1970  
**The Least Squares Problem and Pseudo-Inverse.**  
Computer Journal, Vol. 13, 1970.
- Phillips, C. & Cornelius, B. 1986  
**Computational Numerical Methods**  
Ellis Horwood Limited. 375 pages.
- Pinch, M.C. & Peterson A.E. 1974  
**A Method for Adjusting Survey Networks in Sections.**  
The Canadian Surveyor, Vol. 28, No. 1, March 1974.
- Powell, M. J. D. 1962  
**An Iterative Method for Finding Stationary Values of A Function of Several Variables.**  
The Computer Journal, Vol. 5, 1962.
- Powell, M. J. D. 1965  
**A Method for Minimising A Sum of Squares of Non-linear Functions Without Calculating Derivatives.**  
The Computer Journal, Vol. 7, 1965.
- Robson, S. 1991  
**Some Influence of The Photographic Process on The Accuracy of Close Range Photogrammetry With a Non-metric Camera**  
PhD Thesis, City University, UK.
- Robson, S. & Setan, H.B. 1996  
**The Dynamic Digital Photogrammetric Measurement and Visualisation of a 21m Wind Turbine Rotor Blade Undergoing Structure Analysis.**  
International Archives of Photogrammetry and Remote Sensing.  
Vol. XXXI, Part B5. Vienna 1996, pp. 493-498.
- Schuh, W.D. 1989  
**Non-Conventional Adjustment Techniques**  
Tutorial on "Mathematical Aspects of Data Analysis", ISPRS Proc., 1989.
- Searle, S.R. 1982  
**Matrix Algebra -- Useful for Statistics.**  
John Wiley & Sons, Inc. 438 pages.

- Setan, H.B. 1995  
**Functional and Stochastic Models for Geometrical Detection of Spatial Deformation in Engineering: A Practical Approach**  
PhD Thesis, City University, UK. 261 pages.
- Shih, T.Y. & Faig, W. 1988  
**A Solution for Space Resection in Closed Form**  
International Archives of Photogrammetry and Remote Sensing, Vol.21, 1988.
- Shih, T.Y. 1990  
**An Investigation Into the Computational Procedures of Space Resection By Collinearity Equations**  
Photogrammetric Record, Vol. 13, No. 75, April 1990, pp. 433-440.
- Shmutter, B, & Perlmutter, A. 1974.  
**Spatial intersection**  
Photogrammetric Record, Vol. 8(43): 94-100.
- Shortis, M.R. 1980  
**Sequential Adjustment of Photogrammetric Models**  
PhD Thesis. Department of Civil Engineering, The City University, London.
- Slama, C.C. (Ed), 1980.  
**Manual of Photogrammetry.** (Fourth Edition)  
American Society for Photogrammetry, Falls Church, Virginia, 1056 pages.
- Smith, A.D.N. 1965  
**The Explicit Solution of The Single Picture Resection Problem, With A Least Squares Adjustment to Redundant Control**  
Photogrammetric Record, Vol. V, No. 26, October 1965, pp. 113-121.
- Stefanovic, P. 1978  
**Blunders and Least Squares**  
ITC Journal 1978-1.
- Stefanovic, P. 1981  
**Pitfalls in Blunder Detection Techniques**  
ITC Journal 1981-1.
- Strang van Hees, G.L. 1982  
**Variance and Covariance Transformations of Geodetic Networks**  
Manuscripta Geodetica, 7(1): pp. 1-20.
- Tan, W. 1988  
**Some Design Considerations Using the Bundle Adjustment**  
The Australian Surveyor, Vol. 34, No. 4, December 1988, pp. 400-406.

References and Bibliography

- Teunissen, P.J.G. & Knickmeyer, E.H. 1988  
**Nonlinearity And Least Squares**  
CISM Journal ACAGC, Vol. 42, No. 4, Winter 1988, pp. 321-330.
- Thompson, E.H. 1966  
**Space Resection: Failure Cases**  
Photogrammetric Record, Vol. V, No. 27, April 1975, pp. 201-205.
- Thompson, E.H. 1975  
**Resection in Space**  
Photogrammetric Record, 8(45): April 1975, pp. 333-334.
- Traub, J.F. 1964  
**Iterative Methods for the Solution of Equations**  
Prentice-Hall, Inc., Englewood Cliffs, New Jersey. 310 pages.
- Varga, R.S. 1962  
**Matrix Iterative Analysis.**  
Prentice-Hall, Inc. 322 pages.
- Wampler, R. H. 1969  
**An Evaluation of Linear Least Squares Computer Programs**  
Journal of Research of the National Bureau of Standards - B. Mathematical Sciences, Vol. 73B, 1969.
- Wang, X. 1996  
**An Algorithm for Real-Time 3D Measurement.**  
International Archives of Photogrammetry and Remote Sensing.  
Vol. XXXI, Part B5. Vienna 1996, pp. 587-592.
- Welsh, N. 1986  
**Photogrammetry in Engineering**  
Photogrammetric Record, Vol. 12, No. 67, pp. 25-44.
- Wolf, P.R. 1983  
**Elements of Photogrammetry**  
McGraw-Hill Inc., New York, 628 pages.
- Young, D.M 1971  
**Iterative Solution of Large Linear Systems**  
Academic Press, New York and London. 570 pages.
- Zimmerman, D.S. 1974  
**Least Squares Solution by Diagonal Partitioning**  
The Canadian Surveyor, Vol. 28, No. 5, December 1974.